Geometry & Topology

Volume 29 (2025)

Endperiodic maps, splitting sequences, and branched surfaces

MICHAEL P LANDRY
CHI CHEUK TSANG

msp

msp

Geometry & Topology **29**:9 (2025) 4531–4663
DOI: 10.2140/gt.2025.29.4531
Published: 31 December 2025

Endperiodic maps, splitting sequences, and branched surfaces

MICHAEL P LANDRY
CHI CHEUK TSANG

We strengthen the unpublished theorem of Gabai and Mosher that every depth one sutured manifold contains a very full dynamic branched surface by showing that the branched surface can be chosen to satisfy an additional property we call veering. To this end we prove that every endperiodic map admits a periodic splitting sequence of train tracks carrying its positive Handel–Miller lamination. This completes step one of Gabai and Mosher's unpublished two-step proof that every taut finite-depth foliation of a compact, oriented, atoroidal 3-manifold is almost transverse to a pseudo-Anosov flow. Further, a veering branched surface in a sutured manifold is a generalization of a veering triangulation, and we extend some of the theory of veering triangulations to this setting. In particular we show that the branched surfaces we construct are unique up to a natural equivalence relation, and give an algorithmic way to compute the foliation cones of Cantwell and Conlon.

37E30, 57K32

1 Introduction

1.1 Context

Let $\mathcal{F}$ be a finite-depth cooriented foliation obtained from a sutured hierarchy, ie a sequence of sutured manifold decompositions

$$M = Q_0 \rightsquigarrow Q_1 \rightsquigarrow \cdots \rightsquigarrow Q_n \rightsquigarrow Q_{n+1},$$

where M is a compact 3-manifold with toral boundary and Q_{n+1} is a product sutured manifold (see [Gabai 1983]). The last decomposition $Q_n \rightsquigarrow Q_{n+1}$ induces a *depth one foliation* on Q_n by the well-known "spinning" construction.

A depth one foliation of a sutured manifold is a cooriented foliation whose only compact leaves are the positive and negative tangential boundaries $R_\pm$, and whose noncompact leaves accumulate only on $R_\pm$. In this situation, the complement of $R_\pm$ fibers over S^1 with fibers the noncompact leaves L of the foliation, and the monodromy of the fibration determines an *endperiodic map* $f : L \to L$. The foliated sutured manifold is a compactification of the mapping torus of f.

In the 1980s, Handel and Miller developed a theory of *positive* and *negative laminations* for endperiodic maps, analogous to the Nielsen–Thurston picture of laminations for pseudo-Anosov mapping classes; this theory was definitively exposited only recently by Cantwell, Conlon and Fenley [Cantwell et al. 2021]. Morally, an endperiodic map expands the leaves of the positive lamination Λ_+ and contracts the leaves of the negative lamination Λ_- up to isotopy. Moreover, the isotopy class of the endperiodic map contains a *Handel–Miller representative* which preserves the laminations on the nose. By suspending the 1-dimensional positive and negative Handel–Miller laminations to the compactified mapping torus, one obtains 2-dimensional *unstable* and *stable Handel–Miller laminations*.

Subsequent to the work of Handel and Miller, Gabai developed a theory to build a pseudo-Anosov flow in M almost transverse to the original finite-depth foliation $\mathcal{F}$, essentially by extending the unstable/stable Handel–Miller laminations in Q_n up through the hierarchy. This theory was not written down.

In the 1990s, Mosher set out to prove the existence of Gabai's flows. He introduced the notion of a *dynamic pair*, which is a combinatorial analogue of a pseudo-Anosov flow together with its unstable and stable foliations. Roughly speaking, a dynamic pair consists of a pair of branched surfaces B^u and B^s intersecting transversely whose complementary regions are particularly nice. Mosher [1996, Part I] proves that a dynamic pair in M transverse to $\mathcal{F}$ gives rise to a pseudo-Anosov flow almost transverse to $\mathcal{F}$, thus reducing the construction of a flow in M to the construction of a dynamic pair from a sutured manifold hierarchy.

Mosher outlined his plans for Part II of the monograph in his introduction. Essentially Part II would have been an inductive argument consisting of two parts: a *base step* and a *gluing step*. In the base step, one builds a dynamic pair in Q_n combinatorializing the Handel–Miller laminations. In the gluing step, one aims to show that for each i, a dynamic pair in Q_{i+1} can be promoted to a dynamic pair in Q_i. Inducting up the sutured hierarchy, this would produce a dynamic pair on $M = Q_0$.

The Gabai–Mosher construction has proven useful. For example, Mosher [1992] uses it to show that there exist pseudo-Anosov flows dynamically representing top-dimensional, nonfibered faces of the Thurston norm ball; in the same paper he constructs a pseudo-Anosov flow which does not represent an entire face of the Thurston norm ball. Fenley and Mosher [2001] prove that pseudo-Anosov flows almost transverse to finite-depth foliations in hyperbolic 3-manifolds are quasigeodesic, and appeal to the construction to say such flows are abundant. Calegari and Dunfield [2003] use the construction to show that certain Dehn fillings of torally bounded hyperbolic 3-manifolds admit pseudo-Anosov flows, allowing them to apply their results on universal circles. Calegari [2006] uses the construction for one direction of his proof that the unit ball of the dual Thurston norm of a closed hyperbolic 3-manifold is exactly the convex hull of the Euler classes of quasigeodesic flows.

Unfortunately, thus far a complete proof of Gabai and Mosher's result has not appeared in the literature.

1.2 Summary of results

This paper is part of an attempt to revisit Mosher's program using ideas from the theory of *veering triangulations*. Veering triangulations were introduced by Agol [2011] and recently shown to correspond robustly to pseudo-Anosov flows [Frankel et al. 2019, Introduction]. Tsang [2023, Proposition 3.2] introduced the notion of (*unstable*) *veering branched surfaces* in compact 3-manifolds with toral boundary, and showed that these are dual to veering triangulations. Inspired by Mosher's dynamic pairs, we generalize veering branched surfaces to the setting of sutured manifolds. See Definition 6.11 for the precise formulation.

Using this tool of veering branched surfaces, we prove the following theorem that substitutes for Mosher's base step:

Theorem 7.10 *Let Q be an atoroidal sutured manifold with a depth one foliation $\mathcal{F}$. Then Q contains an unstable veering branched surface carrying the unstable Handel–Miller lamination associated to $\mathcal{F}$.*

In Theorem A.14, we show that Theorem 7.10 in fact implies Mosher's base step. We remark that one can symmetrically define a stable veering branched surface and prove the symmetric version of Theorem 7.10, and in fact of all the results that we state. That we mainly work with unstable veering branched surfaces in this paper is just a choice.

This theorem can be thought of as a generalization of Agol's work [2011] showing that the mapping torus of a pseudo-Anosov map (on a finite-type surface) contains an unstable veering branched surface carrying the unstable foliation of the suspension flow. Indeed, our strategy of proof resembles Agol's proof, though there are some essential differences. In the finite-type case, Agol uses a projectively invariant positive measure for the expanding lamination of the pseudo-Anosov monodromy to get a measured train track carrying the lamination. He then performs *maximal splittings*, ie splitting moves on the branches of maximal weight. He shows that the resulting sequence of train tracks is eventually periodic modulo

the monodromy, and hence can be suspended to obtain a branched surface in the mapping torus. This branched surface carries the unstable lamination of the monodromy and satisfies our definition of veering.

In our setting, this idea does not work since Handel–Miller laminations do not in general carry projectively invariant measures of full support (see [Fenley 1997, Section 5] and Example 10.6). Instead, we perform *core splittings* on endperiodic train tracks carrying the positive Handel–Miller lamination. This means performing every possible splitting within a certain *core* of the surface. To show that this operation is well defined and gives an eventually periodic sequence, we develop the theory of *spiraling train tracks* (Definition 2.9) and utilize properties of the complementary regions of Handel–Miller laminations. In Theorem 4.10, we prove the resulting sequence is eventually periodic modulo the monodromy:

Theorem 4.10 *Let $f\colon L \to L$ be endperiodic, and let τ_0 be an efficient f-endperiodic train track carrying the positive Handel–Miller lamination. Consider the sequence of train tracks (τ_n), where τ_{n+1} is a core split of τ_n. For sufficiently large n, we have $\tau_{n+1} = f(\tau_n)$.*

To prove Theorem 7.10, we essentially suspend a period of this sequence to get a branched surface, which we prove is veering.

We also investigate the uniqueness of the veering branched surface. In the finite-type case, it is known that the veering branched surface carrying the unstable lamination is unique up to isotopy (this follows from results in [Agol 2011; Landry et al. 2024]; see Theorem 9.1). In the endperiodic case the situation is more subtle because two veering branched surfaces B_1 and B_2 carrying the unstable Handel–Miller lamination can have different boundary train tracks $B_1 \cap R_+(Q)$ and $B_2 \cap R_+(Q)$. However, this is the only obstruction to uniqueness:

Theorem 9.22 *Let Q be an atoroidal sutured manifold with depth one foliation $\mathcal{F}$, and let $\mathcal{L}$ be the unstable Handel–Miller lamination associated to $\mathcal{F}$. Any veering branched surface B compatibly carrying $\mathcal{L}$ is determined up to isotopy by $B \cap R_+(Q)$.*

Moreover, from our study of spiraling train tracks, we know that any two veering branched surfaces carrying $\mathcal{L}$ must intersect $R_\pm(Q)$ in two train tracks differing by a sequence of shifts. From this sequence of shifts we have an explicit description of how B_1 and B_2 are related. See Section 9.3 for details.

Finally, we generalize the theory of cones associated to veering triangulations. We briefly review this theory for context. A veering triangulation has an associated *dual graph* and *flow graph*. These are finite directed graphs embedded inside of the triangulation. The dual graph is easily describable as the branch locus of the dual veering branched surface. The flow graph, introduced in [Landry et al. 2024], has a more complicated description.

In [Landry et al. 2023b], it is shown that the cone in H_1 generated by directed cycles of the dual graph equals that of the flow graph. In [Landry 2022; Landry et al. 2024], it is shown that this cone is the cone over a (not necessarily top-dimensional) face of the Thurston norm unit ball. When the veering

triangulation is one whose dual veering branched surface carries the unstable foliation of a pseudo-Anosov mapping torus as above, its associated cone is dual to the cone over the Thurston fibered face containing the fibration. In particular this provides an algorithmic way to compute fibered faces.

In Section 6.4 we generalize the dual graph and flow graph to the sutured setting. We then prove the following theorem:

Theorem 8.5 *Let Q be an atoroidal sutured manifold with depth one foliation $\mathcal{F}$, and let $\mathcal{L}$ be the unstable Handel–Miller lamination associated to $\mathcal{F}$. Let $\mathscr{C}_{\mathcal{F}} \subset H_2(Q, \partial Q)$ be the foliation cone containing the class of $\mathcal{F}$. Meanwhile, let B be an unstable veering branched surface compatibly carrying $\mathcal{L}$, with dual graph Γ and flow graph Φ. Let $\mathscr{C}_\Gamma$ and $\mathscr{C}_\Phi$ be the cones in $H_1(M)$ positively generated by the cycles of Γ and Φ, respectively. Then*

$$\mathscr{C}_{\mathcal{F}}^\vee = \mathscr{C}_\Gamma = \mathscr{C}_\Phi.$$

We refer to Section 8.1 for a review of the theory of foliation cones. Here it suffices to say that these are finitely many rational polyhedral cones in $H_2(Q, \partial Q)$ that contain the classes of depth one foliations transverse to Handel–Miller semiflows, mirroring Fried's theory [1979] of Thurston fibered faces in compact 3-manifolds. Our result provides an algorithmic way to compute foliation cones.

The equality $\mathscr{C}_\Gamma = \mathscr{C}_\Phi$ is shown by generalizing the notion of dynamic planes, introduced in [Landry et al. 2023b], to the sutured setting. The condition "*compatibly carrying*" arises naturally when considering the extra complications in the combinatorics of these dynamic planes; see Definition 8.3. When the unstable veering branched surface compatibly carries an unstable Handel–Miller lamination $\mathcal{L}$ as in the theorem, the dynamic planes are in one-to-one correspondence with the lifts of leaves of $\mathcal{L}$ to the universal cover of Q. This allows us relate the dynamics of the Handel–Miller semiflow to that of the dual graph and flow graph, and show that $\mathscr{C}_\Gamma = \mathscr{C}_\Phi = \mathscr{C}_{\mathcal{F}}^\vee$.

In general, even if an unstable veering branched surface does not carry the unstable lamination associated to a depth one foliation, it is still true that $\mathscr{C}_\Gamma = \mathscr{C}_\Phi$.

There are other aspects of veering triangulation theory that we expect to admit generalizations to the sutured setting. We mention a few in Section 11.

We also include an appendix, the purpose of which is to explain the connection between our veering branched surfaces and Mosher's base step, and to prove results that will be used in our sequel paper [Landry and Tsang $\geq$ 2025]. The main result is the following:

Theorem A.14 *If an atoroidal sutured manifold Q admits an unstable veering branched surface, then it admits a dynamic pair.*

In the case when the unstable veering branched surface carries the unstable lamination associated to a depth one foliation, we can in fact pick the unstable branched surface of the dynamic pair to be the given unstable veering branched surface. Hence we have the following corollary, which recovers Mosher's base step with a little extra information:

Corollary A.15 *Let Q be the compactified mapping torus of an endperiodic map $f : L \to L$. If Q is atoroidal, then there is a dynamic pair (B^u, B^s) on Q such that:*

- *B^u is an unstable veering branched surface.*
- *B^u compatibly carries the unstable Handel–Miller lamination.*
- *The boundary train track $B^u \cap R_+$ is efficient.*

1.3 Future work

The next step of our project is to revisit Mosher's gluing step using veering branched surfaces. The basic idea is that given a sutured decomposition $Q \rightsquigarrow Q'$ and a veering branched surface B' on Q', one would like to construct a veering branched surface B on Q.

Applying such a construction to a sutured hierarchy $M = Q_0 \rightsquigarrow \cdots \rightsquigarrow Q_{n+1}$, one would get a veering branched surface on $M = Q_0$, which is dual to a veering triangulation. One could then apply [Landry 2022, Theorem A] to recover an entire face of the Thurston norm ball on M, the cone over which contains $[S]$; there is also a combinatorial Euler class associated to the triangulation that computes the norm in this cone. Alternatively, using the correspondence between veering triangulations and pseudo-Anosov flows mentioned before, one could obtain a pseudo-Anosov flow φ *without perfect fits* on M. By [Mosher 1992, Flows represent faces, page 244], one could then recover an entire face of the Thurston norm ball using φ and compute the norm in the cone over this face using φ's normal Euler class. While the Gabai–Mosher construction implies that the Thurston norm may be computed by pseudo-Anosov flows, it is a longstanding open question of Mosher whether finitely many pseudo-Anosov flows suffice.

However, there is a nontrivial obstruction to the construction of such a flow for a given hierarchy: the hierarchy must satisfy a property we refer to as *no oppositely oriented parallel orbits*, or *NOOPO* for short. Our program aims to show this is the only obstruction. We discuss this in more detail in Section 11.

1.4 Outline of paper

Sections 2, 3 and 4 deal exclusively with surfaces. In Section 2, we develop the theory of *spiraling train tracks* and *spiraling laminations*. This includes existence and uniqueness statements for splitting sequences of spiraling train tracks carrying spiraling laminations, which play a key role in Section 4. In Section 3, we give a condensed treatment of Handel–Miller theory and prove some useful lemmas. In Section 4 we construct periodic train track splitting sequences for endperiodic maps using the notion of *core splittings*. We also investigate the uniqueness of such a splitting sequence.

In Section 5, we recall the relation between endperiodic maps and depth one foliations on sutured manifolds. In Section 6, we define veering branched surfaces on sutured manifolds. We also define the dual graph and flow graph, and extend the theory of dynamic planes from [Landry et al. 2023b] to our setting. These dynamic planes play a key role in Section 8.

In Section 7, we prove Theorem 7.10 by suspending the splitting sequences constructed in Section 4. We also translate the uniqueness statements about the splitting sequence into uniqueness statements about the veering branched surfaces obtained via this construction. In Section 8, we prove Theorem 8.5. In Section 9, we prove Theorem 9.22. Given the uniqueness results in Section 7, the main task is to show that a veering branched surface as in the theorem must be "layered", ie come from the suspension of a splitting sequence of train tracks.

In Section 10, we discuss some examples of veering branched surfaces. Some examples are obtained from suspending a splitting sequence as in Section 7, while others are constructed directly and may not carry the Handel–Miller lamination associated to a depth one foliation. In Section 11, we discuss some future directions coming out of this paper, including some more details on what we anticipate for the gluing step.

In the appendix, we define dynamic pairs and prove Theorem A.14 and Corollary A.15, showing that our results imply Mosher's base step.

Notational conventions In this paper we adopt the following notational conventions:

- $X \setminus\setminus Y$ denotes the metric completion of $X \setminus Y$ with respect to the induced path metric from X. We refer to this operation as cutting X along Y. In addition, we will call the components of $X \setminus\setminus Y$ the *complementary regions* of Y in X.
- All coefficients for homology and cohomology groups are in $\mathbb{R}$ unless otherwise stated.
- A "cycle" in a directed graph refers to a *directed* cycle unless otherwise stated.

2 Train tracks and laminations

2.1 Review: train tracks, laminations and index

In this section, a surface will mean an orientable surface with (possibly empty) boundary.

Let S be a surface. A *train track* on S is an embedded graph τ in S whose vertices have degree 3 or degree 1 such that the vertices of degree 1 are mapped to ∂S, the edges are C^1 embedded, every point in τ has a well-defined tangent space, and at each vertex of degree 3 there are two edges tangent to one side and one edge tangent to the other side. The vertices of degree 3 are called *switches*, the vertices of degree 1 are called *stops*, and the edges are called *branches*.

We define a vector field on the set of switches and stops of τ by requiring that it points into the side of the tangent space meeting only one end of a branch at each switch, and that it points out of the surface at each stop. This is called the *maw vector field*. If b is a noncircular branch such that the maw vector field points into b at both its ends, we say b is *large*. If the maw vector field points out of b at both ends, b is *small*. Otherwise, b is *mixed*.

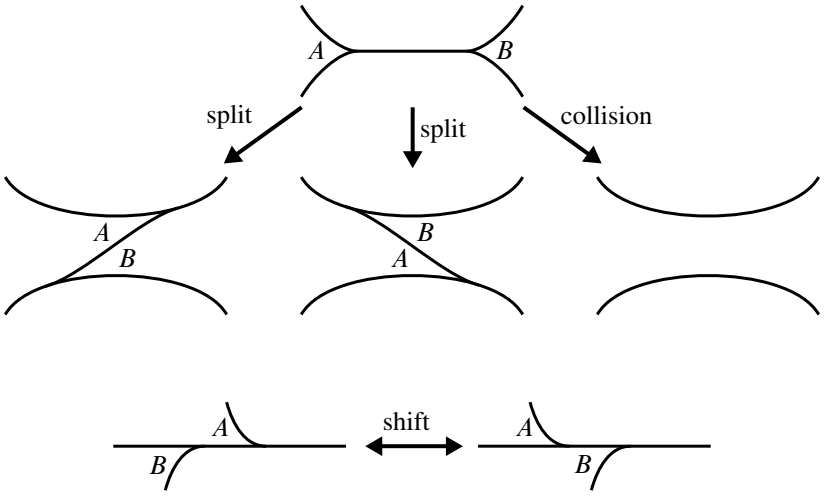

Figure 1: Illustration of split, collision, shift.

A *lamination* Λ on a surface S is a partition of a closed subset of S into connected 1-manifolds such that each point x on S has a neighborhood $\mathbb{R}\times\mathbb{R}$ with elements of the partition intersecting the neighborhood of the form $\mathbb{R}\times C$ (if x is in the interior of S) or a neighborhood $[0,\infty)\times\mathbb{R}$ with elements of the partition intersecting the neighborhood in sets of the form $[0,\infty)\times C$ for some closed set C (if x is on the boundary of S). The elements of the partition are called the *leaves* of Λ. We will often conflate a lamination with the union of its leaves.

Let τ be a train track in S and let Λ be a lamination on S. A *standard neighborhood* of τ is a closed regular neighborhood N of τ which is foliated by line segments, called *ties*, such that each line segment meets the branches of τ transversely. By collapsing the ties, we get a projection map $N\to\tau$. We say that τ *carries* Λ if τ has a standard neighborhood N such that Λ is embedded in N in such a way that its leaves are transverse to the ties. In this case we say that the map $\Lambda\hookrightarrow N\to\tau$ is the *carrying map* and we say that N is a *standard neighborhood* of Λ. Further, we say that τ *fully carries* Λ if the carrying map is onto, ie Λ intersects every tie of N.

There are a few standard local operations on train tracks which are described below and pictured in Figure 1. Let b be a branch of τ that meets two switches A and B of τ at its ends.

- **Split** If b is a large branch, then a split alters a small neighborhood of b by either pushing A and B past each other, or resolving A and B as shown. The latter type of split is also called a *collision*. Including collisions, there are three types of splits that can be performed on b up to isotopy.
- **Fold** A fold is the inverse of a split.
- **Shift** If b is mixed, then a shift moves A and B past each other.

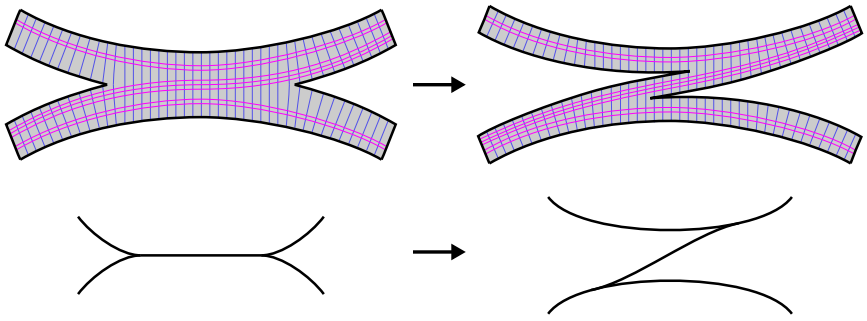

Figure 2: An example of a Λ-split. Note that collisions are also possible.

Note that in our descriptions of these moves we are implicitly making use of a natural identification between the switches of a train track before and after all moves except collisions and their inverses. We will use this identification in the future. In practice our train tracks will carry laminations, and the data of the laminations will control which types of splits we perform.

Let τ be a train track, with standard neighborhood N. A *train route* is a sequence of branches of τ traversed by a C^1-immersed copy of $\mathbb{R}$, $[0,\infty)$ or $[0,1]$. Any curve immersed in N transverse to the ties of T naturally determines a train route. If the sequences associated to two such curves γ, γ' are equal, or if one is a subsequence of the other, we say that γ and γ' *fellow travel* in N. When there is no danger of confusion, we may say that γ and γ' fellow travel in τ. If the sequences associated to γ, γ' are *eventually* equal, we say they *eventually fellow travel*.

If τ is a train track fully carrying a lamination Λ, any large branch of τ can be split in a unique way such that the splitting also fully carries Λ. We call this a Λ-*split*; see Figure 2. Any switch of τ naturally determines a train route, which may be finite or infinite, as follows. Let c be a switch of τ, let I be the tie through c in a standard neighborhood of τ, and let p_1, p_2 be the two endpoints of the component of $I \setminus\setminus \Lambda$ containing c. Let ρ_1 and ρ_2 be the train routes determined by rays in Λ-leaves starting at p_1, p_2, respectively, and traveling in the direction determined by the maw vector field at c. If ρ_1 and ρ_2 are

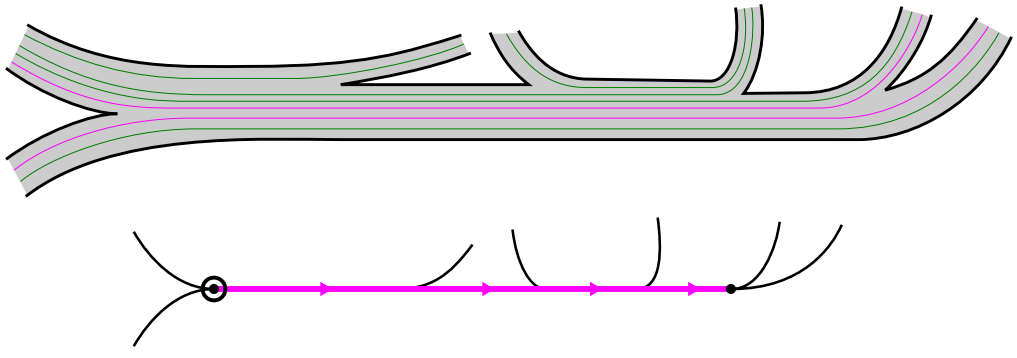

Figure 3: If the train track on the bottom carries Λ as shown on the top, the Λ-route from the circled cusp is the pink segment.

Figure 4: The cusped bigon, the 1-cusped triangle and the rectangle are among the surfaces with cusps and corners that have index 0. Note that if these arise as complementary regions of a train track on S, the unique side of a 1-cusped triangle not incident to a cusp must lie along ∂S, and that any rectangle has two nonadjacent sides lying along ∂S.

equal, define $\rho_c := \rho_1 = \rho_2$. Otherwise, define ρ_c to be the longest route which is an initial subroute of ρ_1 and ρ_2. See Figure 3. We call ρ_c the Λ-*route of* c.

More generally, a Λ-*route* is any train route determined by a parametrization of a part of a leaf of Λ. The *length* of a train route is the number of branches the route traverses counted with multiplicity.

Definition 2.1 (cusps, corners) A *surface with cusps and corners* is a surface S along with the data of two disjoint finite sets of points on ∂S, called *cusps* and *corners*. The motivation for considering surfaces with cusps and corners comes from considering a complementary region C of a train track on a surface, where we take the set of the cusps to be the nonsmooth points of ∂C corresponding to switches, and the set of corners to be the nonsmooth points corresponding to stops. Henceforth we will consider complementary regions of train tracks to be surfaces with cusps and corners in this way, unless specified otherwise. Since the switches of a train track are natural bijection with the cusps of its complementary regions, we will sometimes conflate the two objects. ◁

Definition 2.2 (index of a surface with corners and cusps) The *index* of a compact surface with cusps and corners S is defined to be

$$\operatorname{index}(S) = \chi^{\mathrm{top}}(S) - \tfrac{1}{2}\#\text{cusps} - \tfrac{1}{4}\#\text{corners},$$

where χ^{top} denotes the Euler characteristic of the underlying topological surface. ◁

For example, the (orientable) surfaces with cusps and corners that have index 0 are exactly tori, annuli, *cusped bigons*, 1-*cusped triangles* and *rectangles*. See Figure 4 for an illustration of the last three.

Another common surface with cusps and corners is the *bigon*, which is a topological disk with two corners in its boundary and has index $\frac{1}{2}$.

Notice that the index is additive, that is, if τ is a train track on a surface S, then $\operatorname{index}(S) = \operatorname{index}(S \setminus\setminus \tau)$.

Definition 2.3 (index of complementary regions of a lamination) The complementary regions of a lamination on a compact surface are noncompact surfaces with boundary, but here the noncompactness can be cut off. Precisely, for such a complementary region C, there exists a finite collection of arcs that

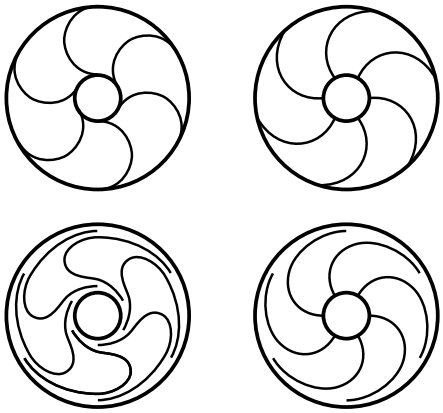

Reeb annulus half Reeb annulus

Figure 5: Reeb and half-Reeb annuli.

cut C up into a union $K \cup V_1 \cup \cdots \cup V_n$ such that K is a surface with corners and each $V_i \cong [0,\infty)\times[0,1]$. See for example [Candel and Conlon 2000, Section 5.2]. We define the *index* of C to be the index of K.

Alternatively, one can complete C by adding a point at infinity for each of its ends, and treating the completion $\overline{C}$ as a surface with cusps and corners by taking the added points as cusps. Then the index of C will be equal to the index of $\overline{C}$. ◁

Definition 2.4 (Reeb annuli) Let S be a surface. Let A be a subsurface of S that is homeomorphic to an annulus. We say that A is *carried* by a train track τ on S if ∂A is smoothly embedded along τ. We say that A is a *Reeb annulus* if $A \cap \tau$ is the union of ∂A and a nonempty collection of arcs with endpoints attached onto both components of ∂A along a consistent direction. (The arcs need not be disjoint from one another.) Similarly, we say that an annulus $A \subset S$ is a *half-Reeb annulus* if one component l_1 of ∂A is smoothly embedded along τ while the other component l_2 lies along ∂S, and if $A \cap \tau$ is the union of l_1 and a nonempty collection of arcs with one endpoint attached onto l_1 along a consistent direction and with the other endpoint on l_2. (Here, again, the arcs need not be mutually disjoint.) See Figure 5, top row.

Similarly, we say that A is carried by a lamination Λ on S if ∂A is smoothly embedded along Λ. We say that A is a *Reeb annulus* if $A \cap \Lambda$ is the union of ∂A and a nonempty collection of noncompact leaves with ends spiraling onto both components of ∂A along a consistent direction. Similarly, we say that an annulus $A \subset S$ is a *half-Reeb annulus* if one component l_1 of ∂A is smoothly embedded along Λ while the other component l_2 lies along ∂S, and if $A \cap \Lambda$ is the union of l_1 and a nonempty collection of noncompact leaves with an end spiraling onto l_1 along a consistent direction and with an endpoint on l_2. See Figure 5, bottom row. ◁

There are various definitions of "nice" train tracks in the literature. In this paper, it is convenient for us to make the following two definitions.

Definition 2.5 (good train tracks and laminations) A train track τ on S is *good* if all of its complementary regions have nonpositive index, except possibly for bigons, and if it has neither Reeb annuli nor half-Reeb annuli.

A lamination Λ on S is *good* if all of its complementary regions have nonpositive index, except possibly for bigons, and if has neither Reeb annuli nor half-Reeb annuli. ◁

Definition 2.6 (efficient train tracks) A train track τ is *efficient* if it is good, has no complementary regions that are cusped bigons, and does not carry an annulus. ◁

The motivation for the above terminology is the fact that a curve or a properly embedded arc can be carried by an efficient train track in at most one way, up to homotopy (rel endpoints).

Remark 2.7 In particular, an efficient train track can have only two types of index 0 complementary regions: rectangles and 1-cusped triangles. See Figure 4. ◁

2.2 Spiraling train tracks and laminations

In this paper we will encounter two special types of laminations on compact surfaces:

(i) laminations such that each end of a noncompact leaf limits on one of finitely many closed leaves, and

(ii) laminations on surfaces with boundary for which all leaves are properly embedded compact intervals.

These two types of laminations share many important properties, so we will consider them to be in the same class of "spiraling laminations" (see Definition 2.12).

Beyond this paper, spiraling laminations will also be important in our future work described in the introduction.

Definition 2.8 (source orientation) A *source orientation* on a 1-manifold (possibly with boundary) l is a choice of points $p_1, \dots, p_k$ and an orientation on each component of $l \setminus \{p_1, \dots, p_k\}$ which points away from $p_1, \dots, p_k$. The points $p_1, \dots, p_k$ are called the *sources*. ◁

Definition 2.9 (spiraling train tracks) Let τ be a good train track, and let V be a continuous vector field tangent to τ. We say (τ, V) is *spiraling* if V restricts to the maw vector field on the set of switches and stops, and induces a source orientation on each branch of τ. ◁

Lemma 2.10 *Let τ be a good train track. Then τ has no large branches if and only if there exists a vector field V on τ such that (τ, V) is spiraling.*

Proof If τ has no large branches, we can define a vector field V as follows. For each branch b which is not a circle, we can extend the maw vector field on its endpoints to a vector field on b which has at most one singularity. Since τ has no large branches, a singularity arises only when the maw vector field points

out of b at each endpoint, in which case the singularity will be a source. For each circular branch, we may choose any nonsingular vector field on that branch. This vector field makes τ a spiraling train track.

Conversely, suppose τ has a large branch b. If V is a vector field on τ extending the maw vector field, then the vector field $V|_b$ points into b at both endpoints and therefore cannot induce a source orientation on b. It follows that there is no vector field making τ spiraling. □

Definition 2.11 Let (τ, V) be a spiraling train track. Notice that the forward trajectory of any point x in τ under V is well defined (possibly) up to the point where it exits the surface through a stop. If x is not a singularity of V and its forward trajectory does not exit the surface, then the trajectory is an infinite ray carried by τ, with limit set equal to a circle carried by τ, the circle being oriented by V. The *sink* of (τ, V) is defined to be the union of the stops of τ and the oriented circles which are the limit sets of the infinite forward trajectories. ◁

Our choice of the term "spiraling" is motivated by the case when τ has no stops, where any ray smoothly immersed in τ eventually periodically traverses a loop in the sink. If a spiraling track τ has stops, then this particular behavior is not necessarily present, but we will see in Section 2.3 that other important properties remain.

Definition 2.12 (spiraling laminations) A good lamination Λ is said to be *spiraling* if:

(1) There are finitely many closed leaves $\ell_1, \dots, \ell_k$ in Λ, each with a fixed orientation.

(2) For all noncompact $\ell \subset \Lambda$, if $\gamma\colon [0, \infty) \to \ell$ is a proper embedding then γ spirals onto some ℓ_i in the direction specified by the orientation of ℓ_i. ◁

It may be useful to think of these as "depth ≤ 1 laminations" in analogy with finite-depth foliations.

The following shows that spiraling laminations naturally decompose into sets of two types, which we define after stating the result.

Proposition 2.13 *Let S be a compact surface and Λ a spiraling lamination on S. Then Λ can be decomposed into a finite union of sets each of which is*

(1) *a good lamination restricted to a (possibly degenerate) annulus carried by Λ, or*

(2) *a pocket of noncircular leaves.*

We have defined an annulus carried by Λ in Definition 2.4. A *degenerate annulus* carried by Λ is just a circular leaf of Λ. A *pocket* of noncircular leaves is a subset $\Lambda' \subset \Lambda$ such that there exists a (not necessarily proper) embedding $R \times [0, 1] \to S$, where R is equal to either $\mathbb{R}$, $[0, \infty)$ or $[0, 1]$, and a closed $C \subset [0, 1]$ such that $R \times C$ maps injectively onto Λ'.

Proof Consider the family F of closed curves in S that comprises the closed leaves of Λ. A maximal collection of these curves in the same isotopy class must be contained in a (possibly degenerate) annulus carried by Λ.

All remaining leaves of Λ are either compact or spiral onto compact leaves. Since S is compact, there can only be finitely many proper homotopy classes of these leaves. Taking maximal collections of properly homotopic leaves, we obtain finitely many pockets. □

Definition 2.14 (consistent lamination) A spiraling lamination Λ is *consistent* if no two (oriented) closed leaves cobound an annulus. ◁

Equivalently, a spiraling lamination Λ is consistent if, whenever Λ carries an annulus A, $\Lambda \cap A$ is a disjoint union of parallel closed leaves.

In this paper, we will be concerned with efficient spiraling train tracks carrying consistent spiraling laminations. Observe that if a train track with no large branches carries a consistent spiraling lamination, there is an (essentially) unique vector field making it into a spiraling train track, so that the spiraling of forward trajectories is compatible with the orientations of the closed leaves of the lamination. We will thus freely refer to such train tracks as spiraling train tracks.

In Lemma 2.16 below, we show that any consistent spiraling lamination is carried by an efficient spiraling train track. In Section 2.3, we will see that an efficient train track carrying a consistent spiraling lamination can be split into a spiraling train track in an essentially unique way.

We make an observation which we will use repeatedly for the rest of this paper. Suppose τ is an efficient spiraling train track fully carrying a consistent spiraling lamination Λ. The image of each closed leaf of Λ in τ under the carrying map is embedded. Also the images of parallel leaves coincide, while the images of nonparallel leaves are disjoint. Hence, if we let $[\lambda_1], \dots, [\lambda_k]$ be the parallel classes of the closed leaves of Λ, each $[\lambda_i]$ will correspond to some circular component of the sink of τ. Conversely, a circular component of the sink of τ must carry some closed leaf of Λ. Hence there is a natural one-to-one correspondence between the parallel classes of the closed leaves of Λ and the circular components of the sink of τ.

Working toward Lemma 2.16, we make the following definition:

Definition 2.15 We say that a finite collection of points $\{x_i\}$ on ∂S *carries* $\Lambda \cap \partial S$ if there exists a closed regular neighborhood N of $\{x_i\}$ on ∂S such that $\Lambda \cap \partial S \subset N$. In this case we say that the map $\Lambda \cap \partial S \hookrightarrow N \to \{x_i\}$ is the *carrying map*. Further, we say that $\{x_i\}$ fully carries $\Lambda \cap \partial S$ if the carrying map is surjective. ◁

Lemma 2.16 *Let Λ be a consistent spiraling lamination. Let $\{x_i\}$ be a finite collection of points on ∂S fully carrying $\Lambda \cap \partial S$, with carrying map $\rho\colon \Lambda \cap \partial S \to \{x_i\}$. Then there exists an efficient spiraling train track τ with the set of stops equal to $\{x_i\}$ such that τ fully carries Λ and the restriction of the carrying map $\Lambda \to \tau$ extends ρ on the boundary.*

Proof Let Λ be a spiraling lamination. We construct a spiraling train track (τ, V) according to Proposition 2.13 in the following way.

From each parallel class of closed leaves of Λ, take one closed leaf to be part of τ with a nonsingular vector field defining its orientation as in Definition 2.12(1). This uses the consistency of Λ.

By subdivision of pockets, we can assume that each end of a pocket spirals around some closed leaf of Λ or is mapped to a single point in the finite collection $\{x_i\}$ by the carrying map, and that each pocket is maximal with respect to this property. For each pocket, we add a branch between the corresponding closed leaves and/or boundary points. When attaching a branch to one of the closed leaves, we smooth so that the branching is compatible with the orientation.

Finally, we slightly zip up the branches at the stops and perturb so that switches are trivalent to get the desired spiraling train track. □

2.3 Splitting train tracks carrying spiraling laminations

For this subsection Λ will denote a consistent spiraling lamination, S a compact surface, and τ a train track fully carrying Λ.

We say a cusp c of τ is *persistent* if the maximal Λ-route from c does not terminate in $\operatorname{int}(S)$, and denote the set of persistent cusps of τ by $\operatorname{pers}(\tau)$.

Let $\lambda_1, \dots, \lambda_k$ be the closed leaves of Λ. Each λ_i determines a bi-infinite periodic train route. If the maximal Λ-route from a cusp c fellow travels λ_i in τ, then we call c a *graft point* for λ_i. We let $\operatorname{graft}(\lambda_i)$ be the (finite) set of graft points of λ_i and circularly order this set according to the order in which λ_i meets the cusps.

If the maximal Λ-route from a cusp c *eventually* fellow travels λ_i, we define the *reduced Λ-route* for c to be the initial segment before its maximal Λ-route fellow travels λ_i. If c is a graft point, then by convention the reduced Λ-route for c is just the constant path c.

If instead the maximal Λ-route from a cusp c terminates at a stop, we define the *reduced Λ-route* for c to be the same as its maximal Λ-route.

We define a partial order $\preceq$ on the set $\operatorname{pers}(\tau)$ as follows. If c_1 and c_2 are two persistent cusps with reduced Λ-routes ρ_{c_1} and ρ_{c_2}, then $c_2 \succeq c_1$ if and only if ρ_{c_2} is a concatenation

$$\rho_{c_2} = \gamma * \rho_{c_1},$$

where γ is some initial train route. See Figure 6.

Suppose τ and τ' are train tracks carrying Λ. If there is a poset isomorphism $\operatorname{pers}(\tau) \to \operatorname{pers}(\tau')$ which also respects the circular orders on $\operatorname{graft}(l_i)$ for each i, then we say that the map $\operatorname{pers}(\tau) \to \operatorname{pers}(\tau')$ is *order-preserving*.

Lemma 2.17 *Any Λ-split is order-preserving. More precisely, if τ carries a spiraling lamination Λ and τ' is obtained from τ by a Λ-split, then the natural identification $\operatorname{pers}(\tau) \to \operatorname{pers}(\tau')$ is order-preserving.*

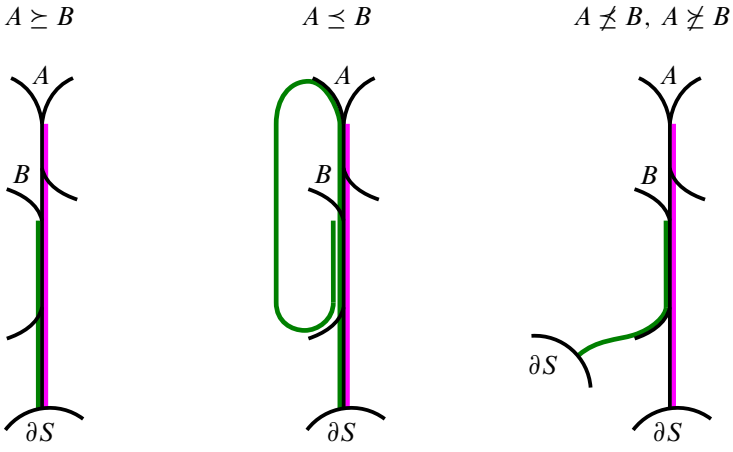

Figure 6: The pink lines represent the Λ-route from A, and the green lines represent possible Λ-routes from B.

Proof Suppose that τ' is obtained by performing a Λ-split on a branch of τ. Let $\widetilde{S}$ be the universal cover of S, and let $\widetilde{\Lambda}$ and $\tilde{\tau}$ be the lifts of Λ and τ to $\widetilde{S}$.

First we explain why the property of being a graft point is preserved by a Λ-split, as is the circular order on the graft points of any circular leaf of Λ. If γ is a closed loop in τ following the same route as a closed leaf λ_i, let $\tilde{\gamma}$ be a lift to $\widetilde{S}$. By the argument in [Penner and Harer 1992, Corollary 1.1.2], $\tilde{\tau}$ is a tree, so $\tilde{\gamma}$ is an oriented line embedded in $\tilde{\tau}$. Let $\widetilde{\text{graft}(\lambda_i)}$ be the set of lifts of points in $\text{graft}(\lambda_i)$ lying on $\tilde{\gamma}$. The orientation of $\tilde{\gamma}$ induces a linear order $\widetilde{\text{graft}(\lambda_i)}$. Any Λ-split on τ lifts to infinitely many disjoint $\widetilde{\Lambda}$-splits, and each point of $\widetilde{\text{graft}(\lambda_i)}$ is involved in at most one of these splits. It is easy to see that no finite collection of splits can reverse the linear order of any two points in $\widetilde{\text{graft}(\lambda_i)}$, or remove any point in $\widetilde{\text{graft}(\lambda_i)}$ from $\tilde{\gamma}$. It follows that any Λ-split of τ preserves graft points and the circular order on $\text{graft}(\lambda_i)$ for each circular leaf λ_i.

Next, let A and B be persistent cusps of τ, and suppose that $A \succeq B$. Hence, if γ_A and γ_B are the reduced Λ-routes from A and B, respectively, we have

$$\rho_A = \gamma * \rho_B$$

for some initial train route γ. Let C be the terminal point of ρ_A and ρ_B. As above, a lift of ρ_A to the universal cover $\widetilde{S}$ is embedded. This makes it clear that no Λ-split can reverse the order of A and B. The same ideas show that any fold on τ' preserves the relation $A \succeq B$. Since any Λ-split can be reversed by a fold, this shows that $A \succeq B$ in $\text{pers}(\tau)$ if and only if $A \succeq B$ in $\text{pers}(\tau')$. □

We will show in Lemma 2.20 that a train track fully carrying a spiraling lamination can be Λ-split to a spiraling train track. To do so, we need a measure of complexity that decreases after each Λ-split. To this end we introduce the following definition:

Definition 2.18 If A and B are cusps of τ, a *large Λ-biroute* connecting A and B is a train route γ in τ from A to B such that

- the maw vector field points into γ at both A and B, and
- γ is an initial subroute of the Λ-route from A, and the reverse of γ is an initial subroute of the Λ-route from B.

We consider two large Λ-biroutes to be the same if they differ by reversing orientation. ◁

Lemma 2.19 *Let Λ be a consistent spiraling lamination. Suppose τ is a train track fully carrying Λ. Then the number of large Λ-biroutes is finite.*

Proof Fix a cusp A of τ. It is enough to show that there are finitely many large Λ-biroutes with an endpoint on A.

Since Λ is spiraling, the Λ-route ρ_A from A either has finite length or eventually periodically traverses a closed oriented route in τ. If ρ_A has finite length, it is clear there are only finitely many large Λ-biroutes ending at A.

If ρ_A eventually fellow travels a closed route ρ in τ, then there are at most finitely many large Λ-biroutes connecting A to any cusp not lying along ρ. If B is any cusp on the closed route ρ such that there is a large Λ-biroute connecting A and B, then the maw vector field at B points against the orientation of ρ. Since Λ is consistent, there cannot a closed leaf of Λ traversing ρ in the opposite direction, so the Λ-route ρ_B from such a cusp B can traverse ρ at most finitely many times before leaving ρ. In particular, there are only finitely many initial subroutes of ρ_A which are initial subroutes of ρ_B when reversed, so there are only finitely many large Λ-biroutes connecting A and B. □

Lemma 2.20 *Let Λ be a consistent spiraling lamination. Suppose τ is a train track fully carrying Λ. Then any sequence of Λ-splits $\tau = \tau_0 \to \tau_1 \to \tau_2 \to \cdots$ must terminate in a spiraling train track. In particular, there exists a sequence of Λ-splits $\tau = \tau_0 \to \cdots \to \tau_n$ such that τ_n is spiraling.*

Proof Let $\mathrm{BR}(\tau)$ be the set of large Λ-biroutes of τ. By Lemma 2.19, $\#\mathrm{BR}(\tau) < \infty$. It is clear that $\mathrm{BR}(\tau)$ is nonempty if and only if τ has large branches. Let b be a large branch of τ, and τ' be the track obtained by performing a Λ-split on b. Note that b itself is an element of $\mathrm{BR}(\tau)$, and there is a natural bijection

$$\sigma\colon (\mathrm{BR}(\tau) - \{b\}) \to \mathrm{BR}(\tau').$$

(See Figure 7 for a visual description of σ and σ^{-1}.) Hence a Λ-split decreases the number of large Λ-biroutes by one, so any sequence of Λ-splits must terminate in a train track with no large Λ-biroutes, ie one with no large branches. □

A splitting sequence $\tau_0 \to \cdots \to \tau_n$ where τ_n has no large branches, as in Lemma 2.20, is said to be a *maximal splitting sequence* for τ_0. The train track τ_n is a *maximal splitting* of τ_0. It turns out that a maximal splitting is unique up to isotopy, and a maximal splitting sequence is unique up to a natural equivalence.

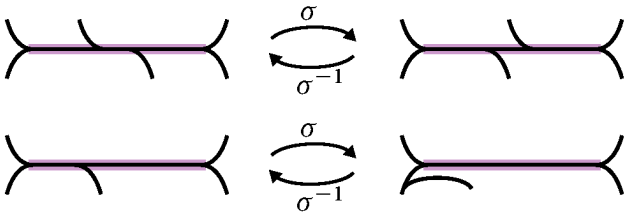

Figure 7: If τ' is obtained by Λ-splitting a branch b, then there is a bijection $\sigma\colon \mathrm{BR}(\tau)-\{b\}\to \mathrm{BR}(\tau)$. Highlighted in purple are Λ-biroutes before (left) and after (right) a Λ-split.

If b_1 and b_2 are disjoint large branches of τ, then the moves splitting b_1 and b_2 commute with each other, and we call the operation of swapping their order a *commutation*.

Lemma 2.21 *If τ is a train track fully carrying a consistent spiraling lamination Λ, then any two maximal splitting sequences for τ are related by commutations. In particular, any two maximal splitting sequences have the same length and end in the same train track.*

Proof Let the two splitting sequences be $\tau=\tau_0\to\cdots\to\tau_k$ and $\tau=\tau_0'\to\cdots\to\tau_{k'}'$. We induct on $\max\{k,k'\}$. When $\max\{k,k'\}=0$, the statement is clear.

Suppose branch b is split in $\tau_0\to\tau_1$. Locate the term in the other splitting sequence where b is split. The terms before that are performed on branches disjoint from b, so we can move the splitting of b to the beginning of the sequence via commutations, then apply the inductive hypothesis to τ_1. □

Definition 2.22 (Λ-compatible) Let Λ be a consistent spiraling lamination, and let τ be an efficient train track carrying Λ. Each complementary region C of Λ is a surface with boundary, possibly noncompact. Its boundary ∂C can be decomposed into $\partial_v C$, which lies along ∂S, and $\partial_h C$, which lies along leaves of Λ. We say that a component of $\partial_v C$ is *associated* to a stop v of τ if both of its endpoints are mapped by the carrying map into v. Note that not every component of $\partial_v C$ need be associated to a stop; see Figure 8.

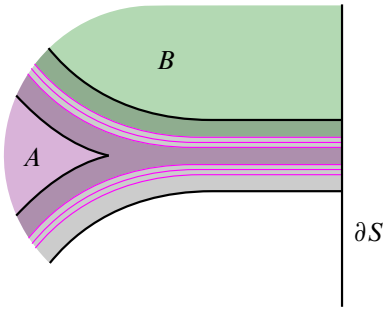

Figure 8: A standard neighborhood (gray) of the pink lamination, and two shaded complementary regions A and B. There is a component of $\partial_v A$ which is associated to the stop obtained by collapsing the standard neighborhood, while the component of $\partial_v B$ shown lying on ∂S is not associated to a stop.

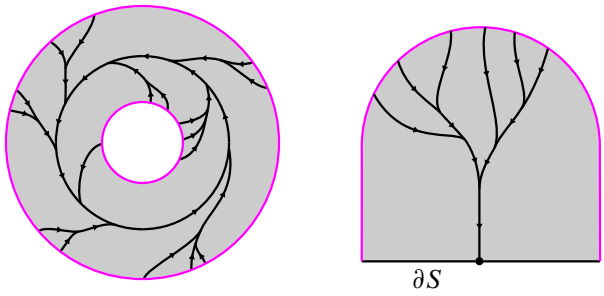

Figure 9: Picture from the proof of Lemma 2.24.

If τ' is another efficient train track carrying Λ, then we say τ and τ' are Λ-*compatible* if the set of stops of τ equals the set of stops of τ', and for each complementary region of Λ, a component of $\partial_v C$ is associated to a stop of τ if and only if it is associated to the same stop of τ'. ◁

Note that if $\partial S = \varnothing$, then the Λ-compatibility condition is vacuous.

Definition 2.23 (Λ-identification) Suppose τ_1 and τ_2 are Λ-compatible. Each complementary region T of τ_i corresponds to a complementary region C of Λ. Since τ_i is efficient, either C has negative index, or some component of $\partial_v C$ is not associated to any stop. Each persistent cusp of τ_i in T corresponds to an end of C or a component of $\partial_v C$ that is associated to a stop of τ_i. Conversely, if C is a complementary region of Λ of negative index or has some component of $\partial_v C$ not associated to a stop of τ_i, then each end of C and each component of $\partial_v C$ that is associated to a stop of τ_i corresponds to some persistent cusp of τ_i. From this, we get a natural identification between $\operatorname{pers}(\tau_1)$ and $\operatorname{pers}(\tau_2)$, which we call the Λ-*identification*. ◁

Lemma 2.24 *Let Λ be a consistent spiraling lamination on S and let τ_1 and τ_2 be two efficient spiraling train tracks fully carrying Λ.*

(a) *If τ_1 and τ_2 are Λ-compatible, then, up to isotopy, they are related by a collection of shifts.*

(b) *If the Λ-identification between their cusps preserves orders, then, up to isotopy, τ_1 and τ_2 are related by Dehn twists around curves isotopic to closed leaves of Λ. The effect of these Dehn twists can be achieved by shifts along the circular components of $\operatorname{sink}(\tau_i)$.*

Proof Since τ_1 and τ_2 are Λ-compatible spiraling train tracks carrying Λ, there is a natural identification of their sinks (recall that the sink of τ_i is a collection of circles and stops).

Let N be the closure of a small neighborhood of the sink of τ_1 and τ_2. Thus N is a collection of annuli and disks, where each disk has two corners and has half of its boundary on ∂S and half of its boundary in $\operatorname{int}(S)$. See Figure 9. Let $S' = S \setminus\setminus N$.

By initial isotopies, we can arrange that all switches of τ_1 and τ_2 lie in N.

We observe that S' is a surface with boundary, and that $N \cap S'$ is a collection of intervals and circles contained in $\partial S'$. Each leaf of the lamination $\Lambda \cap S'$ is a properly embedded interval, both of whose endpoints lie in a component of $N \cap S'$.

Let $i = 1$ or 2. Each component of the train track $\tau_i \cap S'$ is also a properly embedded segment with endpoints in $N \cap S'$. Note that $\tau_i \cap S'$ has no components which are isotopic rel ∂N. If such components existed, there would be a rectangle R with cyclically ordered edges a, b, c, d such that $a, c \subset \tau_i$ and $b, d \subset S' \cap N$. See Figure 10. Since Λ is spiraling, this would give rise to a cusped bigon complementary region of τ_i, contradicting efficiency. It follows that the branches of $\tau_i \cap S'$ are in one-to-one correspondence with the isotopy classes rel $S' \cap N$ of the leaves of $\Lambda \cap S'$. Fix such an isotopy class P. The leaves of P lie in a closed rectangle R_P with two opposite sides on $S' \cap N$, and two opposite sides formed by leaves in P. Up to isotopy, we can assume that the corresponding component of $\tau_i \cap S'$ lies inside R_P. Hence we can perform an isotopy of S supported in a neighborhood of Λ so that $\tau_1 \cap S' = \tau_2 \cap S'$.

Now we turn our attention to $\tau_1 \cap N$ and $\tau_2 \cap N$.

Let C be a disk component of N. Then $\tau_1 \cap C$ and $\tau_2 \cap C$ are both tracks with no large branches whose sets of stops are equal. Their cusps are also identified via the Λ-identification; we will call these cusps $c_1, \dots, c_n$. There is a distinguished stop $v \in \partial C$ such that the Λ-route from each c_j ends at v. It is not hard to show that $\tau_1 \cap C$ and $\tau_2 \cap C$ are related by shifts and isotopy rel boundary; we will do so by showing that each τ_i can be shifted to obtain the same track.

Each c_j is associated to a complementary region R_j of $\Lambda \cap C$ that has a vertical component associated to the stop v. If we choose an orientation of ∂C, we may assume, up to relabeling, that the vertical components of $R_1, \dots, R_n$ move from left to right in a small neighborhood of v. By performing shifts on each $\tau_i \cap C$, we can arrange that $c_1 \preceq c_2 \preceq \cdots \preceq c_n$. See Figure 11. We conclude that $\tau_1 \cap C$ and $\tau_2 \cap C$ are related by shifts.

If the Λ-identification between the cusps of τ_1 and τ_2 preserves orders, then an induction on the number of cusps of $\tau_1 \cap C$ and $\tau_2 \cap C$ shows that the two tracks are isotopic rel stops; that is, no shifts are necessary above.

Next, suppose that A is an annulus component of N containing a circular sink component ℓ. For $i = 1, 2$, we perform shifts on τ_i to obtain a track τ_i' whose only cusps lie on ℓ. We then perform shifts and isotopy on τ_1' and τ_2', obtaining new tracks τ_1'' and τ_2'' such that the circular order on the cusps of τ_1'' and τ_2'' is the same. A further isotopy can arrange so that the sinks and corresponding cusps of τ_1'' and τ_2'' agree as points in A. At this point, τ_1'' and τ_2'' differ only by the application of some number of Dehn twists around curves parallel to ℓ. The effect of applying these Dehn twists can be achieved by shifts and isotopy. We have completed the proof of (a).

Next we suppose that the Λ-identification between the cusps of τ_1 and τ_2 preserves orders. We assume that we have already isotoped τ_1 and τ_2 so that all their cusps lie in N and so that they agree outside N. In

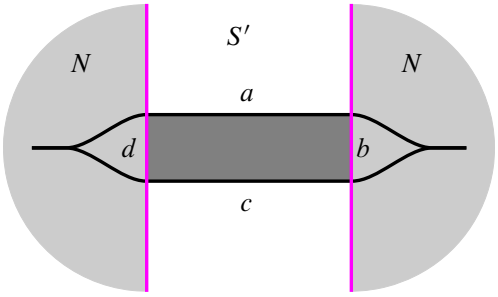

Figure 10: Components of $\tau_i \cap S'$ which are isotopic in S' rel $S' \cap N$ force the existence of cusped bigon complementary components of τ_i for $i = 1, 2$.

a disk component C of N, we have already observed in the proof of (a) that the partial order $\preceq$ determines each $\tau_i \cap C$ up to isotopy rel stops. Hence we need consider only the annulus components of N.

Now let A be an annulus component of N containing a circular sink ℓ. Up to isotopy, we can assume that $\tau_1 \cap A$ and $\tau_2 \cap A$ agree on the circular sink ℓ. Since the Λ-identification preserves orders and the graft points are minimal in the partial order, τ_1 and τ_2 have the same collection of graft points along ℓ. Let v be one of these graft points, and let τ_i^v be the component of $(\tau_i \cap A) \setminus\setminus v$ not containing ℓ. Since the Λ-identification preserves orders and τ_1^v, τ_2^v have the same sets of stops, we see that (up to isotopy rel stops) they can differ only in how many times they wrap around A. Applying this analysis to each cusp along ℓ gives that $\tau_1 \cap A$ and $\tau_2 \cap A$ can only differ by isotopy and by twisting around a curve parallel to ℓ. The twisting can clearly be achieved by performing shift moves involving branches incident to ℓ. □

When restricted to a subclass of spiraling laminations called I-laminations, this lemma yields the important Corollary 2.26, which will play a role later. We first define I-laminations.

Definition 2.25 (I-laminations) Let K be a compact surface with boundary. An *I-lamination* is a lamination in which every leaf is a compact, properly embedded arc in K. ◁

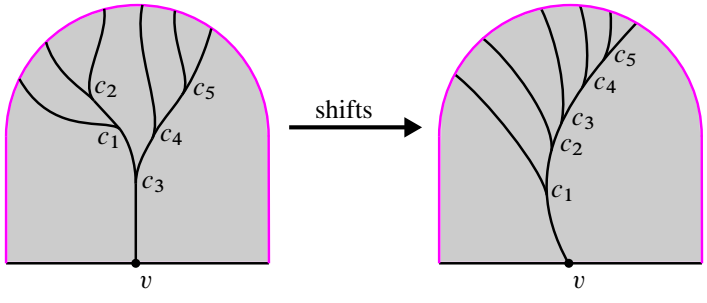

Figure 11: When C is a disk, we can shift both $\tau_1 \cap C$ and $\tau_2 \cap C$ so that, for example, $c_1 \preceq \cdots \preceq c_n$. Hence the two tracks differ by shifts and isotopy rel stops.

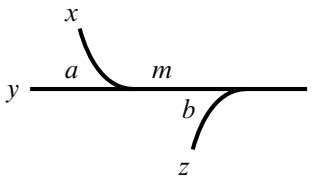

Figure 12: Notation from the definition of divergent neighbors and the proof of Corollary 2.26.

Notice that every I-lamination is spiraling: condition (2) in Definition 2.12 concerning noncompact leaves is vacuous. Furthermore, any I-lamination is consistent since it does not carry any annuli.

Let τ be a train track fully carrying an I-lamination λ, and suppose a and b are cusps of τ at two ends of a mixed branch m as shown in Figure 12. We say that a and b are *divergent neighbors* if either a or b is nonpersistent, or if both a and b are persistent and $\rho_a \neq m * \rho_b$, where, as in Section 2.3, ρ_c denotes the maximal Λ-route from a cusp c. If a and b are divergent neighbors, then we call the shift along m a *shift of divergent neighbors*.

Corollary 2.26 *Let S be a compact surface, Λ an I-lamination in S, and σ, τ two Λ-compatible efficient train tracks which fully carry Λ.*

Let σ' and τ' be maximal splittings of σ and τ, respectively. Then σ' and τ' are isotopic rel stops if and only if the Λ-identification $\operatorname{pers}(\sigma) \to \operatorname{pers}(\tau)$ is an isomorphism of partially ordered sets.

Furthermore, if σ and τ differ by a sequence of shifts of divergent neighbors, then σ' and τ' are isotopic rel stops.

Proof By Lemma 2.17, the natural identifications of $\operatorname{pers}(\sigma)$ with $\operatorname{pers}(\sigma')$ and of $\operatorname{pers}(\tau)$ with $\operatorname{pers}(\tau')$ are poset isomorphisms. If σ' and τ' are isotopic, then the Λ-identification $\operatorname{pers}(\sigma') \cong \operatorname{pers}(\tau')$ is a poset isomorphism, and thus the Λ-identification $c\colon \operatorname{pers}(\sigma) \to \operatorname{pers}(\tau)$, being a composition of these identifications, is a poset isomorphism.

Conversely, if the Λ-identification $\operatorname{pers}(\sigma) \to \operatorname{pers}(\tau)$ is a poset isomorphism, then the Λ-identification $\operatorname{pers}(\sigma') \cong \operatorname{pers}(\tau')$ is a poset isomorphism by the above reasoning. Hence, by Lemma 2.24, σ' and τ' are isotopic since Λ has no closed leaves. This proves the biconditional statement.

For the last statement, in light of the above, it suffices to prove that a single shift of divergent neighbors induces a poset isomorphism. We do this by cases, after setting some notation. As before, ρ_v denotes the maximal Λ-route from a cusp v. Suppose that, prior to the shift, a and b are as shown in Figure 12. If c is a cusp such that $c \succeq a$ (resp. $c \succeq b$), we say that ρ_c "joins a (resp. b) through" x, y or z if x, y or z is the last of $\{x, y, z\}$ traversed by ρ_c before it fellow travels ρ_a (resp. ρ_b).

Suppose c and d are comparable, say $c \succeq d$. Then either

(a) $\{c, d\} \cap \{a, b\} = \varnothing$, or

(b) $c = a$, or

(c) $c = b$, or

(d) $d = a$, or

(e) $d = b$.

In each of (a)–(d), it is clear that shifting a and b does not affect $c \succeq d$. If $d = b$, then $c \succeq d$ holds after shifting a and b unless ρ_c joins a and b through x, which cannot happen because a and b are divergent neighbors.

Since the inverse of a shift of divergent neighbors is also a shift of divergent neighbors, this shows that $c \succeq d$ before such a shift if and only if $c \succeq d$ after such a shift. Hence the shift induces a poset isomorphism. □

3 Endperiodic maps

In this section, we give a condensed treatment of the parts of Handel–Miller theory we need. Other than a few lemmas which we prove, all of the material presented here can be found in more detail in [Cantwell et al. 2021].

3.1 Surfaces and ends

Let L be an orientable surface. Consider a sequence $A_1 \supset A_2 \supset A_3 \supset \cdots$ such that there exists a compact exhaustion $K_1 \subset K_2 \subset K_3 \subset \cdots$ of L and A_i is a connected component of $L - K_i$. We consider two such sequences $\{A_i\}$ and $\{B_i\}$ to be equivalent if each term of one sequence contains all but finitely many terms of the other. An *end* of L is an equivalence class of such sequences. If e is an end of L and $\{A_i\}$ is a sequence in the equivalence class e, we will call $\{A_i\}$ a *regular neighborhood basis* for e. We denote the set of ends of L by $\mathcal{E}(L)$.

It will be useful for our treatment to single out two specific types of ends of L. We say that an end e is an *infinite strip end* if it has a regular neighborhood basis in which each set is homeomorphic to $[0, 1] \times (0, \infty)$. We say that e is an *infinite cylinder end* if it has a regular neighborhood basis in which each set is homeomorphic to an open annulus.

There is a natural topology on $L \sqcup \mathcal{E}(L)$ which compactifies L: a base for this topology is given by the open sets of L together with all sets of the form $\{e\} \cup V$ where V is open in L and contains a term of a regular neighborhood basis for e. Together with this topology, $L \sqcup \mathcal{E}(L)$ is called the *end compactification* of L; the subspace topology on $\mathcal{E}(L)$ makes it into a totally disconnected set. A *neighborhood* of the end e is an open set $A \subset L$ such that $A \cup e$ is an honest neighborhood of e in the end compactification of L. The end compactification motivates our use of the term "regular neighborhood basis" for elements of e: if

$A_1, A_2, A_3, \dots$ is a regular neighborhood basis for e in our sense, then $A_1 \cup \{e\}$, $A_2 \cup \{e\}$, $A_3 \cup \{e\}, \dots$ is a regular neighborhood basis for e in the end compactification, in the traditional point–set topological sense.

3.2 Endperiodic maps

Let $f : L \to L$ be a homeomorphism. Then f induces a homeomorphism of the end compactification, which restricts to a homeomorphism of $\mathcal{E}(L)$. We say an end $e \in \mathcal{E}(L)$ is *periodic* if there exists an integer p such that $f^p(e) = e$. If p is the smallest such integer, we call it the *period* of e.

Let e be a periodic end of L with period p. Then e is *positive* if there exists a neighborhood U of e such that $U, f^p(U), f^{2p}(U), \dots$ is a regular neighborhood basis for e. Symmetrically, e is *negative* if e is a positive end of f^{-1}. We think of the positive ends of L as attracting and the negative ends as repelling.

The set $\{e, f(e), \dots, f^{p-1}(e)\}$ is called a *positive end-cycle* or *negative end-cycle* depending on whether e is positive or negative, respectively.

Definition 3.1 (endperiodic map, Reeb endperiodic map) Let L be an oriented surface with finitely many ends, none of which are infinite cylinder ends. Let $f : L \to L$ be an orientation-preserving homeomorphism. We say that f is *endperiodic* if

(a) all ends of L are positive or negative, and

if L has a noncompact boundary component ℓ with period p, then

(b) ℓ runs between two ends of L with the opposite sign and $f^p|_\ell$ has no fixed points.

We say that f is *Reeb endperiodic* if f satisfies (a) and, if ℓ is a noncompact component of ∂L with period p, then either ℓ satisfies (b) or

(c) ℓ runs between two ends of L with the same sign and $f^p|_\ell$ has a single fixed point x_0, which is a source or sink for f^p in L depending on whether the ends are both positive or negative, respectively. ◁

We remark that if f satisfies (a), then we can homotope f so that each noncompact boundary component running between two ends of the opposite sign satisfies (b) and each noncompact boundary component running between two ends of the same sign satisfies (c).

Reeb endperiodic maps are a convenient generalization of endperiodic maps. We will see in Section 5.3 that they are associated to generalized sutured manifolds, called Reeb sutured manifolds. These will play a part in our future work [Landry and Tsang ≥ 2025].

3.3 Junctures

The construction of Handel–Miller laminations starts by producing a collection of "junctures" associated to an endperiodic map $f: L \to L$, which are cooriented 1-manifolds in L "dual to a cohomology class at infinity" in a certain sense.

Let e be an end of L, and let $\{U_i\}_{i\in\mathbb{Z}_+}$ be any regular neighborhood basis for e. We say a sequence of sets $\{A_i\}_{i\in\mathbb{Z}_+}$ *escapes to* e if each U_j contains all but finitely many A_i. If e is a positive end of L with period p, let

$$\mathcal{U}_e = \big\{q \in L \mid \{f^{np}(q)\}_{n\in\mathbb{Z}^+} \text{ escapes to } e\big\}.$$

Letting $e_0 = e$, if $Z = \{e_0, e_1, \dots, e_{p-1}\}$ is the f-cycle of e_0, let

$$\mathcal{U}_Z = \bigcup_{i=0}^{p-1} \mathcal{U}_{e_i}.$$

Then $\mathcal{U}_Z$ is a surface with connected components $\mathcal{U}_{e_0}, \dots, \mathcal{U}_{e_{p-1}}$, and is in fact a regular covering space of a compact, connected surface $F_Z = \mathcal{U}_Z/\langle f\rangle$ with cyclic deck group generated by f.

The *positive escaping set* $\mathcal{U}_+$ is the union of the $\mathcal{U}_Z$ where Z ranges over all positive end-cycles:

$$\mathcal{U}_+ = \bigcup_{\text{pos. end-cycles } Z} \mathcal{U}_Z.$$

The *negative escaping set* $\mathcal{U}_-$ is the positive escaping set of f^{-1}.

Construction 3.2 (juncture components and tilings) Choose a basepoint $b \in F_Z$, and let γ be an oriented loop based at b. If $\tilde\gamma$ is any lift of γ traveling from $\tilde b_1$ to $\tilde b_2$ in $\mathcal{U}_Z$, there is a unique $n \in \mathbb{Z}$ such that $f^n(\tilde b_1) = \tilde b_2$. This defines a map $\pi_1(F_Z, b) \to \mathbb{Z}$, which gives a cohomology class $u \in H^1(F_Z; \mathbb{Z})$. It is clear from the definition that u must take values only in $p\mathbb{Z}$. Moreover, the smallest positive value taken by u is p. This can be seen as follows: Let x_0 be a lift of b to $\mathcal{U}_{e_0}$, and define $x_i = f^i(x_0)$. We can find a path in $\mathcal{U}_{e_0}$ from x_0 to x_p. This projects to a loop in F_Z evaluating to p under u.

We can choose a weighted, cooriented 1-manifold J_Z in F_Z which is dual to u. The weights come from collapsing parallel components of a representative of the Lefschetz dual of u. Further, we can require that J_Z be nonseparating in F_Z. In this situation, we see that all the weights on components of J_Z will be divisible by p. We require that J_Z be disjoint from our basepoint $b \in F_Z$.

Let F_Z' be $F_Z \setminus\!\setminus J_Z$, and let $\mathcal{J}_Z$ be the preimage of J_Z in $\mathcal{U}_Z$. The surface $\mathcal{U}_Z$ decomposes into compact, connected surfaces, called *tiles*, which are glued along components of $\mathcal{J}_Z$, each of which has a weight in $p\mathbb{Z}_+$ induced by J_Z. Because J_Z is nonseparating, for each $n \in \mathbb{Z}$ there is a unique component t_n of $\mathcal{U}_Z - \mathcal{J}_Z$ that contains x_n. Here are some relevant facts about the tiles t_n:

- f carries t_n to t_{n+1} for all n.
- If j is a component of $\mathcal{J}_Z$ with weight w, then there is a unique n such that j joins t_n to t_{n+w} and the coorientation on j points out of t_n and into t_{n+w}.

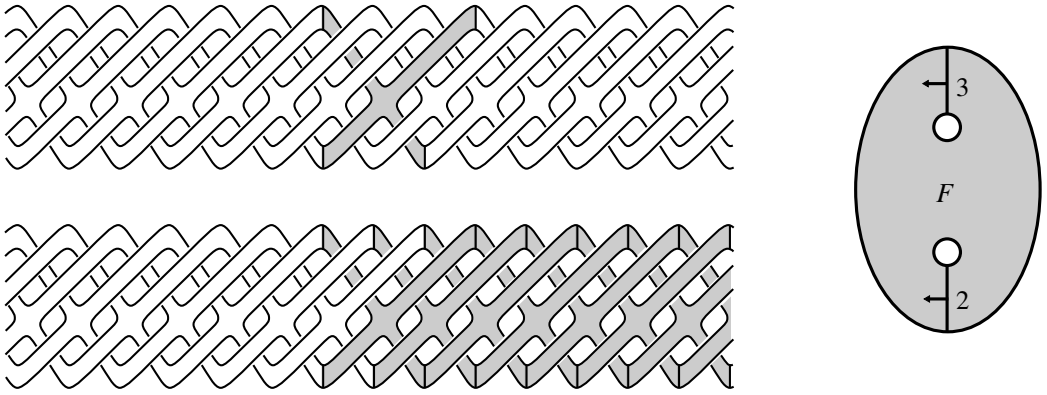

Figure 13: This figure accompanies Example 3.3.

A decomposition of $\mathcal{U}_Z$ into tiles as above is called a *tiling*. Given a tiling $\{t_n \mid n \in \mathbb{Z}\}$ of $\mathcal{U}_Z$, a *tiled neighborhood* of Z is any set of the form $\bigcup_{i=n}^{\infty} t_i$. This is a union of neighborhoods of each of the ends in Z, which are themselves unions of tiles. We call each of these end-neighborhoods a tiled neighborhood of the corresponding end. The boundary of a tiled neighborhood of an end e is called a *juncture* of e.

Now let $\mathcal{J}_+ = \bigcup_Z \mathcal{J}_Z$, where the union is over all f-cycles of positive ends of L. The components of $\mathcal{J}_+$ are called *positive juncture components*. A juncture component j is called *escaping* if $\{f^{np}(j)\}_{n<0}$ escapes to a negative end and *nonescaping* otherwise. ◁

Example 3.3 This example is a special case of [Cantwell et al. 2021, Example 2.29]. Let L be the two-ended surface shown in Figure 13, which is made by gluing together countably many X-shaped pieces like the one shaded on the top of the figure. Let $f : L \to L$ be translation to the right by one X-shaped piece. Let e be the positive end of L. Then $\mathcal{U}_e = L$, F is as shown in Figure 13, right, and we can take J to be the weighted cooriented 1-manifold shown there. With this J, the tiles corresponding to the singleton end-cycle e are exactly the X-shaped pieces. On the bottom of Figure 13 we see a tiled neighborhood of e. Note that because the weights on components of J are greater than the period of e (in this case the period is 1), each juncture component is a part of multiple junctures. ◁

Remark 3.4 If all boundary components of the surface F_Z have zero pairing with the cohomology class u in the above construction of junctures, then J can be chosen to have one component disjoint from ∂F_Z, with weight equal to the period of Z. See the discussion in [Field et al. 2023, Section 2], in which $\partial F = \varnothing$. In this case, each juncture component will belong to just one juncture, unlike the situation in Example 3.3. ◁

3.4 The Handel–Miller laminations

A *geodesic half-plane*, or *half-plane*, is a closed subset of $\mathbb{H}^2$ bounded by a single geodesic. Following [Cantwell et al. 2021], we say a complete hyperbolic metric on a surface L is *standard* if there is no isometric embedding of a half-plane in L and if all components of ∂L are geodesics.

Recall that $\mathcal{J}_+$ is the set of positive juncture components. There is a symmetric definition of the set $\mathcal{J}_-$ of *negative juncture components*.

The following theorem is proved in [Cantwell et al. 2021] and is the foundation of Handel–Miller theory.

Theorem 3.5 (Handel and Miller; Cantwell, Conlon and Fenley) *Let L be endowed with a standard hyperbolic metric and suppose that $f : L \to L$ is an endperiodic map. The geodesic representatives of nonescaping components of $\mathcal{J}_+$ limit on a geodesic lamination Λ_-. Similarly, the geodesic representatives of nonescaping components of $\mathcal{J}_-$ limit on a geodesic lamination Λ_+ which is transverse to Λ_-.*

The geodesic tightenings of the negative (positive) juncture components are mutually disjoint and disjoint from Λ_+ (Λ_-).

Moreover, up to isotopy, we can assume that f preserves the geodesic laminations Λ_+, Λ_- and also permutes the geodesic representatives of positive and negative juncture components.

Remark 3.6 This statement is slightly more general than [Cantwell et al. 2021] in that we allow infinite strip ends, but the methods of proof there work just as well in this case. ◁

The laminations $\Lambda_\pm$ are called the *positive/negative Handel–Miller laminations* for f. Note that they are independent of the representative of the isotopy class of f, since they depend only on the geodesic tightenings of the f-images of curves. Additionally, they are independent of the choice of junctures [Cantwell et al. 2021, Corollary 4.72]. Finally, by [Cantwell et al. 2021, Corollary 10.16], the union $\Lambda_+ \cup \Lambda_-$ is independent of the choice of standard hyperbolic metric on L up to ambient isotopy. As such we will sometimes refer to the Handel–Miller laminations without specifying a choice of metric.

A representative of f which preserves the Handel–Miller laminations as well as the geodesic representatives of the juncture components is called a *Handel–Miller representative* of the homotopy class of f, or simply a *Handel–Miller map*. When the metric on L is not specified, a Handel–Miller map means a Handel–Miller map for some choice of metric.

Suppose we are given a Handel–Miller map f; by definition f comes with some associated (geodesic) juncture components. If we perform the construction of junctures on f from Construction 3.2 to produce some *other* collection of juncture components, then f will permute these new juncture components as well as the leaves of Λ_+ and Λ_-. These new juncture components will not be geodesics in general.

Example 3.7 (translation) Suppose that $f : L \to L$ is endperiodic and that each point in L escapes compact sets of L under positive and negative iteration of f, ie $\mathcal{U}_+ = \mathcal{U}_- = L$. Such an endperiodic map is called a *translation*. In this case, $\Lambda_+ = \Lambda_- = \varnothing$. See [Cantwell et al. 2021, Section 4.8]. One can show that if L is connected then it has exactly two ends. In general, f generates the deck group of an infinite cyclic covering $L \to L/\langle f \rangle$, and the mapping torus $(L \times I)/(x, 1) \sim (f(x), 0)$ is homeomorphic to $(L/\langle f \rangle) \times (0, 1)$. ◁

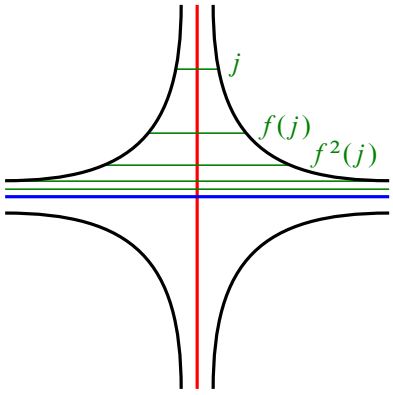

Figure 14: A picture of $\Lambda_\pm$ for the map $f = \left(\begin{smallmatrix} 2 & 0 \\ 0 & 1/2 \end{smallmatrix}\right)$ from Example 3.8. The blue line denotes Λ_+ and the red denotes Λ_-. The green lines depict part of the f-orbit of a negative juncture j.

Example 3.8 The following is one of the simplest examples in which the Handel–Miller laminations are nonempty. Let $L = \{(x, y) \in \mathbb{R}^2 \mid xy \leq 1\}$, and let $f : L \to L$ be given by the matrix $\left(\begin{smallmatrix} 2 & 0 \\ 0 & 1/2 \end{smallmatrix}\right)$. There are two positive and two negative ends of L, all of which are infinite strip ends. The lamination Λ_+ consists of a single line running between the two positive ends, while Λ_- consists of a single line running between the negative ends. See Figure 14. ◁

3.5 Principal regions

We will now assume that $f : L \to L$ is Handel–Miller. The positive and negative escaping sets $\mathcal{U}_+$ and $\mathcal{U}_-$ (defined in Section 3.3) of f are related quite simply to the Handel–Miller laminations Λ_+, Λ_- by the following lemma:

Lemma 3.9 [Cantwell et al. 2021, Lemma 4.71] *For a Handel–Miller map f, we have $\Lambda_+ = \partial\mathcal{U}_-$ and $\Lambda_- = \partial\mathcal{U}_+$.*

Definition 3.10 (principal regions) Let $\mathcal{P}_+ = L - (\Lambda_+ \cup \mathcal{U}_-)$. Each connected component of $\mathcal{P}_+$ is called a *positive principal region*. Symmetrically, a *negative principal region* is a positive principal region of f^{-1}. ◁

We now describe some general structure of principal regions without justification; for more details see [Cantwell et al. 2021, Sections 5.3 and 6.1–6.4].

Let P_+ be a positive principal region. Then P_+ is homeomorphic to the interior of a compact surface with boundary, say Σ. The metric completion $\overline{P}_+$ of P_+ is homeomorphic to Σ minus a finite nonempty set of points on each component of $\partial\Sigma$. Hence, $\partial\overline{P}_+$ consists of finitely many lines $\lambda_1, \ldots, \lambda_n$. Furthermore, each λ_i is a leaf of Λ_+. Assume for now that Σ has only one boundary component. Then each λ_i has the same period under f, say p. For each λ_i, there is a maximal f-invariant closed interval $I_i \subset \ell_i$ such that if $x \in \lambda_i - I_i$, then $\{f^{kp}(x) \mid k \geq 0\}$ escapes an end of λ_i.

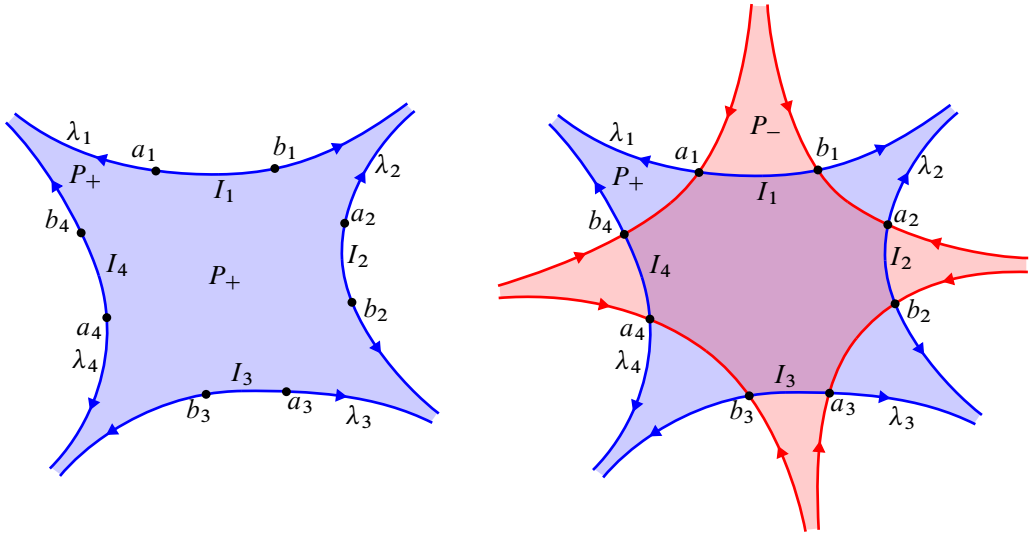

Figure 15: Left: an example of a positive principal region P_+ together with some notation from our description of the structure of principal regions. Right: the dual principal region P_-. Each of P_+ and P_- has four arms, and the nucleus is the 8-sided region in the center. The arrows on leaves indicate the direction in which points move under application of f^p, where p is the period of the leaves. Note that unlike in this example, principal regions need not be simply connected in general.

Orient each λ_i from left to right looking out from P_+, and let a_i and b_i be the left and right endpoints of I_i, respectively (see Figure 15). Then there is a leaf λ_i' of Λ_- passing through b_i and a_{i+1} (indices taken mod n). The leaves $\lambda_1', \dots, \lambda_n'$ are also periodic of period p. The leaf λ_i' has a maximal invariant interval I_i' with endpoints on b_i and a_{i+1}, and if $x \in \lambda_i' - I_i'$ then $\{f^{kp}(x) \mid k \geq 0\}$ escapes an end of λ_i'. The set $P_+ - (I_1' \cup \cdots \cup I_n')$ consists of n unbounded, simply connected components, called the *arms* of P_+, and one bounded component, called the *nucleus* of P_+. The nucleus is homeomorphic to the interior of Σ.

In fact, the leaves $\lambda_1', \dots, \lambda_n'$ bound a negative principal region P_-; the pair P_+ and P_- are said to be *dual principal regions*. See Figure 15. Symmetrically to P_+, the set P_- has n arms and one nucleus, which is equal to the nucleus of P_+.

When the compact surface Σ has more than one boundary component, the description above holds with minor modifications. Namely, the boundary lines of P_+ break into finitely many sets, corresponding to the boundary components of Σ; each of these sets gives rise to finitely many arms, the complement in P_+ of the closure of the arms is the nucleus of P_+, and there exists a dual principal region P_- sharing a nucleus with P_-.

3.6 Useful lemmas about the Handel–Miller representative

For this section, let $f : L \to L$ be a Handel–Miller map.

Since f preserves the laminations $\Lambda_\pm$, it induces quotient laminations $\Lambda_\pm^\infty$ in the quotients $\mathcal{U}_\pm/\langle f\rangle$.

Lemma 3.11 (a) *The laminations $\Lambda_\pm^\infty$ are spiraling and consistent. Each compact leaf of $\Lambda_\pm^\infty$ is the image under the quotient map of a leaf of $\Lambda_\pm \cap \mathcal{U}_\pm$ which has a subray escaping to an end of L. Conversely, each such leaf of $\Lambda_\pm \cap \mathcal{U}_\pm$ gives a compact leaf of $\Lambda_\pm^\infty$.*

For the next two items, see the definitions in Section 5.

(b) *If λ is a compact leaf of Λ_+^∞, then λ is the boundary component of a periodic leaf ℓ of the suspension $\mathcal{L}^u$ of Λ_+, and λ is homotopic in ℓ to a positive multiple of the closed orbit of the suspension semiflow at the core of ℓ.*

(c) *Further, Λ_+^∞ contains parallel closed leaves if and only if f has a positive principal region with an arm bounded by rays in Λ_+ which escape compact sets in L. This arm gives rise to two parallel closed leaves of Λ_+^∞ bounding an annulus disjoint from the lamination. Symmetric statements hold for Λ_-^∞.*

Proof The statements in this lemma are all restatements of the material in [Cantwell et al. 2021, Section 6.7]. □

Lemma 3.12 *Let λ be a leaf of Λ_+, and let $p \in \lambda$. Then no component of $\lambda - \{p\}$ is contained in a compact subset of L.*

Proof This is [Cantwell et al. 2021, Corollary 4.50]. □

Lemma 3.13 *Let K be a compact subsurface of L with $\partial K \pitchfork \Lambda_+$. Then $\Lambda_+ \cap K$ is an I-lamination.*

Proof If λ is a leaf of Λ_+, then, by Lemma 3.12, neither of its ends accumulates in K. The lemma follows. □

Lemma 3.14 *Let λ be a leaf of Λ_+. If there is a side of λ on which negative (geodesic) juncture components do not accumulate, then λ borders a principal region on that side.*

Proof By [Cantwell et al. 2021, Lemma 5.14] (or Definition 3.10), L is the disjoint union of the negative escaping set $\mathcal{U}_-$, the lamination $\Lambda = \Lambda_+$ and the union of positive principal regions $\mathcal{P}_+$.

If λ has a side on which negative juncture components do not accumulate, it follows from the definition of Λ_+ that leaves of Λ_+ do not accumulate on that side either. Hence λ borders a component P of $L - \Lambda$ on that side, which must be either an escaping component or a principal region.

By [Cantwell et al. 2021, Proposition 5.11], negative juncture components accumulate on λ from any side bordering $\mathcal{U}_-$. We conclude that P is a principal region. □

Let $\widetilde{L}$ denote the universal cover of L, where L is endowed with a standard hyperbolic metric. Then $\widetilde{L}$ can be identified with a subset of $\mathbb{H}^2$ with (possibly empty) boundary a collection of geodesics. Thus it has a natural compactification to a closed disk obtained by taking the closure in $\mathbb{H}^2 \cup \partial_\infty \mathbb{H}^2$. We denote

the intersection of this closed disk with $\partial_\infty \mathbb{H}^2$ by $\partial_\infty(\widetilde{L})$. Since $\Lambda_\pm$ are geodesic laminations, each leaf of their lifts $\widetilde{\Lambda}_\pm$ to $\widetilde{L}$ determines well-defined endpoints in $\partial_\infty(\widetilde{L})$.

The following lemma says that the arms of principal regions never "fellow travel". Its proof makes use of the fact that all leaves of Λ^+ and all juncture components are geodesics.

Lemma 3.15 *Let λ_1 and λ_2 be leaves of Λ_+, with distinct lifts $\widetilde{\lambda}_1$ and $\widetilde{\lambda}_2$ sharing a point p in $\partial_\infty(\widetilde{L})$. Then $\widetilde{\lambda}_1$ and $\widetilde{\lambda}_2$ border the same lifted principal region.*

Proof Let A be the component of $\widetilde{L} - (\widetilde{\lambda}_1 \cup \widetilde{\lambda}_2)$ bordered by both $\widetilde{\lambda}_1$ and $\widetilde{\lambda}_2$. We claim that there are no lifted negative juncture components accumulating on $\widetilde{\lambda}_1$ or $\widetilde{\lambda}_2$ from inside A. This is because any such lifted juncture component sufficiently far into such a sequence would have to have p as an endpoint, since the negative junctures are disjoint from Λ_+. If $\tilde{\jmath}$ were such a lift of a juncture component j, then both λ_1 and λ_2 would limit on j in L. However, by Lemma 3.12, both ends of each leaf of Λ_+ pass arbitrarily near at least one end of L, so this is impossible.

By Lemma 3.14, $\widetilde{\lambda}_1$ and $\widetilde{\lambda}_2$ must each border a lift of a principal region lying in A; call these lifts $\widetilde{P}_1$ and $\widetilde{P}_2$, respectively. If $\widetilde{P}_1 \neq \widetilde{P}_2$, then there must be at least one lifted leaf $\widetilde{\lambda}_3 \in \widetilde{\Lambda}$ lying in A and having p as an endpoint. However, this would imply the existence of a sequence of lifted negative junctures accumulating on $\widetilde{\lambda}_3$, each having p as an endpoint, which we have already seen is impossible. It follows that no such $\widetilde{\lambda}_3$ exists, so $\widetilde{P}_1 = \widetilde{P}_2$. □

Lemma 3.16 *Let λ be a periodic leaf of Λ_+. Let $\widetilde{\lambda}$ be a lift of λ to $\widetilde{L}$. Let $\tilde{f}^n$ be a lift of f^n that preserves $\widetilde{\lambda}$ and its ends. For each side of $\widetilde{\lambda}$ such that $\widetilde{\lambda}$ does not border a lifted principal region on that side, there exists a lift $\tilde{\jmath}$ of a (geodesic) juncture component j such that $(\tilde{\jmath}, \tilde{f}^n(\tilde{\jmath}), \tilde{f}^{2n}(\tilde{\jmath}), \dots)$ converges to $\widetilde{\lambda}$ from that side.*

Proof This is a restatement of [Cantwell et al. 2021, Lemma 6.7]. □

When infinite strip ends are present, they interact predictably with the laminations, as the following lemma shows:

Lemma 3.17 *Let e be an infinite strip end of L. If e is positive, then there are either one or two leaves of Λ_+ escaping to e. These are the only leaves that see e, in the sense that there is a neighborhood of e disjoint from all other leaves of $\Lambda_\pm$.*

Proof Let ℓ_1 and ℓ_2 be the two boundary components of L with ends escaping to e. We choose a collection of junctures $\mathcal{J}$ for L. Note that there are infinitely many negative junctures meeting ℓ_i, since ℓ_i connects a negative end to a positive end. If p is the period of e, then f^p maps ℓ_i to ℓ_i with no fixed points, translating points from the negative end to the positive end. Hence there is a sequence of negative junctures for each $i = 1, 2$ such that each juncture has an endpoint on ℓ_i and these endpoints escape to e. Hence each sequence of junctures accumulates on a leaf λ_i of Λ_+ that escapes e. If $\lambda_1 \neq \lambda_2$, then λ_1 and λ_2 border a single principal region by Lemma 3.15, which cannot contain any other leaves of Λ_+. □

Construction 3.18 (endperiodization) Suppose that $f\colon L \to L$ is a Reeb endperiodic map (see Definition 3.1). Assume first that there is a unique component ℓ of ∂L connecting two ends of the same sign. Without loss of generality, assume that ℓ connects two negative ends, so that $f|_\ell$ has a unique fixed point x_0 and all points in $\ell - \{x_0\}$ are attracted to x_0 under iteration of f. By definition, x_0 is a local sink in L, so there is an attracting neighborhood $A \ni x_0$ in L with $\lim_{n\to\infty} f^n(x) = x_0$ for all $x \in A$. Note that $f|_{L-\{x_0\}}$ is now an actual endperiodic map; we have introduced a new infinite strip end corresponding to the point x_0 and no boundary components of $L - \{x_0\}$ connect ends of the same sign. We can therefore speak of the Handel–Miller laminations associated to $f|_{L-\{x_0\}}$. When L has multiple such boundary components of various periods, this construction can be modified in the obvious way to produce an endperiodic map. We call this new map the *endperiodization* of f. ◁

4 Periodic sequences of endperiodic train tracks

4.1 Conventions and definitions

In this section we assume that $f : L \to L$ is a Handel–Miller map. Recall that by our definition of Handel–Miller map, there is a choice of standard hyperbolic metric on L and geodesic juncture components such that $\Lambda_\pm$ are geodesic laminations and such that f permutes the leaves of the laminations as well as the juncture components.

Fix a tiling of each positive and negative end-cycle as in Construction 3.2; we emphasize that the juncture components defining these tilings need not be the geodesic juncture components used to construct the Handel–Miller laminations; this freedom will be useful to us later.

Let $E_\pm$ be a union of mutually disjoint tiled neighborhoods of all end-cycles of L such that Λ_+ (resp. Λ_-) is disjoint from the tiled neighborhoods of the negative (resp. positive) end-cycles. Let $K_0 = L \setminus\setminus E_\pm$. We call K_0 a *core* of L.

Suppose that the positive end-cycles are $Z_1, \dots, Z_n$, and let t_j^i be the j^{th} tile in the tiled neighborhood for Z_i, where the indexing on j starts at 1. Starting with $l = 0$, we inductively define the $(l+1)^{st}$ *core* to be

$$K_{l+1} = K_l \cup (t_{l+1}^1 \cup \cdots \cup t_{l+1}^n).$$

That is, K_{l+1} is obtained from K_l by absorbing a t_j^i for each i, where j is the smallest integer such that t_j^i does not already lie in K_l. Let E_i be the union of components of $L \setminus\setminus K_i$ which are neighborhoods of positive ends.

4.2 Train tracks carrying Λ_+: some geometric arguments

We continue to assume that $f : L \to L$ is a Handel–Miller map.

In this subsection our arguments make use of the standard hyperbolic metric on L and of the geodesic juncture components associated to f by the definition of a Handel–Miller map. However, we emphasize

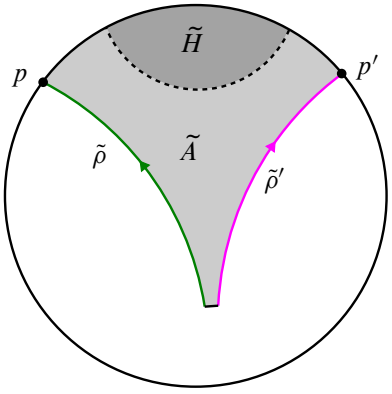

Figure 16: If $p \neq p'$, the metric on L would be nonstandard.

that the results do not depend on this geometric structure since the Handel–Miller laminations are independent of the standard metric up to ambient isotopy.

Lemma 4.1 *Let τ be a train track fully carrying Λ_+. Let ρ, ρ' be two rays in leaves of Λ_+ which eventually fellow travel in τ, and let $\tilde{\rho}$, $\tilde{\rho}'$ be two lifts of these rays eventually fellow traveling in $\tilde{\tau}$. Then the ideal points in $\partial_\infty(\widetilde{L})$ determined by $\tilde{\rho}$ and $\tilde{\rho}'$ are equal.*

The above lemma is obvious for laminations carried by train tracks on hyperbolic surfaces of finite type, but we should convince ourselves that it also holds in our setting. In the finite-type setting, it is immediate that the ties of a standard neighborhood of a lamination have bounded length, which immediately implies the claim. We give a different argument here that does not require a uniform bound on the length of ties.

Proof By truncating, we may assume that the two rays begin on the same tie of τ. Choose parametrizations of $\tilde{\rho}$ and $\tilde{\rho}'$ that are compatible with the ties of $\tilde{\tau}$. That is, for all $t \in [0, \infty]$ there exists a segment a_t connecting $\rho(t)$ to $\rho'(t)$ such that a_t is contained in a tie of $\tilde{\tau}$. Thus the parametrization of ρ' is uniquely determined by the parametrization of ρ. Let $\widetilde{A}_t$ be the region bounded by the tie segments a_0, a_t and the leaf segments $[\tilde{\rho}(0), \tilde{\rho}(t)], [\tilde{\rho}'(0), \tilde{\rho}'(t)]$. Let $\widetilde{A} = \bigcup_{t\in[0,\infty)} \widetilde{A}_t$.

Suppose that the mapping of $\widetilde{A}$ to L under the covering projection is not an embedding. In this case, one can check that ρ and ρ' must follow the same train route as a closed curve γ. Thus the two rays stay in a compact set of L, contradicting Lemma 3.12.

Otherwise $\widetilde{A}$ projects homeomorphically to a set $A \subset L$ which is foliated by segments of ties of τ. Note that $\widetilde{A}$ does not contain any lifts of boundary components of L, since $\widetilde{A}$ is foliated by tie segments disjoint from all such lifts. As a consequence, if $p \neq p'$ then $\widetilde{A}$ contains a half-plane $\widetilde{H}$, which projects isometrically to L. See Figure 16. This contradicts that the hyperbolic metric on L is standard, so $p = p'$, as desired. □

If τ is a train track fully carrying Λ_+, we say a cusp of τ is *principal* if it corresponds to a principal region of Λ_+. All other cusps are *nonprincipal*. Any cusp c of τ determines two rays ρ_1, ρ_2 in leaves of Λ_+ bordering the corresponding complementary component of Λ_+. There are two possibilities: either ρ_1 and ρ_2 fellow travel in τ, or there is some first cusp c' of τ at which the two rays split away from each other. In the second case we say that the cusps c and c' *collide* with one another.

Lemma 4.2 *Let τ be a train track fully carrying Λ_+, and let c be a nonprincipal cusp of τ. Then there exists a cusp c' of τ such that c and c' collide.*

Proof We prove the contrapositive: if there exists no such cusp c' then c is principal.

Let $\tilde{c}$ be a lift of c to the universal cover $\widetilde{L}$. If c does not collide with any cusp then $\tilde{c}$ determines two rays of leaves in $\widetilde{\Lambda}_+$ that follow the same route in $\tilde{\tau}$; these are two border leaves $\widetilde{\lambda}$, $\widetilde{\lambda}'$ of the complementary region determined by $\tilde{c}$. Let λ and λ' be their respective projections to L. By Lemma 4.1, there exists a point $p \in \partial_\infty \widetilde{L}$ which is an endpoint of both $\widetilde{\lambda}$ and $\widetilde{\lambda}'$, so by, Lemma 3.15, there is a lifted principal region bounded by $\widetilde{\lambda}$ and $\widetilde{\lambda}'$. Therefore c is principal. □

4.3 Train tracks carrying Λ_+: topological arguments

In this subsection we prove some more facts about train tracks carrying Λ_+, but using topological arguments that do not rely on the standard hyperbolic metric on L. We also introduce the "core split", an operation on train tracks that will be important going forward.

We make the convention that train tracks carrying Λ_+ will always be transverse to any junctures under consideration. We can always arrange for this to hold by a small perturbation.

Lemma 4.3 *Let τ_1 and τ_2 be efficient train tracks fully carrying Λ_+ which are equal in E_i, ie $\tau_1|_{E_i} = \tau_2|_{E_i}$. Then the train tracks $\tau_1|_{K_j}$ and $\tau_2|_{K_j}$ are $\Lambda|_{K_j}$-compatible as train tracks in K_j for all $j \geq i$.*

Here, τ_1 and τ_2 being efficient implies that $\tau_1|_{K_j}$ and $\tau_2|_{K_j}$ are efficient, so the notion of Λ-compatibility makes sense.

Proof Implicit in our discussion of τ_1 and τ_2 is the existence of standard neighborhoods witnessing the fact that Λ is carried by both of these train tracks, and which agree on E_j for $j \geq i$. Let $N(\tau_1)$ and $N(\tau_2)$ be these standard neighborhoods, respectively. Let A be a complementary region of $\Lambda_+|_{K_j}$, and let c be a component of the vertical boundary $\partial_v A \subset \partial K_j$ associated to the stop s of $\tau_1|_{K_j}$. We must show that c is mapped to s under the carrying map $N(\tau_2) \to \tau_2$. Let A' be the complementary component of $\Lambda_+|_{E_j}$ meeting A along c (see Figure 17). Then c, when viewed as a component of $\partial_v A'$, is also associated to s (viewing s as a stop of $\tau_1|_{E_j}$). We have $N(\tau_1)|_{E_j} = N(\tau_2)|_{E_j}$, so c is also associated to s viewed as a stop of $\tau_2|_{E_j}$. Since the local picture is as in Figure 17, it follows that c is associated to s viewed as a stop of $\tau_2|_{K_j}$. Therefore $\tau_1|_{K_j}$ and $\tau_2|_{K_j}$ are $\Lambda|_{K_j}$-compatible. □

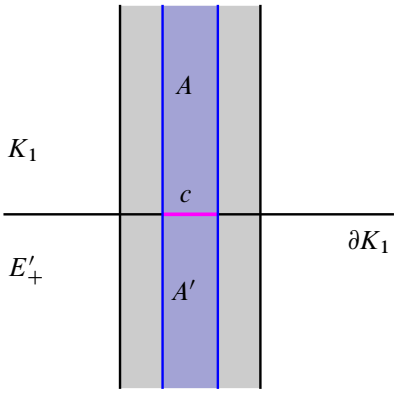

Figure 17: Notation for showing $\Lambda_+|_{K_j}$-compatibility of $\tau_1|_{K_j}$ and $\tau_2|_{K_j}$ in the proof of Lemma 4.3.

Definition 4.4 (core split) Let τ be a train track fully carrying Λ_+. If τ has no large branches, define $\kappa(\tau) = \tau$. Otherwise, let i be the least $i \in \mathbb{Z}_{\geq 0}$ such that $\tau|_{K_i}$ contains a large branch. Let μ be the maximal splitting of $\tau|_{K_i}$, and let $\kappa(\tau) = \mu \cup (\tau \setminus\setminus K_i)$ (recall the maximal splitting is unique by Lemma 2.21). We call the operation of replacing τ by $\kappa(\tau)$ a *core split*. Sometimes we will use a double-headed arrow to denote core splitting, ie $\tau \twoheadrightarrow \tau'$ means that $\tau' = \kappa(\tau)$. ◁

Note that the definition of a core split depends on the tiling fixed in Section 4.1. For an example see Figure 53, where, if we fix the tiling shown, then the composition of the first two splitting moves is a core split.

Lemma 4.5 *Let τ be a efficient train track fully carrying Λ_+. Then core splitting commutes with f, that is, $\kappa(f(\tau)) = f(\kappa(\tau))$.*

Proof If τ has no large branches then $f(\tau)$ also has no large branches, and the statement reduces to $f(\tau) = f(\tau)$; hence we may assume τ has large branches. Suppose that i is the least i such that $\tau|_{K_i}$ has large branches.

It is clear that $f(\kappa(\tau))|_{E_{i+1}} = \kappa(f(\tau))|_{E_{i+1}}$. Moreover, $f(\kappa(\tau))|_{K_{i+1}}$ and $\kappa(f(\tau))|_{K_{i+1}}$ are $\Lambda|_{K_{i+1}}$-compatible by Lemma 4.3, and they are spiraling. Since core splitting and the application of the map f both preserve orders on persistent cusps, we conclude that $f(\kappa(\tau))|_{K_{i+1}}$ and $\kappa(f(\tau))|_{K_{i+1}}$ are isotopic in K_{i+1} rel stops by Corollary 2.26f. This gives a compactly supported isotopy from $\kappa(f(\tau))$ to $f(\kappa(\tau))$. □

4.4 Endperiodic train tracks

We say a train track τ in L fully carrying Λ_+ is *f-endperiodic* if there exists an i such that

$$f(\tau)|_{E_{i+1}} = \tau|_{E_{i+1}}. \tag{4.6}$$

(The sets E_i were defined in Section 4.1.) We say that τ is *f-endperiodic in E_i* if (4.6) holds.

Proposition 4.7 *There exists $i \geq 0$ such that the lamination Λ_+ is fully carried by an efficient endperiodic train track T_+ with the following properties*:

(i) *T_+ is f-endperiodic in E_i.*

(ii) *$T_+ \cap K_i$ has no large branches.*

(iii) *$T_+ \cap E_i$ has no large branches.*

We remark that conditions (ii) and (iii) together are equivalent to the statement that all large branches of T_+ pass through ∂K_i. For an example, see the train track in Figure 53, far left, where the core is the second piece from the top.

Proof Recall the quotient surface $\mathcal{U}_+/\langle f \rangle$, which contains the quotient lamination Λ_+^∞. By Lemma 3.11, parts (a) and (c), Λ_+^∞ is spiraling, and has no closed leaves which are homotopic to each other with the opposite orientation. By Lemma 2.16, Λ_+^∞ is carried by an efficient spiraling train track T_+^∞.

Let $N(\Lambda_+^\infty)$ be a standard neighborhood of T_+^∞ which is also a standard neighborhood of Λ_+^∞. By taking the preimage of $N(\Lambda_+^\infty)$ under the map $E_0 \hookrightarrow \mathcal{U}_+ \to \mathcal{U}_+/\langle f \rangle$, we obtain a standard neighborhood of $\Lambda_+|_{E_0}$. By taking a standard neighborhood of $\Lambda_+|_{K_0}$ which matches up along ∂K_0, we can extend this to a standard neighborhood $N(\Lambda_+)$ of Λ_+.

Similarly, by taking the preimage of T_+^∞, we obtain a train track T_{E_0} on E_0. Let T_{K_0} be a train track for $N(\Lambda_+)|_{K_0}$ that matches up with T_E along ∂K_0. Since $\Lambda_+|_{K_0}$ is an I-lamination by Lemma 3.13, we may replace T_K by its maximal Λ-splitting by Lemma 2.20. Let

$$T_0 = T_{E_0} \cup T_{K_0}.$$

Note that T_0 has no annulus complementary regions since this would force the existence of a circular leaf of Λ_+. Also, T_0 has at most finitely many cusped bigon or cusped monogon complementary regions since T_{E_0} has none such, so any cusped bigon complementary region must pass through K_0. Suppose R is a cusped bigon or monogon complementary region of T_0. At least one of the cusps of R must collide with another cusp, for otherwise Lemmas 4.1 and 3.15 would give a principal region of Λ^+ with nonnegative index, and all of the principal regions of Λ_+ have negative index (Λ^+ is geodesic). Hence there is a finite sequence of splits reducing the number of cusped bigon and monogon complementary regions by one.

Therefore, after finitely many splits we obtain a track T_1 which agrees with T_0 outside some smallest core K_i. We perform a core split on T_1 and call the result T_+. By construction T_+ is efficient, and endperiodic in E_i. Further, (ii) is satisfied because T_+ is the core split of T_1, and (iii) is satisfied because T_+^∞ is spiraling. □

Remark 4.8 In the last paragraph of the proof of Proposition 4.7, note that the uniqueness of maximal splittings implies that T_+ can also be obtained by performing i core splits on T_0. ◁

Theorem 4.9 *There exists an efficient f-endperiodic train track τ which fully carries Λ_+, satisfies properties* (i)–(iii) *from Proposition 4.7, and is the first term of a Λ_+-splitting sequence*

$$\tau \to \cdots \to f(\tau).$$

Proof Let T_+ be the train track furnished by Proposition 4.7. Reindex the E_i so that T_+ and E_0 satisfy properties (i)–(iii) from that proposition. Set $\Lambda_i := \Lambda_+|_{K_i}$.

Let $\tau_0 = T_+$, and let τ_{i+1} be obtained by performing a core split on τ_i for $i \geq 0$. By Lemma 4.3, $\tau_0|_{K_j}$ and $f(\tau_0)|_{K_j}$ are Λ_j-compatible for $j \geq 1$. Since Λ_j-splitting preserves Λ_j-compatibility, this implies that $\tau_1|_{K_j}$ and $f(\tau_0)|_{K_j}$ are Λ_j-compatible for $j \geq 1$. In particular, there is a natural Λ_j-identification of their cusps. Note also that $\tau_1|_{K_1}$ and $f(\tau_0)|_{K_1}$ are both spiraling train tracks, so Lemma 2.24 implies that they differ by at most a collection of shifts.

By Lemmas 3.15 and 4.1, none of the Λ_+-routes from principal cusps of τ_1 or $f(\tau_0)$ eventually fellow travel in their respective train tracks. By Lemma 4.2, the Λ_+-routes from all nonprincipal cusps all experience collisions. We can therefore choose a natural number N such that the following hold:

- If a, b are principal cusps of $\tau_1|_{K_1}$ or $f(\tau_0)|_{K_1}$ such that their maximal Λ-routes in K_1 end at the same point of ∂K_1, then their maximal Λ-routes in K_N diverge at some point.
- Each nonprincipal cusp of $\tau_1|_{K_1}$ and $f(\tau_0)|_{K_1}$ is nonpersistent in K_N.

As noted above, the train tracks $\tau_1|_{K_N}$ and $f(\tau_0)|_{K_N}$ are Λ_N-compatible and differ by a collection of shifts. By the choice of N, each of these is a shift of divergent neighbors. By Corollary 2.26, the two train tracks have identical core splittings in K_N.

We have therefore shown that $\tau_N = \kappa^{N-1}(f(\tau_0)) = f(\tau_{N-1})$ (we have used Lemma 4.5 in the second equality). Renaming $\tau = \tau_{N-1}$, the core split of τ is $f(\tau)$, so there is a splitting sequence from τ to $f(\tau)$, as claimed. □

Theorem 4.9 is phrased so as to be maximally useful to us later in the paper. However, we note that the same proof actually gives the following statement, which mirrors Agol's construction of layered veering triangulations and may be of independent interest to researchers in Handel–Miller theory:

Theorem 4.10 *Let $f\colon L \to L$ be endperiodic, and let τ_0 be an efficient f-endperiodic train track carrying the positive Handel–Miller lamination. Consider the sequence of train tracks $\tau_0, \tau_1, \tau_2, \ldots$ where τ_i is a core split of τ_{i-1}. For sufficiently large n, we have $\tau_n = f(\tau_{n-1})$.*

In particular, note that we do not assume above that the quotient train track in the positive ends of L is spiraling.

4.5 Uniqueness of the splitting sequence

There were several choices involved in the construction of the splitting sequence in Theorem 4.9. However, we claim that, viewed through an appropriate lens, the only choice that mattered was that of the train track T_+^∞. We investigate this now.

Let $\tau_0 \to \tau_1 \to \tau_2 \to \cdots$ be an infinite splitting sequence of train tracks in L (ie for each i, τ_{i+1} is obtained from τ_i by performing a single split. Further, suppose there exists a positive integer p such that $f(\tau_i) = \tau_{i+p}$ for all i and that p is the least such positive integer. Then we say that (τ_n) is an *f-periodic splitting sequence* with period p.

Suppose that (τ_n) is an f-periodic splitting sequence with period $p \geq 2$ and that, for some $i \geq 0$, there exists a track τ_i' such that $\tau_{i-1} \to \tau_i \to \tau_{i+1}$ and $\tau_{i-1} \to \tau_i' \to \tau_{i+1}$ differ by a commutation. Then the operation of replacing τ_{i+np} by $f^n(\tau_i')$ for all n such that $i+np > 0$ is called an *f-periodic commutation*. The result of performing an f-periodic commutation is another f-periodic splitting sequence. (For $p = 0$ or 1, there are no f-periodic commutations.)

If $\tau_0 \to \tau_1 \to \tau_2 \to \cdots$ is a splitting sequence such that some truncation $(\tau_n)_{n \geq N}$ is f-periodic, we say (τ_n) is *eventually f-periodic*. We say that two eventually f-periodic splitting sequences are *equivalent* if they have truncations which are related by finitely many f-periodic commutations. We will see in Section 7.6 that an eventually f-periodic splitting sequence determines a certain branched surface in the compactified mapping torus $\overline{M}_f$ of f, and that equivalent sequences determine the same branched surface up to isotopy.

Recall that in the construction of the splitting sequence in Theorem 4.9, we made the following choices:

(a) an efficient spiraling train track T_+^∞ carrying Λ_+^∞,

(b) a tiling of the end-cycles of L,

(c) an initial core $K = K_0$, and

(d) a train track $\tau_K = \tau_{K_0}$ fully carrying $\Lambda|_{K_0}$, which together with T_+^∞ gives rise to a train track τ_0 fully carrying Λ_+ which is endperiodic in E_0 and whose image in E_0/f is equal to T_+^∞.

In the proofs of Proposition 4.7 and Theorem 4.9, we showed that repeatedly performing core splits yields a sequence $\tau_0 \twoheadrightarrow \tau_1 \twoheadrightarrow \tau_2 \twoheadrightarrow \cdots$ such that for large i, τ_i is efficient and $f(\tau_i) = \tau_{i+1}$. We can then factor the core splits $\tau_i \twoheadrightarrow \tau_{i+1}$ into sequences of individual splits such that the result is an eventually f-periodic splitting sequence. By Lemma 2.21, the equivalence class of this resulting f-periodic splitting sequence is well defined. We denote the equivalence class by $\mathcal{S}(T_+^\infty, \mathcal{T}, K, \tau_K)$, where $\mathcal{T}$ denotes our choice of tiling.

We claim that $\mathcal{S}(T_+^\infty, \mathcal{T}, K, \tau_K)$ is determined up to equivalence by the train track T_+^∞. That is, up to equivalence, $\mathcal{S}(\cdot, \cdot, \cdot, \cdot)$ is independent of the last three arguments.

Lemma 4.11 *Let τ_K' be another choice of input for the function $\mathcal{S}(T_+^\infty, \mathcal{T}, K, \cdot)$. Then*

$$\mathcal{S}(T_+^\infty, \mathcal{T}, K, \tau_K) = \mathcal{S}(T_+^\infty, \mathcal{T}, K, \tau_K').$$

Proof For notational simplicity, in this proof we write τ for a train track on L constructed from τ_K and τ' for a train track constructed from τ_K'.

By the proof of Proposition 4.7 (see Remark 4.8), there is a number i such that the train tracks obtained by performing i core splits on τ and τ' are efficient. Hence by truncating and relabeling, we may assume that τ and τ' are efficient. By Lemma 4.3, $\tau|_{K_i}$ and $\tau'|_{K_i}$ are $\Lambda|_{K_i}$-compatible.

Now, as in the proof of Theorem 4.9, there exists a number N such that the $\Lambda_+|_{K_N}$-identification of the persistent cusps of $\tau|_{K_N}$ and $\tau'|_{K_N}$ is a poset isomorphism. Therefore τ and τ' have common core splittings, so $\mathcal{S}(T_+^\infty, \mathcal{T}, K, \tau_K) = \mathcal{S}(T_+^\infty, \mathcal{T}, K, \tau_K')$. □

In light of Lemma 4.11 above, we will drop the fourth argument of $\mathcal{S}(\cdot,\cdot,\cdot,\cdot)$ and write simply $\mathcal{S}(\cdot,\cdot,\cdot)$ going forward.

Lemma 4.12 *For all $i \geq 0$, $\mathcal{S}(T_+^\infty, \mathcal{T}, K) = \mathcal{S}(T_+^\infty, \mathcal{T}, K_i)$ (recall our convention $K = K_0$).*

Proof Up to equivalence, to obtain a sequence representing $\mathcal{S}(T_+^\infty, \mathcal{T}, K_i)$ we may start with the train track $\kappa^i(\tau)$ and take iterative core splits. On the other hand, a sequence representing $\mathcal{S}(T_+^\infty, \mathcal{T}, K)$ is obtained by taking iterative core splits of τ. The two sequences are related by truncation, so $\mathcal{S}(T_+^\infty, \mathcal{T}, K) = \mathcal{S}(T_+^\infty, \mathcal{T}, K_i)$. □

Lemma 4.13 *Given our fixed tiling $\mathcal{T}$ of the positive and negative end-cycles of L, let $K' = K_0'$ be another choice of core. Then $\mathcal{S}(T_+^\infty, \mathcal{T}, K) = \mathcal{S}(T_+^\infty, \mathcal{T}, K')$.*

Proof By our definition of a core, Λ_+ is disjoint from the components of $L \setminus\setminus K$ and $L \setminus\setminus K'$ which are neighborhoods of negative ends. Hence it suffices to assume that K and K' contain exactly the same negative tiles, and differ only by the positive tiles they contain.

Let Z be a positive end-cycle of L, and let t_1 be the lowest-index tile in the tiling of $\mathcal{U}_Z$ which is not already contained in K. We will first prove the statement of the lemma for $K' = K \cup t_1$.

For all $i \geq 0$, define K_i' so that K_{i+1}' is to K_i' as K_{i+1} is to K_i; that is, K_{i+1}' is obtained by adding to K_i', for each positive end-cycle, the tile of lowest index not already lying in K_i'.

Let τ_0 be the track chosen in (d) above. For $i \geq 0$, let τ_i be the maximal splitting of τ_0 in K_i, and τ_i' be the maximal splitting of τ_0 in K_i'. Note that there exists a natural number N such that for all $i \geq N$, we have $f(\tau_i) = \tau_{i+1}$ and $f(\tau_i') = \tau_{i+1}'$.

By factoring maximal splits into individual splits, the sequence $\tau_0, \tau_0', \tau_1, \tau_1', \tau_2, \tau_2', \dots$ may be factored into splits to give an eventually f-periodic splitting sequence

$$\tau_0 \to \cdots \to \tau_0' \to \cdots \to \tau_1 \to \cdots \to \tau_1' \to \cdots \to \tau_2 \to \cdots \to \tau_2' \to \cdots$$

representing $\mathcal{S}(T_+^\infty, \mathcal{T}, K)$. By truncating the sequence above to begin with τ_0', we see that $\mathcal{S}(T_+^\infty, \mathcal{T}, K) = \mathcal{S}(T_+^\infty, \mathcal{T}, K')$.

The special case we have just proven can be applied iteratively to prove the lemma for general K'. □

In light of Lemma 4.13, we will drop the third argument of $\mathcal{S}(\cdot,\cdot,\cdot)$ and write simply $\mathcal{S}(\cdot,\cdot)$ going forward.

We recall from our construction of junctures and tilings in Section 3.3 that an end-cycle Z gives rise to a compact surface F_Z and a homology class $u \in H^1(F_Z;\mathbb{Z})$. Any nonseparating $\mathbb{Z}$-weighted 1-manifold J which represents u and intersects ∂F_Z with consistent coorientation then defines a tiling $\mathcal{T}_Z$ of $\mathcal{U}_Z$.

Let Z be an end-cycle of L. We say that two tilings $\mathcal{T}_Z, \mathcal{T}'_Z$ of Z respectively determined by weighted cooriented 1-manifolds $J, J' \subset F_Z$ are *interleaved* if J and $-J'$ cobound an embedded subsurface in F_Z.

Lemma 4.14 *Let Z be a positive end-cycle of L. Suppose that $\mathcal{T}'$ is obtained from $\mathcal{T}$ by replacing the tiling $\mathcal{T}_Z$ of Z by an tiling $\mathcal{T}'_Z$ of Z which is interleaved with $\mathcal{T}_Z$. Then $\mathcal{S}(T_+^\infty, \mathcal{T}) = \mathcal{S}(T_+^\infty, \mathcal{T}')$.*

Proof Suppose that $\mathcal{T}$ and $\mathcal{T}'$ are induced by J and $J' \subset F_Z$. Then, because $\mathcal{T}$ and $\mathcal{T}'$ are interleaved, $F_Z - (J \cup J')$ consists of two surfaces, into one of which J points and into one of which J' points. Let these surfaces be called $W_{0.5}$ and W_1.

Let $\{t_i \mid i \in \mathbb{Z}\}$ be the tiles of $\mathcal{T}_Z$, each of which is naturally identified with $F_Z \setminus\!\setminus J$. Let $t_{i.5}$ be the subsurface of t_i corresponding to $W_{0.5}$.

By relabeling we can assume that t_0 is the lowest-index tile of $\mathcal{T}$ not contained in K_0.

Let $K_{i.5} = K_i \cup t_{i.5}$. Then $K_0 \subset K_{0.5} \subset K_1 \subset K_{1.5} \subset \cdots$. Let $\tau_{i.5}$ be the maximal splitting of τ in $K_{i.5}$. Now, similarly to the proof of Lemma 4.13, the sequence $\tau_0, \tau_{0.5}, \tau_1, \tau_{1.5}, \tau_2, \tau_{2.5}, \dots$ can be factored to give an eventually periodic splitting sequence

$$\tau_0 \to \cdots \to \tau_{0.5} \to \cdots \to \tau_1 \to \cdots \to \tau_{1.5} \to \cdots \to \tau_2 \to \cdots \to \tau_{2.5} \to \cdots$$

representing $\mathcal{S}(T_+^\infty, \mathcal{T})$. Truncating gives a sequence representing $\mathcal{S}(T_+^\infty, \mathcal{T}')$. Hence $\mathcal{S}(T_+^\infty, \mathcal{T}) = \mathcal{S}(T_+^\infty, \mathcal{T}')$. □

The following is a fairly well-known lemma:

Lemma 4.15 *Let F be a compact oriented surface, and let C and C' be two cooriented multicurves such that, for each boundary component α of F, all components of C and C' which meet α do so with consistent coorientation.*

If $[C] = [C']$ in $H_1(F, \partial F)$, then there exists a sequence of cooriented multicurves

$$C = C_0, C_1, \dots, C_n = C'$$

such that:

- *For each boundary component α of F, all components of $C_0, \dots, C_n$ which meet α do so with consistent coorientation.*
- *For $0 \le i \le n-1$, C_i and $-C_{i+1}$ are the boundary of an embedded subsurface W_i.*

Proof This is asserted in [Gabai 1987], and we provide a proof here for completeness. We make the convention that the boundary of an oriented manifold is cooriented into the manifold.

In the case where F is closed, the lemma follows from [Hatcher 2008]. We will use this to treat the case when F has nonempty boundary. We can double C and C' across ∂F to get collections of closed curves DC and DC' on the doubled surface F such that $[DC] = [DC']$ in $H_1(DF)$. Then, applying [Hatcher 2008], we have a sequence of cooriented multicurves

$$DC = \widehat{C}_0, \widehat{C}_1, \dots, \widehat{C}_n = DC'$$

such that, for $0 \le i \le n-1$, $\widehat{C}_i$ and $-\widehat{C}_{i+1}$ are the boundary of an embedded subsurface $\widehat{W}_i$. What we will do is to restrict $\widehat{C}_i$ and $\widehat{W}_i$ to F, and then perform some operations to obtain the desired sequence $C = C_0, C_1, \dots, C_n = C'$ on F.

The details are as follows. For each $\widehat{C}_i$, consider the restriction $\widehat{C}_i \cap F$. Up to a small perturbation, we can assume that this is a multicurve on F. However, its components might not meet components of ∂F with consistent coorientations. To fix this, we inductively perform cut-and-paste along innermost pairs of intersection points $\widehat{C}_i \cap \partial F$ that are cooriented toward each other. See Figure 18, top. Call the resulting multicurve C_i. Notice that DC and DC' meet each boundary component of F with consistent coorientations, so in this case the cut-and-paste operation is not necessary and we have $C_0 = C$ and $C_n = C'$.

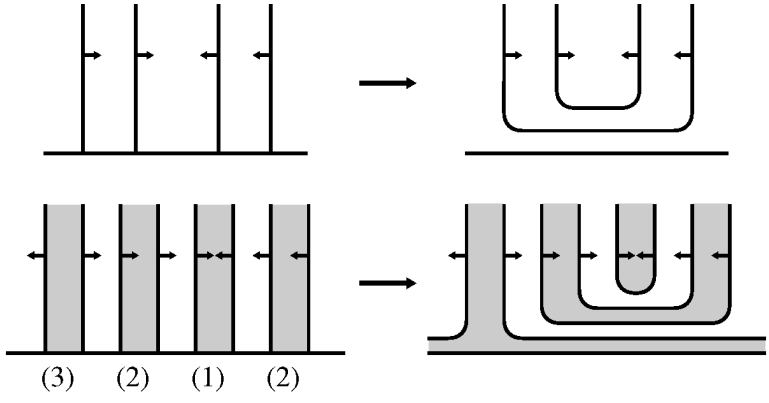

Figure 18: A sequence on DF restricts to a sequence on F, up to performing cut-and-paste along ∂F if necessary.

We claim that for each $0 \le i \le n-1$, C_i and $-C_{i+1}$ bound an embedded subsurface W_i. To define W_i, consider the restriction $\widehat{W}_i \cap F$. For each boundary component α of F, if $\widehat{W}_i \cap \alpha$ is a union of intervals, then each such interval I is one of three types:

(1) The endpoints of I lie on $\widehat{C}_i$, and hence are both cooriented inwards.

(2) One endpoint of I lies on $\widehat{C}_i$ and the other lies on $\widehat{C}_{i+1}$; hence they are cooriented in the same direction.

(3) The endpoints of I lie on $\widehat{C}_{i+1}$, and hence are both cooriented outwards.

We first move $\widehat{W}_i \cap \alpha$ away from α near intervals of type (1). Then, inductively, for innermost pairs of intervals of type (2) whose endpoints are cooriented toward each other, we join $\widehat{W}_i \cap \alpha$ along the pair. Finally, if there are any intervals of type (3), we append a small collar neighborhood of α to $\widehat{W}_i \cap \alpha$. See Figure 18, bottom. Call the resulting surface W_i.

It is straightforward to check that the boundary of W_i is the union of C_i and $-C_{i+1}$, as desired. □

Lemma 4.16 *Let $\mathcal{T}'$ be another tiling of L. Then $\mathcal{S}(T_+^\infty, \mathcal{T})$ is equivalent to $\mathcal{S}(T_+^\infty, \mathcal{T}')$.*

Proof By applying Lemma 4.15 to one end-cycle at a time, $\mathcal{T}$ and $\mathcal{T}'$ are related by a sequence of tilings such that each one is interleaved with the next. The lemma then follows from Lemma 4.14. □

Combining the sequence of lemmas in this subsection gives the following theorem:

Theorem 4.17 *Up to equivalence, the splitting sequence $\mathcal{S}(T_+^\infty, \mathcal{T}, K, \tau_K)$, which is defined by factoring repeated core splits of an efficient f-endperiodic train track τ_0 carrying the positive Handel–Miller lamination, depends only on the train track T_+^∞ induced by τ_0 on $\mathcal{U}_+/\langle f \rangle$.*

Hence we are justified in dropping the last three arguments of $\mathcal{S}(\cdot,\cdot,\cdot,\cdot)$ and simply writing $\mathcal{S}(\cdot)$ to denote the equivalence class of any sequence obtained from the core splitting construction of Theorem 4.9.

5 Endperiodic maps and sutured manifolds

Up to this point in the paper, we have been dealing with surfaces and automorphisms on surfaces. An equivalent way of studying this data is to consider the mapping tori of automorphisms and their associated suspension flows. This will be our perspective from this point forward. To this end, in this section we will describe how one passes from the 2-dimensional to the 3-dimensional picture, and prove some lemmas for later use.

5.1 Sutured manifolds and compactified mapping tori

A *sutured manifold* (Q, γ) is an oriented, compact 3-manifold Q with decorated boundary. We have $\gamma \subset \partial Q$ and $\gamma = A(\gamma) \cup T(\gamma)$, where $A(\gamma)$ is a union of annuli and $T(\gamma)$ is a union of tori. Each component of $A(\gamma)$ contains an oriented curve at its core called a *suture*. Let $R(\gamma) = \partial Q \setminus\setminus \gamma$; sometimes

$R(\gamma)$ is called the *tangential boundary* of Q and γ the *transverse boundary*. We require that each component of $R(\gamma)$ be oriented, and that each component of $\partial R(\gamma)$, when given the boundary orientation, have the homology class of a suture in $H_1(\gamma)$. Since Q is oriented, each component of $\partial R(\gamma)$ has a well-defined coorientation either pointing out of or into Q. The sets of components whose coorientations point out of and into Q are denoted by $R_+(\gamma)$ and $R_-(\gamma)$, respectively. A consequence of this definition is that, for every component A of $A(\gamma)$, one component of A lies on R_+ and the other lies on R_-. Often, when there is no chance of confusion, we omit reference to γ, for example writing Q instead of (Q,γ) or $R_\pm$ instead of $R_\pm(\gamma)$.

A sutured manifold is *atoroidal* if any essential torus is boundary parallel.

A *foliation* $\mathcal{F}$ of a sutured manifold (Q,γ) is a 2-dimensional cooriented foliation of Q which is transverse to γ and tangent to $R(\gamma)$ in such a way that the coorientation of $\mathcal{F}$ restricts to the coorientation of $R(\gamma)$. We say $\mathcal{F}$ is *taut* if each leaf of $\mathcal{F}$ intersects either a closed curve transverse to $\mathcal{F}$ or an interval transverse to $\mathcal{F}$ with one endpoint on R_- and the other on R_+. We say that $\mathcal{F}$ is *depth one* if $Q-(R_+\cup R_-)$ fibers over S^1 with fibers the noncompact leaves of $\mathcal{F}$.

A *depth one sutured manifold* is a sutured manifold admitting a depth one foliation and having no torus components in $R_\pm$.

For us, a *semiflow* on a sutured manifold (Q,γ) is a 1-dimensional oriented foliation φ, whose leaves we call *orbits*, that points inward along R_- and outward along R_+, and which is tangent to γ in such a way that each orbit contained in $A(\gamma)$ is a properly embedded oriented interval with initial endpoint on $R_-(\gamma)$ and terminal endpoint on $R_+(\gamma)$. For us it will not be important to explicitly parametrize a semiflow. However, if one chooses a parametrization, orbits are not generally defined for all forward or backward time.

The following is well known and appears as [Cantwell et al. 2021, Lemma 12.5].

Lemma 5.1 *Let $f: L\to L$ be an endperiodic map. Then there exists a sutured manifold $\overline{M}_f$, a taut depth one foliation $\mathcal{F}$ of $\overline{M}_f$, and a semiflow φ_f of $\overline{M}_f$ such that L is homeomorphic to each noncompact leaf of $\mathcal{F}$ and the first return map induced by φ_f is equal to f.*

We call the semiflow φ_f the *suspension semiflow* of f.

The manifold $\overline{M}_f$ is called the *compactified mapping torus* of f because it is constructed by compactifying the mapping torus $M_f = L\times[0,1]/\big((x,1)\sim(f(x),0)\big)$. The compactification works by attaching copies of the surfaces $\mathcal{U}_+/\langle f\rangle$ and $\mathcal{U}_-/\langle f\rangle$ to M_f. (Recall that $\mathcal{U}_+$ and $\mathcal{U}_-$ are the positive and negative escaping sets of f, respectively. See Section 3.3.) Thus this compactification is obtained by gluing on one ideal point for each escaping end of an f-orbit. For the details of this construction, see [Field et al. 2023, Section 3]; they work only with "irreducible" endperiodic maps on boundaryless surfaces but their construction goes through in our setting also.

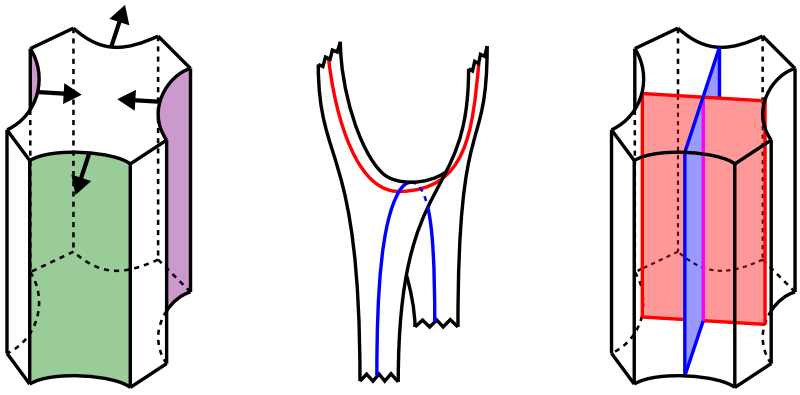

Figure 19: Left: the compactified mapping torus $\overline{M}_f$ for the map $f = \left(\begin{smallmatrix} 2 & 0 \\ 0 & 1/2 \end{smallmatrix}\right)$, where the top should be identified with the bottom to give a solid torus. The green and purple annuli are R_+ and R_-, respectively. Center: the surface L sits inside $\overline{M}_f$ as shown, with two ends spiraling onto R_+ and two ends spiraling onto R_-. Right: the laminations $\mathcal{L}_+$ and $\mathcal{L}_-$.

The sutured structure on $\overline{M}_f$ is as follows. The tangential boundary $R_\pm$ arises from the copy of $\mathcal{U}_\pm/\langle f \rangle$ added to M_f during the compactification. A component of $T(\gamma)$ arises from a compact boundary component of L whose f-orbit has finitely many components. A component of $A(\gamma)$ can arise in two ways: from a noncompact boundary component of L, or from a compact boundary component of L whose f-orbit has infinitely many components.

If f is a Handel–Miller map, then f preserves the Handel–Miller laminations and induces the spiraling laminations $\Lambda^\infty_\pm$ on $\mathcal{U}_\pm/\langle f \rangle$ (see Lemma 3.11). We can canonically identify $R_\pm$ with $\mathcal{U}_\pm/\langle f \rangle$ (see [Cantwell et al. 2021, Lemma 12.36], so we can think of $\Lambda_\pm$ as a subset of $R_\pm$. Moreover, if we consider the union of all φ_f-orbits passing through points in $\Lambda_\pm \subset L \subset \overline{M}_f$, we obtain a pair of 2-dimensional laminations $\mathcal{L}^u$, $\mathcal{L}^s$ such that $\mathcal{L}^u \cap R_+ = \Lambda^\infty_+$ and $\mathcal{L}^s \cap R_- = \Lambda^\infty_-$. We call these the *unstable* and *stable Handel–Miller laminations*, respectively.

Example 5.2 Let $L = \{(x, y) \mid xy \le 1\}$ and let $f : L \to L$ be the map $\left(\begin{smallmatrix} 2 & 0 \\ 0 & 1/2 \end{smallmatrix}\right)$ from Example 3.8. Then $\overline{M}_f$ is a solid torus with four longitudinal sutures, each one homotopic to the core of the solid torus. Each of R_+ and R_- has two components, both of which are annuli. The depth one foliation of $\overline{M}_f$ is known as a "stack of chairs". Each of $\mathcal{L}^u$ and $\mathcal{L}^s$ consists of a single annulus connecting the two components of R_+ and the two components of R_-, respectively. The laminations Λ^∞_+ and Λ^∞_- each have two components, each of which is a circle. See Figure 19. ◁

5.2 Useful lemmas about the unstable lamination

In this subsection, we will state and prove some lemmas about the unstable Handel–Miller lamination $\mathcal{L}^u$ in the setting above. These facts will play a role in Sections 8 and 9. Symmetric statements hold for the stable Handel–Miller lamination, even though those will not play a role in this paper.

Lemma 5.3 *$\mathcal{L}^u$ has no I-fibered complementary regions whose boundary components lie along $\mathcal{L}^u$. Here a complementary region C is I-fibered if C fibers over some surface F with I fibers.*

Proof Suppose otherwise. Let us identify the surface L with a fixed leaf of $\mathcal{F}$. L intersects ∂C in leaves of Λ_+, hence each component of this intersection is a copy of $\mathbb{R}$. Meanwhile, L is incompressible in $\overline{M}_f$ hence in C. Since L is incompressible in $\overline{M}_f$, $L \cap C$ is incompressible in C, from which it can deduced that each component of $L \cap C$ is homeomorphic to $\mathbb{R} \times [0,1]$, meaning that there is a complementary region of Λ_+ in L homeomorphic to $\mathbb{R} \times [0,1]$. But this is impossible since the leaves of Λ_+ are geodesics for some standard hyperbolic metric on L. □

Lemma 5.4 *Let γ be a closed orbit of φ_h on a leaf A of $\mathcal{L}^u$. Suppose A is nonisolated from some side. Then the holonomy of $\mathcal{L}^u$ along γ is topologically contracting on that side, ie there is an immersion of a rectangle $\alpha\colon [0,1]_t \times [0,1]_s \to \overline{M}_f$ such that $\alpha([0,1] \times \{0\})$ traverses γ for increasing t, $\alpha([0,1] \times \{1\})$ lies on a leaf of $\mathcal{L}^u$, and $\alpha(\{1\} \times [0,1]) \subsetneq \alpha(\{0\} \times [0,1])$.*

Proof The leaf A is the suspension of some periodic leaf l_+ of Λ_+. Applying [Cantwell et al. 2021, Corollary 6.11] to l_+, there is a leaf l_- of Λ_- and a periodic point $x \in l_+ \cap l_-$.

Notice that l_+ is nonisolated from the side that suspends to the nonisolated side of A. Now, applying [Cantwell et al. 2021, Corollary 6.11] again but to l_- this time (and also using [Cantwell et al. 2021, Corollary 6.15]), we see that the holonomy is contracting on our fixed side of l_+, which implies the lemma. □

5.3 Reeb sutured manifolds

We now define Reeb sutured manifolds, which generalize sutured manifolds in the same way that Reeb endperiodic maps generalize endperiodic maps. We will also explain Construction 5.5, which converts a Reeb sutured manifold into a sutured manifold, analogous to endperiodization (Construction 3.18).

A *Reeb sutured manifold* (P, γ) is defined similarly to a sutured manifold. The only difference is that $A(\gamma)$ is allowed to contain components that have both boundary components on R_+ or both boundary components on R_-. Such an annulus is called a *Reeb annulus* and does not have a suture at its core.

A *foliation* of a Reeb sutured manifold is defined just as for foliations of sutured manifolds, with the additional requirement that the restriction of the foliation to each Reeb annulus be a Reeb foliation.

A *semiflow* on a Reeb sutured manifold is defined like a semiflow on a sutured manifold except on the Reeb annuli. If A is a Reeb annulus touching only R_+ (resp. R_-), orbits of the semiflow do not end on R_+ (resp. R_-) in the backward (resp. forward) direction.

If (P, γ) is a Reeb sutured manifold, there is a naturally associated sutured manifold obtained by performing the following procedure for each Reeb annulus of $A(\gamma)$. Suppose without loss of generality

that A connects R_+ to R_+. Subdivide A into three annuli A_1, A_2, A_3, labeled so that A_1 and A_3 touch ∂A and $A_2 \subset \operatorname{int} A$. Then modify $A(\gamma)$ and $R(\gamma)$ by adding A_2 to $R_-(\gamma)$, and replacing A by A_1 and A_3 in $A(\gamma)$. Place sutures in A_1 and A_3, oriented so as to be compatible with the orientations of R_+ and R_-. The result is an honest sutured manifold (P', γ'), called the *de-Reebification* of (P, γ).

Construction 5.5 (mapping tori of Reeb endperiodic maps) Let $f : L \to L$ be a Reeb endperiodic map. There is a compactified mapping torus $\overline{M}_f$ of f defined just as for endperiodic maps, but $\overline{M}_f$ is in general only a Reeb sutured manifold. However, there is still a depth one foliation $\mathcal{F}$ of $\overline{M}_f$ whose depth one leaves are homeomorphic to L, and a semiflow on $\overline{M}_f$ whose first return map is conjugate to f under this identification.

Let $f' : L' \to L'$ be the endperiodization of f (Construction 3.18), where L' is L minus finitely many boundary points. Let $\mathcal{F}'$ be the associated depth one foliation of $\overline{M}_{f'}$. Then $\overline{M}_{f'}$ is naturally identified with the de-Reebification of $\overline{M}_f$, and $\mathcal{F}'$ is obtained from "spinning" $\mathcal{F}$ around the annuli added to the tangential boundary of $\overline{M}_f$ in the de-Reebification. ◁

6 Veering branched surfaces

In this section we start working with branched surfaces and laminations in 3-manifolds. The prototype of the laminations we consider is the unstable Handel–Miller lamination in a compactified mapping torus. In this context, the natural type of branched surfaces to consider are (unstable) dynamical branched surfaces. In the first two subsections, we will recall the definition of these and some related ideas. Essentially all the definitions presented in these subsections are due to Mosher.

Then we define veering branched surfaces in sutured manifolds, the main objects of study in the rest of the paper. The rest of the section develops some of the theory of these veering branched surfaces, most of it being adapted from the theory in nonsutured manifolds.

6.1 Dynamic branched surfaces

A *branched surface* B is a 2-complex embedded in a 3-manifold such that every point in B has a neighborhood smoothly modeled on a point in the space shown in Figure 20, top left. In particular, every point in B has a well-defined tangent space.

If (Q, γ) is a sutured manifold, a *vertical branched surface* in Q is a 2-complex $B \subset Q$ such that $B \cap \operatorname{int} Q$ is a branched surface, and each point in $B \cap \partial Q$ has a neighborhood modeled on a point in the space in Figure 20, top right.

The union of the nonmanifold points of a vertical branched surface B is called the *branch locus* of B and denoted by $\operatorname{brloc}(B)$. This set decomposes as a union of smooth, properly immersed curves and arcs, called *branch curves* and *branch arcs*, respectively. A *component* of $\operatorname{brloc}(B)$ refers to a branch curve or branch arc (note that in general this is not a connected component of $\operatorname{brloc}(B)$). A *branch segment* is the

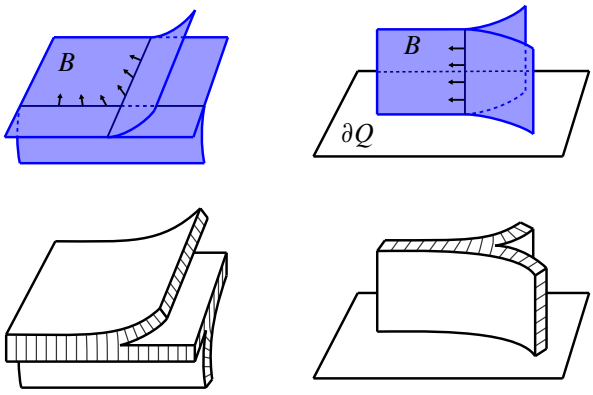

Figure 20: Top: the local models for vertical branched surfaces at points in $\mathrm{int}(Q)$ and in ∂Q. The maw vector field is indicated using arrows along the branch locus. Bottom: the local models for a standard neighborhood of a vertical branched surface.

image of a smooth immersion $I \to \mathrm{brloc}(B)$. The nonmanifold points of $\mathrm{brloc}(B)$ are called the *triple points* of B. A mnemonic for this definition is that near such a point, the branched surface is the quotient of a stack of three disks such that each disk is C^1 embedded.

There is a continuous vector field on $\mathrm{brloc}(B)$, called the *maw vector field*, defined up to homotopy by the property that away from triple points it always points from the 2-sheeted side to the 1-sheeted side of $\mathrm{brloc}(B)$. The maw vector field induces a coorientation on each branch arc and branch loop, which we call the *maw coorientation*.

A *sector* is a component of $B \setminus\setminus \mathrm{brloc}(B)$. Note that each sector is naturally a surface with corners, with the sides lying along $\mathrm{brloc}(B)$ and ∂Q.

The intersections $B \cap R_+$ and $B \cap R_-$ are train tracks on R_+ and R_-, respectively. We refer to these as the *boundary train tracks* of B, and denote their union by ∂B.

A *lamination* Λ in a sutured manifold Q is a partition of a closed subset of Q into connected 2-manifolds such that each point $x \in Q$ has a neighborhood $\mathbb{R}^2 \times \mathbb{R}$ with elements of the partition intersecting the neighborhood of the form $\mathbb{R}^2 \times C$ (if x is in the interior of Q) or a neighborhood $[0,\infty) \times \mathbb{R} \times \mathbb{R}$ with elements of the partition intersecting the neighborhood in sets of the form $[0,\infty) \times \mathbb{R} \times C$ for some closed set C (if x is on the boundary of Q). The elements of the partition are called the *leaves* of Λ. As with 1-dimensional laminations, we will often conflate a lamination with the union of its leaves.

If Λ is a lamination in Q, then $\Lambda \cap R_+$ and $\Lambda \cap R_-$ are laminations on R_+ and R_-, respectively. We refer to these as the *boundary laminations* of Λ.

Let B be a branched surface in Q and let Λ be a lamination on Q. A *standard neighborhood* of B is a closed regular neighborhood N of τ which is foliated by line segments, called *ties*, such that each line segment meets the sectors of B transversely. See Figure 20, bottom.

The *vertical boundary* of N, denoted by $\partial_v N$, is the complement of the union of endpoints of the ties in $\partial N \setminus \partial Q$. The *horizontal boundary* of N, denoted by $\partial_h N$, is the complementary region of $\partial_v N$ in $\partial N \setminus \partial Q$. Notice that in this definition, $\partial_v N$ is a union of 1-manifolds, which may differ from some conventions in the literature. We chose to define N in this way for better analogy with the definitions for train tracks in Section 2.

We remark that $\partial N \cap \partial Q$ is neither in the horizontal boundary nor in the vertical boundary of N. Also notice that $\partial N \cap R_\pm$ is a standard neighborhood of the boundary train track $B \cap R_\pm$.

By collapsing the ties, we get a projection map $N \to B$. We say that B *carries* Λ if B has a standard neighborhood N such that Λ is embedded in N in such a way that its leaves are transverse to the ties. In this case, we say that the map $\Lambda \hookrightarrow N \to B$ is the *carrying map* and N is a *standard neighborhood* of Λ. Further, we say that τ *fully carries* Λ if Λ intersects every tie of N.

We now bring dynamics into the picture. An *unstable dynamic branched surface* in Q is an ordered pair (B, V) where B is a vertical branched surface and V is a nonvanishing C^0 vector field on M such that

- V is tangent to γ, inward-pointing along R_- and outward-pointing along R_+,
- V is tangent to B, and
- $V|_{\mathrm{brloc}(B)}$ is a maw vector field for B.

V in this definition is said to be *smooth* if it is smooth on $B \setminus \mathrm{brloc}(B)$ and has a unique forward trajectory starting at each point of B.

Symmetrically, a *stable dynamic branched surface* in Q is an ordered pair (B, V) where B is a vertical branched surface and V is a nonvanishing C^0 vector field on M such that

- V is tangent to γ, inward-pointing along R_- and outward-pointing along R_+,
- V is tangent to B, and
- $-V|_{\mathrm{brloc}(B)}$ is a maw vector field for B.

V in this definition is said to be *smooth* if it is smooth on $B \setminus \mathrm{brloc}(B)$ and has a unique backward trajectory starting at each point of B.

In this paper, except for the appendix, V will always be smooth. Hence, for the sake of brevity, we will implicitly include V being smooth as part of the definition of an unstable or stable branched surface. In the appendix we will need to relax the definitions slightly in order to have a single vector field V such that (B^u, V) and (B^s, V) are unstable and stable dynamic branched surfaces, respectively.

Remark 6.1 As Mosher [1996, Section 1.5] points out, the existence of a dynamic vector field V for a given branched surface $B \subset M$ is a purely combinatorial property of B. Indeed, such a vector field can always be constructed along $\mathrm{brloc}(B)$. Whether it can be extended to all of B and then to M depends only on the combinatorics of the sectors of B and the combinatorics of the components of $M \setminus\setminus B$, respectively.

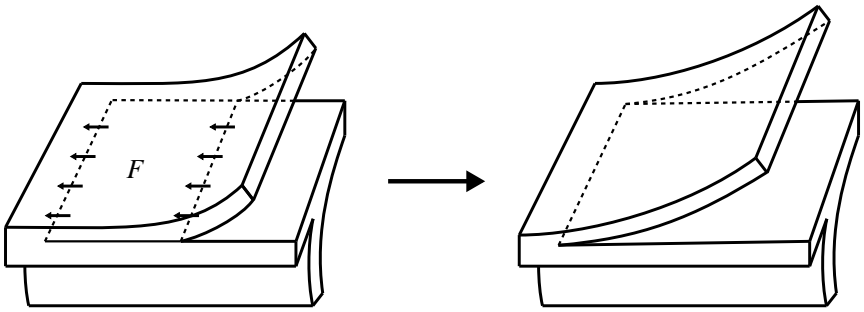

Figure 21: Dynamically splitting a dynamic branched surface along a dynamic splitting surface F.

As such we generally think of V as a placeholder for some combinatorial data, unless we are explicitly using it for one of our arguments. ◁

Finally, we recall the definition of dynamically splitting an unstable dynamic branched surface B.

Let $N(B)$ be a standard neighborhood of B. Let F be a surface embedded in $N(B)$ such that $\partial F = \partial_v F \cup \partial_i F$, where $\partial_v F \subset \partial_v N(B)$ and $\partial_i F \subset \operatorname{int} N(B)$, and such that F is transverse to the ties of $N(B)$. Then we can pull back the vector field V on B to F via the composition $F \to N(B) \to B$. If the image of $\partial_i F$ under $N(B) \to B$ is transverse to $\operatorname{brloc}(B)$, and if the pulled-back vector field points outwards along $\partial_i F$, then we call F a *dynamic splitting surface*. By *dynamically splitting along* F, we refer to the operation of cutting $N(B)$ along F, then collapsing the remaining intervals to get a branched surface B_F. There is a natural choice of vector field making B_F an unstable branched surface. See Figure 21.

Let $F \looparrowright B$ be an immersed surface with $\partial F = \partial_v F \cup \partial_i F$, where $\partial_v F$ lies along $\operatorname{brloc}(B)$. Suppose F can be lifted to a dynamic splitting surface $F' \subset N(B)$. Then, as long as F' is clear from context, we will refer to dynamically splitting B along F' as *dynamically splitting B along F*.

6.2 Dynamic manifolds

Following [Mosher 1996], we define a 3-*manifold with corners* to be a 3-manifold M with boundary such that every point p has a neighborhood modeled on one of the following six closed subsets of $\mathbb{R}^3$, where p is identified with the origin:

- Interior point: all of $\mathbb{R}^3$.
- Boundary point: the upper half-space $\{(x, y, z) \mid z \geq 0\}$.
- Apex: the closed orthant $\{(x, y, z) \mid x, y, z \geq 0\}$.
- (Convex) corner edge: $\{(x, y, z) \mid x, y \geq 0\}$.
- Gable: $\{x, y, z \mid x \geq 0, z \leq f(y)\}$, where $f : \mathbb{R} \to (-\infty, 0]$ is a cusp function, eg $f(y) = -\sqrt{|y|}$.
- Cusp edge: $\{x, y, z \mid z \leq f(y)\}$, where f is as above.

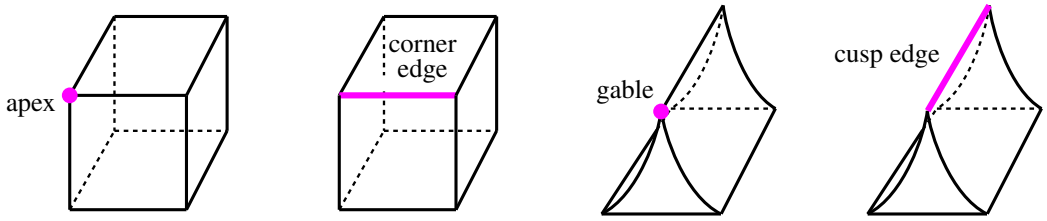

Figure 22: Illustrations of an apex, corner edge, gable and cusp edge.

See Figure 22. A connected component of the set of boundary points is called a *face* of the manifold with corners. A connected component of the set of corner edge points or cusp edge points is called a *corner edge* or *cusp edge*, respectively.

Example 6.2 A sutured manifold (Q,γ) can be considered as a 3-manifold with corners by taking the set of (convex) corner edges to be the curves of intersection between $R_+(\gamma)$ and $A(\gamma)$ and between $R_-(\gamma)$ and $A(\gamma)$. There are no apexes, gables or cusp edges in this example. ◁

Going forward, we will always view sutured manifolds as 3-manifolds with corners in this way.

We next define a dynamic manifold. Consider a triple (D,V,λ), where D is a 3-manifold with corners, V is a continuous nonvanishing vector field on D, and λ is a labeling

$$\lambda\colon\{\text{faces of } D\}\to\{\boldsymbol{p},\boldsymbol{m},\boldsymbol{b},\boldsymbol{s},\boldsymbol{u}\},$$

where the labels stand for plus, minus, bare, stable and unstable, respectively. This assigns each cusp edge and corner edge a pair of labels and we can classify edges by this pair of labels. For example a $\boldsymbol{uu}$-edge is one which has a $\boldsymbol{u}$-face on both of its sides.

A *dynamic manifold* is such a triple (D,V,λ) which satisfies the following:

(a) V points out of D along all $\boldsymbol{p}$-faces and into D along all $\boldsymbol{m}$-faces.

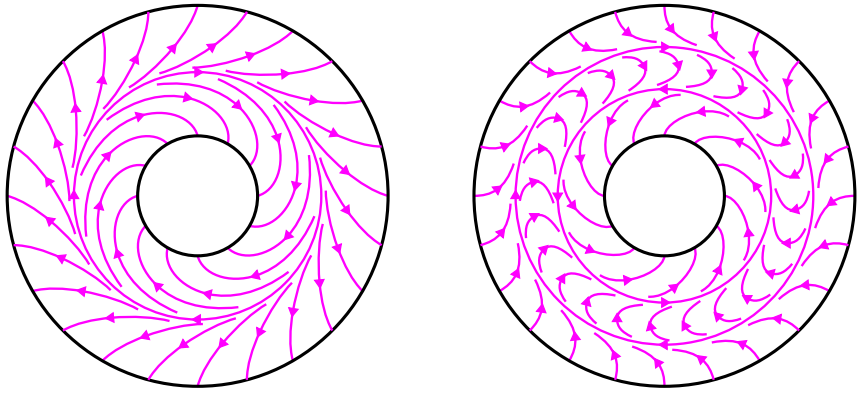

Figure 23: The trajectories of two different vector fields on an annulus. The vector field on the left is circular, while the vector field on the right is not.

(b) V is tangent to all $\boldsymbol{b}$-, $\boldsymbol{s}$- and $\boldsymbol{u}$-faces.

(c) All $\boldsymbol{ss}$-, $\boldsymbol{uu}$- and $\boldsymbol{pm}$-edges are cusp edges.

(d) V points into D along all $\boldsymbol{ss}$-edges and points out of D along all $\boldsymbol{uu}$-edges.

(e) There are no $\boldsymbol{pp}$-, $\boldsymbol{mm}$-, $\boldsymbol{bb}$-, $\boldsymbol{bs}$- or $\boldsymbol{bu}$-edges.

The motivation behind the above axioms is that a dynamic manifold should be thought of as a complementary component of the union of a stable dynamic branched surface B^s and an unstable dynamic branched surface B^u intersecting transversely (the $\boldsymbol{b}$/bare labels correspond to sutures). For example, condition (a) corresponds to the fact that a dynamic vector field points outward along R_+ and inward along R_-. Condition (d) corresponds to the fact that a dynamic vector field restricts to the maw vector field on $\operatorname{brloc}(B^u)$, and to the negative of the maw vector field on $\operatorname{brloc}(B^s)$.

Remark 6.3 It follows from the axioms that all $\boldsymbol{u}$-faces which are not incident to $\boldsymbol{s}$-faces (and vice versa) are annuli or tori. Indeed, the vector field V must point outward (inward) along the entire boundary of such a $\boldsymbol{u}$-face ($\boldsymbol{s}$-face), so this follows from Poincaré–Hopf and the fact that V is nonsingular. ◁

Definition 6.4 (circular, dynamic orientation, (in)coherent cusp circle) Let V be a nonvanishing vector field generating a forward semiflow on a manifold M, possibly with boundary. We say V is *circular* if there exists a map $g\colon M \to S^1$ such that, if $\gamma(t)$ is a monotonic parametrization of a trajectory of V, then $g(\gamma(t))$ is a monotonic path in S^1. See Figure 23 for an example and a nonexample.

If γ is a $\boldsymbol{uu}$-cusp circle of a dynamic manifold, then, by Remark 6.3, the $\boldsymbol{u}$-faces A_1 and A_2 to either side of γ are annuli. If V is circular on both of these faces, then there are induced orientations on $H_1(A_1)$ and $H_1(A_2)$. This orientation of $H_1(A_i)$ is called the *dynamic orientation*. If the dynamic orientations of $H_1(A_1)$, $H_1(A_2)$ match up along γ, we say γ is a *coherent* cusp circle. Otherwise we say γ is *incoherent*. ◁

The following lemma proves that a vector field of the type shown in Figure 23, left, is circular:

Lemma 6.5 *Let $\mathcal{R}$ be a cooriented Reeb foliation of an annulus A, and let V_A be a vector field on A which is positively transverse to $\mathcal{R}$. Then V is circular.*

Proof If we place a Riemannian metric on A, then, by compactness, there is some ϵ such that the vector field V_A makes an angle of at least ϵ with any vector tangent to $\mathcal{R}$. Hence we can perturb the tangent distribution of $\mathcal{R}$ slightly to obtain a foliation $\mathcal{R}'$ with tangent distribution close enough to that of $\mathcal{R}$ so that V_A is positively transverse to $\mathcal{R}'$, but whose leaves are properly embedded line segments. The map to the leaf space of $\mathcal{R}'$ now certifies the circularity of V_A. □

As examples, we now define two types of dynamic manifolds following Mosher. Later, these types of dynamic manifolds will feature in the definition of a "very full" dynamic branched surface.

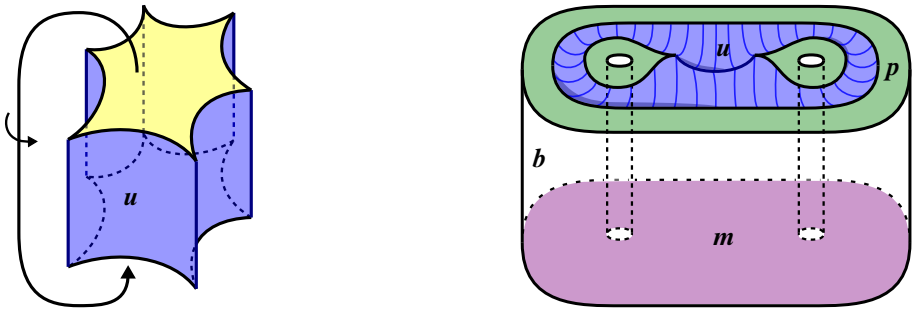

Figure 24: A $\boldsymbol{u}$-cusped solid torus (left) and a $\boldsymbol{u}$-cusped product (right).

Definition 6.6 ($\boldsymbol{u}$-cusped torus) Let Δ be a closed disk whose boundary is smooth with the exception of $n \geq 2$ cusps, and let $f\colon \Delta \to \Delta$ be a diffeomorphism. The mapping torus M of f is a 3-manifold with corners homeomorphic to a solid torus. There are $\frac{n}{p}$ circular cusp edges of M, where p is the period of a cusp of Δ under f. Likewise, there are $\frac{n}{p}$ annular faces of M. We label each of these faces $\boldsymbol{u}$. Take a circular vector field V on M that gives it the structure of a dynamic manifold. Equipped with such a vector field, M is called a *$\boldsymbol{u}$-cusped solid torus*. See Figure 24, left. Define the *index* of M to be $1 - \frac{n}{2}$, which is the index of a meridional disk intersecting the $\boldsymbol{uu}$-cusp curves minimally.

A *$\boldsymbol{u}$-cusped torus shell* is defined similarly, but replacing Δ by a closed annulus whose boundary is smooth with the exception of $n \geq 1$ cusps on a single boundary component. The annulus faces are labeled $\boldsymbol{u}$, the torus face is labeled $\boldsymbol{b}$, and circularity of the vector field is defined as for the $\boldsymbol{u}$-cusped solid torus. Notice that there is no canonical meridian in a $\boldsymbol{u}$-cusped torus shell, so there is no canonical way to assign an index as in the nonpunctured case.

A *$\boldsymbol{u}$-cusped torus* refers to a $\boldsymbol{u}$-cusped solid torus or a $\boldsymbol{u}$-cusped torus shell. We define *$\boldsymbol{s}$-cusped solid tori*, *$\boldsymbol{s}$-cusped torus shells* and *$\boldsymbol{s}$-cusped tori* symmetrically. ◁

Definition 6.7 ($\boldsymbol{u}$-cusped product) Suppose that D is homeomorphic to $S \times [0,1]$, where S is a compact surface with $\operatorname{index}(S) \leq 0$. We say that (D, V, λ) is a *$\boldsymbol{u}$-cusped product* if the following hold:

(a) $S \times \{0\}$ is an $\boldsymbol{m}$-face.

(b) Each component of $\partial S \times [0,1]$ is a $\boldsymbol{b}$-face.

(c) $S \times \{1\}$ is a union of $\boldsymbol{p}$-faces and $\boldsymbol{u}$-faces.

(d) Each orbit of the V-semiflow that does not accumulate on a $\boldsymbol{u}$-face either terminates on a $\boldsymbol{p}$-face or a $\boldsymbol{uu}$-cusp.

(e) Each $\boldsymbol{p}$-face has nonpositive index.

(f) V is circular on each $\boldsymbol{u}$-face.

(g) Each $\boldsymbol{uu}$-cusp circle is incoherent.

The definition of *s-cusped product* is symmetric. See Figure 24 for an example of a $\boldsymbol{u}$-cusped product. Note that because $\boldsymbol{bu}$-edges are prohibited, the $\boldsymbol{u}$-faces in $S \times \{1\}$ must lie entirely in $\operatorname{int}(S \times \{1\})$. ◁

Remark 6.8 In this paper the $\boldsymbol{u}$-cusped products we encounter will not have $\boldsymbol{uu}$-cusp circles, but we include condition (g) to be consistent with [Mosher 1996] and with our future work. ◁

The following lemma is inspired by [Mosher 1996, Remark preceding Proposition 4.6.1], and allows for the recognition of $\boldsymbol{u}$-cusped products. We record it here for later use.

Lemma 6.9 [Mosher 1996] *Let (Q, V, λ) be a connected dynamic manifold such that*

(1) *Q has no $\boldsymbol{s}$-faces,*

(2) *each backward trajectory not lying in a $\boldsymbol{u}$-face terminates on an $\boldsymbol{m}$-face,*

(3) *each $\boldsymbol{b}$-face is an annulus with boundary consisting of one $\boldsymbol{pb}$-circle and one $\boldsymbol{mb}$-circle, and*

(4) *there are no $\boldsymbol{pm}$-edges.*

If each $\boldsymbol{m}$-face has nonpositive index, then Q is homeomorphic to $S \times [0,1]$ for some compact surface S with index $S \leq 0$ *and satisfies items* (a)–(d) *in the definition of a $\boldsymbol{u}$-cusped product.*

Proof We first claim that S has exactly one $\boldsymbol{m}$-face. Suppose points p, q lie in $\boldsymbol{m}$-faces. Take a path α in the interior of Q from p to q. We can flow α backward so that it lies on an $\boldsymbol{m}$-face by (2), so p and q lie in the same $\boldsymbol{m}$-face.

Let us denote the unique $\boldsymbol{m}$-face of Q by S. We now claim that Q is homeomorphic to the product $S \times [0,1]$ with S corresponding to $S \times \{0\}$. Pick a basepoint $x \in S$. Consider the map $\pi_1(S, x) \to \pi_1(Q, x)$ induced by inclusion. This map is surjective because any closed curve in the interior of Q can be flowed backward to a curve on S by (2). Similarly, the map is injective because any nullhomotopy of a curve on S in Q can be homotoped off of the $\boldsymbol{u}$-faces of N, and then flowed backward to lie on S. Thus the claim follows from [Hempel 1976, Theorem 10.2], for example.

This shows (a) in Definition 6.7. (b) follows from (4), while (c) follows from (1) and (3).

Finally, for (d), suppose some orbit neither accumulates on a $\boldsymbol{u}$-face nor terminates on a $\boldsymbol{p}$-face or a $\boldsymbol{uu}$-cusp. Then it must have some accumulation point x in the interior of Q. But then the backward trajectory of x cannot terminate on S, contradicting (2). □

6.3 Veering branched surfaces

In this subsection, we define veering branched surfaces, which will be the main class of objects we study in the rest of this paper.

Definition 6.10 An unstable dynamic branched surface (B, V) in a sutured manifold Q is said to be *very full* if the complementary regions of B in Q are all $\boldsymbol{u}$-cusped tori and $\boldsymbol{u}$-cusped products. A very full stable dynamic branched surface is defined symmetrically. ◁

In particular, notice that a very full unstable dynamic branched surface B does not meet $R_- \cup \gamma$ and a very full stable dynamic branched surface B does not meet $R_+ \cup \gamma$.

Let B be a very full unstable dynamic branched surface. Recall that $\mathrm{brloc}(B)$ is a union of branch loops and branch arcs. Suppose that we have chosen a source orientation (recall Definition 2.8) on each branch loop and each branch arc. We say that this data specifies a *source orientation* of $\mathrm{brloc}(B)$.

Definition 6.11 A very full unstable dynamic branched surface (B, V), along with the choice of a source orientation, is called an *unstable veering branched surface* if:

(1) For each triple point p meeting branch segments γ and δ, the orientation of γ points into the same side of $T_p\delta$ in T_pB as the maw coorientation of δ does. See Figure 25.

(2) The *boundary train track* $\beta = B \cap R_+$ is efficient and has no large branches.

(3) For each branch loop l, let c be the unique $\boldsymbol{uu}$-cusp circle of $Q \setminus\setminus B$ which is identified to l. We require that the orientation on l agree with the dynamic orientations of both $\boldsymbol{u}$-faces adjacent to c.

(4) There are no annulus or Möbius band sectors with both boundary components having inward-pointing maw coorientations.

(5) B does not carry any tori or Klein bottles.

By Lemma 2.10, there exists a choice of source orientations on the boundary train track making it into a spiraling train track. In fact, a canonical choice exists here: The only freedom is how the circular branches are oriented. Each of these lie on a $\boldsymbol{u}$-face of $Q \setminus\setminus B$, so we orient it according to the dynamic orientation of the $\boldsymbol{u}$-face. In the following we will implicitly assume that the boundary train track of a veering branched surface is endowed with this source orientation, thus making it a spiraling train track. ◁

Remark 6.12 There is a symmetric definition for a stable veering branched surface. In this paper all the veering branched surfaces we encounter will be unstable, so we will sometimes omit the word "unstable" and refer to these as veering branched surfaces. Everything done in this paper can be performed for stable veering branched surfaces as well. ◁

Recall that sectors of a vertical branched surface are surfaces with corners. In particular, sectors of a veering branched surface are surfaces with corners, with sides along the branch locus and R_+. Moreover, the sides along the branch locus are naturally cooriented inwards or outwards by the vector field V (equivalently, by the maw coorientation), and the sides along R_+ are naturally cooriented outwards by the vector field V. The sides of the sectors also inherit a source orientation from that of $\mathrm{brloc}(B)$ and β. Henceforth we will implicitly coorient and orient edges in this manner.

Proposition/Definition 6.13 *A sector s of a veering branched surface on a sutured manifold must be one of the following*:

- *A* ***diamond*** *that possibly has*
  - ***scalloped top***, *ie the two top sides and the top vertex of the diamond can be replaced by $n \geq 3$ adjacent top sides and $n-1$ top corners, or*
  - ***rounded bottom***, *ie the two bottom sides and the bottom vertex of the diamond can be replaced by one bottom side.*

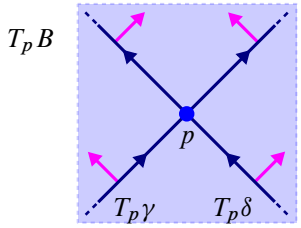

Figure 25: In a veering branched surface, the orientations (dark blue) and maw coorientations (pink) of branch segments are compatible at triple points.

The outermost top sides are oriented toward the top vertices, while the other top sides have sources. All the top sides are cooriented outwards. If the bottom is not rounded, the bottom sides are oriented away from the bottom vertex, otherwise the bottom side has a source. All the bottom sides are cooriented inwards. See the first two columns of Figure 26.

- *An* ***annulus/Möbius band*** *that possibly has*
  - ***scalloped boundary components****, ie each of the boundary components can be replaced by $n \geq 1$ sides and n corners.*

In this case, s lies on a ***u****-face F of $Q \setminus\setminus B$, and we have an injection $H_1(F) \hookrightarrow H_1(s)$. We call the orientation on $H_1(s)$ induced by the dynamic orientation of F the* ***dynamic orientation*** *on s. Here F*

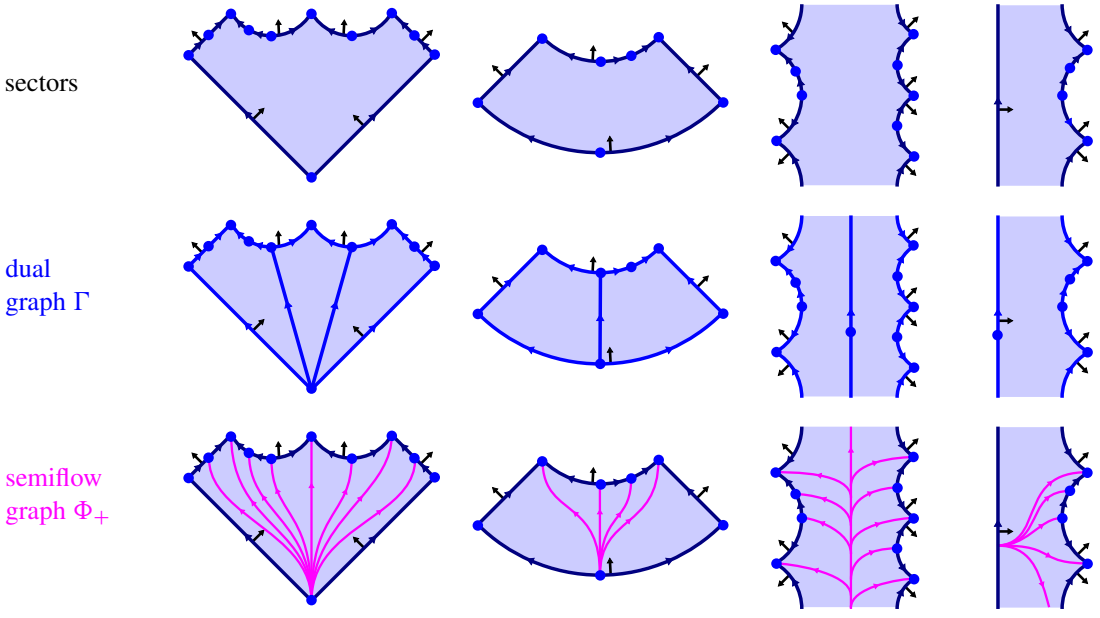

Figure 26: The possible sectors of a veering branched surface and the portion of the dual graph Γ and semiflow graph Φ_+ on each of them. Column 1: a diamond with scalloped top. Column 2: a diamond with scalloped top and rounded bottom. Column 3: a source sector. Column 4: a transient annulus.

may not be unique but the dynamic orientation on s is well defined as the orientation of a closed orbit on s if s is a source, and by Definition 6.11(3) if s is transient.

The orientation of a nonscalloped boundary component agrees with the dynamic orientation of s. Nonscalloped boundary components can be cooriented inwards or outwards. Each side on a scalloped boundary component has a source. Scalloped boundary components must be cooriented outwards.

We say s is a ***source*** *sector if all of ∂s is cooriented outwards. See Figure 26, third column. Otherwise, by Definition 6.11(4), s must be an annulus with one inward and one outward boundary component, and we say s is a* ***transient*** *annulus. See Figure 26, fourth column.*

Proof Since V is nonsingular, by the Poincaré–Hopf theorem, $\chi(s) = \text{degree}(V|_{\partial s})$. In particular, since V is transverse to $\text{brloc}(B)$ and all corners are convex, s must be a disk, an annulus or a Möbius band.

If s is a disk, $\text{index}(V|_{\partial s}) = 1$, so s must have some number of consecutive sides cooriented outwards followed by some number of consecutive sides cooriented inwards. But, given Definition 6.11(1), a side with no source must be adjacent to both an inwardly and outwardly cooriented edge; and a side with a source must be adjacent to two outwardly cooriented edges.

If s is an annulus or a Möbius band, $\text{index}(V|_c) = 0$ for each boundary component c of s, so each boundary component must consist of a number of consecutive edges all cooriented outwards or all cooriented inwards. But, as above, the two edges to the sides of an edge with no source cannot be cooriented in the same direction, and the two edges to the sides of an edge with a source must be cooriented outwards. □

Remark 6.14 In Definition 6.11, the requirements that β has no large branches and (4) are not actually very restrictive, in the sense that if B is a very full dynamic branched surface satisfying all the axioms except these, then they can be arranged to hold. For suppose B is such a branched surface. Then a similar proof as in Proposition/Definition 6.13 shows that a sector s of B must be one of the following:

- A diamond that possibly has
  - scalloped top, or
  - rounded top, ie the two top sides and the top vertex of the diamond can be replaced by one top side lying on R_+, or
  - rounded bottom.

  If the top is rounded, the top side has a source. Otherwise, the same statements as in Proposition/Definition 6.13 still hold.
- An annulus/Möbius band that possibly has
  - scalloped boundary components.

  There are now no restrictions on the coorientations of the boundary components. The same statements about their orientations as in Proposition/Definition 6.13 still hold.

To arrange for β to have no large branches, we can dynamically split B to get rid of all diamonds with rounded top (see Figure 61 in the appendix). This might change the corner structure of some cusped

product pieces, but they remain cusped product pieces, hence B is still very full. The result of the splitting may contain new undesirable sectors, so we split again to get rid of those inductively. Since the splittings reduce the number of sectors, the process stops eventually, and β now has no large branches.

Similarly, we can do dynamic splittings to arrange for (4) to hold. Suppose there is an annulus/Möbius band sector s with both boundary components cooriented inwards. For a fixed boundary component c of s, locate an immersed annulus A with one boundary component on c and another boundary component c' on $\mathrm{brloc}(B)\cup\beta$ that is cooriented out of A, by, for example, following along the boundary of a complementary region of B meeting s, using the fact that B is very full. We can then dynamically split along A minus a small neighborhood of c' to reduce the number of annulus/Möbius band sectors that violate (4). ◁

6.4 The dual graph and flow graph

In this section, we define the dual graph and flow graphs of a veering branched surface. These definitions are motivated by the corresponding objects in the nonsutured setting (see eg [Landry et al. 2023b]). Within the context of this paper, the dual graph will play a part in Sections 8 and 9, while the main use of flow graphs is to prove the main result of the appendix: that veering branched surfaces give rise to dynamic pairs.

Definition 6.15 (dual graph) Let B be a veering branched surface. The *dual graph* Γ of B is a directed graph embedded in B determined by requiring its intersection with each sector s of B be as follows:

- If s is a diamond, then $\Gamma\cap s$ is the union of ∂s with an edge from the bottom vertex (if the bottom is not rounded) or the bottom source (if the bottom is rounded) of s to each source on a top side.
- If s is a source, then $\Gamma\cap s$ is the union of ∂s with an edge connecting a vertex in the interior of s to itself forming a core of s, oriented by the dynamic orientation of s.
- If s is a transient annulus, then $\Gamma\cap s=\partial s$ (with a vertex placed on each cycle). ◁

See Figure 26 for an illustration of the dual graph.

Definition 6.16 Let c be an oriented path immersed in B. We say that c is *positively transverse* to $\mathrm{brloc}(B)$ if

- c intersects $\mathrm{brloc}(B)$ nontrivially, and, at every intersection point, the orientation of c agrees with the maw coorientation on $\mathrm{brloc}(B)$, or
- c is contained in an annulus or Möbius band sector, and is homotopic within the sector to a positive multiple of the core oriented by the dynamic orientation. ◁

Proposition 6.17 *Any closed curve c on a veering branched surface B that is positively transverse to* $\mathrm{brloc}(B)$ *is homotopic to a directed cycle of the dual graph* Γ.

Proof If c does not intersect $\mathrm{brloc}(B)$, then the proposition is clear from definition, so we can assume that c intersects $\mathrm{brloc}(B)$. We claim that c does not intersect any annulus or Möbius band sectors in this case. Indeed, c cannot enter a source sector. If c intersects a transient annulus s, then it must enter s

at some point x on a nonscalloped boundary component of s. But c must lie on a transient annulus immediately before x as well, so, repeating this argument, we eventually get a union of annuli that glue up to form a torus or Klein bottle carried by B (in fact a torus because the dynamic orientations agree), contradicting Definition 6.11(5).

Now, by a small perturbation, we can assume c does not meet $\mathrm{brloc}(B)$ in a triple point or source. We analyze the form of c within each sector s that it meets. By the paragraph above, s must be a diamond. Then c must enter through a bottom side and exit through a top side. For each intersection point between c and $\mathrm{brloc}(B)$, we homotope c in a neighborhood to push the intersection point against the orientation on $\mathrm{brloc}(B)$ until it hits a triple point or a source. After this homotopy, c then enters each sector through the triple point or source in the interior of the union of bottom sides and exits through a triple point or source on the top sides. We can then clearly homotope c sector-by-sector to lie on Γ such that its orientation is compatible with that of Γ. □

Definition 6.18 (the (semi)flow graph) Let B be a veering branched surface. Construct an oriented train track embedded in B in the following way. First, for each component of $\mathrm{brloc}(B)$ with no triple points, pick a point lying on it. Similarly, for each component of $B \cap R_+$ with no switches, pick a point lying on it.

- For each diamond s, take a union of disjoint branches going from the bottom vertex (if the bottom is not rounded) or the bottom source (if the bottom is rounded) to each corner, triple point, and source contained in the interior of the union of the top sides.
- For each source sector s, take the core of s oriented by the dynamic orientation. Then, for each boundary component t of s:
  - If t is a smooth circle with some triple points, attach to the core a branch from the core to each triple point on t.
  - If t is a smooth circle with no triple points, attach to the core a branch from the core to the chosen vertex on t.
  - If t has corners, attach to the core a branch from the core to each corner, triple point and source on t.
- For each transient annulus s with one boundary component t_1 cooriented inwards and the other boundary component t_2 cooriented outwards:
  - If t_2 is a smooth circle with some triple points, take a union of disjoint branches going from the chosen vertex on t_1 to each triple point on t_2.
  - If t_2 is a smooth circle with no triple points, take a branch going from the chosen vertex on t_1 to the chosen vertex on t_2.
  - If t_2 has corners, take a union of disjoint branches going from the chosen vertex on t_1 to each corner, triple point and source on t_2.

Notice that such an oriented train track is not uniquely defined. There is freedom in choosing the points on components of $\mathrm{brloc}(B)$ with no triple points and components of $B \cap R_+$ with no switches, and in the case when s is a source, there is freedom in choosing how the branches connect the vertices on ∂s to the core of s.

However, these operations do not meaningfully change the information contained by the oriented train track, so by a slight abuse of language we will refer to an oriented track defined by the above description as *the semiflow graph* Φ_+ of B. See Figure 26.

Now consider the set

$$\{x \in \Phi_+ : \text{every directed train route starting at } x \text{ ends on } R_+\}.$$

Let Φ be the result of removing this set from Φ_+, which is still an oriented train track embedded in B. We call Φ the *flow graph*. As with the semiflow graph, the flow graph is not uniquely defined, but the ambiguity is inconsequential. ◁

In the appendix, we will show that the flow graph is a "dynamic train track", which will imply that one can construct a dynamic pair starting with only a veering branched surface. See the appendix for definitions of the terms. Even without this motivation, a flow graph is a natural companion object for the dual graph, as we will see in the next subsection.

6.5 Dynamic planes

In this section we will generalize some discussion from [Landry et al. 2023b]. The authors of that paper introduced "dynamic planes", which are combinatorial objects associated to a veering triangulation that correspond to different leaves of the stable/unstable foliations of pseudo-Anosov flows. Here we will define dynamic planes for veering branched surfaces that correspond to leaves of the suspension of the Handel–Miller laminations.

Our first order of business will be to show that a veering branched surface B fully carries a lamination $\mathcal{L}$ for which every leaf is π_1-injective. This is so that we can use the leaves of $\mathcal{L}$ to understand our dynamic planes.

We remark that in the setting of [Landry et al. 2023b], one starts with a pseudo-Anosov flow and gets a veering branched surface, which one can check is *laminar* and hence carries an essential lamination by [Li 2002]. The leaves of such a lamination must be π_1-injective, so this preliminary step was automatically true in that paper.

Proposition 6.19 *A veering branched surface B on a sutured manifold Q carries a lamination $\mathcal{L}$ with no spherical leaves and such that every leaf is π_1-injective.*

Proof If B carries a surface F, then we can construct a nonsingular vector field on F by pulling back the vector field V on B. In particular, if F is closed then it must have zero Euler characteristic. This shows that if B carries a lamination $\mathcal{L}$ then no leaf of $\mathcal{L}$ can be a sphere.

Now, to construct $\mathscr{L}$ we use the tool of *laminar branched surfaces*, introduced in [Li 2002]. Recall that a branched surface B in a compact 3-manifold M where $B \cap \partial M = \varnothing$ is laminar if:

(1) $\partial_h N(B)$ is incompressible in $M \setminus\setminus N(B)$, no component of $\partial_h N(B)$ is a sphere, and $Q \setminus\setminus N(B)$ is irreducible.

(2) There are no *monogons* in $M \setminus\setminus N(B)$.

(3) B does not carry a torus that bounds a solid torus.

(4) B has no *trivial bubbles*.

(5) B has no *sink disks*.

We refer to [Li 2002] for the definitions of the italicized terms. By [Li 2002, Theorem 1], a laminar branched surface fully carries an *essential lamination* $\mathscr{L}$. We will not go into the full definition of an essential lamination here. We only need the property that every leaf of an essential lamination is π_1-injective.

Returning to our setting, let DQ be the double of Q over R_+ and R_-, and let $DB \subset DQ$ be the double of B. We claim that DB is laminar.

The complementary regions of $N(DB)$ in DQ are the doubles of those of $N(B)$ in Q over their $\boldsymbol{p}$- and $\boldsymbol{m}$-faces. In particular, it is straightforward to check that no component of $\partial_h N(DB)$ is a sphere, $Q \setminus\setminus N(DB)$ is irreducible, and B has no trivial bubbles.

To show that $\partial_h N(DB)$ is incompressible in $DQ \setminus\setminus N(DB)$, assume that there is a compressing disk. Then, by an innermost disk argument using the incompressibility of $R_\pm$ and the irreducibility of Q, there is a compressing disk or boundary compressing disk for $\partial_h N(B)$ in $Q \setminus\setminus N(B)$. But it is straightforward to check that these do not exist. Similarly, one can show that there are no monogons in $DQ \setminus\setminus N(DB)$.

If DB carries a torus that bounds a solid torus, then, by the same standard arguments, now using the efficiency of the boundary train track $B \cap R_+$ as well, either B carries a torus bounding a solid torus T or B carries a properly embedded annulus that bounds a solid torus T with another annulus on R_+. The former case is ruled out by Definition 6.11(5). In the latter case, every complementary region of B in Q inside T must be a cusped torus piece, but then this implies that T has no $\boldsymbol{p}$-face, giving a contradiction.

Finally, that DB has no sink disks follows from Proposition/Definition 6.13.

Now apply [Li 2002, Theorem 1] to get an essential lamination $\mathscr{L}'$ fully carried by DB, then restrict it to a lamination $\mathscr{L}$ fully carried by B. To show that every leaf ℓ of $\mathscr{L}$ is π_1-injective, it suffices to show that if ℓ' is the leaf of $\mathscr{L}'$ that contains ℓ, then $\pi_1(\ell) \to \pi_1(\ell')$ is injective. Assume otherwise; then there is a disk D in ℓ' intersecting R_+ in a union of circles. We take an innermost such circle which bounds a disk D' in D. Then D' is carried by B. However, the vector field on B induces one on D' which points outwards along $\partial D'$, contradicting the Poincaré–Hopf theorem. □

Remark 6.20 The above gives a proof of a version of Li's result [2002] in the setting of sutured manifolds. Note that Li himself [2003] generalized the result to include torally bounded manifolds. ◁

Let B be a veering branched surface on a sutured manifold Q and let $\widetilde{B}$ be the lift of B to the universal cover $\widetilde{Q}$. Let $\widetilde{\Gamma}$ be the lift of the dual graph Γ to $\widetilde{B}$.

Definition 6.21 Let σ be a sector of $\mathrm{brloc}(\widetilde{B})$. The *future set of* σ, which we denote as $\nabla(\sigma)$, is the union of sectors s of $\widetilde{B}$ for which there is a path from σ to s that points in the same direction as the maw vector field whenever it intersects $\mathrm{brloc}(\widetilde{B})$.

Let x be a point of $\mathrm{brloc}(\widetilde{B})$. Let $\sigma(x)$ be the sector of B that meets x and at which the coorientation is pointing inwards. The *future set of* x is defined to be $\nabla(\sigma(x))$.

Let γ be a bi-infinite directed edge path of $\widetilde{\Gamma}$ that is not a subset of $\partial\widetilde{B}$. We denote by $D(\gamma)$ the union of sectors s of $\widetilde{B}$ for which there is a path from γ to s that is positively transverse to $\mathrm{brloc}(\widetilde{B})$. If γ does not eventually lie along a single component of $\mathrm{brloc}(\widetilde{B})$ in the backward direction, then we call $D(\gamma)$ the *dynamic plane* associated to γ. Otherwise we call $D(\gamma)$ the *dynamic half-plane* associated to γ. See Figure 27 for a depiction of a portion of a dynamic place tiled by sectors of $\widetilde{B}$. ◁

Proposition 6.22 (1) *Each future set* $\nabla(\sigma)$ *is a surface with corners, with interior homeomorphic to a plane and boundary along* $\partial\widetilde{B}$ *and* $\mathrm{brloc}(\widetilde{B})$. *Furthermore,*

- *If* σ *is a diamond, then* $\partial\nabla(\sigma)\cap\mathrm{brloc}(\widetilde{B})$ *is precisely the rays along the components of* $\mathrm{brloc}(\widetilde{B})$ *starting from the bottom vertex (if the bottom is not rounded) or the bottom source (if the bottom is rounded) of* σ.
- *If* σ *is the lift of an annulus/Möbius band, then* $\partial\nabla(\sigma)\cap\mathrm{brloc}(\widetilde{B})$ *is precisely the components of* $\mathrm{brloc}(\widetilde{B})$ *containing the sides of* σ *that are cooriented inwards (if any).*

(2) *Each dynamic plane* $D(\gamma)$ *is a surface with boundary, with interior homeomorphic to a plane and boundary along* $\partial\widetilde{B}$.

(3) *Each dynamic half-plane* $D(\gamma)$ *is a surface with boundary, with interior homeomorphic to a plane and boundary along* $\partial\widetilde{B}$ *and one component of* $\mathrm{brloc}(\widetilde{B})$.

Proof This follows from the discussion in [Landry et al. 2023b, Section 3], which can almost be applied word for word here. We outline the idea, emphasizing the slight modifications that one has to perform in our setting.

By Proposition 6.19, B fully carries a lamination $\mathcal{L}$ with no spherical leaves and for which every leaf is π_1-injective. Lifting this to $\widetilde{Q}$, $\widetilde{B}$ fully carries $\widetilde{\mathcal{L}}$, for which each leaf is a surface with boundary with interior homeomorphic to a plane. For each leaf ℓ of $\widetilde{\mathcal{L}}$, we will abuse notation and use the same name for the homeomorphic image under the collapsing map $\widetilde{\mathcal{L}}\subset N(\widetilde{B})\to\widetilde{B}$. As such, ℓ inherits a decomposition into surfaces with corners that are among the sectors of $\widetilde{B}$.

Now, for a sector σ, let ℓ be a leaf of $\widetilde{\mathcal{L}}$ containing σ. Then $\nabla(\sigma)$ is naturally a subset of ℓ. The boundary of $\nabla(\sigma)$ in ℓ will be $\partial\nabla(\sigma)\cap\mathrm{brloc}(\widetilde{B})$. One shows that $\nabla(\sigma)$ coincides with the region bounded by the claimed form of $\partial\nabla(\sigma)\cap\mathrm{brloc}(\widetilde{B})$ using the argument in [Landry et al. 2023b, Lemma 3.1].

To prove (2) and (3), notice that every directed path α in $\widetilde{\Gamma}$ starting at some point x can be homotoped to be positively transverse to $\mathrm{brloc}(\widetilde{B})$ rel x by pushing it along the flow on $\widetilde{B}$ slightly. Hence given a bi-infinite directed edge path γ, $D(\gamma) = \cup\nabla(x_i)$ for a sequence of points x_i on γ converging to the negative end.

We have $\nabla(x_i) \subset \operatorname{int}\nabla(x_{i+1})$ unless γ stays within a constant component c of $\mathrm{brloc}(\widetilde{B})$ between x_i and x_{i+1}. In the latter case, we at least have $\nabla(x_i)\setminus c \subset \operatorname{int}\nabla(x_{i+1})\setminus c$. Hence, taking the union, we see that $\bigcup\nabla(x_i)$ is always a plane in its interior, and has boundary entirely along $\partial\widetilde{B}$, unless the component c above eventually stays constant, in which case the boundary of $\bigcup\nabla(x_i)$ will have one side along that c.

Note that the latter case occurs exactly when γ eventually lies along a constant component of $\mathrm{brloc}(\widetilde{B})$ in the backward direction, which is precisely the case when $D(\gamma)$ is a dynamic half-plane. □

Let $\widehat{\Phi}_+$ be the lift of the semiflow graph Φ_+ to $\widetilde{Q}$. Each dynamic plane $D(\gamma)$ inherits the restriction of $\widehat{\Phi}_+$. This will be an oriented train track on $D(\gamma)$ with only diverging switches. In particular, every point has an infinite, unique backward trajectory.

Definition 6.23 (triangles, rectangles, tongues, following) Let Φ_+ be the semiflow graph. Notice that, by construction, for each sector s of B, the components of $s \setminus\setminus \Phi_+$ are of the following forms:

- *Triangles*, ie triangles with two sides on $\mathrm{brloc}(B)$ or R_+, one cooriented outwards and one cooriented inwards, and the remaining side on Φ_+.
- *Rectangles*, ie rectangles with two opposite sides on $\mathrm{brloc}(B)$ or R_+, one cooriented outwards and one cooriented inwards, and the remaining two opposite sides on Φ_+.
- *Tongues*, ie one-cusped triangles with the side opposite to the cusp on $\mathrm{brloc}(B)$ or R_+ cooriented outwards, and the remaining two sides on Φ_+.

If s is a diamond, then the components of $s \setminus\setminus \Phi_+$ are triangles and tongues; if s is an annulus/Möbius band, then the components of $s \setminus\setminus \Phi_+$ are rectangles and tongues. See Figure 26.

Let t_1 and t_2 be two such components. We say that t_1 is *followed by* t_2 if t_1 is adjacent to t_2 along an edge of $\mathrm{brloc}(B)$ which is cooriented from t_1 to t_2. ◁

Lemma 6.24 *We have the following two properties*:

- *A triangle cannot be followed by a rectangle.*
- *There cannot be an infinite sequence of rectangles following one another.*

Proof Suppose that we have a triangle followed by a rectangle. Then we would have a diamond sector s_1 and an annulus/Möbius band sector s_2 that are adjacent along an edge e that is cooriented from s_1 to s_2. This implies that the component of ∂s_2 on which e lies is cooriented inwards, and hence meets no triple points of B. This contradicts the fact that s_1 is a diamond.

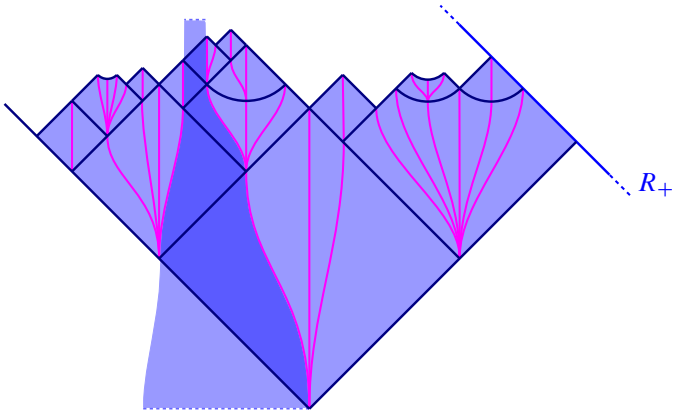

Figure 27: A portion of a dynamic plane containing an AB strip. We remark that the entire dynamic plane could intersect R_+ in infinitely many components.

Now suppose that there is an infinite sequence of rectangles following one another. Then we would have an infinite sequence of transient annulus sectors each adjacent to the previous one along a circular edge. This produces a torus that is carried by B, contradicting Definition 6.11(5). □

Definition 6.25 An *AB strip* on a dynamic plane $D(\gamma)$ is a region with boundary along $\hat{\Phi}_+$ which is homeomorphic to $[0,1]\times\mathbb{R}$ and made out of a bi-infinite sequence of triangles following one another. An *AB half-strip* on a dynamic plane $D(\gamma)$ is a region with boundary along $\hat{\Phi}_+$ which is homeomorphic to $[0,1]\times(-\infty,0]$ with the infinite end being in the direction of backward flow along $\hat{\Phi}_+$, and made out of an infinite sequence of triangles following one another. See Figure 27 for an example. ◁

Lemma 6.26 *Two infinite backward $\hat{\Phi}_+$ rays lying on a dynamic plane $D(\gamma)$ either eventually coincide or both eventually lie on the boundaries of AB half-strips.*

Proof This follows nearly word for word from the proof of [Landry et al. 2023b, Lemma 3.7]. As in the proof of Proposition 6.22, we outline the idea here and point out small modifications for our setting.

Recall that $D(\gamma)=\bigcup\nabla(x_i)$ for a sequence x_i converging to the negative end of γ. Let α_1,α_2 be two infinite backward $\hat{\Phi}_+$ rays lying on $D(\gamma)$. By inspection of the complementary regions of $\hat{\Phi}_+$ in sectors, the distance between $\alpha_k\cap\partial\nabla(x_i)$ on $\partial\nabla(x_i)$ is larger or equal to that between $\alpha_k\cap\partial\nabla(x_j)$ on $\partial\nabla(x_j)$ for $i<j$, and equality holds if and only if the region bounded by the portion of α_k in between $\partial\nabla(x_i)$ and $\partial\nabla(x_j)$ is made out of triangles and rectangles.

But, by Lemma 6.24, a triangle cannot be followed by a rectangle and there cannot have an infinite sequence of rectangles following one another. Hence we conclude that if the α_k do not eventually coincide, they will eventually bound some AB half-strips. □

In particular, just as in [Landry et al. 2023b, Proposition 3.10], this lemma easily implies that all AB half-strips in a dynamic plane are adjacent.

Proposition 6.27 *Let B be a veering branched surface, let Γ be its dual graph, and let Φ be its flow graph. If c is a cycle of Γ, then c or c^2 is homotopic to a cycle of Φ in Q.*

Proof Let $\tilde{c}$ be the lift of c to an infinite directed path in $\widetilde{\Gamma}$.

Suppose first that $D(\tilde{c})$ is a dynamic plane. Similarly to above, the proposition follows essentially from the proof of [Landry et al. 2023b, Proposition 3.15], and we outline the idea here.

Let $g = [c] \in \pi_1(Q)$. Notice that the dynamic plane $D(\tilde{c})$ is g-invariant. If $D(\tilde{c})$ does not contain an AB strip, then pick some infinite backward trajectory α of $\widehat{\Phi}_+$ on $D(\tilde{c})$. From Lemma 6.26, we know that α and $g \cdot \alpha$ eventually coincide, hence α is eventually g-periodic, and the periodic part projects to a cycle of Φ_+ with homotopy class g.

On the other hand, if $D(\tilde{c})$ contains AB strips, then the projection of the boundary components of an AB strip is a cycle of Φ_+ with homotopy class g or g^2 (depending on whether g reverses the orientation of the AB strip).

Now, if $D(\tilde{c})$ is a dynamic half-plane, then c must be a component of $\mathrm{brloc}(B)$. Hence c must lie on an annulus face of some complementary region of B. The restriction of Φ_+ to this annulus face is a (nonempty) oriented train track with only diverging switches and with branches leaving through the boundary. Hence it must consist of some cycles and some branches from the cycles to the boundary. The cycles will have homotopy class g or g^2.

Finally, notice that by definition a cycle of Φ_+ must lie in Φ. □

Corollary 6.28 *The cone spanned by cycles of Γ in $H_1(Q)$ agrees with that of Φ.*

Proof Proposition 6.27 implies that the former cone is a subset of the latter cone. For the converse, observe that each cycle of Φ is positively transverse to $\mathrm{brloc}(B)$ in the sense of Definition 6.16, and hence can be homotoped to a cycle of Γ by Proposition 6.17. □

To conclude this section, we illustrate the utility of dynamic planes by discussing the correspondence between periodic dynamic planes and periodic leaves. This will be applied in Section 8.

Suppose B is a veering branched surface on Q fully carrying a lamination $\mathcal{L}$ as in Proposition 6.19. Lift B and $\mathcal{L}$ to the universal cover $\widetilde{Q}$. A dynamic plane of $\widetilde{B}$ is said to be *periodic* if it is invariant under some element of $\pi_1(Q)$ acting on $\widetilde{Q}$. Similarly, a leaf of $\widetilde{\mathcal{L}}$ is said to be *periodic* if it is invariant under some element of $\pi_1(Q)$; equivalently, a leaf of $\widetilde{\mathcal{L}}$ is said to be periodic if its image in $\mathcal{L}$ is a leaf that has interior homeomorphic to an open annulus or Möbius band.

Given a periodic leaf ℓ of $\widetilde{\mathscr{L}}$, consider the union of sectors that the leaf passes through. This is a surface with boundary along $\partial\widetilde{B}$ and with interior homeomorphic to a plane, which we abuse notation and call ℓ as well. If ℓ does not contains the lift of an annulus or Möbius band sector, then, since each vertex of Γ has at least one incoming edge on ℓ, one can construct a bi-infinite $\widetilde{\Gamma}$-path γ on ℓ that does not lie entirely on $\partial\widetilde{B}$. If γ can be chosen such that $D(\gamma)$ is a dynamic plane, then $\ell = D(\gamma)$. If not, then it must be the case that ℓ contains the lift of an annulus or Möbius band sector. In this case, ℓ contains the lift of a source sector, for otherwise B would carry a closed surface. We pick γ to be the lift of the core of such a sector, then $\ell = D(\gamma)$ in this case as well.

Conversely, given a periodic dynamic plane D, we can write it as a nested union $\bigcup_{i=0}^{\infty} \nabla(\sigma_i)$. The sets of leaves of $\widetilde{\mathscr{L}}$ passing through σ_i gives a nested sequence of compact sets in the space of leaves of $\widetilde{\mathscr{L}}$. Taking the intersection, we get a nonempty collection of leaves of $\widetilde{\mathscr{L}}$ passing through exactly the sectors that tile the dynamic plane. For general $\mathscr{L}$, this determines a packet of leaves, but, when $\mathscr{L}$ is an unstable Handel–Miller lamination, such a leaf must be unique by Lemma 5.3, and hence periodic.

This discussion implies the following proposition:

Proposition 6.29 *Suppose $\mathscr{L}^u$ is an unstable Handel–Miller lamination carried by a veering branched surface B. Then there is a one-to-one correspondence between the periodic leaves of $\widetilde{\mathscr{L}^u}$ and the periodic dynamic planes of B. Moreover, this correspondence is such that a leaf of $\widetilde{\mathscr{L}^u}$ is invariant under $g \in \pi_1(\overline{M}_f)$ if and only if its corresponding dynamic plane is invariant under g.*

7 Veering branched surfaces for Handel–Miller laminations

In this section we construct veering branched surfaces carrying unstable Handel–Miller laminations in compactified mapping tori. The construction itself, contained in Section 7.2, essentially consists in suspending a splitting sequence of train tracks carrying the positive Handel–Miller lamination, the existence of which is guaranteed by Theorem 4.9. Checking for the axioms of a veering branched surface requires some in-depth analysis of the splitting sequence, which we perform in Sections 7.4 and 7.3, allowing us to prove our main existence result, Theorem 7.10, in Section 7.5. Finally, in Section 7.6, we promote the uniqueness result of Section 4.5 regarding splitting sequences to a uniqueness result about veering branched surfaces carrying Handel–Miller laminations.

7.1 Staircases

It is now convenient to consider an enlargement of the category of sutured manifolds, which by our convention have convex corner points, to include *concave corner points*, which by definition have neighborhoods modeled on the following closed set in $\mathbb{R}^3$:

- (Concave) corner edge: $\{(x, y, z) \mid x \leq 0 \text{ or } y \leq 0\}$.

A *sutured manifold with concavity* is defined in the same way as a sutured manifold, but now we allow the existence of annular sutures with both boundary components meeting the positive (or negative) tangential boundary, and require that, for any such annular suture A, one component of ∂A consist of concave corner points and the other consist of convex corner points.

A *positive staircase* is a sutured manifold with concavity (P, γ) satisfying the following:

(i) P is homeomorphic to $S \times [0,1]$ for some compact oriented surface S.

(ii) $R_+(P) = S \times \{1\}$.

(iii) $T(\gamma) = \varnothing$ and $A(\gamma) = (\partial S \times [0,1]) \cup A_1 \cup \cdots \cup A_n$ for a collection of annuli $A_1, \dots, A_n \subset \operatorname{int}(S) \times \{0\}$.

(iv) $R_-(\gamma) = (S \times \{0\}) - \bigcup_1^n A_i$.

A *negative staircase* is defined symmetrically by switching the roles of R_+ and R_-. See Figure 28.

7.2 Construction of (B^u, V)

Let $f : L \to L$ be a Handel–Miller map, and let (Q, γ) be the sutured manifold $\overline{M}_f$ endowed with the suspension semiflow φ_f. We view L as sitting inside Q. Let $\mathcal{F}$ be the depth one foliation of (Q, γ) whose noncompact leaves are parallel to L. Let $\mathcal{L}^u$ be the suspension of the Handel–Miller lamination Λ_+.

Definition 7.1 (staircase determined by a tiled neighborhood) Let E_+ be a tiled neighborhood of a positive end-cycle of L corresponding to a component Y of $R_+(Q)$. The union of all forward φ_f-orbits starting in E_+ naturally has the structure of a positive staircase S with $R_+(S) = Y$. We call this the *staircase neighborhood* of Y *determined by* the tiled neighborhood E_+. ◁

In Theorem 4.9, we showed that there exists a finite splitting sequence from τ to $f(\tau)$ for a certain train track τ fully carrying the lamination Λ_+. Reversing this sequence, we obtain a sequence

$$f(\tau) = \tau_0 \to \tau_1 \to \cdots \to \tau_n = \tau,$$

where τ_{i+1} is obtained from τ_i by a single fold.

We first assume that $n > 0$. As Q is the compactified mapping torus of f, we have $Q \setminus \partial_\pm Q = (L \times [0,1])/\big((x,1) \sim (f(x),0)\big)$. Let $L_i = L \times \{\frac{i}{n}\} \subset Q$ for $i = 0, \dots, n-1$.

For each end-cycle Z, choose a tiling of $\mathfrak{U}_Z$. Let $N(\mathcal{E}_+)$ be a tiled neighborhood of all positive end-cycles which is small enough so that τ_0 is f-endperiodic in $N(\mathcal{E}_+)$ and the folding sequence from τ_0 to τ_n is supported in $K = L \setminus\setminus N(\mathcal{E}_+)$. Let $N(R_+)$ be the staircase neighborhood of R_+ determined by $N(\mathcal{E}_+)$. Note that K is not compact: it is the union of a core of L with neighborhoods of all negative ends.

Let $M_i = K \times \big[\frac{i}{n}, \frac{i+1}{n}\big] \subset Q$ and $K_i = K \times \{\frac{i}{n}\}$. Thus M_i is a region in Q lying between L_i and L_{i+1}, and $K_i \subset L_i$. Let

$$A = R_- \cup \left(\bigcup_{i=0}^{n-1} M_i \right) = Q \setminus\setminus N(R_+).$$

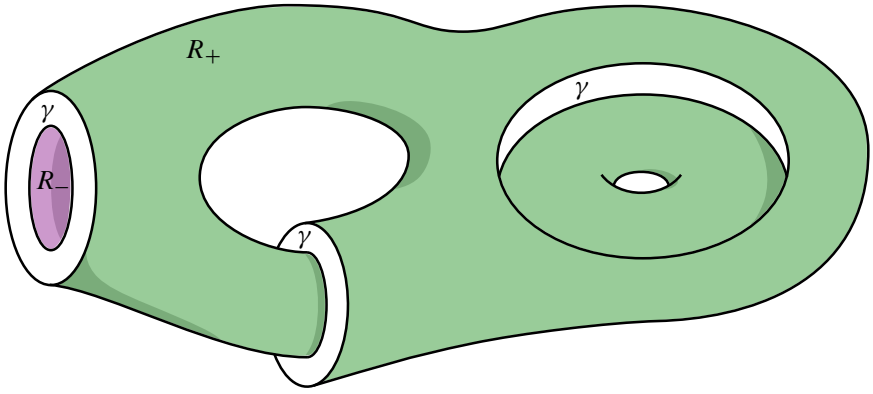

Figure 28: A negative staircase. By switching R_+ and R_-, we obtain a positive staircase.

Under our identification of L with $L_0 = L \times \{0\}$, there is a natural embedding of τ_0 in L_0. Given an embedding of τ_i in K_i, we fix an embedding of τ_{i+1} in K_{i+1} as follows: we flow τ_i forward into K_{i+1} under φ_f, and then perform the fold $\tau_i \to \tau_{i+1}$.

Now, for $i = 0, \dots, n-2$ (if $n = 1$ we skip this step), we define a dynamic branched surface (M_i, B_i, V_i) with the following properties:

(i) B_i intersects K_i in τ_i and K_{i+1} in τ_{i+1}.

(ii) Between the parts of τ_i and τ_{i+1} involved in the fold, there is a piece of B_0 that is modeled on Figure 29, center or right, according to whether the fold is the reverse of a collision or not, respectively.

(iii) Away from the pieces of B_i described in (ii), B_i is topologically a product.

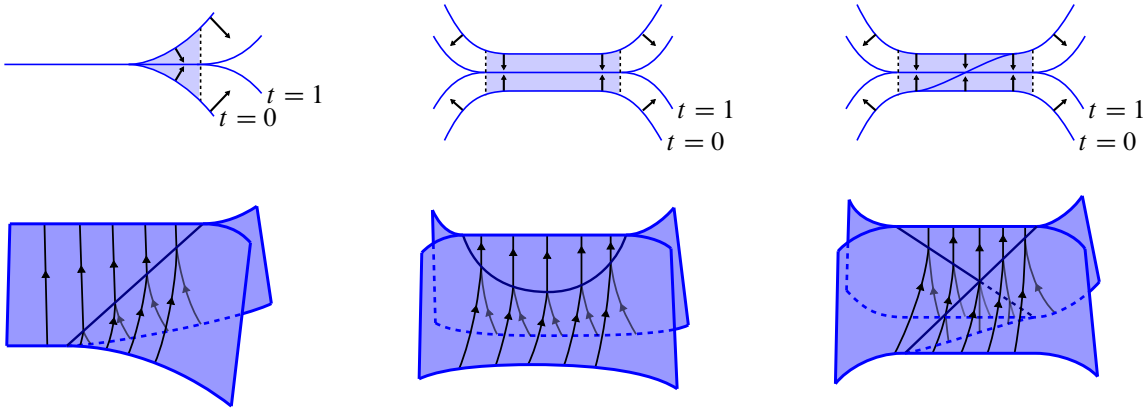

Figure 29: Building a dynamic branched surface from a train track folding sequence. The shaded regions in the top row indicate the sets in K_i whose forward trajectories under V_i merge with others (ie they enter B_i).

(iv) $\operatorname{brloc}(B_i)$ has a source orientation which is positively transverse to $\mathcal{F}$ at oriented points and tangent to $\mathcal{F}$ at sources. If $\tau_i \to \tau_{i+1}$ is the reverse of a collision, there is a single source of $\operatorname{brloc}(B_i)$(see Figure 29, center), and otherwise there are no sources.

(v) V_i has unique forward trajectories, points forward along $\operatorname{brloc}(B_i)$, and is positively transverse to $\mathcal{F}|_{M_i}$. All points in $M_i - B_i$ have unique backward trajectories.

Between switches of τ_i and τ_{i+1} which are not involved in the fold $\tau_i \to \tau_{i+1}$, condition (iii) requires that B_i be a product and (v) requires that V point forward along $\operatorname{brloc}(B_i)$. This can be achieved by using the model shown in Figure 29, left.

We next describe $(M_{n-1}, B_{n-1}, V_{n-1})$. This is built the same way as for $i = 1, \dots, n-2$, but with the additional requirement that the top of $(M_{n-1}, B_{n-1}, V_{n-1})$ line up smoothly with the bottom of (M_0, B_0, V_0) on the overlap of K_0 and $K_n = f(K_0)$.

Let $B_A = \bigcup_{i=0}^{n-1} B_i$, and V_A be the vector field on A which restricts to V_i on each M_i.

Finally, we define a vector field on $N(R_+)$. Let B_N be the union of all forward φ_f-orbits starting in $B_A \cap \partial N(R_+)$. Away from B_N, let V_N be equal to the vector field generating φ_f; near B_N, we choose V_N so that each branch line of (B_N, V_N) has a neighborhood modeled in Figure 29, left.

Let $B^u = B_A \cup B_N$, and let V be the vector field on Q restricting to V_A on A and V_N on N. Then evidently (Q, B^u, V) is an unstable dynamic branched surface. Furthermore, because B^u was constructed from an f-periodic train track folding sequence for a train track fully carrying Λ_+, we see that B^u fully carries $\mathcal{L}^u$.

Now we treat the case when $n = 0$. We construct a neighborhood of the positive end-cycles $N(\mathcal{E}_+)$ just as before, and similarly we construct the sets $N(R_+)$, $K = L \setminus\setminus N(R_+)$, $N(\mathcal{E}_+)$ and $A = Q \setminus\setminus N(R_+)$. The construction works just as above, the only difference being that the branched surface we build in A has no triple points or sources in its branch locus.

Hence we have shown the following, which is suggested by Mosher [1996] as an intermediate step:

Proposition 7.2 *Let $h\colon L \to L$ be a Handel–Miller endperiodic map. There exists an unstable dynamic branched surface (B^u, V) in $\overline{M}_f$ fully carrying $\mathcal{L}^u$, the suspension of the Handel–Miller lamination Λ_+.*

7.3 Principal and nonprincipal regions of (B^u, V)

We let φ_V denote the forward semiflow of V. Note that orbits of φ_V are uniquely determined in the forward direction but may not be in the backward direction.

Recall that there are two types of complementary region of Λ_+ in L: principal regions and components of the negative escaping set $\mathcal{U}_-$. Let C_τ be a complementary region of τ_0. Then C_τ corresponds naturally to a complementary region C_Λ of Λ_+. If C_Λ is a principal region, we call C_τ a *principal region of* τ_0. Since τ_0 is efficient and fully carries Λ_+, there is only one principal region of τ_0 corresponding to a given

principal region of Λ_+. In the case that C_τ is a principal region homeomorphic to an annulus with one boundary component equal to a component of ∂L, we say that C_τ is a *peripheral principal region*. If C_Λ is not a principal region (and hence is a component of $\mathcal{U}_-$), then we say C_τ is a *nonprincipal region of* τ.

If U is a complementary region of B^u, then $U \cap L_0$ consists of either entirely principal regions or entirely nonprincipal regions of τ_0. As such we will speak of (*peripheral*) *principal* and *nonprincipal* regions of B^u.

The following two lemmas describe the vector fields induced on principal and nonprincipal regions:

Lemma 7.3 (V in principal regions) *Let U be a principal region of B^u, and let V_U be the vector field on U induced by V. Then V_U is circular. As a consequence, if U is a solid torus or is peripheral, then U is a $\boldsymbol{u}$-cusped torus or $\boldsymbol{u}$-cusped torus shell, respectively.*

Proof If U is a principal region of B^u, then the foliation of U induced by $\mathcal{F}$ defines a map to S^1. Since V is positively transverse to $\mathcal{F}$, we see that the induced vector field on U is circular. The last claim follows immediately. □

By Handel–Miller theory, backward orbits from points in nonprincipal regions of $\mathcal{L}^u$ terminate on $R_-(\overline{M}_f)$. We will need the corresponding fact for (B^u, V):

Lemma 7.4 (V in nonprincipal regions) *Let U be a nonprincipal region of B^u, and let V_U be the vector field on U induced by V. The branched surface in Proposition 7.2 can be constructed so that the backward trajectory from each point in U not lying in a $\boldsymbol{u}$-face ends on $R_-(\overline{M}_f)$.*

Proof In this proof we refer to each complementary region of a standard neighborhood of B^u as "principal" or "nonprincipal" according to whether it is contained in a principal or nonprincipal region of B^u, respectively.

The hard part of the proof is the construction of a standard neighborhood $\mathcal{N}(B^u)$ of B^u with the property that the Handel–Miller suspension flow points inward along each component of $\partial\mathcal{N}(B^u)$ meeting a nonprincipal region.

In this construction we make use of the fact that f preserves geodesic juncture components (see Theorem 3.5).

Recall from our construction of B^u in Proposition 7.2 that N is a staircase neighborhood of $R_+(\overline{M}_f)$ and $A = \overline{M}_f \setminus\setminus N$.

Let U be a nonprincipal region of B^u, and let $U_{\mathcal{L}}$ be the associated nonprincipal region of $\mathcal{L}^u$. Let F be a $\boldsymbol{u}$-face of U. Then F corresponds to a leaf ℓ of $\mathcal{L}^u$ which borders $U_{\mathcal{L}}$ and is carried by F. Let λ be one component of $\ell \cap L$, which is evidently a semi-isolated leaf of Λ_+ (ie leaves of Λ_+ do not accumulate on λ from the side corresponding to $U_{\mathcal{L}}$). By [Cantwell et al. 2021, Theorem 6.5], λ is periodic with some period $p > 0$. Since U is a nonprincipal region, Lemma 3.16 gives that there exists a negative juncture component j such that the sequence $j, f^p(j), f^{2p}(j), \ldots$, accumulates on λ monotonically

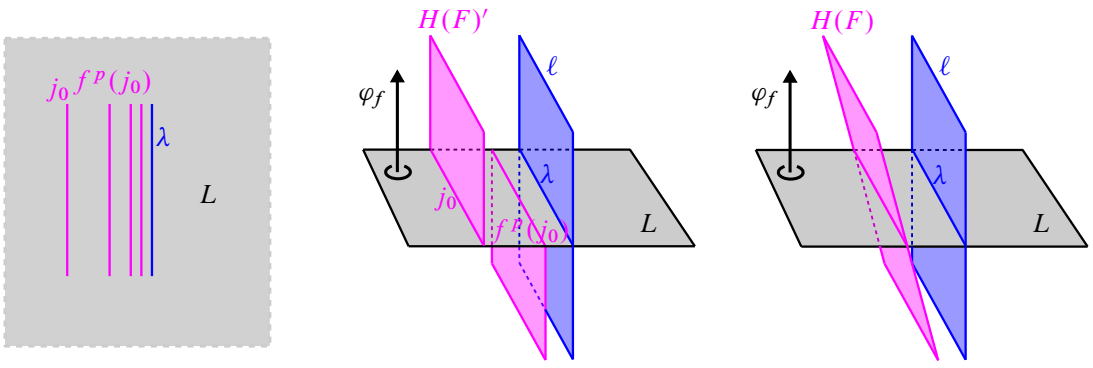

Figure 30: The construction of $H(F)$ in the proof of Lemma 7.4. In the center and right pictures, the flow φ_f is vertical.

from the side corresponding to U. Let λ_K be the component of $\lambda \cap K$ containing a periodic point; we are evidently free to assume that there is a component j_0 of $j \cap K$ such that j_0 is as close as we like to λ_K.

Let $H(F)'$ be obtained by flowing j_0 around $\overline{M}_f$ p times. Since $f^p(j_0)$ is closer to λ than j is, $H(F)'$ can be homotoped slightly so that it is an annulus $H(F)$ transverse to φ_f, and φ_f points through $H(F)$ toward ℓ. See Figure 30. The letter H indicates $H(F)$ will correspond to a component of the horizontal boundary of the standard neighborhood we are building.

Next let c be a ***uu***-cusp curve of U. Since U is nonprincipal, c is an interval and not a circle (see Lemma 4.2). There are two leaves of $\mathcal{L}^u$, say ℓ_1 and ℓ_2, which correspond to the faces of U adjacent to c. Let $V(c)$ be a rectangle embedded in A which has one edge along ℓ_1, an opposite edge along ℓ_2, and the remaining two edges along ∂A. Further, choose $V(c)$ to stay close to c. See Figure 31.

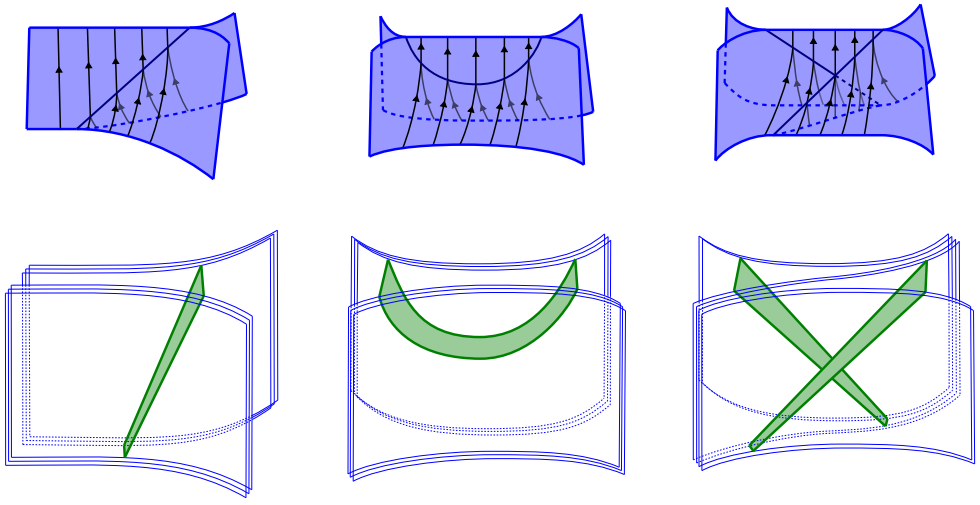

Figure 31: Locally constructing $V(c)$ for different cusp curves c. In the bottom row, the flow φ_f is vertical.

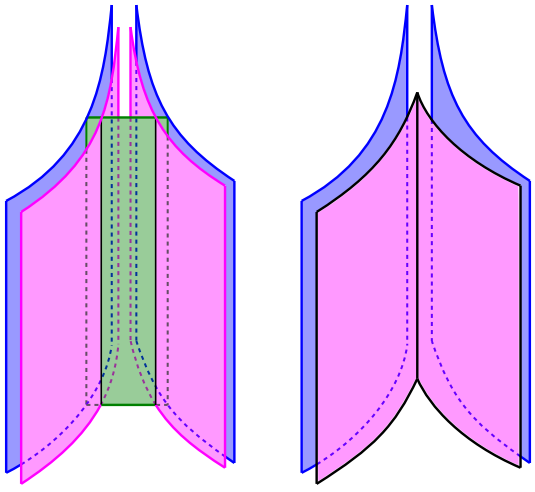

Figure 32: The view from a nonprincipal region U of B^u, looking at two leaves of $\mathscr{L}^u$ (blue) coming together near a cusp curve of B^u (B^u not pictured). On the left, the darker pink sheets are parts of $H(F)$ for the corresponding faces of B^u, and the green rectangle is part of $V(c)$ for the cusp curve c. The boundary of $\widehat{U}_A$ is formed by surgering and perturbing the pieces as shown.

Let $\widehat{U}_A$ be equal to the component of $(U \cap A) \setminus\!\setminus \left(\left(\bigcup V(c)\right) \cup \left(\bigcup H(F)\right)\right)$ containing $U \cap R_-(\overline{M}_f)$, where the unions are taken over all $\boldsymbol{uu}$-cusp curves c and $\boldsymbol{u}$-faces F of U.

For each principal region P of B^u, let $\widehat{P}$ be equal to P minus some (any) standard neighborhood of B^u.

Form $A \setminus\!\setminus \left(\left(\bigcup \widehat{P}\right) \cup \left(\bigcup \widehat{U}_A\right)\right)$, where the unions are taken over all principal regions and all nonprincipal regions. This is a neighborhood of $B^u|_A$ which we can make into a standard neighborhood by smoothing out corners and adding cusps near the nonprincipal cusp curves of B^u. We call the resulting standard neighborhood $\mathcal{N}_A(B^u)$. See Figure 32.

Now we extend this neighborhood to N. Let $\mathcal{N}_N(B^u)$ be a standard neighborhood of $\mathscr{L}^u|_N$ that lines up smoothly with $\mathcal{N}_A(B^u)$, with the additional property that φ_f points into $\mathcal{N}_N(B^u)$ at every point of $\partial\mathcal{N}_N(B^u)$. Such a neighborhood exists because the flow is quite simple on N: each flow line is an interval. See Figure 33.

Let $\mathcal{N}(B^u) = \mathcal{N}_A(B^u) \cup \mathcal{N}_N(B^u)$. This is a standard neighborhood of B^u with the promised property that φ_f points into $\mathcal{N}(B^u)$ along the boundary of each of its nonprincipal regions.

Now that we have the neighborhood $\mathcal{N}(B^u)$, we can redo the construction of (B^u, V) from Proposition 7.2 so that V is equal to the generating vector field for φ_f outside of $\mathcal{N}(B^u)$ and points into $\mathcal{N}(B^u)$ along the boundary of each nonprincipal region. Inside $\mathcal{N}(B^u)$ we are free to require that flow lines not lying in B^u do not accumulate in $\mathcal{N}(B^u)$ in backward time.

Next we let U be any nonprincipal region of B^u, and consider any point $p \in U$ not lying in a $\boldsymbol{u}$-face. If p lies in $\mathcal{N}(B^u)$, then its backward orbit must exit $\mathcal{N}(B^u)$ by construction, so we can assume $p \notin \mathcal{N}(B^u)$.

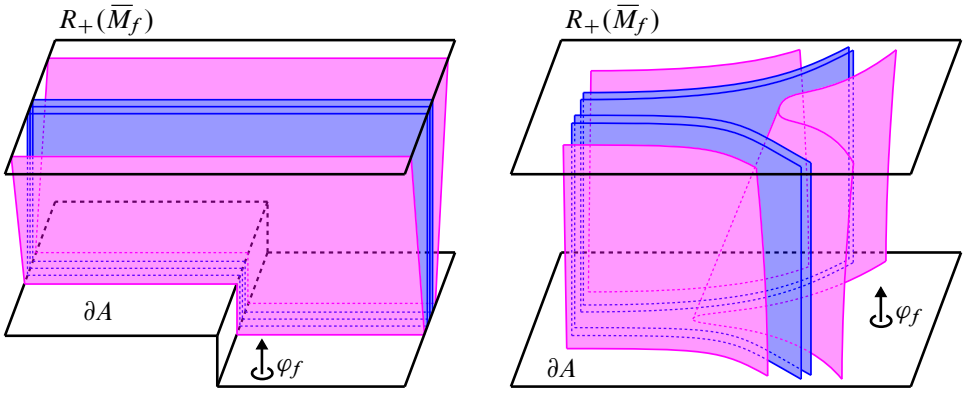

Figure 33: Construction of $\mathcal{N}_N$. The flow $\varphi_f|_N$ is vertical in this picture.

If we flow p backward until it hits L at a point p', we see that p' must lie in a nonprincipal region. Hence p lies in the negative escaping set of f by the definition of principal regions (Definition 3.10), so the backward orbit must terminate on $R_-(\overline{M}_f)$. □

In light of Lemma 7.4, we will henceforth assume that V has been chosen so that each backward trajectory in a nonprincipal regions not lying in a $\boldsymbol{u}$-face terminates on $R_-(\overline{M}_f)$. We now begin an extended analysis of the nonprincipal regions of (B^u, V), which will lead to the following proposition:

Proposition 7.5 *Each nonprincipal region of (B^u, V) is a $\boldsymbol{u}$-cusped product with no $\boldsymbol{uu}$-cusp circles.*

Fix a nonprincipal region U of B^u, and let F be a $\boldsymbol{u}$-face of U. By Remark 6.3, F is an annulus. Hence F is of one of the forms shown in Figure 34; that is, each boundary component either lies entirely on R_+ or alternates between lying on R_+ and lying in $\operatorname{brloc}(B^u)$. Each segment of ∂F lying in $\operatorname{brloc}(B^u)$ must have a source orientation with a single source in its interior. If a component of ∂F does not lie completely in R_+, we say that component is *scalloped*.

Recall that $\mathcal{F}$ is the depth one foliation of Q. Let $\{L_\theta \mid \theta \in S^1\}$ denote the collection of leaves in $\operatorname{int}(Q)$, each isotopic to L. For each $\theta \in S^1$, let τ_θ be the intersection $B^u \cap L_\theta$.

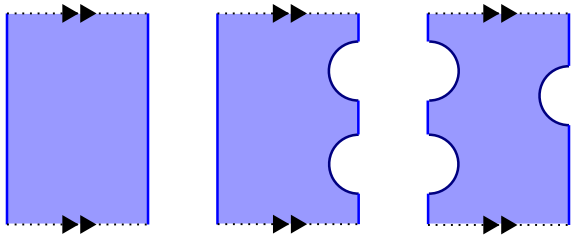

Figure 34: Possible $\boldsymbol{u}$-faces of a component of $Q \setminus\!\setminus B^u$ containing a component of R_-. The blue pieces of boundary indicate parts of the branch locus of B^u, while the black pieces lie on R_+.

By intersecting with $\mathcal{F}$, we obtain a cooriented foliation $\mathcal{F}_F$ of F. The foliation $\mathcal{F}$ is compatible with ∂F in the sense that

- the pieces of F along R_+ are leaves of $\mathcal{F}_F$,
- $\mathcal{F}_F$ is tangent to ∂F at the sources, and
- $\mathcal{F}_F$ is positively transverse to ∂F at all oriented points of $\operatorname{brloc}(B^u) \cap F$.

Furthermore, a given leaf of $\mathcal{F}_F$ is tangent to at most one source in ∂F. This is because, in our folding sequence, folds are performed one at a time.

Fix $\theta \in S^1$, and let γ be a component of $L_\theta \cap F$. In L_θ, γ is a piece of the boundary of a nonprincipal region of τ_θ. Note that γ cannot be a circle, or else Λ_+ would have a circular leaf. Since γ is a 1-manifold, it is homeomorphic to either $[0,1]$, $[0,\infty)$ or $(-\infty,\infty)$.

We can see that γ does not accumulate in $\operatorname{int}(F)$, for otherwise L_θ would accumulate in $\operatorname{int}(Q)$, a contradiction. As a consequence, if γ is noncompact, then each end of γ (there may be one or two) must accumulate on a component of ∂F. It is not possible for γ to accumulate on $\operatorname{brloc}(B^u) \cap F$ since γ must be transverse to $\operatorname{brloc}(B^u)$ except at sources. We conclude that each neighborhood $\nu \cong [a,\infty)$ of an end of γ limits on a boundary component of F lying entirely on R_+, and hence that ν limits on R_+. We remark that, when viewed as a curve in L_θ, the end-neighborhood ν must be an escaping ray.

Let ∂_1 and ∂_2 be the two boundary components of F. We say that a leaf λ of $\mathcal{F}_F$ *spans* F if, for each ∂_i $(i = 1, 2)$, λ either spirals onto ∂_i (if ∂_i is nonscalloped) or terminates on ∂_i.

Lemma 7.6 *There exists a leaf of $\mathcal{F}_F$ spanning F.*

Proof Suppose that ∂_1 is nonscalloped. Since $\mathcal{F}_F$ has no circle leaves, there must be leaves spiraling onto ∂_1; let λ be such a leaf. Choose an orientation for λ and suppose that λ spirals on ∂_1 in the backward direction. In the forward direction, the coorientation of λ prevents λ from spiraling on ∂_1. Also, as noted above, λ cannot accumulate in $\operatorname{int}(F)$. Thus λ must either accumulate on ∂_2 if ∂_2 is nonscalloped or terminate on ∂_2 if ∂_2 is scalloped.

It remains to show only that there exists a spanning leaf when ∂_1 and ∂_2 are both scalloped. Suppose that ∂_1 is scalloped and contains k sources of $\operatorname{brloc}(B^u)$. Let $\lambda_1, \dots, \lambda_k$ be the leaves of $\mathcal{F}_F$ which are tangent to the sources. Choose an orientation of ∂_1, which we will refer to as *clockwise*. Thus every oriented portion of $\operatorname{brloc}(B^u) \cap F$ is either *clockwise* or *counterclockwise*. If s_i is the source contained in λ_i, then $\lambda_i \setminus\setminus s_i$ consists of two components. Orient each of these components *away* from s_i, and let $\lambda_i^{\circlearrowright}$ and $\lambda_i^{\circlearrowleft}$ denote the components whose orientations at s_i are clockwise and counterclockwise, respectively.

If $\lambda_i^{\circlearrowright}$ terminates on ∂_2, then it must be the case that $\lambda_i^{\circlearrowleft}$ terminates on ∂_1. Indeed, if λ_i had both its endpoints on ∂_2 then an index argument shows that there would be a component of $F \setminus\setminus \lambda_i$ on which $\mathcal{F}_F$ is singular, a contradiction. We conclude that if $\lambda_i^{\circlearrowright}$ terminates on ∂_2, then λ_i spans F.

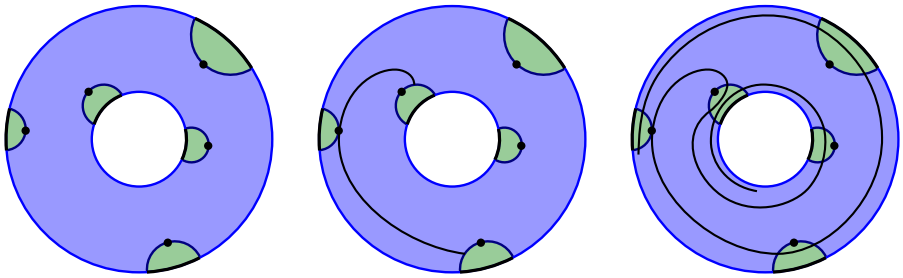

Figure 35: Left: embedding F (purple) in a larger annulus A without corners. Center: a spanning leaf λ as furnished by Lemma 7.6. Right: extending λ to an embedded cooriented line $\overline{\lambda}$ by adding segments which are alternately paths in $A - F$ and leaves of $\mathcal{F}_F$, so that both ends of $\overline{\lambda}$ spiral onto ∂A compatibly with the coorientation of ∂A. Coorientations are not drawn.

Now suppose that none of $\lambda_1^{\circlearrowleft}, \dots, \lambda_k^{\circlearrowleft}$ terminates on ∂_2, whence they all terminate on ∂_1. Then because the coorientation of $\mathcal{F}_F$ is compatible with the orientation of $\mathrm{brloc}(B^{\boldsymbol{u}})$, each $\lambda_i^{\circlearrowleft}$ must terminate on a counterclockwise portion of $\mathrm{brloc}(B^{\boldsymbol{u}})$ (recall that each λ_i contains at most one source). Consider $F' = F \setminus\!\setminus \left(\bigcup_{i=1}^{k} \lambda_i^{\circlearrowleft}\right)$. By assumption, there exists an annular component of F' containing ∂_2. Without loss of generality, assume that $\lambda_1^{\circlearrowleft} \subset \partial F'$. Then $\lambda_1^{\circlearrowleft}$ must either terminate on a clockwise portion of ∂_1 or terminate on ∂_2. Observe that F' contains no clockwise portions of ∂_1, since each clockwise component of ∂F is separated from F' by some $\lambda_i^{\circlearrowleft}$. We conclude that $\lambda_1^{\circlearrowleft}$ terminates on ∂_2, and that λ_1 spans F. □

Lemma 7.7 *The vector field V_F is circular.*

Proof Let A be an annulus with smooth boundary, and choose an embedding of F into A so that $\partial F \cap R_+$ is mapped into ∂A and the interior of each component of $\partial F \cap \mathrm{brloc}(B^{\boldsymbol{u}})$ is mapped to $\mathrm{int}(A)$. See Figure 35, left. By Lemma 7.6, there exists a leaf λ of $\mathcal{F}|_F$ spanning F. We can extend λ to an embedded copy $\overline{\lambda}$ of $\mathbb{R}$ with both ends spiraling onto ∂A by adding to λ line segments which are alternately contained in $A - F$ and in leaves of $\mathcal{F}_F$. See Figure 35, right.

Next, we may extend $\mathcal{F}_F$ to a foliation F_A of A such that $\overline{\lambda}$ is a leaf, and such that each component of ∂A is also. Moreover, V extends to a vector field V_A on A transverse to $\mathcal{F}_A$. The spiraling of $\overline{\lambda}$ forces $\mathcal{F}_A$ to be a Reeb foliation. By Lemma 6.5, V_A is circular, so V_F must also be circular. □

Now we can prove Proposition 7.5, as promised, which states that each nonprincipal region of (B, V) is a $\boldsymbol{u}$-cusped product.

Proof of Proposition 7.5 We will start by using Mosher's $\boldsymbol{u}$-cusped product recognition lemma, Lemma 6.9.

Let P be a nonprincipal region. We will check that P satisfies the hypotheses of Mosher's $\boldsymbol{u}$-cusped product recognition lemma, Lemma 6.9, namely the conditions labeled (1)–(4) and the property that each $\boldsymbol{m}$-face has nonpositive index. Evidently P contains no $\boldsymbol{s}$-faces, so (1) is satisfied. Recall that V was chosen so that each backward orbit of the V-semiflow not contained in a $\boldsymbol{u}$-face terminates on R_-; thus

(2) holds. Every $\boldsymbol{b}$-face of P comes from the orbit of a boundary component of L that accumulates on R_-. This orbit can either consist of finitely many line boundary components, each with one end in a positive end of L and one end in a negative end of L; or of infinitely many compact boundary components that escape into the positive and negative ends under positive and negative iteration of f. In either case, the corresponding $\boldsymbol{b}$-face is an annulus with boundary consisting of one $\boldsymbol{pb}$-circle and one $\boldsymbol{mb}$-circle; this shows (3) holds. Also, note that there are no $\boldsymbol{pm}$-edges since components of $R_+(\overline{M}_f)$ and $R_-(\overline{M}_f)$ are never adjacent, so (4) holds. Further, each $\boldsymbol{m}$-face of P is a component of $R_-(\overline{M}_f)$, so has nonpositive index. Hence we can apply Lemma 6.9 to conclude that P is homeomorphic to $S \times [0,1]$ for some component S of $R_-(\overline{M}_f)$, and P satisfies (a)–(d) in the definition of $\boldsymbol{u}$-cusped product (Definition 6.7).

It remains to check the following conditions from Definition 6.7: that

(e) each $\boldsymbol{p}$-face has nonpositive index,

(f) V is circular on each $\boldsymbol{u}$-face, and

(g) each $\boldsymbol{uu}$-cusp circle is incoherent.

For (e), note that each $\boldsymbol{p}$-face is a complementary component of $B^{\boldsymbol{u}} \cap R_+ = T_+^\infty$, which is an efficient train track; hence each $\boldsymbol{p}$-face has nonpositive index. Condition (f) is satisfied by Lemma 7.7. Finally, for (g), note that a $\boldsymbol{uu}$-cusp circle of a complementary region of $B^{\boldsymbol{u}}$ corresponds to a cusp in our construction's train track splitting sequence which experiences no collisions. By Lemma 4.2, such a cusp corresponds to a principal region, so we conclude that the nonprincipal region P is a $\boldsymbol{u}$-cusped product with no $\boldsymbol{uu}$-cusp circles, as claimed. □

7.4 Annulus and Möbius band sectors of $B^{\boldsymbol{u}}$

In Sections 7.5 and A.3, it will be important to understand how annulus and Möbius band sectors of $B^{\boldsymbol{u}}$ without corners arise in our construction.

Lemma 7.8 *Suppose that A is an annulus sector of $B^{\boldsymbol{u}}$ with no corners. Then A either*

(i) *is a face of a principal region of $B^{\boldsymbol{u}}$, or*

(ii) *has one boundary component on R_+ and another on a cusp circle of a principal region of $B^{\boldsymbol{u}}$, or*

(iii) *has both its boundary components on R_+.*

Furthermore, A is adjacent to at least one nonprincipal complementary region of $B^{\boldsymbol{u}}$.

Proof Suppose that γ is a boundary component of A lying in $\operatorname{brloc}(B^{\boldsymbol{u}})$. Then, in the periodic splitting sequence used to construct $B^{\boldsymbol{u}}$, γ corresponds to a cusp c of τ which never collides with another cusp, so is a principal cusp by Lemma 4.2. Let b be the branch incident to c and lying in A. One property of the splitting sequence is that every large branch is eventually split, so b must not be a large branch.

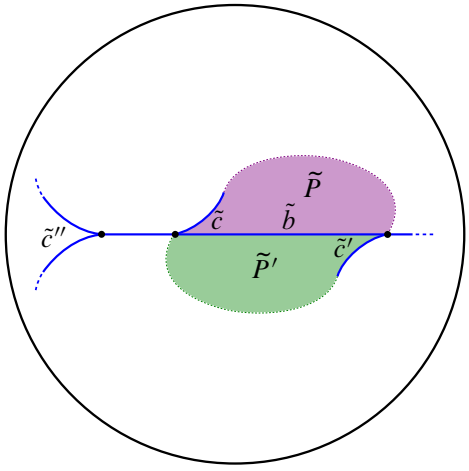

Figure 36: From the proof of Lemma 7.8 that $\tilde{b}$ cannot abut principal regions on both its sides.

Suppose that c points into b. If b is not incident to another switch, then (ii) holds. If b is incident to another switch c' (necessarily principal), then the Λ-routes from c and c' must fellow travel, contradicting the fact that principal cusps never fellow travel (Lemma 3.15).

Otherwise b is a small branch. Lift b to the universal cover $\widetilde{L}$, call its lift $\tilde{b}$ and suppose that the two cusps incident to $\tilde{b}$ are $\tilde{c}$ and $\tilde{c}'$, corresponding to c and c', respectively.

The reader should reference Figure 36 while reading this argument. Suppose for a contradiction that $\tilde{c}$ and $\tilde{c}'$ correspond to lifted principal regions of τ on each side of the small branch $\tilde{b}$. There are two lifts P and P' of principal regions of Λ_+ corresponding to these train track complementary regions. Note that there are multiple $\widetilde{\Lambda}_+$-leaves separating P and P' by [Cantwell et al. 2021, Lemma 5.20]. Also, by Lemma 3.15, none of the border leaves for P and P' share ideal points in $S_\infty(\widetilde{L})$. Let ℓ and ℓ' be the border leaves of P and P' carried by $\tilde{b}$, respectively. Following ℓ and ℓ' from b through $\tilde{c}$ and toward $\partial\widetilde{L}$, the corresponding train routes must diverge, forcing the existence of a cusp $\tilde{c}''$ that projects to a cusp in L that eventually is involved in a split through b, a contradiction.

Since $\tilde{c}$ and $\tilde{c}'$ are both principal cusps, the contradiction above forces them to lie on the same side of $\tilde{b}$. We conclude that if b is small, then (i) holds: A is a face of a principal region of B^u.

The only other possibility is that b is not incident to any cusps. In this case, both ends of b escape, giving two closed curves in R_+, so possibility (iii) holds.

It remains only to show that A cannot border a principal region on both sides. Since any sector touching R_+ is incident to nonprincipal regions on both sides, we can assume that A has both its boundary components in $\mathrm{brloc}(B^u)$ and thus corresponds to a compact branch b of a train track in our splitting sequence. By the above arguments, b must be incident to a nonprincipal region of the train track, forcing A to border a nonprincipal region of B^u. □

Lemma 7.9 *Let M be a Möbius strip sector of B^u with no corners. Then $\partial M \subset R_+$.*

Proof Let b be the branch of τ which suspends to give M. As in the previous proof, the cusps incident to b (if any) must be principal. Suppose there is at least one cusp incident to b. Since M has only one boundary component, this forces b to be incident to two cusps. Since f sends b to itself with the orientation reversed while preserving the orientation of L, these cusps must lie on opposite sides of b. But this gives a similar contradiction to the previous proof by looking at the picture in $\widetilde{L}$.

We conclude that b is not incident to any switches, so both of its ends must escape to positive ends and correspond to a boundary component of M lying in R_+. □

7.5 Our branched surface (B^u, V) is very full and veering

Theorem 7.10 *Let Q be an atoroidal sutured manifold with a depth one foliation $\mathcal{F}$. Then Q contains an unstable veering branched surface carrying the unstable Handel–Miller lamination associated to $\mathcal{F}$.*

Proof Let $\mathcal{F}$ be a depth one foliation of Q. Let L be a particular noncompact leaf of $\mathcal{F}$, and let $f : L \to L$ be a Handel–Miller representative of the monodromy for L determined by $\mathcal{F}$. Let (B^u, V) be an unstable dynamic branched surface as constructed in Proposition 7.2 whose nonprincipal regions are $\boldsymbol{u}$-cusped products (this exists by Proposition 7.5).

Suppose that f has a principal region P which is nonperipheral and not simply connected. Then the border of the nucleus of P, when flowed forward under the suspension flow of f, sweeps out a π_1-injective nonperipheral torus in Q, violating atoroidality.

Otherwise all principal regions of f are simply connected or peripheral, so all principal regions of B^u are $\boldsymbol{u}$-cusped tori or $\boldsymbol{u}$-cusped torus shells. By assumption, all nonprincipal regions of B^u are $\boldsymbol{u}$-cusped products, so B^u is very full in this case. It remains to show that B^u is veering. Veering branched surfaces are defined in Definition 6.11 and in this proof we will refer to properties (1)–(5) from that definition.

- Condition (1) regarding triple points is satisfied because each triple point of B^u comes from a train track folding move.

- Condition (2) on the boundary train track is satisfied because we chose the boundary train track T_+^∞ to be efficient and spiraling.

- Condition (3) requires that the orientation on each branch loop agree with the dynamic orientation (Definition 6.4) on each adjacent face of the corresponding complementary region. This is true because each branch loop is positively transverse to $\mathcal{F}$ by the construction, as is the core of each annulus face of a principal region of B^u. Meanwhile, there are no branch loops in nonprincipal regions by Proposition 7.5.

- Condition (4) on annulus and Möbius band sectors holds by Lemmas 7.8 and 7.9.

• Condition (5) says that B^u does not carry any tori or Klein bottles. Suppose that T is a torus or Klein bottle carried by B^u. Since $T \subset \operatorname{int} Y$, the intersection $T \cap L$ is compact. It follows that $\mathcal{F}|_T$ is a foliation of T by circles. By reversing the folding sequence used to construct (B^u, V), we get a splitting sequence

$$\tau_0 \to \tau_1 \to \cdots \tau_n \to \tau_{n+1} \to \cdots,$$

where each τ_i is a train track in L carrying the Handel–Miller lamination Λ_+, and $\tau_{i+n} = f(\tau_i)$ for all i. Since $\mathcal{F}|_T$ is a foliation by circles, there exists a closed curve $c \subset L$ which is carried by τ_0 and survives each splitting move in the above sequence. Fix a (local) side of c. After finitely many splits, all switches on this side of c must point in the same direction around c. Since each τ_i fully carries Λ_+, this forces the existence of a compact leaf of Λ_+. This contradicts that all leaves of Λ_+ are noncompact; see eg Lemma 3.12.

Having verified that (B^u, V) satisfies all the conditions in the definition of veering branched surface, we are done. □

Theorem 7.11 *Let Y be an atoroidal depth one Reeb sutured manifold, and let Y' be the de-Reebification of Y. Then Y' contains a very full unstable veering branched surface. For each annulus component A of $R_+(Y')$ that was added in the de-Reebification process, the veering branched surface intersects A in a circle.*

Proof In light of Theorem 7.10, the only case that needs our attention here is when ∂Y has at least one Reeb annulus. Since Y is depth one, there is a depth one foliation of Y with Reeb endperiodic monodromy f (see Definition 3.1). We can replace f with its endperiodization (see Construction 3.18), obtaining a depth one foliation of Y'. Each annulus of $R_+(Y')$ corresponds to an infinite strip end. By Lemma 3.17, the Handel–Miller lamination for the endperiodization has one or two leaves that exit each such end. When we construct the very full unstable veering branched surface (B^u, V) of Proposition 7.2, each such annulus will meet B^u in a single circle. □

7.6 Uniqueness of the veering branched surface construction

In this subsection, we will prove some uniqueness results about the veering branched surface constructed in Theorem 7.10. Taken together with the results in Section 4.5, they show that our construction of such a veering branched surface ends up being quite canonical.

The construction of a dynamic branched surface in Proposition 7.2 depends on three inputs, namely

(a) a f-periodic splitting sequence of f-endperiodic train tracks $S = \{\tau_0 \to \tau_1 \to \tau_2 \to \cdots\}$,

(b) a tiling $\mathcal{T}$ of the end-cycles of L, and

(c) a core K large enough such that the truncated sequence $\tau_0 \to \cdots \to f(\tau_0)$ is supported in K.

Our construction of the branched surface could be summarized as follows. First we reversed the splitting sequence to obtain a folding sequence from $f(\tau_0)$ to τ_0. Outside a neighborhood of $R_+(\overline{M}_f)$, we let the branched surface be the suspension of this folding sequence; in the neighborhood of $R_+(\overline{M}_f)$, we

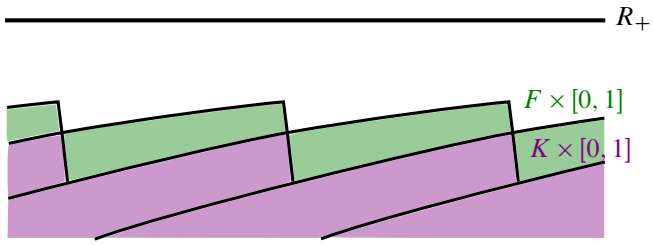

Figure 37: Schematic of the proof of Lemma 7.12.

constructed the branched surface to be $T_+^\infty \times I$ (recall that T_+^∞ is chosen during the construction of the splitting sequence). The choices of tiling and core simply served the purpose of fixing a neighborhood of $R_+(\overline{M}_f)$, so it should come as no surprise that the construction is independent of those choices. In Lemmas 7.12 and 7.13 we make this precise.

Later, in Lemma 7.14, we show that the branched surface is unchanged if we replace S by an equivalent f-periodic splitting sequence (using the equivalence relation from Section 4.5). By Theorem 4.17, this implies that the branched surface depends only on the choice of train track T_+^∞.

Let us write $B(S, \mathcal{T}, K)$ for the branched surface constructed with the data (a)–(c), considered up to isotopy.

Lemma 7.12 *For a fixed splitting sequence S and tiling $\mathcal{T}$, let K and K' be two choices of cores such that $\tau_0 \to \cdots \to f(\tau_0)$ is supported inside K and K'. Then $B(S, \mathcal{T}, K) = B(S, \mathcal{T}, K')$.*

Proof For convenience, let $B = B(S, \mathcal{T}, K)$ and $B' = B(S, \mathcal{T}, K')$. Since there is always a core containing both K and K', it suffices to assume that $K \subset K'$. Let $F = K' \setminus\setminus K$. Using the notation from the construction in Section 7.2, we can write Q as the union $A \cup (F \times [0,1]) \cup N'(R_+)$, with $N(R_+) = (F \times [0,1]) \cup N'(R_+)$ and $A' = A \cup (F \times [0,1])$. See Figure 37 for a schematic picture.

Notice that $B|_{F\times[0,1]}$ is the product branched surface $\tau_0|_F \times [0,1]$ and that $B|_{A'} = B|_A \cup B|_{F\times[0,1]} = B'|_{A'}$, since $\tau_0 \to \cdots \to f(\tau_0)$ is supported inside K_i. In particular, $B|_{\partial A'} = B'|_{\partial A'}$, and so, upon taking the forward flow completion, we have $B|_{N'(R_+)} = B'|_{N'(R_+)}$. Hence $B = B'$. □

In light of Lemma 7.12, we will drop the third argument of $B(\cdot,\cdot,\cdot)$ and write simply $B(\cdot,\cdot)$.

Lemma 7.13 *For a fixed splitting sequence S, let $\mathcal{T}$ and $\mathcal{T}'$ be two choices of tiling of the end-cycles of L. Then $B(S, \mathcal{T}) = B(S, \mathcal{T}')$.*

Proof For convenience, let $B = B(S, \mathcal{T})$ and $B' = B(S, \mathcal{T}')$. Using Lemma 4.15 as in the proof of Lemma 4.16, it suffices to prove the lemma in the case that $\mathcal{T}$ and $\mathcal{T}'$ are interleaved. Recall that this in particular means that $K_i \subset K_i' \subset K_{i+1}$ up to reindexing, where K_i are the cores determined by $\mathcal{T}$ and K_i' are the cores determined by $\mathcal{T}'$. Suppose $\tau_0 \to \cdots \to f(\tau_0)$ is supported inside K_i. Let $F = K_i' \setminus\setminus K_i$. We will show that $B(S, \mathcal{T}, K_i) = B(S, \mathcal{T}, K_i')$.

This proof of this is exactly as in Lemma 7.12: We write Q as the union $A \cup (F \times [0,1]) \cup N'(R_+)$, observe that $B|_{A'} = B|_A \cup B|_{F\times[0,1]} = B'|_{A'}$, then $B|_{N'(R_+)} = B'|_{N'(R_+)}$, and hence $B = B'$. □

In light of Lemma 7.13, we will drop the second argument of $B(\cdot,\cdot)$ and write simply $B(\cdot)$.

Lemma 7.14 *Let S and S' be two equivalent f-periodic splitting sequences. Then $B(S)$ is ambient isotopic to $B(S')$.*

Proof Let $B = B(S)$ and $B' = B(S')$. It suffices to prove the lemma in the case when S and S' differ by one f-periodic commutation.

In this case, using the notation from the construction of Section 7.2, there exist M_i and M_{i+1} such that $B(S)$ and $B(S')$ agree outside of $M_i \cup M_{i+1}$. In $M_i \cup M_{i+1}$, the restrictions of $B(S)$ and $B(S')$ are the suspensions (in the downward direction) of splits along the same two disjoint branches, but in different orders. This description makes it clear that the restrictions, and hence the entire branched surfaces, are isotopic. □

This gives the following:

Corollary 7.15 *Up to isotopy, our construction of a veering branched surface in Theorem 7.10 depends only on the choice of the boundary train track.*

It turns out that an even stronger statement is true, namely that any veering branched surface in Theorem 7.10 (satisfying some obviously necessary conditions) comes from our construction; see Theorem 9.22. Hence our construction produces the unique veering branched surface satisfying these conditions given a boundary train track. We prove this stronger statement in Section 9, where we also show that when the boundary train track is allowed to vary, the resulting branched surface transforms via moves that can be explicitly described. This will round off our investigation of uniqueness.

8 Foliation cones

In this section, we will port some results of [Landry et al. 2024] regarding veering triangulations and Thurston fibered faces over to the sutured setting. The main goal will be Theorem 8.5, which we need in order to complete the uniqueness discussion in Section 9. We remark that this discussion opens up some interesting questions, in particular regarding how to generalize Thurston norm faces to sutured manifolds, which we will discuss in Section 11.

8.1 Depth one foliations and foliation cones

We first review some of the theory of foliation cones for atoroidal sutured manifolds. For more detail, see [Cantwell and Conlon 1999; 2017; Cantwell et al. 2021].

Let Q be an atoroidal sutured manifold. Every depth one foliation $\mathcal{F}$ on Q determines a class $[\mathcal{F}] \in H^1(Q)$ whose value on any oriented loop in $\mathrm{int}(Q)$ is given by taking its algebraic intersection with a noncompact leaf of $\mathcal{F}$. An alternative way of describing $[\mathcal{F}]$ is to cut away staircase neighborhoods of $R_\pm$ and look at the restriction of a noncompact leaf, which is now a properly embedded surface; the class of this surface in $H_2(Q, \partial Q) \cong H^1(Q)$ is $[\mathcal{F}]$. It is shown in [Cantwell and Conlon 1994, Theorem 1.1] that the isotopy class of $\mathcal{F}$ is determined by $[\mathcal{F}]$.

Cantwell and Conlon [1999, Theorem 4.3] also showed that, for fixed Q, there exist finitely many cones in $H^1(Q)$, called *foliation cones*, such that the class of any depth one foliation on Q lies in the interior of one of these cones, and, conversely, any integral point interior to a cone corresponds to a depth one foliation. We remark that Cantwell and Conlon refer to these as "Handel–Miller foliation cones".

Suppose we fix a foliation $\mathcal{F}_1$ associated to C, with a Handel–Miller representative f_1 of its monodromy. By suspending the 1-dimensional positive Handel–Miller lamination of f_1, we obtain the 2-dimensional Handel–Miller lamination $\mathcal{L}$. Now suppose $\mathcal{F}_2$ is another depth one foliation associated to C. By [Cantwell and Conlon 2017, Theorem 4.9 and Proposition 6.20], $\mathcal{F}_2$ can be isotoped to be transverse to the suspension semiflow of f_1. The proof of the transfer theorem of [Cantwell et al. 2021, Theorem 12.7] gives that the intersection Λ_2 of $\mathcal{L}$ with a noncompact leaf of $\mathcal{F}_2$ is ambient isotopic to the 1-dimensional positive Handel–Miller lamination Λ for the first return map to that leaf. (In fact, using this ambient isotopy to pull back a hyperbolic metric for which Λ is geodesic shows that Λ_2 is the positive Handel–Miller lamination associated to this pullback metric.) Hence, as we vary the depth one foliation within the foliation cone C, the 2-dimensional Handel–Miller lamination is invariant up to isotopy. Hence there exists a semiflow φ_C on Q such that every depth one foliation $\mathcal{F}$ associated to C is transverse to φ_C up to isotopy, and such that the first return map of φ_C preserves the Handel–Miller lamination for a given noncompact leaf of $\mathcal{F}$.

Remark 8.1 The papers [Cantwell and Conlon 2017; Cantwell et al. 2021] assume that $R_\pm$ have no annulus or torus components. However, we have explained in Section 3 that Handel–Miller theory works for surfaces with infinite strip ends. Reading these papers with that in mind, one sees the results also hold when annular components of $R_\pm$ are allowed. ◁

Finally, it is explained in [Cantwell and Conlon 2017, Section 6.2] how one can compute foliation cones in practice using Markov partitions. We will not need to use the full knowledge of this, but rather we just need the fact that each foliation cone C is dual to the cone in $H_1(Q)$ positively generated by the periodic orbits of the Handel–Miller semiflow φ_C described above.

We remark that the atoroidal case described here is simpler than the general case, where one must choose the Handel–Miller representative with an additional property called tightness to define the correct foliation cone. This complication arises in the presence of principal regions which are not disks.

Note the significant parallels between the theory of foliation cones and the flow-theoretic perspective on cones over fibered faces of the Thurston norm ball developed by Fried [1979] in the setting of compact

hyperbolic manifolds. However, the analogy is not perfect because, unlike fibered cones, foliation cones cannot be interpreted as cones over faces of the unit ball of a norm on $H^1(Q)$: they are in general not invariant under multiplication by -1, as demonstrated by examples in [Cantwell and Conlon 1999].

8.2 Cone of dual cycles

In the setting of pseudo-Anosov mapping tori, the following is true:

Theorem 8.2 *Let $f : S \to S$ be a pseudo-Anosov homeomorphism on a finite-type surface, let $M = S \times [0,1]/(x,1) \sim (f(x),0)$ be the mapping torus of f with its foliation $\mathcal{F}$ by the leaves $S \times \{t\}$, and let $\mathcal{L}$ be the unstable 2-dimensional lamination in M associated to f. Let $\mathcal{C}_{\mathcal{F}} \subset H_2(M, \partial M)$ be the Thurston fibered cone associated to $\mathcal{F}$.*

Meanwhile, let B be a veering branched surface fully carrying $\mathcal{L}$. Let Γ be the dual graph of B and let Φ be the flow graph of B. Let $\mathcal{C}_\Gamma \subset H_1(M)$ be the cone positively generated by the cycles of Γ, and let $\mathcal{C}_\Phi$ be the cone positively generated by the cycles of Φ.

Then $\mathcal{C}_{\mathcal{F}}^\vee = \mathcal{C}_\Gamma = \mathcal{C}_\Phi$ in $H_1(M)$.

The branched surface B in the statement of Theorem 8.2 is actually unique up to isotopy; see Theorem 9.1. The statement above is phrased to motivate and maximize symmetry with Theorem 8.5, which we later use to prove the corresponding uniqueness statement in our setting.

In the cases when S is closed and when S is fully punctured (ie when the singularities of f all occur at punctures), Theorem 8.2 is a consequence of results in [Landry et al. 2024; Landry 2022]. The general case does not pose any added difficulty, so we sketch a proof using the ideas of [Landry et al. 2023b]. Our goal for the rest of this section is to transport this proof to the setting of sutured manifolds.

Proof Let M° be the fully punctured mapping torus of f (obtained by deleting the singular orbits of the suspension flow of f), and let Δ be the veering triangulation on M° dual to B. Then Γ is the dual graph of Δ and Φ is the dual graph of Δ.

By [Fried 1979, Theorems 6 and 7], $\mathcal{C}_{\mathcal{F}}^\vee$ is spanned by the closed orbits of the pseudo-Anosov suspension flow. (Strictly speaking, Fried treats only the case where S is closed; a proof of the general case appears in [Landry 2023, Appendix A].) Now every closed orbit of the flow, say of homotopy class g, lies on some annulus or Möbius band leaf of $\mathcal{L}$. The lift of such a leaf to $\widetilde{M}$ determines a g-invariant dynamic plane, which has to contain a g-invariant bi-infinite $\widetilde{\Gamma}$-line. The quotient of the line is a Γ-cycle of homotopy class g. Conversely, a Γ-cycle, say of homotopy class g, determines a g-invariant dynamic plane, and thus a g-invariant leaf of $\widetilde{\mathcal{L}}$, the image of which contains a closed orbit of homotopy class g. See [Landry et al. 2023b] for more details about this argument. This shows that $\mathcal{C}_{\mathcal{F}}^\vee = \mathcal{C}_\Gamma$. Meanwhile it is shown in [Landry et al. 2024, Theorem 5.1] that $\mathcal{C}_\Gamma = \mathcal{C}_\Phi$. □

To generalize the above result to the sutured setting, fix, for the rest of this section, a Handel–Miller map $f : L \to L$. Let $\overline{M}_f$ be the compactified mapping torus of f with depth one foliation $\mathcal{F}$ and associated unstable Handel–Miller lamination $\mathcal{L}$. Let B be an arbitrary veering branched surface fully carrying $\mathcal{L}$. We emphasize that while such a branched surface was constructed in Proposition 7.2, we are *not* assuming that B comes from our construction. However, in Section 9 we show that B indeed arises from our construction.

We have defined the dual graph and flow graph of B in Section 6.5. If we define $\mathscr{C}_\Gamma$ and $\mathscr{C}_\Phi$ exactly as in Theorem 8.2, Proposition 6.27 tells us that $\mathscr{C}_\Gamma = \mathscr{C}_\Phi$. Also, in Section 8.1, we discussed how foliation cones serve as a natural generalization to Thurston fibered cones.

However, some thought reveals that the equality between $\mathscr{C}^\vee_{\mathcal{F}}$ and $\mathscr{C}_\Gamma = \mathscr{C}_\Phi$ and its proof will not carry over immediately. The branched surface may contain annulus sectors, which do not carry a canonical dynamic orientation. See Example 10.7 for an instance where this happens. To address this, we need to impose a requirement on dynamic orientation separately. Before we do that we set up some notation.

Recall the correspondence between periodic leaves of $\widetilde{\mathcal{L}}$ and periodic dynamic planes of $\widetilde{B}$ in Proposition 6.29. Going forward, we will be implicitly applying this correspondence.

The quotient of a periodic leaf A in $\overline{M}_f$ is a leaf of $\mathcal{L}$ whose interior is homeomorphic to an open annulus or Möbius band. Such a leaf must contain a periodic orbit of the Handel–Miller suspension flow as a core. While such a periodic orbit may not be unique, the flow directions on all of them will be oriented in the same way. With this in mind, we will refer to the dynamic orientation determined by the flow direction on this core as *the dynamic orientation on* A.

Meanwhile, a periodic dynamic plane D, which is, say, invariant under $g \in \pi_1(M)$, contains a g-invariant bi-infinite $\widetilde{\Gamma}$-line. Indeed, the proof of Proposition 6.27 shows that unless D has an odd number of AB strips, there is a g-invariant bi-infinite $\widetilde{\Phi}$-line, and, applying Proposition 6.17 to the quotient of D under g, we can homotope this to a g-invariant bi-infinite $\widetilde{\Gamma}$-line. If D has even width, the zigzag in the middle AB region is a g-invariant bi-infinite $\widetilde{\Gamma}$-line. The quotient of such a line is an oriented core of the quotient of D, and again, with a slight abuse of notation, we refer to the corresponding dynamic orientation on the image of D as *the dynamic orientation on* D.

One should of course check that this is well defined, since there could be more than one g-invariant bi-infinite line on D. Suppose otherwise: that we can find two such lines on D which descend to two Γ-cycles of opposite homotopy class. Then, by Proposition 6.27, we would be able to find two bi-infinite $\widetilde{\Phi}$-lines which descend to two (possibly nonprimitive) Γ-cycles of opposite homotopy class. But, by Lemma 6.26, any two periodic $\widetilde{\Phi}$-lines must bound a union of AB strips, and thus be oriented in the same way. Hence this shows that the dynamic orientation of a periodic dynamic plane is well defined.

If a periodic leaf A corresponds to a periodic dynamic plane D, we say that the dynamic orientation on A is *compatible* with that on D if the dynamic orientations on the images of A and D agree. The condition

that we need for the generalization of Theorem 9.1 is that the dynamic orientation on each periodic leaf be compatible with that on its associated periodic dynamic plane.

However, such a condition is difficult to verify in practice, since there are infinitely many periodic leaves to check. Fortunately, it turns out a simpler criterion suffices here, which we take as our definition in Definition 8.3 below. In Proposition 8.4, we will show the equivalence between Definition 8.3 and the condition stated in the last paragraph.

To state Definition 8.3, we need some more setup. Recall that, by Lemma 3.11(a), $\Lambda^\infty_+ = \mathcal{L} \cap R_+$ is spiraling. In fact, if we use the language of this section, Lemma 3.11(b) says further that the orientation of each closed leaf of Λ^∞_+ is compatible with the dynamic orientation of the closed leaf of $\mathcal{L}$ that contains it. Similarly, each circular sink component of the boundary train track $T^\infty_+ = B \cap R_+$ carries an orientation coming from the source orientation of T^∞_+. Each circular leaf of Λ^∞_+ corresponds to a circular sink component of the boundary train track, so we can ask if the orientations of these loops agree.

Also recall that each leaf in the boundary of a complementary region of $\mathcal{L}$ contains a periodic orbit of the Handel–Miller suspension flow, and thus carries a natural dynamic orientation. Similarly, each face of a complementary region of B by definition carries a dynamic orientation. Each leaf in the boundary of a complementary region of $\mathcal{L}$ corresponds to a face of a complementary region of B, so we can compare their dynamic orientations.

Definition 8.3 A veering branched surface $B = (B, V)$ in M is said to *compatibly carry* $\mathcal{L}$ if:

(1) B fully carries $\mathcal{L}$.

(2) Every circular leaf of the boundary lamination $\mathcal{L} \cap R_+$ is oriented compatibly with the corresponding circular sink component of the boundary train track $\beta = B \cap R_+$.

(3) Every leaf in the boundary of a complementary region of $\mathcal{L}$ is oriented compatibly with the corresponding face of the corresponding complementary region of B. ◁

Proposition 8.4 *Suppose a veering branched surface $B = (B, V)$ fully carries $\mathcal{L}$. Then B compatibly carries $\mathcal{L}$ if and only if the dynamic orientation on each periodic leaf is compatible with that on its associated periodic dynamic plane.*

Proof Suppose the dynamic orientation on each periodic leaf is compatible with that on its associated periodic dynamic plane. Then, for every circular leaf l of the boundary lamination, there is some annulus or Möbius band leaf of $\mathcal{L}$, containing l, whose dynamic orientation is given by the orientation of l. Such a leaf lifts to a periodic leaf of $\widetilde{\mathcal{L}}$, and the corresponding periodic dynamic plane of $\widetilde{B}$ must have a boundary component along $\widetilde{B} \cap \widehat{R}_+ \subset \widetilde{\Gamma}$ which projects down to the circular sink component of β carrying l, and its orientation determines the dynamic orientation of the dynamic plane. Since the dynamic orientation of the leaf agrees with that of the dynamic plane, the orientation of l agrees with that of the circular sink component.

For every leaf in the boundary of a complementary region of $\mathscr{L}$, consider a lift to $\widetilde{\mathscr{L}}$ and the corresponding dynamic plane. The quotient of this dynamic plane meets the corresponding face of the complementary region of B, and we claim that their dynamic orientations agree. This can be seen by taking a periodic orbit of V on the face, which defines the dynamic orientation of the face, and applying Proposition 6.17 to homotope it to a Γ cycle, which defines the dynamic orientation of the dynamic plane. Since the dynamic orientation of the leaf agrees with that of the dynamic plane, it in turn agrees with that of the face.

For the converse, it suffices to show that the dynamic orientation condition always holds for leaves of $\mathscr{L}$ that do not have a circular boundary component that lies on R_+, since, for those leaves, the argument in the first paragraph goes through.

To that end, consider a periodic leaf A of $\widetilde{\mathscr{L}}$ whose image in $\mathscr{L}$ does not have a circular boundary component that lies on R_+, and let D be its corresponding periodic dynamic plane. We first consider the case when D does not contain the lift of an annulus or Möbius band sector.

Consider a bi-infinite periodic $\widetilde{\Phi}$-line on D. It is positively transverse to $\mathrm{brloc}(\widetilde{B})$, ie sectors of $\widetilde{B}$ must merge with D in the forward direction. Equivalently, this can be expressed by saying that the holonomy of $\mathscr{L}$ around the image of this line is contracting on at least one side. By the transversely contracting dynamics of the unstable Handel–Miller lamination (Lemma 5.4), the periodic orbit in the image of A must be oriented in the same direction as the Φ-cycle.

If D contains the lift of an annulus or Möbius band sector, the sector must lie on the face of some complementary region of B. As reasoned in the second paragraph above, the dynamic orientation of D agrees with that of the face, which by assumption agrees with that of the corresponding leaf of $\mathscr{L}$. This completes the proof of the converse. □

Equipped with the notion of compatibly carrying, we can proceed with the proof of our theorem.

Theorem 8.5 *Let $f : L \to L$ be an endperiodic map, let Q be the compactified mapping torus of f with depth one foliation $\mathcal{F}$, and let $\mathscr{L}$ be the unstable Handel–Miller lamination in Q associated to f. Let $\mathscr{C}_{\mathcal{F}} \subset H_2(Q, \partial Q)$ be the foliation cone associated to $\mathcal{F}$. Meanwhile, let B be a veering branched surface compatibly carrying $\mathscr{L}$, with dual graph Γ and flow graph Φ. Let $\mathscr{C}_\Gamma$ and $\mathscr{C}_\Phi$ be the cones in $H_1(Q)$ positively generated by the cycles of Γ and Φ, respectively. Then*

$$\mathscr{C}_{\mathcal{F}}^\vee = \mathscr{C}_\Gamma = \mathscr{C}_\Phi.$$

Proof As pointed out before, Proposition 6.27 implies that $\mathscr{C}_\Gamma = \mathscr{C}_\Phi$; hence, it suffices to show that $\mathscr{C}_{\mathcal{F}}^\vee = \mathscr{C}_\Gamma$. By the discussion in Section 8.1, it suffices to show that every closed orbit of the Handel–Miller suspension flow is homotopic to a Γ-cycle, and that every Γ-cycle is homotopic to a closed orbit of the Handel–Miller suspension flow.

Every closed orbit of the flow lies on some leaf of $\mathscr{L}$, whose lift to $\widetilde{\mathscr{L}}$ is a periodic leaf, and thus corresponds to some periodic dynamic plane. The periodic dynamic plane carries some periodic Γ-line,

which quotients down to a Γ-cycle. By Proposition 8.4, the Γ-cycle is homotopic to the closed orbit (as opposed to its opposite).

Conversely, every Γ-cycle determines a periodic dynamic plane, which corresponds to a periodic leaf of $\widetilde{\mathcal{L}}$ whose image contains a closed orbit. By Proposition 8.4, the Γ-cycle is homotopic to the closed orbit. □

9 Uniqueness of veering branched surfaces which carry Handel–Miller laminations

The following theorem about veering triangulations is essentially known to experts, although perhaps with different terminology. We include a proof for completeness.

Theorem 9.1 *Let $f : S \to S$ be a pseudo-Anosov map on a finite-type surface. Let $\mathcal{L}$ be the unstable lamination of the suspension flow on the mapping torus. If (B, V) and (B', V') are two unstable veering branched surfaces fully carrying $\mathcal{L}$, then B is isotopic to B'.*

That is, the unstable veering branched surface carrying $\mathcal{L}$ has a unique underlying branched surface. Note the vector field cannot be expected to be unique since there are many vector fields that make a branched surface into an unstable branched surface (this was discussed in Remark 6.1).

Proof Let Γ be the dual graph for B. By [Landry et al. 2024, Proposition 5.11], there exists an oriented surface S such that $M \setminus\setminus S \cong S \times [0,1]$ (so S is a fiber of a fibration $M \to S^1$), S is positively transverse to Γ, and S pairs positively with each cycle in Γ. It follows that $\Gamma \setminus\setminus S$ is an acyclic digraph. As such, we can choose a function $h\colon \Gamma \setminus\setminus S \to [0,1]$ which is monotonically increasing on edges of $\Gamma \setminus\setminus S$, and takes the values 1 and 0 at all points of $\Gamma \setminus\setminus S$ lying on $R_+(M \setminus\setminus S)$ and $R_-(M \setminus\setminus S)$, respectively.

Each sector of $B \setminus\setminus S$ is a disk, over which we can continuously extend h so that each level set in a sector is a single properly embedded line segment transverse to Γ, and h takes the values 1 and 0 exactly on points of $R_+(M \setminus\setminus S)$ and $R_-(M \setminus\setminus S)$, respectively.

Finally, each component of $(M \setminus\setminus S) \setminus\setminus (B \setminus\setminus S)$ is diffeomorphic to $A \times [0,1]$, where A is either a disk with ≥ 3 cusps on its boundary or an annulus with one smooth boundary component and ≥ 1 cusps on the other. We can extend h to each $A \times [0,1]$ region so that each level set of $h|_{A\times[0,1]}$ is diffeomorphic to A. Together, the level sets determine an isotopy from $S \times 1$ to $S \times 0$. Looking at the intersection with B at each time slice of this isotopy, we obtain a splitting sequence of train tracks which is periodic under f. The branched surface B is the suspension of this splitting sequence.

Note that every sector of B is a disk: otherwise there would be two parallel $\boldsymbol{u}$-cusped tori. These would correspond to complementary regions of the unstable lamination with core curves c_1, c_2 such that $c_1^{k_1}$ is homotopic to $c_2^{k_2}$ for some positive integers k_1, k_2, a contradiction. Hence B has a dual ideal triangulation, which we call Δ. By [Tsang 2023, Proposition 3.22], Δ is a veering triangulation; by the arguments above, Δ is layered. This determines Δ up to isotopy by [Agol 2011]. As its dual, B is unique up to isotopy also. □

We note that a shorter proof of Theorem 9.1 is possible using [Landry et al. 2024, Theorem E]. In fact, such a proof would show a stronger version of the theorem, where we just need to assume that the dual graphs of B and B' generate the same cone in homology. See Section 11.2 for more discussion.

The goal of this section is to transport this particular proof of Theorem 9.1 to our setting of endperiodic maps. Some care is needed because, as mentioned earlier, when we construct a veering branched surface carrying $\mathcal{L}$ in Proposition 7.2, the resulting branched surface depends on the initial choice of boundary train track. However, we will show that this is the only obstacle to uniqueness, in the sense that a veering branched surface fully carrying $\mathcal{L}$ with a specified efficient boundary train track is unique up to isotopy. Our strategy is to mimic the proof of Theorem 9.1 above: given a veering branched surface B carrying $\mathcal{L}$, we will construct a surface whose intersection with B gives us a splitting sequence of train tracks as we sweep it around the sutured manifold. This will show that B can be obtained from our construction in Section 7 using this splitting sequence. We will then apply the results in Section 7.6 to conclude that B is the only veering branched surface fully carrying $\mathcal{L}$ with this boundary train track.

A natural question, then, is *how* these veering branched surfaces differ from one another as we vary the boundary train track. We address this question in Section 9.3 by showing that they are related by a family of moves which we describe explicitly.

9.1 Building surfaces from veering branched surfaces

In this section we let (B, V) be an unstable veering branched surface in a sutured manifold Q.

We let N be a standard neighborhood of B with the property that along each component of ∂N lying in a $\boldsymbol{u}$-cusped product, V points into N. This can be arranged by, in a $\boldsymbol{u}$-cusped product $P \cong \Sigma \times [0,1]$, isotoping $\Sigma = \Sigma_0$ along the orbits of $V|_P$ to obtain a family of surfaces $\{\Sigma_t \mid t \in [0,1]\}$ such that the $\boldsymbol{u}$-faces of P are within some small $\epsilon > 0$ from Σ_1 and the points in Σ_1 further than ϵ from the $\boldsymbol{u}$-faces lie in R_+. We then set the components of $\Sigma_1 \setminus\!\setminus R_+$ to be components of ∂N. See Figure 38 for a schematic.

Let a be a transient annulus sector of B. Since $V|_a$ points inward on one component of ∂a and outward on the other, we can always replace V by a vector field V' such that each orbit of $V'|_a$ is a properly embedded arc, with the additional properties that V and V' agree outside of a and (B, V') is a veering branched surface. This simplifies some upcoming definitions and constructions, so we will make the following assumption going forward:

Convention 9.2 For any transient annulus a of (B, V), all orbits of $V|_a$ are properly embedded arcs. ◁

Recall the definition of the dual graph Γ of B from Definition 6.15. The complementary regions of Γ in B are disks and annuli, and it is now to our advantage to subdivide the latter into disks. There are multiple ways to do this that would work for our purposes, but we have chosen one that feels relatively natural.

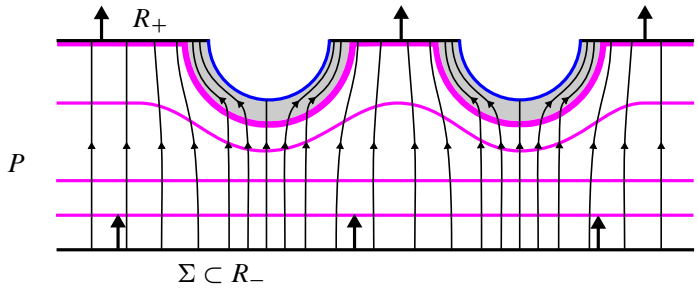

Figure 38: By using the product structure of $\boldsymbol{u}$-cusped products, we can build a standard neighborhood N of B with the property that along each component of ∂N lying in a $\boldsymbol{u}$-cusped product, V points into N. Here the gray areas indicate parts of N in the $\boldsymbol{u}$-cusped product P.

Definition 9.3 An *extended dual graph* for B is a directed graph embedded in B, containing the dual graph Γ as a subgraph, intersecting each sector s of B as follows:

- If s is a source sector, then for each vertex v on ∂s we augment Γ by adding a directed edge from the core Γ-cycle of s to v.
- If s is a transient annulus, then, for each vertex v in the outwardly cooriented component of ∂s, we augment Γ by adding the V-trajectory connecting v to the other boundary component of s, oriented compatibly with V. (This uses Convention 9.2.)
- For any other sector s, we let $\Gamma^+|_s = \Gamma|_s$.

See Figure 39. ◁

Lemma 9.4 *Let s be a source sector of B. Let γ be a properly embedded arc in s that is positively transverse to Γ^+. Then γ is homotopic in s, rel $\partial\gamma$, to an arc positively transverse to V.*

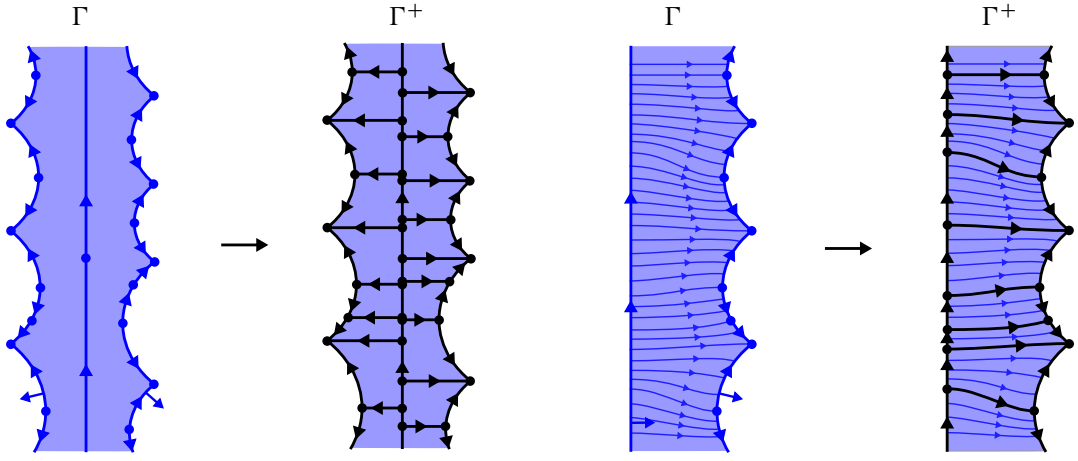

Figure 39: Obtaining the extended dual graph Γ^+ from the dual graph Γ. For transient annulus sectors we use the data of V, while for source sectors we do not.

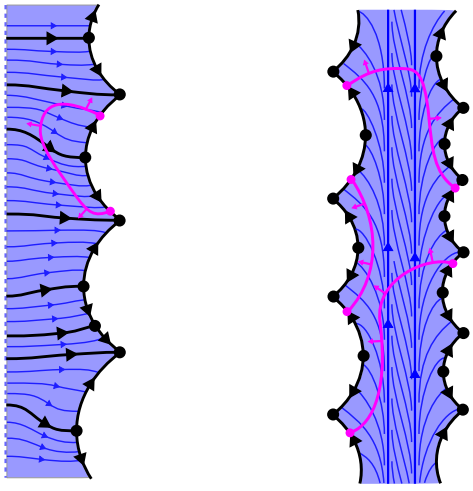

Figure 40: Left: an impossible configuration of γ in s. Right: a possible configuration.

Proof In general, the structure of $V|_s$ is as follows. Since $V|_s$ points outward along ∂s, there is at least one closed orbit of $V|_s$, and possibly infinitely many. All closed orbits have orientation agreeing with the dynamic orientation of s. Every orbit ending on ∂s spirals onto a closed orbit in the backward direction, and the direction of the spiraling is compatible with the closed orbit's orientation. Every nonclosed orbit disjoint from ∂s spirals onto closed orbits in both directions such that all orientations are compatible. See Figure 40, right.

Let $\tilde{s}$ be the universal cover of s, let $\tilde{\gamma}$ be the lift of γ to $\tilde{s}$, and let $V_{\tilde{s}}$ be the lift of $V|_s$ to $\tilde{s}$.

Suppose that γ has inessential intersection with the core of s. In this case, since γ is positively transverse to Γ^+, the lift $\tilde{\gamma}$ must connect two portions of $\partial\tilde{s}$ which point toward each other. That is, the picture cannot be as shown in Figure 40, left. Hence $\tilde{\gamma}$ can be homotoped into a neighborhood of $\partial\tilde{s}$ where it can evidently be made positively transverse to $V_{\tilde{s}}$. See Figure 40, right. This homotopy projects to one in s. If the resulting arc γ' is not embedded, then there is an innermost bigon complementary region of γ' in s foliated by flow segments of V joining the two sides of the bigon. Such a bigon can be eliminated while maintaining transversality by flowing part of γ' along V. After finitely many steps we have produced the desired homotopy of γ.

Alternatively, suppose that γ intersects the core of s essentially. Since γ is positively transverse to the core Γ^+-cycle in s, the endpoints of γ must lie on segments of $\tilde{s}$ that are oriented compatibly with the dynamic orientation of s. From the description of $V|_s$ given at the beginning of the proof, we see that we can homotope γ so that it is positively transverse to V. See Figure 40, right. □

Let e be an edge of Γ which lies at the bottom of a disk sector s, meaning that the sector s of B into which the maw vector field points along e is not an annulus or Möbius band. Let p be the terminal vertex of e.

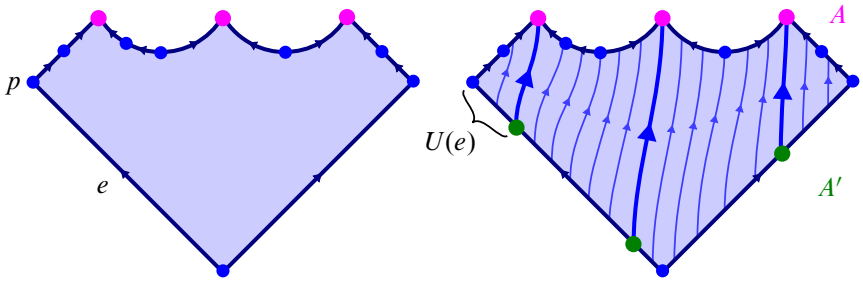

Figure 41: Defining the set $U(e)$ for a Γ-edge e in the bottom of a disk sector.

Let A be the collection of points in the top of s which are sinks of s (these will all be corners). Let A' be the set of points in the bottom of s obtained by flowing backward along V from points in A. Let $U(e)$ be the component of $e \setminus A'$ containing p (see Figure 41). If e is an edge of Γ that does not lie at the bottom of a disk sector, let $U(e) = e$. Let

$$U = \bigcup_e U(e),$$

where the union is taken over all Γ-edges.

Lemma 9.5 *Let γ be a cooriented arc which is properly embedded in a disk sector s of b and positively transverse to Γ. Further suppose that $\partial s \subset U$. Then γ can be made positively transverse to $V|_s$ by a homotopy fixing the endpoints of γ.*

Proof It is either the case that

(a) both endpoints of γ lie in the top of s,

(b) both lie in the bottom of s, or

(c) one lies in the top and the other in the bottom.

In case (a), the fact that γ is positively transverse to Γ implies that the Γ-edges on which the endpoints of γ lie point toward each other. Similarly, in case (b), the Γ-edges on which the endpoints of γ lie point away from each other. A picture then makes clear that γ is positively transverse to V after an endpoint-fixing homotopy (see Figure 42).

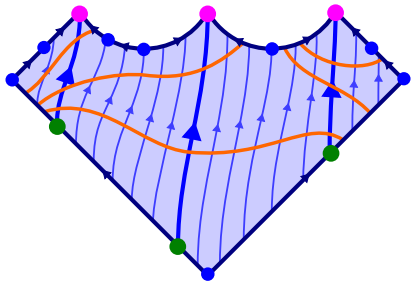

Figure 42: Any properly embedded arc in a disk sector with endpoints in U, positively transverse to Γ, can be made transverse to V by an endpoint-fixing homotopy.

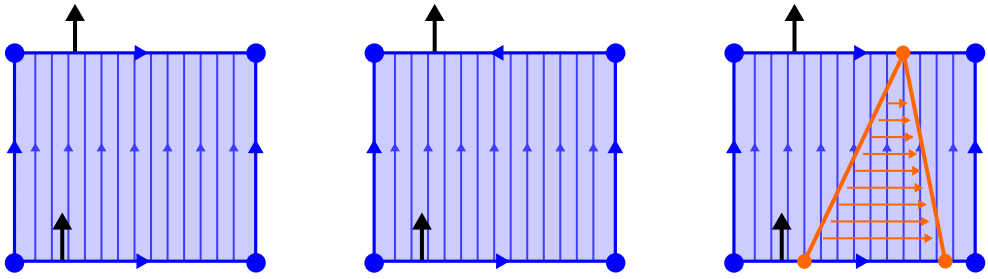

Figure 43: Left and center: for a transient annulus sector s, each component of $s \setminus\setminus \Gamma^+$ is of one of these forms. Right: any properly embedded cooriented arc positively transverse to ∂s may be homotoped rel ∂s to be positively transverse to v; shown is the only case where it is necessary to move a boundary point of the arc.

In case (c), we use the fact that in particular the endpoint of γ lying on the bottom of s lies in the set U. Figure 42 shows that this is precisely the condition needed to guarantee that γ is positively transverse to V after an endpoint-fixing homotopy. □

Lemma 9.6 *Let s be a transient annulus sector of B, and let γ be a cooriented arc properly embedded in s which is positively transverse to Γ^+. Let p be the endpoint of γ lying on the inward-pointing component of ∂s. Then γ can be made positively transverse to $V|_s$ by a homotopy which either fixes both endpoints of γ or moves p closer to the terminal vertex of the Γ-edge on which it lies.*

Proof Each component of $s \setminus\setminus \Gamma^+$ is of the form shown in Figure 43, left and center. The arc γ intersects each such component c in an subarc γ_c which is positively transverse to ∂c. We may clearly homotope γ_c to be positively transverse to V, and we can even choose the homotopy to fix the endpoints of γ_c unless γ_c joins the outward- and inward-pointing portions of ∂c. In this case it may be necessary to move the endpoint on the inward-pointing boundary along the orientation coming from Γ^+ (see Figure 43). Applying this to all subarcs of γ proves the lemma. □

Note that, as remarked above, an extended dual graph is not uniquely determined. However, by the next proposition, this freedom does not affect the cycles of Γ^+ (recall our convention is that cycles are directed).

Proposition 9.7 *Each cycle in Γ^+ lies in Γ.*

Proof Suppose there is a cycle c in Γ^+ containing an edge e of $\Gamma^+ \setminus \Gamma$. By the definition of Γ^+, the edge e must lie interior to an annulus or Möbius band sector s. We see that s is in fact a transient annulus, for the only cycles passing through the interior of sources are the cycles contained in their cores, which are also Γ-cycles.

Following c backward, c must contain an edge entering s from another annulus or Möbius band sector s'. Repeating the argument on s', and so on, we get a cycle of transient annuli whose union is a torus, contradicting Definition 6.11. □

In particular, Proposition 9.7 implies that the cone in $H_1(Q)$ generated by directed cycles of Γ^+ is independent of the choice of extension.

Lemma 9.8 *Let $z \in H^1(\Gamma^+)$ be an integral class such that, for every directed cycle γ of Γ^+, we have $z([\gamma]) \geq 0$. Then z is represented by a nonnegative rational 1-cocycle on Γ^+.*

Proof The proof directly follows ideas from [McMullen 2015; Landry et al. 2024]. Let $W = \mathbb{R}^E$ be the space of real weights on the edges of Γ_+ and let $A\colon W \to H^1(\Gamma^+)$ be the map to cohomology. We can choose rational bases for W and $H^1(\Gamma^+)$ so that A is given by an integral matrix.

By [Landry et al. 2024, Lemma 5.10], there exists a nonnegative cocycle c on Γ^+ representing z. Let S be the set of solutions to $Ax = z$, and let F be the face of $\mathbb{R}^E_{\geq 0}$ containing c in its relative interior. Since $S \cap F$ is nonempty (it contains c) and cut out by integer equations and inequalities, it contains a rational point; this gives the required cocycle. □

We next describe a construction that takes as input a certain type of cohomology class and produces a surface properly embedded in N, transverse to V. While reading the construction, the reader should consult Figure 44.

Before beginning, we briefly describe the structure of complementary regions of $B \setminus\setminus \Gamma^+$. By construction, each component c is diffeomorphic to a square. The edges on ∂c are oriented so that exactly one vertex is a source and one is a sink. The source is called the *bottom vertex* of c and the sink is the *top vertex* of c. The components of $c \setminus\setminus \{\text{top and bottom vertices}\}$ are called the *sides* of c.

Construction 9.9 (N-surfaces) Let $z \in H^1(Q)$ be an integral class such that, for every directed cycle γ of Γ^+, we have $z([\gamma]) \geq 0$; we will also think of z as a class in $H^1(Q)$. By Lemma 9.8, there exists a nonnegative $\mathbb{Q}$-valued 1-cocycle c on Γ^+ representing the pullback of z to $H^1(\Gamma^+)$ (Figure 44(a)). Let n be the least integer such that nc is integer-valued. For each Γ^+ edge e, place $nc(e)$ points on e, close enough to the terminal vertex so that they all lie in U (recall the definition of U preceding Lemma 9.5).

Let σ be a component of $B \setminus\setminus \Gamma^+$, and recall that σ is a topological disk with a top t and bottom b, and edges in each side of σ oriented from b to t. Since $\partial\sigma$ is contractible in Q, we must have $nz([\partial\sigma]) = 0$, so the number of points we have placed on each side of σ is equal (Figure 44(b)). Hence we can join the points on each side of σ by cooriented arcs, each arc joining the two sides of σ and with coorientation compatible with the orientation of Γ^+ (Figure 44(c)).

Doing this for each component of $B \setminus\setminus \Gamma^+$, we obtain a cooriented train track η in B; at each point of intersection between the train track and Γ^+, the coorientation of η is compatible with the orientation of Γ^+ (Figure 44(d)).

We now homotope η to be positively transverse to $V|_B$. First we arrange for all branches of η contained in transient annulus sectors to be positively transverse to $V|_B$. This is possible by Lemma 9.6, and, because

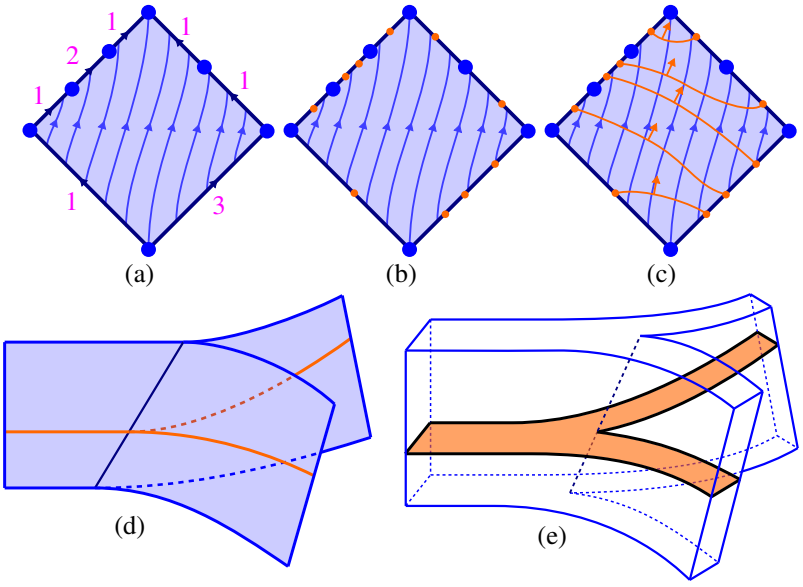

Figure 44: Some steps in Construction 9.9.

there are no cycles of adjacent transient annulus sectors (as noted in the proof of Proposition 9.7, the union of such sectors would produce a torus carried by B). This homotopy does not affect the property that all intersections of η with Γ lie in U. Hence we are free to apply Lemmas 9.4 and 9.5 in order to homotope the branches of η to be positively transverse to $V|_B$.

We now extend η to a cooriented surface T properly embedded in N and positively transverse to V (Figure 44(e)). By [Thurston 1986, Lemma 1], T is a union of n cooriented surfaces that each represent the Lefschetz dual of z. Pick one of these components and call it S. We call S an *N-surface for z*. ◁

Lemma 9.10 *Suppose S is an N-surface for z. Then S is Lefschetz dual to $i^*(z) \in H^1(N)$, where $i : N \to Q$ is inclusion.*

Proof Since N deformation retracts to B and B is cut into disks by Γ^+, it suffices to show that, for any cycle γ in Γ^+ (not necessarily directed), the algebraic intersection of S with γ is equal to $i^*(z)([\gamma])$. This property is immediate from the fact that S was constructed using a cocycle representing the pullback of z to $H^1(\Gamma)$. □

We will now explain how to extend an N-surface for a cohomology class z over $Q \setminus\setminus N$ to obtain a surface properly embedded in Q. One can do this for any N-surface, but we restrict ourselves to the case when z pairs positively with each Γ^+-cycle since this is the only case we need and it simplifies the presentation.

For convenience, we will denote $Q \setminus\setminus N$ by N^c. The components of N^c are in bijection with the components of $Q \setminus\setminus B$, and accordingly we will refer to them as $\boldsymbol{u}$-cusped tori and $\boldsymbol{u}$-cusped products.

For the statement of this lemma, recall that γ denotes $\partial Q \setminus\setminus (R_+ \cup R_-)$ (see Section 5.1).

Lemma 9.11 *Let $z \in H^1(Q)$ be an integral class that pairs positively with the class of every directed cycle of Γ^+. Let S be an N-surface for z, and let C be a component of N^c. Then*:

(a) *If C is a $\boldsymbol{u}$-cusped torus shell, then $S \cap C$ is a collection of closed parallel curves with compatible coorientation, each essential in ∂C with slope distinct from that of the $\boldsymbol{uu}$-cusp curves of C.*

(b) *If C is a $\boldsymbol{u}$-cusped solid torus, then $S \cap C$ is a collection of meridians of C.*

(c) *If C is a $\boldsymbol{u}$-cusped product, then $S \cap C$ is a collection of closed curves and arcs. If we coorient the arcs using the coorientation of S, they may be completed by cooriented arcs in $C \cap R_+$ to obtain a family of arcs and curves whose boundary points lie only in $R_+ \cap \gamma$.*

Proof Let C be a component of N^c, and let C' be the corresponding complementary region of B.

Let c be a component of $S \cap C$, and suppose that c bounds a disk D in ∂C. Since S was constructed to be positively transverse to Γ^+, c is disjoint from any $\boldsymbol{uu}$-cusp curves of C. Hence, corresponding to D is a disk D' immersed in B with boundary lying in $S \cap B$. Since $S \cap B$ is positively transverse to V, this disk violates the Poincaré–Hopf theorem. We conclude that no component of $S \cap C$ bounds a disk in the $\boldsymbol{u}$-faces of C.

If C is a $\boldsymbol{u}$-cusped torus, $S \cap C$ must intersect the $\boldsymbol{uu}$-cusp curves of C since z pairs positively with each such curve. Also, ∂S is positively transverse to the $\boldsymbol{uu}$-cusp curves by construction, so the orientations of the components of $S \cap C$ must agree. This proves part (a).

Consider the long exact sequence of the triple $(Q, N^c \cup \partial Q, \partial Q)$, which contains the subsequence

$$H_2(N^c \cup \partial Q, \partial Q) \to H_2(Q, \partial Q) \to H_2(Q, N^c \cup \partial Q) \to H_1(N^c \cup \partial Q, \partial Q) \to \cdots. \tag{9.12}$$

Here $H_2(Q, N^c \cup \partial Q) \cong H_2(N, \partial N)$ by excision and

$$H_i(N^c \cup \partial Q, \partial Q) \cong H_i(N^c, N^c \cap \partial Q) \cong \bigoplus_C H_i(C, C \cap \partial Q),$$

where the first isomorphism is induced by the inclusion $(N^c, N^c \cap \partial Q) \hookrightarrow (N^c \cup \partial Q, \partial Q)$, and the direct sum is over all complementary regions C of N in Q. By Lemma 9.10, the image of $[S]$ in $H_1(N^c \cup Q, \partial Q)$ is the image of the image of z, viewing z as a class in $H_2(Q, \partial Q)$. Therefore $S \cap C$ is nullhomologous in $H_1(C, C \cap \partial Q)$ for each complementary region C.

If C is a $\boldsymbol{u}$-cusped solid torus, this means that $S \cap C$ must be either a union of meridians or an even-sized collection of parallel curves essential in ∂C whose coorientations cancel each other out in homology. The latter case is impossible because z pairs positively with the $\boldsymbol{uu}$-cusp curves as noted above, proving (b).

If C is a $\boldsymbol{u}$-cusped product, we consider the following subsequence of the long exact sequence associated to $(C, C \cap \partial Q, C \cap R_-)$:

$$H_i(C, C \cap R_-) \to H_i(C, C \cap \partial Q) \to H_{i-1}(C \cap \partial Q, C \cap R_-) \to H_{i-1}(C, C \cap R_-).$$

Note $H_i(C, C \cap R_-) \cong 0$ since C is homeomorphic to $(C \cap R_-) \times [0,1]$. Hence

$$H_i(C, C \cap \partial Q) \cong H_{i-1}(C \cap \partial Q, C \cap R_-) \cong H_{i-1}(C \cap R_+, C \cap R_+ \cap \gamma). \tag{9.13}$$

Using the fact that $S \cap C$ is nullhomologous in $H_1(C, C \cap \partial Q)$, together with the isomorphism $H_1(C, C \cap \partial Q) \cong H_0(C \cap R_+, C \cap R_+ \cap \gamma)$, we see that the (signed) boundary points of $S \cap C$ give a nullhomologous 0-chain in $H_0(C \cap R_+, C \cap R_+ \cap \gamma)$. Hence they can be connected by paths in $C \cap R_+$ to form a collection of cooriented arcs and loops, all of whose boundary points lie in $C \cap R_+ \cap \gamma$. This completes the proof of (c). □

Proposition 9.14 *Let $z \in H^1(Q)$ be an integral class which pairs positively with the homology class of every directed cycle of Γ^+. Let S be an N-surface for z. Then there exists a surface which extends S, is properly embedded in Q, is transverse to the vector field V, and represents z (viewed as a class in $H_2(Q, \partial Q)$).*

Proof By Lemma 9.11(a)–(b), we can cap off S in the $\boldsymbol{u}$-cusped solid tori and the $\boldsymbol{u}$-cusped torus shells of N^c by gluing on disks and annuli. Since V is circular in these $\boldsymbol{u}$-cusped tori, we can choose these disks and annuli to be transverse to V.

For each $\boldsymbol{u}$-cusped product $C \cong \Sigma \times [0,1]$ in N^c, we can extend $S \cap C$ by the family of arcs furnished by Lemma 9.11(c) to obtain a family A of arcs and curves in $\Sigma \times \{1\}$. If we flow A backward along V until it hits R_-, it sweeps out a properly embedded surface tangent to V that we can use to cap off S in C. We then homotope the result slightly so that it is transverse to V. After doing this in each $\boldsymbol{u}$-cusped product, we have produced a cooriented surface $\bar{S}$ which is properly embedded in Q and positively transverse to V. Moreover, if we consider the maps of (9.12) from the proof of Lemma 9.11, the images of z and $[\bar{S}]$ in $H_2(Q, N^c \cup \partial Q) \cong H_2(N, \partial N)$ are equal by Lemma 9.10. As such, they differ by an element $\alpha \in H_2(Q, \partial Q)$ in the image of $H_2(N^c \cup \partial Q, \partial Q) \cong H_2(N^c, N^c \cap \partial Q)$. Since $H_2(C, C \cap \partial Q) = 0$ for each $\boldsymbol{u}$-cusped torus component of N^c, we have $H_2(N^c, N^c \cap \partial Q) \cong \bigoplus_C H_2(C, C \cap \partial Q)$, where the sum is over all the $\boldsymbol{u}$-cusped product components.

We will now construct a cooriented surface S_α which is positively transverse to V and represents α. By (9.13) from the proof of Lemma 9.11, for each $\boldsymbol{u}$-cusped product C we have $H_2(C, C \cap \partial Q) \cong H_1(C \cap R_+, C \cap \partial R_+)$. An element of $H_1(C \cap R_+, C \cap \partial R_+)$ is represented by a collection of cooriented closed loops and arcs in $C \cap R_+$, which can be flowed backward to R_- along V to sweep out a cooriented surface representing the corresponding class in $H_2(C, C \cap \partial Q)$. By a small homotopy we can make the swept-out surface positively transverse to V. Doing this for all $\boldsymbol{u}$-cusped products, we obtain our surface S_α.

To finish the proof, we perform an oriented cut-and-paste on $\bar{S}$ and S_α so that the result is positively transverse to V. □

9.2 Uniqueness argument

In this subsection, we establish our uniqueness result. We fix some notation:

- $f : L \to L$ is a Handel–Miller endperiodic map.
- $\mathring{Q} := M_f$ is the mapping torus of f.
- $Q := \overline{M}_f$ is the compactified mapping torus of f with associated depth one foliation $\mathcal{F}$.
- φ is the suspension semiflow of f in Q.
- $\mathcal{L}$ is the unstable Handel–Miller lamination in Q (recall this is the suspension by f of the positive Handel–Miller lamination $\Lambda_+ \subset L$).

Suppose we have an unstable veering branched surface (B, V) in Q compatibly carrying $\mathcal{L}$. Let $\mathring{B} = B \cap \mathring{Q}$.

By Theorem 8.5, the cone spanned by cycles in the dual graph Γ of B in $H_1(Q)$ is dual to the foliation cone associated to $\mathcal{F}$ in $H_2(Q, \partial Q)$. Fix an extended dual graph Γ^+ for B. Let $z = [\mathcal{F}] \in H_2(M, \partial M) \cong H^1(M)$. By Proposition 9.7, the dual of z pairs positively with every cycle of Γ^+. By Proposition 9.14, there exists a surface S_z representing z properly embedded in Q, which is positively transverse to V and Γ^+.

Lemma 9.15 *Let $p \in Q$. Then the forward V-trajectory from p meets S_z or $R_+(Q)$.*

Proof First let $p \in B$ and suppose that the forward trajectory from p does not intersect R_+. Then, by compactness, there is a segment ρ of the forward V-trajectory from p that starts and ends in the same sector of $B \setminus\setminus S_z$. By adding a segment in this sector, we can close up ρ to a closed curve ρ' that is positively transverse to $\mathrm{brloc}(B)$. By Proposition 6.17, ρ' is homotopic to a directed Γ-cycle. Since z pairs positively with this directed cycle, ρ' must also intersect S_z positively, so ρ itself must intersect S_z positively.

Next suppose $p \notin B$. If p lies in a u-cusped product, then the forward trajectory from p either enters B, which then intersects S_z by the above paragraph, or terminates on R_+. Similarly, if p lies in a $\boldsymbol{u}$-cusped torus T then its forward trajectory either enters B and intersects S_z by the above, or remains in T. In this case, by circularity of $V|_T$, it intersects one of the pieces we used to cap off S_z inside of T. □

It follows from Lemma 9.15 that the sutured manifold obtained by decomposing Q along S_z is a product (as in the proof of Lemma 6.9 on $\boldsymbol{u}$-cusped product recognition). In particular, S_z can be spun around $R_\pm(Q)$ to produce a surface L_z which is the fiber of a fibration

$$L_z \hookrightarrow \mathring{Q} \twoheadrightarrow S^1$$

(see [Altman 2014, Lemma C]). This gives rise to a depth one foliation of Q, which we call $\mathcal{F}_z$. We wish to show that $L_z \cap \mathcal{L}$ is the Handel–Miller lamination associated to the fibration above, which turns out to be a surprisingly subtle point.

The cohomology class of $\mathcal{F}_z$ is equal to that of $\mathcal{F}$, so, by [Cantwell and Conlon 1993, Theorem 1.1], there exists an ambient isotopy of Q which is smooth in $\mathring{Q}$, fixes each point in $R_\pm(Q)$, and carries $\mathcal{F}$ to $\mathcal{F}_z$ and L to L_z. Further, it follows from the arguments in [Cantwell and Conlon 1993] that we can require the existence of a neighborhood N_ϵ of $R_\pm(Q)$ such that the ambient isotopy moves points along flow lines of φ in N_ϵ.

We now replace $\mathcal{F}$, φ and $\mathcal{L}$ by their images under this ambient isotopy. However, we leave B in its original position. The reason for this is that L_z is in a particularly nice position with respect to (B, V) that we would like to preserve. The cost of leaving B in place is that we can no longer assume $\mathcal{L}$ is in a carried position with respect to B.

Choose a tiling $\mathcal{T}_\mathcal{F}$ of all f-cycles of ends of L. We can choose tiled neighborhoods of all the end-cycles which are small enough that the associated staircase neighborhoods of components of $R_\pm(Q)$ are contained in N_ϵ. Let N_+ and N_- be the unions of the positive and negative staircases, respectively, and let $N_\pm = N_+ \cup N_-$.

We now set some more notation, describing natural objects that live in the complement of $N_\pm$:

- Manifolds:
  - Let $Q^\dagger = Q \setminus\setminus N_\pm$ (the dagger notation indicates that we are cutting away $N_\pm$).
  - Let $L^\dagger = (L \cap Q^\dagger) \setminus\setminus (L \cap \partial Q^\dagger)$ be the core of L complementary to the tiled neighborhoods defining $N_\pm$.
  - Let $L^\dagger_{-1} = L \cup R_+(N_-)$ and $L^\dagger_1 = L \cup R_-(N_+)$. In words, $L^\dagger_1$ ($L^\dagger_{-1}$) is obtained by adding to $L^\dagger$ the first tile in each positive (negative) end-cycle that doesn't already lie in $L^\dagger$.
  - Let $\widetilde{Q^\dagger}$ be the $\mathbb{Z}$-cover of $Q^\dagger$ associated to $L^\dagger$. This can be constructed by gluing together $\mathbb{Z}$-many copies of $Q^\dagger \setminus\setminus L^\dagger$.
- Maps and flows:
  - Let $\varphi^\dagger = \varphi|_{Q^\dagger}$.
  - Let $f^\dagger\colon L^\dagger_{-1} \to L^\dagger_1$ be the homeomorphism induced by $\varphi^\dagger$. Note that $Q^\dagger$ is the "mapping torus" of $f^\dagger$, ie
$$Q^\dagger = L^\dagger_{-1} \times [0,1] / \big((x,1) \sim (f^\dagger(x), 0) \text{ if } f^\dagger(x) \in L^\dagger\big).$$
    To visualize this it may be helpful to consider Figure 45.
- Laminations and branched surfaces:
  - Let $\mathcal{L}^\dagger = \mathcal{L}|_{Q^\dagger}$.
  - Let $B \cap L = \tau$ and let $\tau^\dagger = \tau|_{L^\dagger}$.
  - Since f is Handel–Miller, $\mathcal{L} \cap L$ is the positive Handel–Miller lamination. For convenience we will suppress the $+$ subscript and denote the positive Handel–Miller lamination by Λ. Let $\Lambda^\dagger = \Lambda|_{L^\dagger}$.

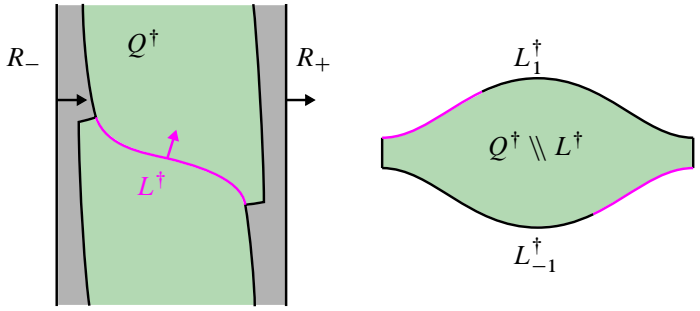

Figure 45: A cartoon of $Q^\dagger$ and the product manifold obtained by cutting $Q^\dagger$ along $L^\dagger$.

– Note that there is an isotopy of $\mathcal{L}^\dagger$, fixing its boundary, so that the result is fully carried by $B^\dagger$ (this is induced by the ambient isotopy carrying $\mathcal{F}$ to $\mathcal{F}_z$). Let $\mathcal{L}_0^\dagger$ denote this isotoped lamination, and let $\Lambda_0^\dagger = \mathcal{L}_0^\dagger \cap L^\dagger$.

Lemma 9.16 *The train track τ carries no closed curve which is nullhomotopic in L.*

Proof If τ carried a curve bounding a disk $D \subset L$, the disk D could be decomposed into compact complementary regions of τ, at least one of which would have to have positive index. However, all the compact complementary regions of τ are pieces we used to cap off an N-surface in $\boldsymbol{u}$-cusped torus pieces, which all have negative index. □

Lemma 9.17 *The laminations $\Lambda_0^\dagger$ and $\Lambda^\dagger$ are isotopic in $L^\dagger$ fixing their boundary points.*

Proof Let $\widetilde{\mathcal{L}^\dagger}$ and $\widetilde{\mathcal{L}_0^\dagger}$ be the lifts of $\mathcal{L}^\dagger$ and $\mathcal{L}_0^\dagger$ to $\widetilde{Q^\dagger}$, respectively. Let $\widetilde{L^\dagger}$ be a lift of $L^\dagger$ to $\widetilde{Q^\dagger}$, and let $\widetilde{\Lambda^\dagger}$ and $\widetilde{\Lambda_0^\dagger}$ be the preimages of $\Lambda^\dagger$ and $\Lambda_0^\dagger$ in $\widetilde{L^\dagger}$ under the covering projection, respectively.

We can lift the isotopy between $\mathcal{L}^\dagger$ and $\mathcal{L}_0^\dagger$ in $Q^\dagger$ to a proper isotopy ι in $\widetilde{Q^\dagger}$ between $\widetilde{\mathcal{L}^\dagger}$ and $\widetilde{\mathcal{L}_0^\dagger}$ fixing their common boundary. Each leaf of $\widetilde{\mathcal{L}^\dagger}$ is properly embedded in $\widetilde{Q^\dagger}$ and homeomorphic to $[0,1]\times\mathbb{R}$, so the same is true of each leaf of $\widetilde{\mathcal{L}_0^\dagger}$.

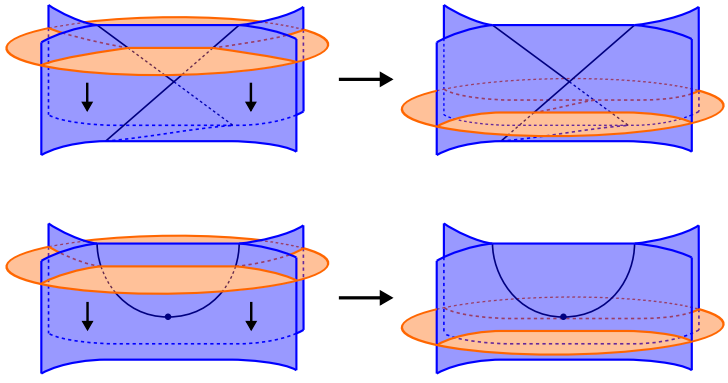

Figure 46: Downward flips.

Immediately we see that each leaf of $\widetilde{\Lambda}^\dagger_0$ is a compact 1-manifold properly embedded in $\widetilde{L}^\dagger$. If such a leaf were a closed curve, it would be nullhomotopic in the corresponding leaf of $\widetilde{\mathscr{L}}^\dagger_0$, hence nullhomotopic in $\widetilde{L}^\dagger$ by π_1-injectivity of $\widetilde{L}^\dagger$; projecting to $Q^\dagger$ would then give a contradiction to Lemma 9.16. Thus, we see that $\widetilde{\Lambda}^\dagger_0$ is an I-lamination, and each leaf of $\widetilde{\mathscr{L}}^\dagger$ intersects $\widetilde{L}^\dagger$ in a unique leaf of the I-lamination.

Let λ be a leaf of $\widetilde{\Lambda}^\dagger$, which is equal to $\ell \cap \widetilde{L}^\dagger$ for some leaf ℓ of $\widetilde{\mathscr{L}}^\dagger$. Note that λ connects the two components of $\partial\ell$. If ℓ_0 is the image of ℓ under ι, $\ell_0 \cap \widetilde{L}^\dagger$ is a union of $\widetilde{\mathscr{L}}^\dagger_0$-leaves with boundary equal to $\partial\lambda$. It cannot contain any closed curves by above, so consists of a single curve λ_0 such that $\partial\lambda = \partial\lambda_0$. Since ℓ and ℓ_0 are isotopic rel boundary in $\widetilde{Q}^\dagger$ and λ and λ_0 have the same boundary points, they are isotopic rel boundary in $\widetilde{Q}^\dagger$. Since $\widetilde{L}^\dagger$ is π_1-injective in $\widetilde{Q}^\dagger$, they are in fact isotopic in $\widetilde{L}^\dagger$. Projecting to $L^\dagger$, we see that every leaf of the I-lamination $\Lambda^\dagger$ is isotopic, fixing endpoints, to a leaf of the I-lamination $\Lambda^\dagger_0$. □

Corollary 9.18 *The train track $\tau^\dagger$ fully carries $\Lambda^\dagger$ up to an isotopy of $\Lambda^\dagger$ rel boundary. Hence τ fully carries Λ.*

Proof Since $B^\dagger$ fully carries $\mathscr{L}^\dagger_0$, the train track $\tau^\dagger$ fully carries $\Lambda^\dagger_0$. The isotopy from Lemma 9.17 between $\Lambda^\dagger$ and $\Lambda^\dagger_0$ rel boundary certifies that $\Lambda^\dagger$ is fully carried by $B^\dagger$. Since τ already carries Λ^+ outside $L^\dagger$, this proves the claim. □

Now that we have shown that τ fully carries Λ, we wish to show that B is obtained from this paper's main construction, which can be summarized in two steps:

(1) Given a Handel–Miller map $f : L \to L$ with positive Handel–Miller lamination Λ and 2-dimensional unstable Handel–Miller lamination $\mathscr{L}$, fix an efficient spiraling train track carrying $\mathscr{L} \cap R_+(\overline{M}_f)$. Using core splits, produce an eventually f-periodic splitting sequence of train tracks fully carrying Λ. In Theorem 4.17, we prove the resulting sequence is unique up to equivalence.

(2) Suspend the periodic part of this splitting sequence in $\overline{M}_f$. In Lemma 7.14, we prove the resulting veering branched surface is unique up to isotopy.

Hence we must show that B is obtained as the suspension of a splitting sequence obtained from performing core splits.

Definition 9.19 (downward flip) Let s be a diamond sector of B, and suppose that a component of $L^\dagger \cap s$ has both its boundary points along the bottom of s, so that the corresponding branch b of τ is large. Further suppose b is lowermost in s, meaning that b is the only piece of $L^\dagger \cap s$ contained in the component of $s \setminus\setminus b$ containing the bottom point of s. Then there exists an isotopy of $L^\dagger$ supported in a neighborhood of b, as shown in Figure 46, which has the effect of splitting τ along b. This isotopy is called a *downward flip*. It is straightforward to see that a downward flip can always be performed in such a way that it preserves the property of $L^\dagger$ being positively transverse to V and Γ. ◁

Lemma 9.20 *After finitely many downward flips, we may assume that $\tau^\dagger$ is a spiraling train track.*

Proof We first claim that whenever we see a large branch of $\tau^\dagger$, it is possible to perform a downward flip on $L^\dagger$.

Suppose that b is a large branch of $\tau^\dagger$, and let s be the sector of $B^\dagger$ containing b. Note that the part of s below b is disjoint from $\partial Q^\dagger$, since the orientation of $\mathrm{brloc}(B^\dagger)$ points outward along $\partial Q^\dagger$. Note also that s is not a Möbius band or annulus, by the definition of veering branched surfaces (Definition 6.11(4)), so it must be part of a diamond sector of B. We can now locate a bottommost arc of $L^\dagger$ in s (this may or may not be b) and perform a downward flip.

Since τ carries the I-lamination $\mathscr{L}_0^\dagger$, the train track $\tau^\dagger$ will become spiraling after finitely many downward flips. □

Lemma 9.21 *The branched surface B is obtained as the suspension of a splitting sequence representing the equivalence class $\mathcal{S}(B \cap R_+(Q))$.*

Proof Recall from Lemma 9.15 (and the subsequent discussion) that $\mathring{Q} \setminus\setminus L_z$ is homeomorphic to a product $L_z \times [0,1]$. The strategy of the proof, similar to our proof of Theorem 9.1, is to construct a "height" function $h\colon \mathring{Q} \setminus\setminus L_z \to [0,1]$ such that:

(1) $h = 0$ on the bottom face $L_z \times \{0\}$ and $h = 1$ on the top face $L_z \times \{1\}$.

(2) h is monotonically increasing on the trajectories of $V|_{\mathring{Q} \setminus\setminus L_z}$.

(3) h is monotonically increasing on the directed paths of $\Gamma^+|_{\mathring{Q} \setminus\setminus L_z}$.

Given such a function h, the fibers $h^{-1}(t)$ define an isotopy from $L_z \times \{1\}$ to $L_z \times \{0\}$. Item (3) guarantees that the intersections $h^{-1}(t) \cap B$ give a movie of train tracks which undergo splits at each t for which $h^{-1}(t)$ passes through a triple point or source of $\mathrm{brloc}(B)$. Each train track $h^{-1}(t) \cap B$ carries $\mathscr{L} \cap h^{-1}(t)$ by Corollary 9.18. Moreover, the sequence of splits, taken together, gives a core split of $\tau|_{L_1^\dagger}$. Therefore it determines a representative of $\mathcal{S}(B \cap R_+(Q))$.

To construct h, observe that, by the construction of L_z, $\Gamma|_{\mathring{Q} \setminus\setminus L_z}$ has no directed cycles. Hence we can first define h on $\Gamma|_{\mathring{Q} \setminus\setminus L_z}$ to satisfy (1) and (3). Then we can extend h over the 2-cells of $\mathring{B} \setminus\setminus L_z$ to satisfy (1) and (2).

Finally, we have to extend h over each complementary region C of $\mathring{B} \setminus\setminus L_z$ in $\mathring{Q} \setminus\setminus L_z$. If C lies in a solid cusped torus component C' of $Q \setminus\setminus B$, then this is straightforward since L_z intersects C' in meridional disks. If C lies in a cusped torus shell component, then extending h over C is similarly straightforward.

If C lies in a cusped product piece C', we make use of the neighborhood N of B constructed in Section 9.1. Recall the key feature of N is that along each component of $\partial N \cap C'$, V points into B. For N small enough, we can extend h into $N \cap C$ so that (2) and (1) still hold. Now using the fact that the trajectory of every point on $C \cap (L_z \times \{0\})$ meets N or $L_z \times \{1\}$ in finite time, we can extend h into $C \setminus\setminus N$ as well. □

In summary, the branched surface B is obtained from this paper's main construction. Since that construction depends only on the choice of the boundary train track (Corollary 7.15), we have proven the following:

Theorem 9.22 (veering branched surface uniqueness) *Let Q be an atoroidal sutured manifold with depth one foliation $\mathcal{F}$, and let $\mathcal{L}$ be the unstable Handel–Miller lamination associated to $\mathcal{F}$. Any veering branched surface B compatibly carrying $\mathcal{L}$ is determined up to isotopy by $B \cap R_+(Q)$.*

9.3 Shifting moves

As promised in the introduction of this section, we will also explain how the veering branched surfaces with different boundary train tracks in Theorem 9.22 are related to each other. To do so, we introduce some moves that one can use to modify veering branched surfaces in general, then claim that the veering branched surfaces in Theorem 9.22 are exactly related by these moves.

Let B be a veering branched surface with boundary train track β.

Definition 9.23 A *shift-source triangle* is a triangle t carried by B such that:

(1) One side of t is a mixed branch b of β.

(2) The other two sides of t lie along components of $\mathrm{brloc}(B)$.

Note that by (1), among the two sides of t lying along $\mathrm{brloc}(B)$, one side is cooriented outwards while the other is cooriented inwards; let these two sides be a and c, respectively. Then a must be oriented from c to b, while c must contain a source since B is veering. ◁

We claim that a shift-source triangle, with the above notation, is the union of a number of adjacent diamonds (unscalloped) with a bottom side along c and a diamond (unscalloped) with rounded bottom whose bottom side is on c. See Figure 47, top left. This follows from Proposition/Definition 6.13 concerning the structure of sectors of veering branched surfaces as follows. Consider the sector b lies on. If it is a diamond with rounded bottom, then the shift-source triangle only consists of this sector and the sector is not scalloped. If the sector is a diamond without rounded bottom, then the sector is not scalloped, one of its top sides lies on a and one of its bottom sides lies on c. We call the other bottom side b' and repeat the argument on b'. Since there are finitely many triple points on c, this process terminates eventually.

When b is embedded, we define the *shifting move along a shift-source triangle t* to be the operation of dynamically splitting c across a small neighborhood of t. The effect on the boundary train track is a shift on the branch b. We retain the source orientations on the components of the branch locus after splitting, so that the resulting branched surface B' satisfies the triple point condition of being veering (Definition 6.11(1)). See Figure 47, top.

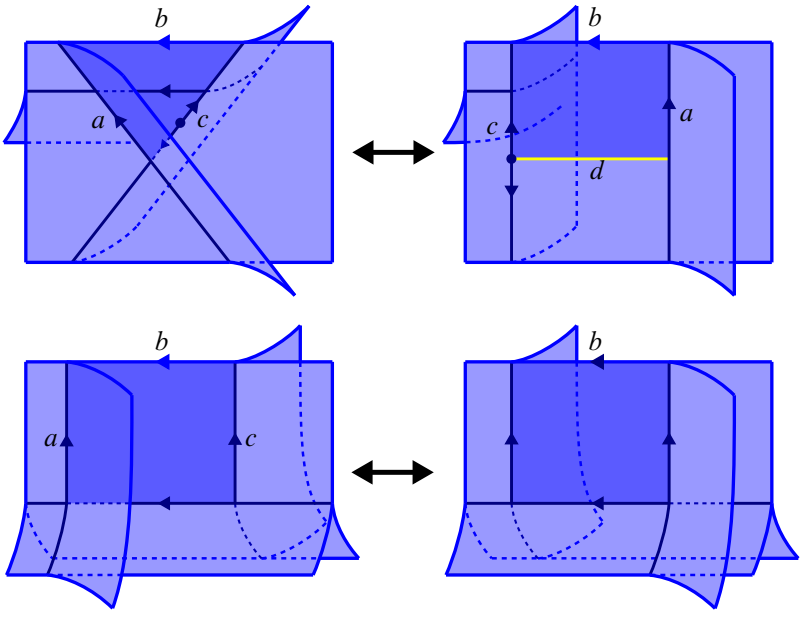

Figure 47: Top: shifting along a shift-source triangle or rectangle. Bottom: shifting along a shift rectangle.

We note that a shift-source triangle t might not be embedded; indeed, it could pass twice through a diamond sector s (see Figure 48, left). While c intersects itself in this situation, the component of $\partial_v N(B)$ corresponding to c is embedded. This gives a canonical relative positioning to the parts of a lift of t to $N(B)$ that project to s such that the lift embeds in $N(B)$. Hence there is no ambiguity in what we mean by dynamically splitting along s. See Figure 48, middle and right, and recall the discussion of dynamic splittings at the end of Section 6.1 if necessary.

We demonstrate that B' is a veering branched surface by verifying the other conditions in Definition 6.11:

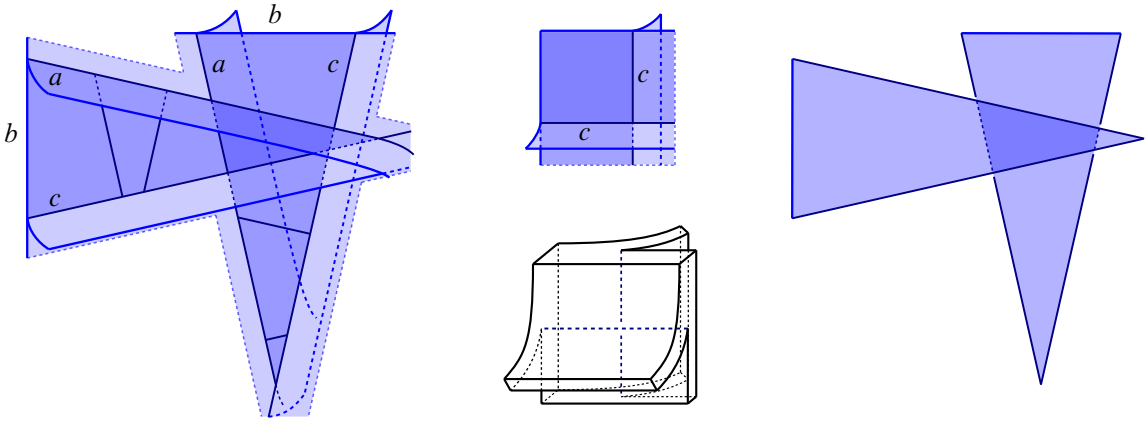

Figure 48: There is a canonical way to lift a shift-source triangle to $N(B)$ even if it passes through a diamond sector twice.

The topology of the complementary regions is not changed; hence, B' is still very full. As noted above, the boundary train track of B' is obtained from that of B via a shift, and hence is still efficient and has no large branches. The dynamic orientations of the $\boldsymbol{u}$-faces are not changed; hence, Definition 6.11(3) is preserved.

For Definition 6.11(4), suppose B' contained an annulus/Möbius band sector with both boundary components cooriented inwards. Then B would carry an annulus/Möbius band with boundary components along branch loops of $\mathrm{brloc}(B)$ that are cooriented inwards. But then the dynamic half-plane $D(\gamma)$ determined by one of these branch loops would not be homeomorphic to a half-plane, contradicting Proposition 6.22. Finally, B' does not carry any tori or Klein bottles, otherwise B would carry such a closed surface as well.

This shows that the shifting move along a shift-source triangle is an operation that transforms a veering branched surface into another veering branched surface.

Definition 9.24 A *shift-source rectangle* is a rectangle r carried by B such that:

(1) One side of r is a mixed branch b of β.

(2) The two sides of r adjacent to b lie along components of $\mathrm{brloc}(B)$. As in Definition 9.23, note that, by (1), one of these sides is cooriented outwards while the other is cooriented inwards; let these two sides be c and a, respectively.

(3) The side of r opposite to b, which we call d, lies in the interior of a sector.

(4) The corner formed by c and d is a source on $\mathrm{brloc}(B)$. ◁

Similarly to the case of shift-source triangles, one can use Proposition/Definition 6.13 to deduce that a shift-source rectangle, with the above notation, is a union of a number of adjacent (unscalloped) diamonds with a bottom side along a and a rectangular neighborhood of a nonscalloped top side of a sector with a bottom side along a. See Figure 47, top right.

Within this last sector, d is an interval connecting an interior point of a bottom side to a source on a top side. Up to modifying the vector field V locally, we can always assume that V is transverse to d pointing out of r.

When b is embedded and with the vector field V modified as described, we define the *shifting move along a shift-source rectangle* r to be the operation of splitting c across a small neighborhood of r. The effect on the boundary train track is a shifting move on the branch b. See Figure 47, top. We retain the source orientations on the components of the branch locus after splitting. By reasoning similarly as above, we see that the resulting branched surface is veering.

As in the case of shift-source triangles, shift-source rectangles might not be embedded, but the shifting move is still well defined.

Shifting moves along shift-source triangles are inverse to shifting moves along shift-source rectangles, in the following sense: After shifting along a shift-source triangle t, there is a natural shift-source rectangle r,

shifting along which recovers the original veering branched surface. After shifting along a shift-source rectangle r, there is a natural shift-source triangle t, shifting along which recovers the original veering branched surface. See Figure 47, top row.

Definition 9.25 A *shift rectangle* is a rectangle r carried by B such that:

(1) One side of r is a mixed branch b of β.

(2) The two sides of r adjacent to b lie along components of $\mathrm{brloc}(B)$. As in Definition 9.23, note that, by (1), one of these sides is cooriented outwards while the other is cooriented inwards; let these two sides be a and c, respectively.

(3) The side of r opposite to b, which we call d, lies along a component of $\mathrm{brloc}(B)$ that is cooriented into r. ◁

As above, one can use Proposition/Definition 6.13 to deduce that a shift rectangle, with the above notation, is a union of a number of adjacent (unscalloped) diamonds with a bottom side along c. See Figure 47, bottom.

When b is embedded, we define the *shifting move along* r to be the operation of splitting B across a neighborhood of r. The effect on the boundary train track is a shifting move on the branch b. See Figure 47, bottom. As above, we retain the source orientations on the components of the branch locus after splitting. By similar reasoning, we see that the resulting branched surface is veering. Also as above, shift rectangles might not be embedded but the operation is still well defined.

Shifting moves along shift rectangles are inverse to themselves, in the following sense: after shifting along a shift rectangle r, there is a natural shift rectangle r', shifting along which recovers the original veering branched surface. See Figure 47, bottom row.

Proposition 9.26 *For every mixed branch b embedded in the boundary train track β, there is a shift-source triangle, a shift-source rectangle or a shift rectangle with a side along b.*

Proof The strategy is to move iteratively downward from b into B using Proposition/Definition 6.13, much like the reasoning employed above.

Let a and c be the components of $\mathrm{brloc}(B)$ on which the outward- and inward-pointing endpoints of b lie, respectively. Consider the sector s_1 in whose boundary b lies. If a has a source on s_1, then one can pick a shift-source rectangle for b within s_1. If c has a source on s_1 and a does not, then s_1 is a diamond with rounded bottom and thus a shift triangle for b. If neither a nor c has a source on s_1, then s_1 is an unscalloped diamond. Let b_1 be the side of s_1 opposite to b, which must be cooriented into s_1. Locally there are two sheets of B converging along b_1. If a and c do not follow the same sheet when crossing b_1, then s_1 is a shift rectangle.

If a and c follow the same sheet of B after crossing b_1, consider the sector s_2 meeting s_1 along b_1 and containing a and c in its boundary. We can perform the above analysis on s_2: if $s_1 \cup s_2$ is not a

shift-source triangle, shift-source rectangle or shift rectangle, then there is a sector s_3 containing a and c in its boundary on which we can continue our analysis. This process terminates when we reach the source of either a or c, which is guaranteed because each branch component has finitely many triple points. □

This proposition implies that given any embedded mixed branch b of β, we can construct a new veering branched surface B' with boundary train track β' given by β with a shifting move done along b. If the original veering branched surface B carried a lamination Λ, then B' carries Λ as well, since the shifting moves are defined by dynamic splittings. In particular, we have the following:

Proposition 9.27 *Let B be a veering branched surface on a sutured manifold Q with boundary train track β. Suppose β' is another train track on $R_+(Q)$ differing from β by shifts. Then there exists a veering branched surface B' on M with boundary train track β'. Furthermore, if B carries a lamination Λ in M, then B' also carries Λ.*

Proof Each shift in the sequence of shifts from β to β' is performed on an embedded mixed branch. Hence, by Proposition 9.26, there exists a (2-dimensional) shifting move as defined above. Each of these moves preserves the property of being a veering branched surface, so we obtain a veering branched surface with boundary track β'. Furthermore, as reasoned above, if B carries a lamination Λ in M, then B' also carries Λ. □

By applying our uniqueness result Theorem 9.22, we obtain our goal of this subsection:

Corollary 9.28 *Let $f : L \to L$ be an endperiodic map, Q be the compactified mapping torus with depth one foliation $\mathcal{F}$, and $\mathcal{L}$ be the unstable Handel–Miller lamination on Q. Then, if B and B' are two veering branched surfaces compatibly carrying $\mathcal{L}$, then they are related by shifting moves.*

10 Examples

In general it is difficult to explicitly describe the Handel–Miller lamination of an endperiodic map f. However, by iterating f and observing the images of junctures, it is sometimes possible by inspection to see that the iterated images are accumulating on a lamination carried by a specific endperiodic train track, as in [Cantwell et al. 2021, Example 4.13]. Then one can use this track to find an f-periodic splitting sequence of endperiodic train tracks. We now present some examples of periodic splitting sequences of endperiodic train tracks carrying Handel–Miller laminations, which give rise to veering branched surfaces using the methods of this paper. Since the intent of this section is simply to help give intuition for our methods, we suppress the work of actually drawing the iterated junctures to find the train tracks.

Example 10.1 (translation) This is the simplest possible example of our construction. If $f : L \to L$ is a translation (recall Example 3.7), then the Handel–Miller laminations of f are empty. In this case the associated veering branched surface is empty as well. ◁

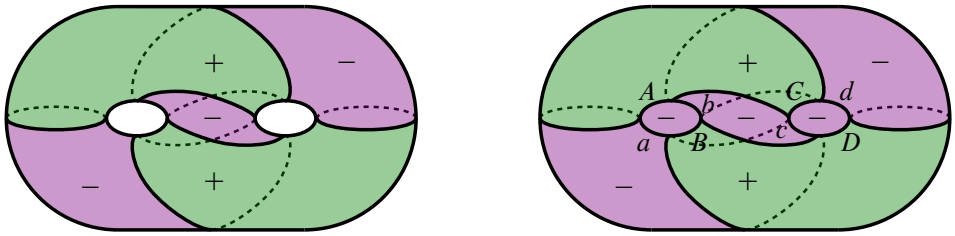

Figure 49: Left: the sutured manifold Q considered in Example 10.3. Right: a disk decomposition of Q.

Example 10.2 (stack of chairs) Consider the map f of Examples 5.2 and 3.8. In this case the positive Handel–Miller lamination Λ_+ is a single properly embedded line λ, which is preserved by the map f preserving orientation. Thus λ itself is an endperiodic train track carrying Λ_+ and there is a trivial splitting sequence from λ to $f(\lambda)$. The associated veering branched surface is an annulus which we can identify with the unstable Handel–Miller lamination $\mathscr{L}^u$ (see Figure 19). ◁

It is convenient for us to use the language of sutured manifold decompositions to describe examples of depth one foliations (see [Gabai 1983]). Roughly, a sutured manifold decomposition is the operation of cutting a sutured manifold along a suitable properly embedded surface, keeping track of boundary information.

Example 10.3 Let Q be the *complement* in S^3 of the handlebody shown in Figure 49, left. Here R_+ is shaded in green, R_- is shaded in purple, and the sutures are drawn as black lines. This is conjectured to be the minimal-volume acylindrical taut sutured manifold by Zhang [2023, Conjecture 1.4].

In Figure 49, right, we consider a disk decomposition of Q, ie a sutured manifold decomposition along a union of disks. The disks are the two "holes" of the handlebody. We convey the information of how we coorient the disks by labeling a side of a decomposing disk $\pm$ if it belongs to $R_\pm$ after decomposition.

One can check that this disk decomposition reduces Q to the product sutured manifold $D^2 \times I$, and hence represents Q as a depth one sutured manifold and, in particular, determines an endperiodic map. In Figure 50, middle, we illustrate this endperiodic map. Here we label the junctures by the same letters as Figure 49 to aid the reader's understanding.

Using the method described at the start of the section, we find a periodic splitting sequence of endperiodic train tracks that carries the positive Handel–Miller lamination, which we illustrate in Figure 50, bottom.

By suspending this periodic splitting sequence as in Section 7.2, we obtain an unstable veering branched surface on Q. We draw its boundary train track in Figure 51, first row, middle.

As pointed out in the introduction, we could have done everything in this paper for negative/stable laminations instead. In particular, one can find a periodic *folding* sequence of train tracks carrying the

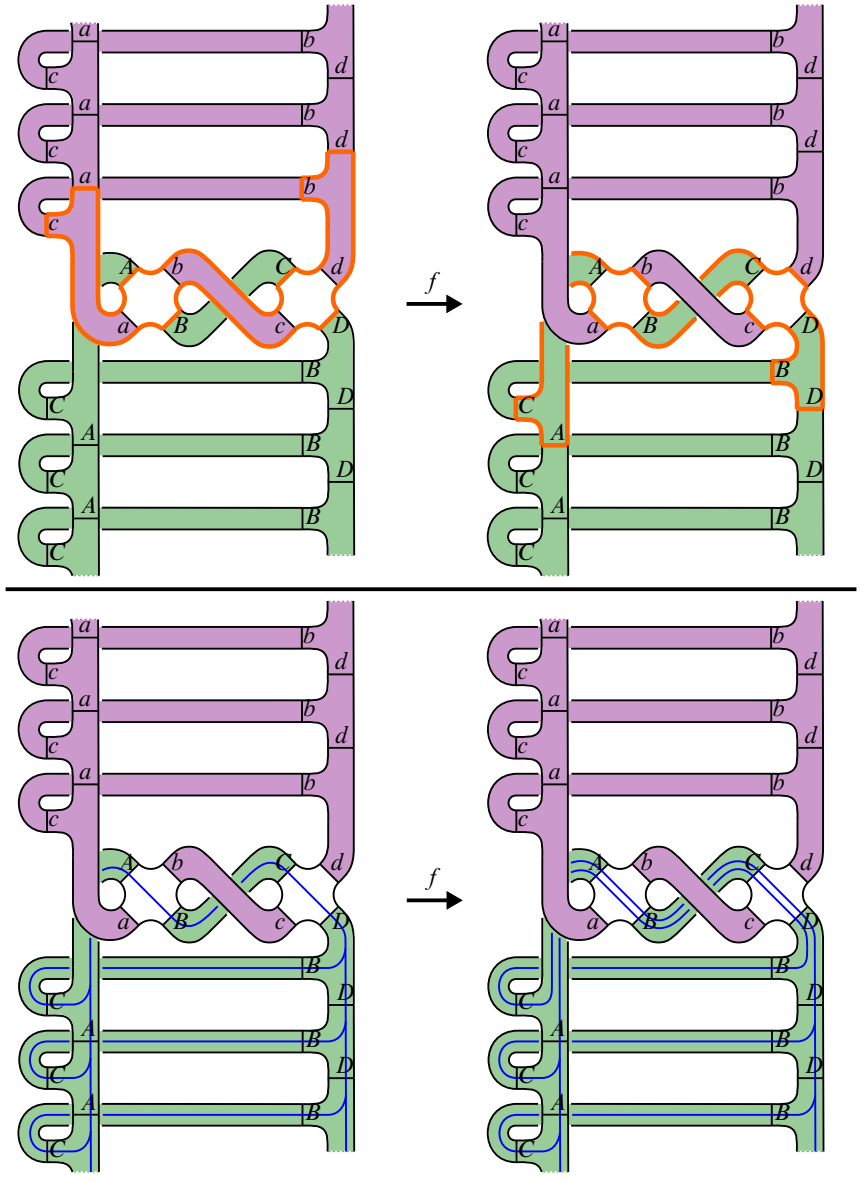

Figure 50: Top: the monodromy of the depth one foliation is determined by the fact that it maps the outlined region on the left to the outlined region on the right so that labels match. Bottom: an f-periodic splitting sequence of endperiodic train tracks carrying the positive Handel–Miller lamination.

negative Handel–Miller lamination, which suspends to a stable veering branched surface. The boundary train track of this branched surface is illustrated in Figure 51, first row, right. ◁

Example 10.4 In Figure 51, second row, we consider a different disk decomposition of the sutured manifold Q in Example 10.3, which determines another endperiodic map.

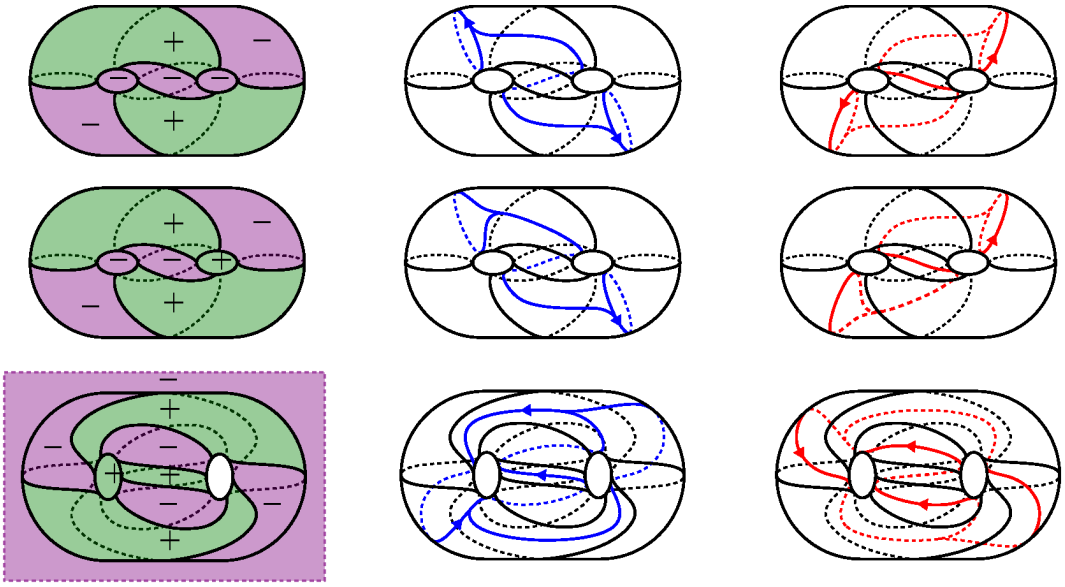

Figure 51: Boundary train tracks of unstable and stable veering branched surfaces associated to some depth one foliations.

Using a similar computation as above, we find periodic splitting/folding sequences of train tracks for this endperiodic map. These suspend to unstable/stable veering branched surfaces on Q, the boundary train tracks of which we record in Figure 51, second row, middle and right. ◁

Example 10.5 In Figure 51, third row, we consider a different sutured manifold. This sutured manifold, as well as the illustrated disk decomposition, was considered in [Cantwell and Conlon 1999, Example 5].

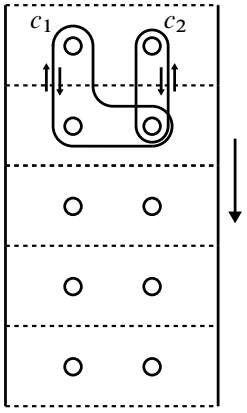

Figure 52: An endperiodic map f where the positive Handel–Miller lamination Λ_+ of f does not admit a f-invariant transverse measure of full support. The map is obtained by performing a twist around curve 2, then a twist around curve 1, and then shifting downward by one unit.

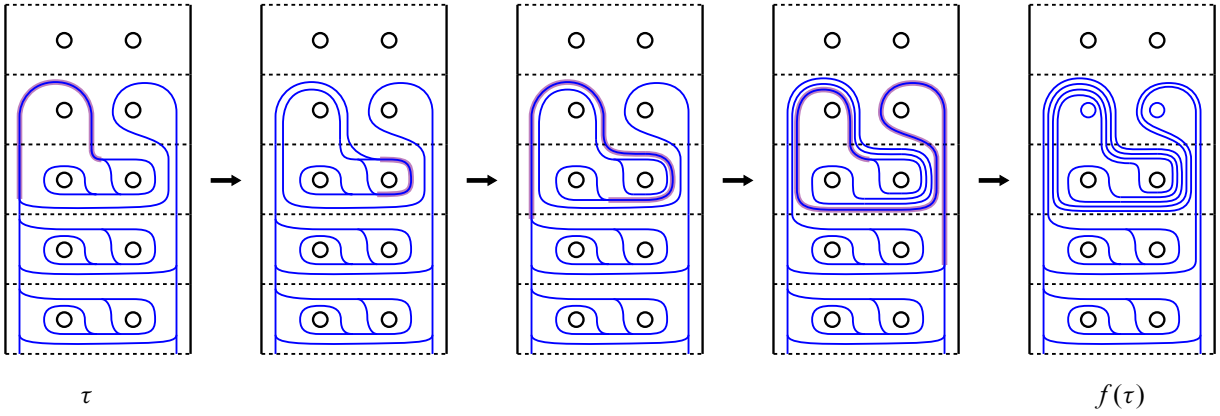

Figure 53: A splitting sequence carrying the unstable Handel–Miller lamination Λ_+. At each step, the edge to be split next is highlighted in purple.

Using a similar computation as above, we find periodic splitting/folding sequences of train tracks for the corresponding endperiodic map. These suspend to unstable/stable veering branched surfaces, the boundary train tracks of which we record in Figure 51, third row, middle and right. ◁

Example 10.6 Fenley [1997, Section 5] gave an example of an endperiodic map $f : L \to L$ where the positive Handel–Miller lamination Λ_+ of f does not admit an f-invariant transverse measure of full support.

We present a version of Fenley's map in Figure 52. The map is the composition of a Dehn twist τ_2 of the indicated sign on c_2, a Dehn twist τ_1 on c_1 of the opposite sign, and a downward shift by one unit σ, ie $f = \sigma \circ \tau_1 \circ \tau_2$.

In Figure 53, we show a f-periodic splitting sequence $\tau = \tau_0 \to \tau_1 \to \tau_2 \to \tau_3 \to \tau_4 = f(\tau) \to \cdots$ carrying the positive Handel–Miller lamination Λ_+.

This splitting sequence admits a subsplitting sequence, ie subtrain tracks $\tau_i' \subset \tau_i$ such that each splitting move $\tau_i \to \tau_{i+1}$ takes τ_i' to τ_{i+1}'. The corresponding sublamination Λ_+' admits a transverse measure μ of full support such that $f_*(\mu) = 2\mu$, which we represent as weights on the branches of τ' in Figure 54.

The reason why Λ_+ does not admit an f-invariant transverse measure of full support is roughly because the branches in τ' fold up at a higher rate than those outside of τ', so any invariant measure will vanish on the latter branches. See [Fenley 1997, Section 5] for details of this argument. ◁

Example 10.7 Take two copies C_1, C_2 of the compactified mapping torus in Example 10.2 (see Figure 19), each admitting an associated disk decomposition intersecting each of the four sutures once, and take the product sutured manifold $P = S_{1,2} \times [0, 1]$, where $S_{1,2}$ is a torus with two boundary components.

Note that the core of each suture of C_i has a natural orientation arising from the coorientation of the decomposing disk. By fixing an orientation of $S_{1,2}$, we also get orientations on the cores of the sutures of P.

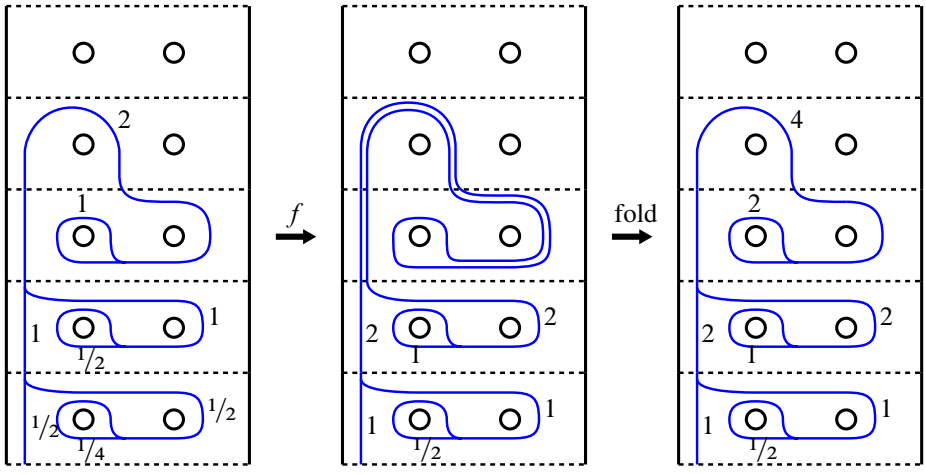

Figure 54: A subsplitting sequence of the splitting sequence in Figure 53 that carries an f-invariant sublamination of Λ_+. The sublamination admits a transverse measure μ such that $f_*(\mu) = 2\mu$.

We define Q to be the sutured manifold obtained by gluing one suture of P to a suture of C_1, and the other suture of P to a suture of C_2. Here the former gluing is done in a way that preserves the orientations on the cores, while the latter gluing reverses the orientations on the cores. See Figure 55, top.

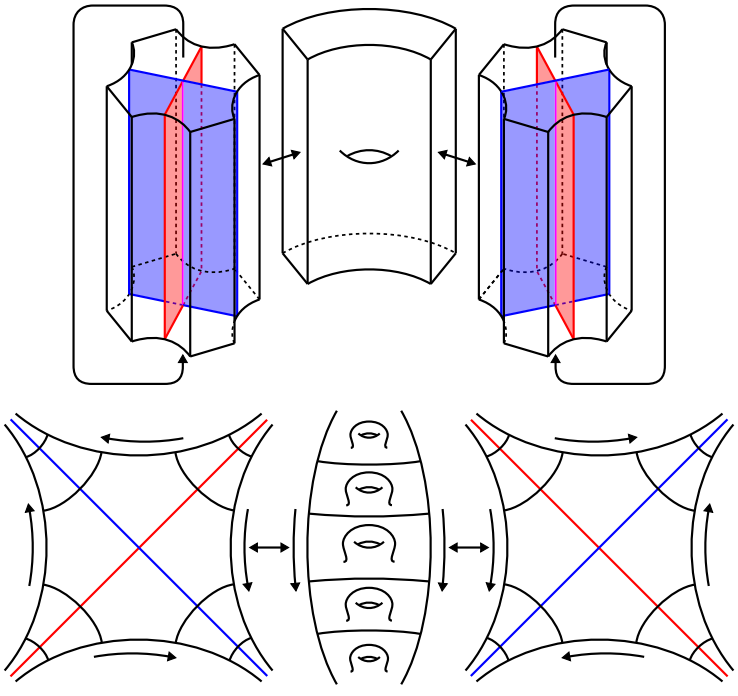

Figure 55: Top: a cartoon of the sutured manifold Q considered in Example 10.7. Bottom: the endperiodic monodromy of a depth one foliation on Q.

Up to an isotopy, we can assume that the decomposing disk D_i of C_i intersects P in an arc of the form $\{x_i\} \times [0,1]$ for $x_i \in \partial S_{1,2}$. By our orientation requirements, we can take an arc a in $S_{1,2}$ connecting x_1 and x_2 and coorient $a \times [0,1] \subset P$ so that $D_1 \cup (a \times [0,1]) \cup D_2$ determines a disk decomposition of Q to a product sutured manifold.

This disk decomposition determines a depth one foliation on Q. We illustrate the endperiodic monodromy of this foliation, together with its positive and negative Handel–Miller laminations, in Figure 55, bottom.

One can construct a veering branched surface B on Q compatibly carrying the suspended unstable Handel–Miller lamination $\mathcal{L}^u$ by simply taking the union of the veering branched surfaces B_i constructed on C_i in Example 10.2 (and extending the vector field to go from $S_{1,2} \times \{0\}$ to $S_{1,2} \times \{1\}$ on P).

Now notice that, in the construction, if we instead glue both pairs of sutures in orientation-preserving ways, we would end up with the same sutured manifold Q. Under this choice of gluings, we can again take the union of the veering branched surfaces B_i constructed on C_i in Example 10.2 to get a veering branched surface B' on Q.

Intuitively, B' is obtained from B by reversing the dynamic orientation in exactly one of the C_i. In particular, B and B' have the same underlying branched surface but differ as dynamic branched surfaces. Hence B' fully carries the unstable Handel–Miller lamination $\mathcal{L}^u$ considered above, but does not *compatibly* carry it.

The flow graph Φ' of B' consists of two cycles, which are the oriented cores of the C_i. By assumption on the orientations, the two cycles are mutually inverse in $H_1(Q)$; hence, the dual of the cone generated by the Φ'-cycles, $\mathcal{C}^\vee_{\Phi'}$, cannot be top-dimensional in $H_2(Q, \partial Q)$. In particular, $\mathcal{C}^\vee_{\Phi'}$ is not a foliation cone.

Thus B' gives an example illustrating why "compatibly carrying" cannot be replaced by "fully carrying" in Theorems 8.5 and 9.22.

This example can be generalized to any sutured manifold that is a *book of I-bundles*. These are sutured manifolds that can be written as $Q = T \cup_A (S \times I)$, where T is a nonempty disjoint union of solid tori, called the *bindings*, S is a (possibly disconnected) surface with components of negative Euler characteristic, and $S \times I$ is glued along certain components of $\partial S \times I$ onto homotopically nontrivial annuli on ∂T.

There are $2^{\#\text{bindings}}$ ways of picking dynamic orientations on each binding of Q. For each choice one can construct a veering branched surface on Q which is the disjoint union of suspensions of prongs inside each binding and possessing the prescribed dynamic orientation. As we vary the choice of dynamic orientations, these veering branched surfaces all have the same underlying branched surface but differ as dynamic branched surfaces. In particular, the cones generated by their dual/flow graph cycles in $H_1(Q)$ are not in general foliation cones. ◁

11 Questions

As explained in the introduction, the subject of our work in progress [Landry and Tsang ≥ 2025] is an alternative approach to Mosher's gluing step. Together with the base step, which we tackled in this paper, such a construction would give a way of building a veering triangulation from a sutured hierarchy $M = Q_0 \rightsquigarrow \cdots \rightsquigarrow Q_{n+1} = \text{surface} \times I$: first construct a veering branched surface on Q_n, then induct up the hierarchy to construct a veering branched surface on $M = Q_0$, and finally take the dual triangulation (but notice that the veering triangulation is not of M but rather M minus some closed orbits in general).

In turn, the goal of this is to obtain a pseudo-Anosov flow without perfect fits on M that is almost transverse to the finite-depth foliation $\mathcal{F}$ corresponding to the sutured hierarchy. By a theorem of Mosher [1992] (see also [Landry 2022, Theorem A]), such a flow would recover the Thurston face containing the compact leaves of $\mathcal{F}$. This flow would exist by the correspondence theory between veering triangulations and pseudo-Anosov flows, provided that the final veering branched surface on M has no index 0 cusped solid tori complementary regions. This is the reason for our aversion to index 0 cusped solid tori in the appendix.

However, this should not be possible for all hierarchies. To see why, consider the depth one case, ie the case when $n = 1$. Applying Theorem 7.10, we get a veering branched surface B_1 on Q_1, and we want to extend this into a veering branched surface B_0 on $M = Q_0$, say without index 0 cusped solid tori complementary regions. Since B_0 is an extension of B_1, the dynamics on B_0 should contain that of B_1; in particular, the (isotopy classes of) closed orbits of the vector field on B_1 should be a subset of that on B_0. But the latter is the set of closed orbits of a pseudo-Anosov flow φ with no perfect fits; in particular, φ has *no oppositely oriented parallel orbits*, ie closed orbits c_1, c_2 for which c_1 is homotopic to $-c_2$ in M. So the same has to be true for the closed orbits of the vector field on B_1 as well.

In other words, a necessary condition for the construction to work is for the gluing map $R_+(Q_1) \cong R_-(Q_1)$ determined by the sutured decomposition to be such that no closed orbits on B_1 become oppositely oriented parallel in M. By the same reasoning, such a condition is necessary for the intermediate gluing steps as well. We believe that this condition is also sufficient, and plan to show this in the sequel to this paper.

Below we explain a few other possible lines of inquiry raised by our work here.

11.1 Veering and taut polynomials

In this paper we generalized some aspects of the theory of veering triangulations to veering branched surfaces on sutured manifolds, namely existence (Theorem 7.10) and uniqueness (Theorem 9.22) in the "fibered" case, and the equality between cones of cycles (Theorem 8.5). There are more aspects of the veering triangulation theory that should admit direct generalizations.

One of these is the veering and taut polynomials defined in [Landry et al. 2024]. The edge and face modules defined in [Landry et al. 2024] should generalize to the sutured setting, and, possibly up to a

slight modification accounting for annulus/Möbius band sectors, one should be able to repeat much of the theory developed in [Landry et al. 2024].

Here a generalization of the taut polynomial is particularly interesting. In the nonsutured layered case, it is shown in [Landry et al. 2024] that the taut polynomial is equal to the Teichmüller polynomial defined in [McMullen 2000]. Thus a generalization of the taut polynomial in the sutured case would provide a generalization of the Teichmüller polynomial for endperiodic maps, possibly giving a polynomial invariant.

In [Landry et al. 2023a], it is shown that any endperiodic map f is isotopic to a "spun pseudo-Anosov (spA) map", and the entropy of the restriction of an spA map to its maximal compact invariant subset generalizes the entropy of a pseudo-Anosov map. In particular, it equals the growth rate of closed orbits of the Handel–Miller suspension flow, as well as the maximal growth rate of the intersection number between α and $f^n(\beta)$ over all closed curves α, β. A generalization of the Teichmüller polynomial is expected to contain information about this entropy, analogous to the nonsutured case as explained in [Landry et al. 2023b].

11.2 (Foliation) cones

Another particular result to hope for a generalization of is [Landry et al. 2024, Theorem 5.15], or, more specifically, the statement that the cone generated by cycles of the dual/flow graph is dual to a foliation cone in $H^1(Q)$ if and only if these cycles lie in an open half-space of $H_1(Q)$. The backward direction is the difficult part here. One should be able to generalize the argument of [Landry et al. 2024, Proposition 5.16] to show that the veering branched surface B is layered, and thus corresponds to a splitting sequence of endperiodic train tracks. In the nonsutured setting, we know that the train tracks in such a splitting sequence must carry the unstable foliation of the pseudo-Anosov monodromy, due to some strong uniqueness results (see for example [Fathi et al. 1979]). However, in the sutured setting, we do not have a strong enough uniqueness statement to allow us to relate the dynamics of the Handel–Miller suspension flow to B.

In general, the cone generated by dual cycles of a veering triangulation determines the cone over some (not necessarily top-dimensional) face of the Thurston norm ball, as shown in [Landry 2022]. The cones associated to veering branched surfaces on sutured manifolds are a generalization of these cones. Meanwhile, there is a generalization of the Thurston norm to the *sutured Thurston norm* on sutured manifolds. One can ask if the cones associated to veering branched surfaces are related to the cones over faces of the sutured Thurston norm ball. The answer might be rather subtle here, however, since foliation cones do not generally agree with cones over sutured Thurston norm faces.

11.3 Correspondence with pA flows

As mentioned before, a key fact about veering triangulations is that they correspond to pseudo-Anosov flows. In the appendix, we will show that a veering branched surface forms one half of a dynamic pair à

la Mosher, and hence, in particular, induces what Mosher [1996, Section 4.10] calls a pA flow on the sutured manifold. One can ask whether a construction in the other direction — a pA flow to a veering branched surface — is possible, and whether the two constructions are inverse to each other (in a suitable sense), as in the nonsutured case.

Note that the technical condition of no perfect fits plays a key role in this correspondence theory in the nonsutured setting. One might have to invent a similar condition before developing a correspondence theory in the sutured case.

11.4 Stable veering branched surfaces

In the nonsutured setting, a veering triangulation is dual to both its stable and unstable branched surfaces. In this paper we have been dealing with unstable dynamical branched surfaces mainly. Symmetrically, we could have dealt with stable dynamical branched surfaces. However, since there is no middle triangulation to tie them together, it is not clear if the two approaches fit together exactly.

More precisely, suppose we have the compactified mapping torus of an endperiodic map. One constructs an unstable veering branched surface carrying the unstable Handel–Miller lamination as in Theorem 7.10, and symmetrically constructs a stable veering branched surface carrying the stable Handel–Miller lamination. Is there a combinatorial way to recover the stable and unstable veering branched surfaces from some cellular decomposition, as in the nonsutured case?

If one can find a positive answer to this last question than it should be possible to associate a stable veering branched surface to a general unstable veering branched surface (and vice versa). One can then ask whether such a pair of stable and unstable veering branched surface can be isotoped to form a dynamic pair. In the nonsutured case, this is shown to be possible in [Schleimer and Segerman 2023].

11.5 Census of veering branched surfaces

The examples of veering branched surfaces which we worked out in Section 10 are all quite simple. In particular, many of them just have one interior vertex in their branch locus, ie one triple point or one source. It might be an interesting question to classify all veering branched surfaces with one interior vertex. In particular, do all of these carry the unstable Handel–Miller lamination of some endperiodic map? We note that, in comparison, the veering branched surfaces with no interior vertices should be easy to classify.

In general, it might be interesting to generate a census of veering branched surfaces with a small number of interior vertices. This has been done in the nonsutured case up to 16 vertices by Giannopolous, Schleimer and Segerman [Giannopolous et al. 2019]. Such a census might in particular give more examples of veering branched surfaces that are not layered, and hence do not carry the unstable Handel–Miller lamination of an endperiodic map.

Appendix Dynamic pairs

This appendix proves that given a veering branched surface in an atoroidal sutured manifold Q, one can construct a "dynamic pair" in Q. We also prove that this implies the existence of a dynamic pair as defined by Mosher (called a "Mosher pair" in what follows). This recovers the base step in Mosher's program discussed in the introduction. The ideas in this appendix will also feature prominently in the sequel paper [Landry and Tsang $\geq$ 2025], where we will explore the gluing step of Mosher's program. Although in some cases one might ultimately care only about the existence of a single dynamic branched surface B^u at the top of a sutured hierarchy, it is necessary for us to keep track of a complementary branched surface B^s to guide the construction of B^u.

As the name suggests, a dynamic pair consists of both a stable and an unstable branched surface. Mosher [1996] introduced a tool called a "dynamic train track" for promoting an unstable branched surface to a dynamic pair. We will prove that the flow graph of a veering branched surface is a dynamic train track. Thus, by Mosher's results together with our construction of veering branched surfaces, any depth one sutured manifold contains a dynamic pair (B^u, B^s) as defined by Mosher.

Crucially, however, Mosher's recipe for producing a dynamic pair involves dynamically splitting along annuli and Möbius bands, thereby introducing index 0 cusped tori. In using the correspondence between veering branched surfaces and pseudo-Anosov flows, one needs to avoid index 0 cusped tori in order to ensure a flow has no perfect fits. Since a main goal of our ongoing project is to understand when it is possible to produce a pseudo-Anosov flow with no perfect fits at the top level of a sutured hierarchy (see Section 11 for more discussion), we need to modify Mosher's theory of dynamic pairs and dynamic train tracks. In particular, we give a definition of dynamic pair which is slightly different than Mosher's, which then requires us to rework the proof that promotes a branched surface with a dynamic train track to a dynamic pair. Many of the arguments liberally use ideas of Mosher, rearranged so as to be compatible with our setup.

A.1 Dynamic pairs

A dynamic pair consists of a pair of dynamic branched surfaces, one stable and one unstable. To give a precise definition, we first have to define a few more classes of dynamic manifolds (continuing from Definitions 6.6 and 6.7) which can arise as complementary regions of such a pair of branched surfaces.

Definition A.1 (dynamic tori) Let Δ be a closed disk whose boundary is smooth with the exception of $2n \geq 4$ corners, and let $f : \Delta \to \Delta$ be a diffeomorphism. The mapping torus M of f is a 3-manifold with corners homeomorphic to a solid torus. There are $\frac{2n}{p}$ circular corner edges of M, where p is the period of a cusp of Δ under f. Likewise there are $\frac{2n}{p}$ annular faces of M. We label these faces $\boldsymbol{u}$ and $\boldsymbol{s}$ alternatingly. Take a circular vector field V that gives it the structure of a dynamic manifold. Equipped with such a vector field, M is called a *dynamic solid torus*. See Figure 56, left. Define the *index* of M to be $1 - \frac{n}{2}$.

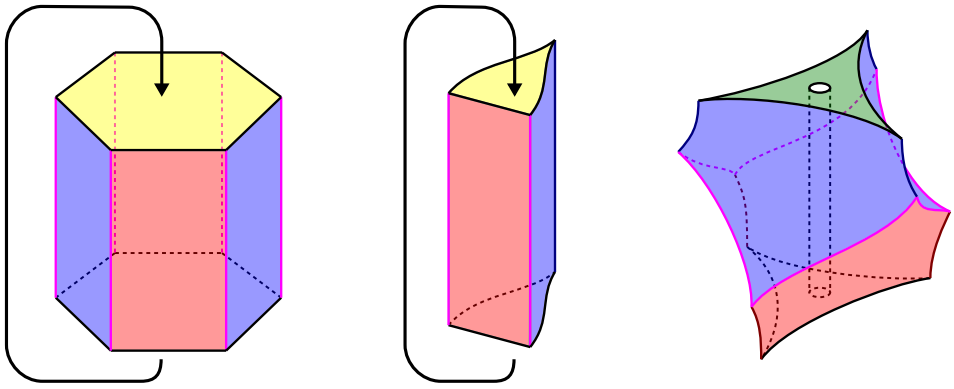

Figure 56: Left: a dynamic solid torus. Middle: an ***suu***-maw piece. Right: a drum.

A *dynamic torus shell* is defined similarly, but replacing Δ by a closed annulus whose boundary is smooth with the exception of $2n \geq 2$ corners on a single boundary component. The annulus faces are labeled ***u*** and ***s*** alternatingly, the torus face is labeled ***b***, and circularity of the vector field is defined as for the dynamic solid torus.

We refer to a dynamic solid torus or a dynamic torus shell as a *dynamic torus*. ◁

Definition A.2 (maw piece) Let Δ be a closed disk whose boundary is smooth with the exception of two corners and one cusp. $M = \Delta \times S^1$ is a 3-manifold with corners homeomorphic to a solid torus, with two corner edges and one cusp edge, and three annulus faces. Label the two annulus faces adjacent to the cusp edge ***u*** and the remaining annulus face ***s***, and take a circular vector field V that gives it the structure of a dynamic manifold. We call M an ***suu****-maw piece*. See Figure 56, middle. The definition of a ***uss****-maw piece* is symmetric. ◁

Construction A.3 (pinching an edge) If e is a ***ps***-edge connecting two ***psu***-corners of a dynamic manifold, then we can *pinch* e as shown in Figure 57. This produces a ***uu***-edge connecting a ***puu***-gable to an ***suu***-gable. Symmetrically, we can pinch an ***mu***-edge connecting two ***msu***-corners to produce an ***ss***-edge connecting an ***mss***-gable to a ***uss***-gable. ◁

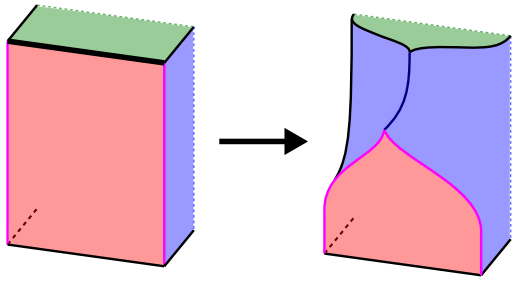

Figure 57: Pinching a ***ps***-edge (thickened) connecting two ***psu***-corners.

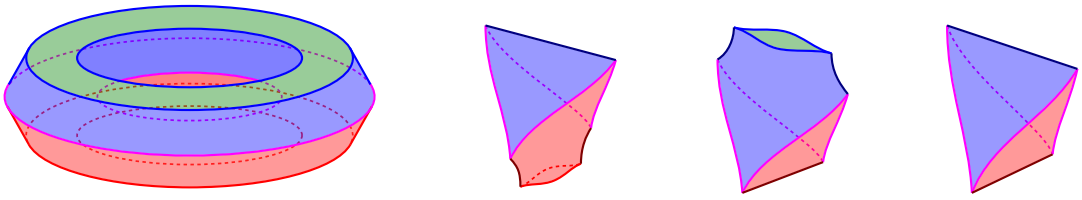

Figure 58: From left to right: a coherent annulus drum, a $\boldsymbol{p}$-pinched rectangle drum, an $\boldsymbol{m}$-pinched rectangle drum, and a pinched tetrahedron.

Definition A.4 (drum) Let S be a surface with an even number of corners at each boundary component and with $\operatorname{index}(S) \leq 0$. For each boundary component c of S, make some choice as follows:

- If c has $2n \geq 2$ corners, label the sides by $\boldsymbol{u}$ and $\boldsymbol{s}$ alternatingly.
- If c has no corners, either label the side by $\boldsymbol{b}$ or choose an orientation of c.

Now $S \times [0,1]$ is a 3-manifold with corners. We can modify it in the following ways:

- Let c be a boundary component of S with $2n \geq 2$ corners. Pinch each $\boldsymbol{ps}$ edge of $c \times \{1\}$, and pinch each $\boldsymbol{mu}$-edge of $c \times \{0\}$.
- For a boundary component c of S with no corners and labeled $\boldsymbol{b}$, label $c \times [0,1]$ by $\boldsymbol{b}$.
- For a boundary component c of S with no corners and not labeled $\boldsymbol{b}$, label $c \times \left[0, \frac{1}{2}\right]$ by $\boldsymbol{s}$ and $c \times \left[\frac{1}{2}, 1\right]$ by $\boldsymbol{u}$.
- If S is not a rectangle, label the image of $S \times \{1\}$ by $\boldsymbol{p}$ and the image of $S \times \{0\}$ by $\boldsymbol{m}$.
- If S is a rectangle, either label the image of $S \times \{1\}$ by $\boldsymbol{p}$ or pinch it into a $\boldsymbol{uu}$-cusp edge; symmetrically, either label the image of $S \times \{0\}$ by $\boldsymbol{m}$ or pinch it into an $\boldsymbol{ss}$-cusp edge.

Now choose a vector field V that gives the resulting 3-manifold with corners the structure of a dynamic manifold, and such that V is circular on the annulus faces on $c \times [0,1]$ for every boundary component c without corners and not labeled $\boldsymbol{b}$, and induces the dynamic orientation on them which is specified by the chosen orientation on c. We call this dynamic manifold a *drum*. ◁

In Figure 56, right, we show one example of a drum. Here we start with an annulus with six corners on one boundary component and no corners on the other. We label the boundary component without corners by $\boldsymbol{b}$.

Among all drums, there are some that deserve specific names. A *coherent annulus drum* is the drum obtained by taking S to be an annulus without corners and with both boundary components oriented in the same direction around S. A *$\boldsymbol{p}$-pinched rectangle drum* is the drum obtained by taking S to be a rectangle and pinching only the $\boldsymbol{p}$-face in the last step above. An *$\boldsymbol{m}$-pinched rectangle drum* is the drum obtained by taking S to be a rectangle and pinching only the $\boldsymbol{m}$-face. A *pinched tetrahedron* is the drum obtained by taking S to be a rectangle and pinching both the $\boldsymbol{p}$- and $\boldsymbol{m}$-faces. See Figure 58.

Definition A.5 Let Q be a sutured manifold, B^u and B^s be branched surfaces in Q, and V be a C^0 vector field on Q. (B^u, B^s, V) is said to be a *dynamic pair* if:

(1) (Q, V) is a dynamic manifold.

(2) (B^u, V) is an unstable dynamic branched surface and (B^s, V) is a stable dynamic branched surface. Note that, unlike in the main text, we are not assuming that V is smooth, and in fact V cannot be smooth here.

(3) V is smooth on Q except along $\operatorname{brloc}(B^u)$, where it has locally unique forward trajectories, and along $\operatorname{brloc}(B^s)$, where it has locally unique backward trajectories.

(4) Each component of $Q \setminus\setminus (B^u \cup B^s)$ is a dynamic torus, a drum or a maw piece. (Notice that $Q \setminus\setminus (B^u \cup B^s)$ is a dynamic manifold with the faces corresponding to $B^{u/s}$, $R_\pm$ and γ labeled $\boldsymbol{u/s}$, $\boldsymbol{p/m}$ and $\boldsymbol{b}$, respectively.)

(5) There is a collection S^u of annuli and Möbius bands, called the *sinks*, which are carried by $B^u \setminus\setminus B^s$ and with boundary components on $B^u \cap B^s$, such that:

   (a) Every $\boldsymbol{uss}$-maw piece component μ of $Q \setminus\setminus (B^u \cup B^s)$ is attached to an element F of S^u, ie the $\boldsymbol{u}$-face of μ is identified with F, and is *boundary parallel*, ie there exists an annulus carried by B^s with one boundary component on the maw circle of μ and the other boundary component on R_-.

   (b) For every component K of $B^u \setminus\setminus B^s$, either it contains an element F of S^u and F is a sink of K, or every forward trajectory of $K \setminus (B^u \cap B^s)$ is finite and ends on R_+.

   (c) The boundary components of elements of S^u do not overlap, ie there does not exist boundary components c_1, c_2 of elements of S^u which map to the same curve in Q, nor can a boundary component c of an element of S^u double cover a curve in Q.

   Similarly, there is a collection S^s of annuli and Möbius bands, called the *sources*, satisfying the symmetric properties.

(6) The boundary train tracks $\beta^u = B^u \cap R_+$ and $\beta^s = B^s \cap R_-$ do not carry Reeb annuli.

(7) No component of $Q \setminus\setminus (B^u \cup B^s)$ is a coherent annulus drum. ◁

In Definition A.5, a dynamic pair is slightly more general than what Mosher [1996, Section 4.5] calls a "dynamic pair", which we will call a *Mosher pair*.

The following lemma explains the relationship between dynamic pairs and Mosher pairs for those interested. We do not use Mosher pairs here, so we will not provide the definition, instead referring the reader to [Mosher 1996, Section 4.5].

Lemma A.6 *Any Mosher pair is a dynamic pair, and any dynamic pair (B^u, B^s, V) can be transformed into a Mosher pair by dynamically splitting along elements of S^u and S^s.*

Proof If (B^u, B^s, V) is a Mosher pair, one can take S^u to be the set of annulus/Möbius band sinks of components of $B^u \setminus\setminus B^s$ and choose S^s symmetrically. Then it is straightforward to check that (B^u, B^s, V) satisfies Definition A.5.

Conversely, if one has a dynamic pair (B^u, B^s, V) à la Definition A.5, the only axioms in the definition of a Mosher pair that could possibly fail are: *every maw piece is attached to a torus piece*, *transience of forward/backward trajectories*, and *separation of torus pieces*. *Separation of torus pieces* in fact holds because if two torus pieces are glued along some pair of, say, $\boldsymbol{u}$-faces, then the $\boldsymbol{s}$-faces of the torus pieces must lie in S^s, and the boundary components of the $\boldsymbol{s}$-faces that are adjacent to the glued $\boldsymbol{u}$-faces will then be identified.

We can transform (B^u, B^s, V) into a Mosher pair by splitting along sources and sinks so that all the resulting sources and sinks are faces of dynamic tori; this property implies the transience and maw piece axioms.

Here is how the splitting works. Suppose there is a sink F of S^u that is not a face of a torus piece. Enlarge F to a slightly larger annulus/Möbius band F' still carried by B^u and containing ∂F in its interior. Dynamically split B^u along F'. This creates an index 0 dynamic solid torus and some $\boldsymbol{suu}$-maw pieces and/or pinched tetrahedra, while the topology of the other components of $Q \setminus (B^u \cap B^s)$ is unchanged. One can modify V so that this new (B^u, B^s, V) satisfies (1)–(4) in Definition A.5.

The new S^u is obtained by replacing F in the original collection by the annuli double covering it under the splitting. That axioms (5a)–(5c) for S^u are preserved is clear from construction. The new S^s is obtained by adding in the $\boldsymbol{s}$-faces of the dynamic solid torus that is created. New $\boldsymbol{suu}$-maw pieces are created on the sides of $F' \setminus F$ with no branches spiraling out. Those components of $F' \setminus F$ are contained in components of $B^u \setminus B^s$ for which every forward trajectory ends on R_+, otherwise (5c) will fail for F. Hence the new $\boldsymbol{suu}$-maw pieces are attached to the new $\boldsymbol{s}$-faces and are boundary parallel, verifying (5a) for S^s for the new (B^u, B^s, V). (5b) is clear from construction. For (5c), the only way this could fail is if there were elements of S^s sharing a boundary curve with F. But then F is a face of a dynamic torus in the first place.

Axioms (6) and (7) are clearly preserved by construction as well. Now we repeat the argument by splitting elements in the new S^u or S^s that are not faces of dynamic tori. Since this kind of splitting always reduces the number of elements in S^u or S^s that are not faces of dynamic tori, the process terminates eventually and we get a Mosher pair. □

In particular, a sutured manifold contains a dynamic pair if and only if it contains a Mosher pair. We will use this fact implicitly going forward.

Proposition A.7 [Mosher 1996, Proposition 4.10.1] *If a sutured manifold Q contains a dynamic pair, then Q is irreducible, each face of Q is incompressible, and no two torus components of γ are isotopic.*

When constructing a dynamic pair, it will be useful to ignore axioms (5c) and (7) during the initial stages, later adjusting for them to hold. We record a proposition explaining this adjustment:

Proposition A.8 *Let Q be an atoroidal sutured manifold with no torus components of $R_\pm$, let B^u and B^s be dynamic branched surfaces in Q, and let V be a vector field on Q. Suppose (B^u, B^s, V) satisfies all but* (5c) *and* (7) *in Definition A.5. If B^u and B^s do not carry closed surfaces, then Q contains a dynamic pair (B'^u, B'^s, V').*

Furthermore:

- *If (B^u, B^s, V) satisfies* (7) *as well, then B'^u can be chosen to be a subbranched surface of B^u, and B'^s can be chosen to be a subbranched surface of B^s.*
- *If (B^u, B^s, V) satisfies* (7) *and B^u satisfies* (5c) *as well, then B'^s can be chosen to be B^s, and B'^u can be chosen to be a subbranched surface of B^u. The symmetric statement holds.*

Proof This is essentially proven in [Mosher 1996, Section 4.12]. We outline an argument here, emphasizing the places that are slightly different due to our definition of a dynamic pair, and referring to the relevant sections of [Mosher 1996] for details.

Given a coherent annulus drum D, we now describe how to add an annulus sector to B^u and an annulus sector to B^s, and then eliminate the $\boldsymbol{m}$- and $\boldsymbol{p}$-faces of D, to create a dynamic torus and some other types of pieces. This is depicted in Figure 59 together with an additional zipping step, and is essentially [Mosher 1996, "An example", pages 193–195]. When attaching the new sectors, we need to take into consideration the branching of B^s and B^u on ∂D. Let A be a $\boldsymbol{u}$-face of D which has a $\boldsymbol{us}$-circle c of D on its boundary.

(a) If $c \cap \mathrm{brloc}(B^u)$ is nonempty, then we also attach the extra s sector very close to c outside D. This creates some number of pinched tetrahedra.

(b) If $c \cap \mathrm{brloc}(B^u) = \varnothing$ and $\mathrm{brloc}(B^u) \cap A = \varnothing$, then we attach the extra B^s sector very close to c outside D. The component of $Q \setminus\setminus (B^u \cup B^s)$ on the other side of A from D is necessarily a drum in this case, so this attachment creates a boundary parallel maw piece.

(c) If $c \cap \mathrm{brloc}(B^u) = \varnothing$, then one can show that $\mathrm{brloc}(B^u) \cap A$ contains some loop that is the $\boldsymbol{uu}$-cusp circle of an $\boldsymbol{suu}$-maw piece, and that there is a (possibly larger) maximal family of maw pieces whose union w has the smooth structure of a maw piece as shown in Figure 59. Let c' be the other $\boldsymbol{us}$-curve of w besides c. We attach the extra B^s sector just outside of w near c' so that it passes through w near its $\boldsymbol{s}$-face as shown in Figure 59. This creates some additional index 0 dynamic solid tori and either pinched tetrahedra (as in (a)) or a boundary parallel $\boldsymbol{uss}$-maw piece (as in (b)), depending on whether c' intersects $\mathrm{brloc}(B^u)$.

We attach the other boundary component of the new annulus sector of B^s using the same recipe applied to the other $\boldsymbol{u}$-face of D. Then we attach a new annulus sector of B^u symmetrically.

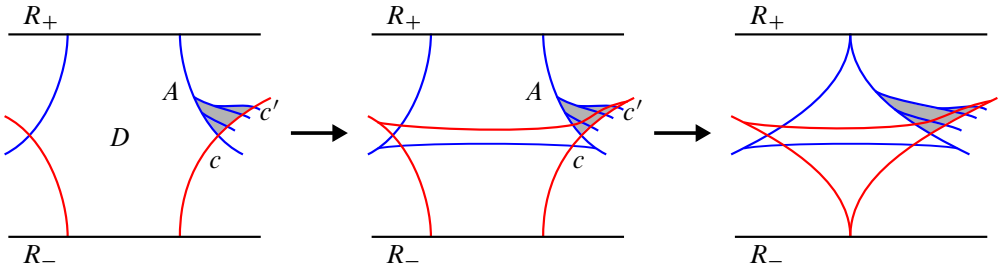

Figure 59: Modifying a coherent annulus drum to obtain a dynamic solid torus and some other pieces. Middle: attaching a sector to B^s near a $\boldsymbol{us}$-circle of a coherent annulus drum when a $\boldsymbol{u}$-face of the drum intersects $\operatorname{brloc}(B^u)$ in a collection of circles, as in case (c) from the proof of Proposition A.8. The region w is shaded.

Finally, we zip up the $\boldsymbol{p}$- and $\boldsymbol{m}$-faces of D, as shown in Figure 59, right. This is possible by our assumption that there are no torus components of $R_\pm$.

We augment S^u and S^s by adding the $\boldsymbol{u}$-faces and $\boldsymbol{s}$-faces, respectively, of all dynamic tori created by the above steps. This process reduces the number of coherent annulus drums by one. After performing it finitely many times, we can arrange that (B^u, B^s, V) satisfies all but (5c) in Definition A.5.

Suppose there exists boundary components c_1, c_2 of elements of S^u which map to the same curve c in Q. Then c is a core of an annulus sector s of B^s; this uses the hypothesis that B^s does not carry a closed surface, for otherwise c could lie in a torus or Klein bottle sector. Also $B^u \cap s$ is a train track on s with only converging switches and it contains the cycle c; hence, it must be a union of parallel cycles with branches going from ∂s to the outermost cycles. See Figure 60.

We first claim that each of the annulus regions between the cycles abuts a torus piece on both of its sides. This is true for those regions that meet c, since the components of $Q \setminus\!\setminus (B^u \cup B^s)$ meeting those regions has a sequence of $\boldsymbol{u}$-, $\boldsymbol{s}$-, $\boldsymbol{u}$-, $\boldsymbol{s}$-annulus faces, and only dynamic tori satisfy this property. Then we can repeat the argument on the annulus regions of s that meet the $\boldsymbol{s}$-faces of these torus pieces, and induct outwards.

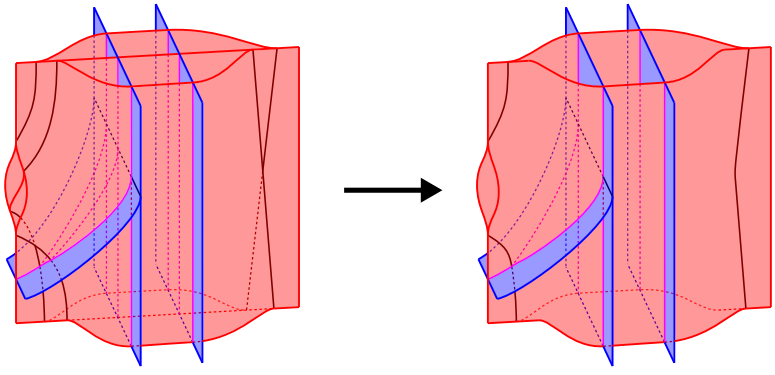

Figure 60: Locating a sector at which (5c) is violated and deleting it.

Then we claim that a region of s outside of an outermost cycle containing no branches of τ is adjacent to maw pieces on both of its sides. This follows from a similar argument as above: each of the components of $Q \setminus\setminus (B^u \cup B^s)$ meeting those regions has a sequence of s-, u-, s-annulus faces, meaning it is either a maw piece or dynamic torus; they cannot both be torus pieces because then the cycle would not have been outermost. Hence at least one is a maw piece. If the other component of $Q \setminus\setminus (B^u \cup B^s)$ is a dynamic solid torus, then there would be a cusp circle on an annulus s-face of a dynamic torus, contradicting (5b) in Definition A.5. Hence the other component of $Q \setminus\setminus (B^u \cup B^s)$ is also a maw piece.

For a region of s outside of an outermost cycle containing branches of τ, we claim that it is adjacent to pinched tetrahedra or p-pinched rectangle drums on both of its sides. This follows from the same line of argument: the components of $Q \setminus\setminus (B^u \cup B^s)$ meeting those regions have two u-faces meeting at a uu-cusp, and some V-trajectories starting on those u-faces enter u-faces of dynamic tori and hence never end at R_+. Only pinched tetrahedra and p-pinched rectangle drums satisfy these properties.

Now remove s from B^s, as indicated in Figure 60. This glues up maw pieces to form bigger maw pieces, and glues up pinched tetrahedra and p-pinched rectangle drums to form bigger pinched tetrahedra/p-pinched rectangle drums. (This uses the hypothesis that B^u does not carry closed surfaces; otherwise, at some point a maw piece/pinched tetrahedron/p-pinched rectangle drum might be glued onto itself.) Dynamic torus pieces are glued up along s-faces. Any dynamic torus admits a Seifert fibration with at most one singular fiber such that the restriction to any u- or s-face is a foliation by circles, and hence the pieces obtained by gluing the dynamic tori admit Seifert fibrations.

If there exists a boundary component c of an element of S^u which double covers a curve in Q, we can locate a sector and remove it similarly as above. And symmetrically the same thing can be done with S^u replaced by S^s. This idea of removing sectors is essentially [Mosher 1996, Proposition 4.12.1, Step 2].

Let T_i be a disjoint collection of tori parallel to the boundary components of the Seifert fibered pieces. We may modify V so that it is tangent to the T_i. Cutting along $\bigcup T_i$ returns sutured manifolds with the restricted (B^u, B^s, V) satisfying all but (5c) in Definition A.5 and some Seifert fibered spaces disjoint from B^u and B^s. This is [Mosher 1996, Proposition 4.12.1, Step 3].

On the components of $Q \setminus\setminus \bigcup T_i$ with nonempty B^u and B^s, we inductively repeat the above argument, deleting sectors and cutting along tori at each stage. Eventually the process will stop since there are only finitely many sectors of B^u and B^s. When the process terminates, we get a disjoint collection of tori T_i such that each component of $Q \setminus\setminus \bigcup T_i$ either contains a dynamic pair or is a Seifert fibered space. We claim that each T_i corresponds to the boundary of a dynamic torus. Indeed, otherwise T_i would be essential in Q by Proposition A.7 and an innermost disk argument, violating atoroidality. Hence we have in fact produced a dynamic pair in Q.

For the additional statements: If there are no coherent annulus drums, then we do not have to modify the branched surfaces as in the first part of the proof. Thus we only have to carry out the part of the proof

where we remove sectors. If furthermore (5c) is satisfied for S^u, then we do not even need to carry out that part of the proof for B^s, and so B^s is left unchanged throughout. The symmetric statement is of course true for B^u as well. □

We remark that without the atoroidality assumption, the above proof still produces a family of essential tori separating Q into a collection of pieces admitting dynamic pairs, and a collection of pieces admitting Seifert fibrations.

A.2 Dynamic train tracks

Definition A.9 Let B be an unstable dynamic branched surface. A oriented train track τ embedded in B is said to be a *dynamic train track* if τ is disjoint from ∂Q and if there exists a dynamic vector field V such that:

(1) V is tangent to τ.

(2) The set of converging switches of τ is equals to $\tau \cap \operatorname{brloc}(B)$.

(3) V is smooth on $B - \operatorname{brloc}(B)$ except at diverging switches of τ.

(4) Every component K of $B \setminus\setminus \tau$ either carries an annulus or Möbius band A such that $\partial A \subset \partial K$ and A is a sink of K, or every forward trajectory of $K \setminus \tau$ is finite and ends at a point of $B \cap R_+$.

A dynamic train track on a stable dynamic branched surface is defined symmetrically. ◁

Our terminology differs from [Mosher 1996] slightly. There, dynamic train tracks were only required to satisfy (1)–(3) in Definition A.9, and those that in addition satisfy (4) were said to be *filling*. However, since we do not need to deal with nonfilling dynamic train tracks, we include (4) in our definition for brevity.

Before stating the next proposition, we explain a construction called "splitting for goodness". This construction is a slightly streamlined version of the material in [Mosher 1996, Section 4.7 and Proposition 4.11.1, Step 2e].

Construction A.10 (splitting for goodness) Let B be an unstable dynamic branched surface and τ be a dynamic train track on B. Let K be a component of $B \setminus\setminus \tau$ that meets R_+. By definition, all forward trajectories starting in the interior of K are finite and end on R_+. Take a small regular neighborhood of $\tau \cap K$ in K and let τ' be the boundary of this regular neighborhood in K. Meanwhile, let β' be $K \cap R_+$. The forward trajectories in the interior of K induce a map from τ' to β'.

For each interval component of $\operatorname{brloc}(K)$ with one endpoint on τ and one endpoint on R_+, dynamically split K along a triangle so that this component of $\operatorname{brloc}(K)$ now lies close to the forward trajectory of a point on the component close to the endpoint on τ. This is [Mosher 1996, Figure 4.10]. See Figure 61, first row.

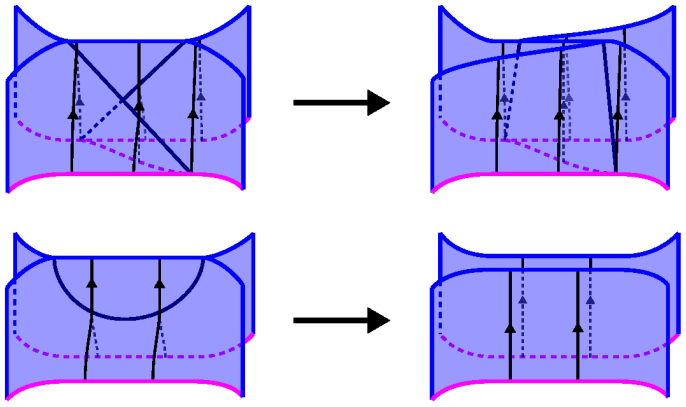

Figure 61: Splitting for goodness refers to the operation of doing these two types of splittings.

For each interval component of $\mathrm{brloc}(K)$ with both endpoints on R_+, dynamically split K along the bigon with one side on this component, so that this component of $\mathrm{brloc}(K)$ disappears. See Figure 61, second row.

We refer to the operation of performing these dynamic splittings as *splitting B for goodness*. ◁

Proposition A.11 *Let (B^u, V) be a very full unstable dynamic branched surface equipped with a dynamic train track τ. If $\beta^u = B^u \cap R_+$ does not carry Reeb annuli, B^u does not carry closed surfaces, and Q is atoroidal, then there is a dynamic pair (B'^u, B^s, V') on Q.*

Furthermore, if

- *β^u has no annulus or cusped bigon complementary regions,*

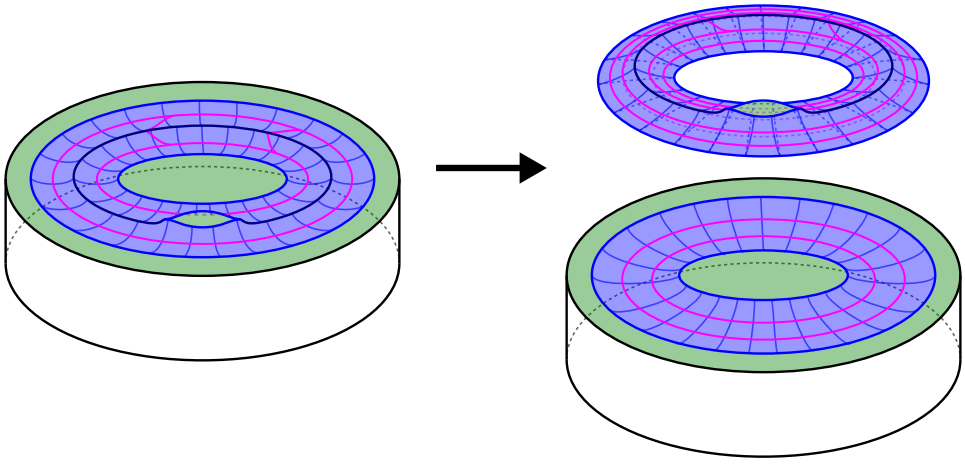

Figure 62: Cutting off breached $\boldsymbol{u}$-cusped torus pieces from $\boldsymbol{u}$-cusped product pieces (and splitting lone cycles on annulus faces of the breached $\boldsymbol{u}$-cusped torus).

- *the $\boldsymbol{u}$-cusped product complementary regions of B^u have no cusp circles*, *and*
- *there is no annulus or Möbius band sector of B^u which meets $\boldsymbol{u}$-cusped torus pieces on both sides*,

then B'^u can be chosen to be B^u after splitting for goodness.

Proof Again, this is essentially proven in [Mosher 1996]. We outline an argument here, emphasizing the places that are slightly different due to our definition of a dynamic pair and splitting for goodness, and referring to the relevant sections of [Mosher 1996] for details.

We first modify τ by removing any "extraneous sinks". An extraneous sink is a sink γ of τ for which there exists an annulus or Möbius band R carried by B^u containing γ in its interior, with boundary components lying on τ. As Mosher [1996, Proposition 4.11.1, Step 2b] describes, there is a process for removing γ along with branches of τ spiraling into γ such that the result still satisfies our definition of dynamic train track. We remove γ in this way and denote the new dynamic train track by τ also.

Then we split B^u for goodness. As remarked above, this step is essentially [Mosher 1996, Proposition 4.11.1, Step 2e].

Next consider a $\boldsymbol{u}$-cusped product complementary region of B^u, homeomorphic to $S \times [0,1]$. Suppose there are annulus $\boldsymbol{u}$-faces on $S \times \{1\}$ that are parallel, have parallel dynamic orientations, and cobound a collection of cusped bigon $\boldsymbol{p}$-faces. Consider a maximal collection of such annulus $\boldsymbol{u}$-faces and add an annulus sector s to B^u with boundary components on the outermost faces. Also augment τ by adding two copies of the core of s, oriented by the dynamic orientation of the $\boldsymbol{u}$-faces. See Figure 62.

This cuts off pieces from the $\boldsymbol{u}$-cusped product, which we call breached $\boldsymbol{u}$-cusped tori, and are defined as follows:

Definition A.12 A *breached $\boldsymbol{u}$-cusped torus* is a $\boldsymbol{u}$-cusped torus with some cusped bigon $\boldsymbol{p}$-faces added along the $\boldsymbol{uu}$-cusp edges. *Breached $\boldsymbol{s}$-cusped tori* are similarly defined.

A *breached $\boldsymbol{suu}$-maw piece* is a dynamic manifold which is an $\boldsymbol{suu}$-maw piece with some cusped bigon $\boldsymbol{p}$-faces added along the $\boldsymbol{uu}$-cusp edge. *Breached $\boldsymbol{uss}$-maw pieces* are similarly defined. ◁

Now modify V so that B^u is still a very full unstable dynamic branched surface, with τ a dynamic train track on B^u.

Finally, for every complementary region of B^u which is a (breached) $\boldsymbol{u}$-cusped torus piece, we inspect the restriction of τ to each of its annulus faces. Since we have removed all extraneous sinks, the restriction of τ to each face contains one or two cycles. If the restriction of τ only has one cycle, split τ along the cycle. The result is still a dynamic train track, which we denote again by τ. This is exactly as described in [Mosher 1996, Proposition 4.11.1, Step 2d].

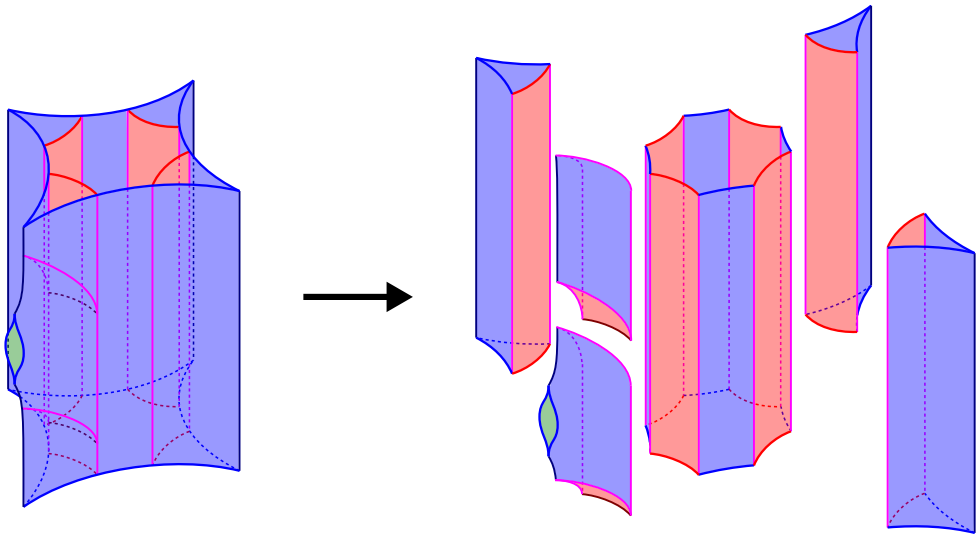

Figure 63: Cutting (breached) $\boldsymbol{u}$-cusped torus pieces into dynamic torus pieces, $\boldsymbol{suu}$-maw pieces, pinched tetrahedra and $\boldsymbol{m}$-pinched rectangle drums.

We record some useful facts about B^u and τ after these modifications:

(i) The complementary regions of B^u are (breached) $\boldsymbol{u}$-cusped torus pieces and $\boldsymbol{u}$-cusped product pieces, and τ is still a dynamic train track on B^u.

(ii) Every loop component of $\operatorname{brloc}(B^u)$ that does not meet τ is boundary parallel. This follows from the definition of dynamic train tracks.

(iii) Every component of $\operatorname{brloc}(B^u)$ which is not a loop meets τ. This is a consequence of splitting for goodness.

(iv) No $\boldsymbol{u}$-cusped product complementary region of B^u has parallel dynamically oriented $\boldsymbol{u}$-annulus faces that meet along $\boldsymbol{uu}$-cusp circles or cobound cusped bigons. This follows from the axiom that cusp circles have to be incoherent in a cusped product piece (Definition 6.7(g)), and also from the annulus sectors we chose to add to B^u.

Next we construct the stable branched surface B^s. We do so by capping off τ within each complementary region of B^u.

For every complementary region of B^u which is a (breached) $\boldsymbol{u}$-cusped torus, place annuli with boundary components lying along cycles of τ on the faces to divide the $\boldsymbol{u}$-cusped torus into a dynamic torus and (breached) $\boldsymbol{suu}$-maw pieces. Then attach tongues to the annuli to subdivide the (breached) $\boldsymbol{suu}$-maw pieces into $\boldsymbol{suu}$-maw pieces, pinched tetrahedra and $\boldsymbol{m}$-pinched rectangle drums. See Figure 63. This is essentially as described in [Mosher 1996, Proposition 4.11.1, Step 3].

For every complementary region of B^u which is a $\boldsymbol{u}$-cusped product homeomorphic to $D \times [0,1]$, consider the restriction of τ to $D \times \{1\}$, which we temporarily denote as τ'. Take $\tau' \times [0,1]$ inside $D \times [0,1]$. If

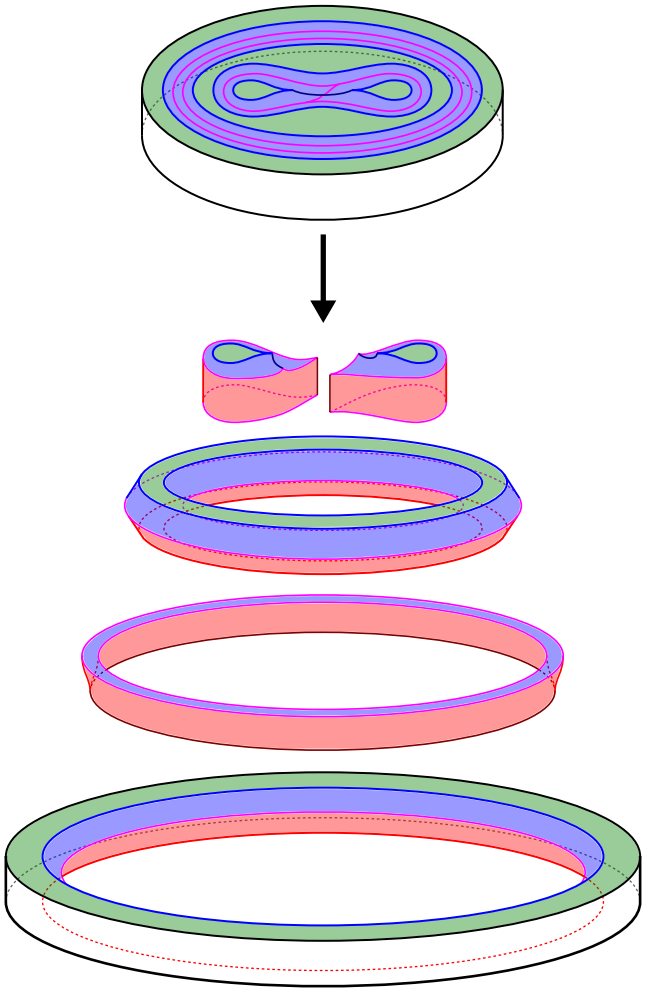

Figure 64: Cutting $\boldsymbol{u}$-cusped product pieces into drums and $\boldsymbol{uss}$-maw pieces.

an annulus $\boldsymbol{u}$-face on $D \times \{1\}$ contains two cycles c_1, c_2 of τ', zip together $c_1 \times [0, \epsilon]$ and $c_2 \times [0, \epsilon]$ for small ϵ. This divides the $\boldsymbol{u}$-cusped product piece into drums and $\boldsymbol{uss}$-maw pieces. See Figure 64. This is exactly as described in [Mosher 1996, Proposition 4.11.1, Step 3], and uses properties (iii) and (iv) above.

Now take the union over all the complementary regions of B^u to get B^s, and modify the vector field V so that (B^u, B^s, V) satisfies (1)–(4) of Definition A.5.

The rest of the construction consists in checking (5a), (5b), (6) of Definition A.5 on (B^u, B^s, V), as well as showing that B^s does not carry closed surfaces, for then we can apply Proposition A.8.

Take S^u to be the set of annulus and Möbius band sinks of the components of $B^u \setminus\setminus \tau$. Since every $\boldsymbol{uss}$-maw piece arises from parallel cycles of τ on the boundary of a $\boldsymbol{u}$-cusped product piece, it is clear that these are attached to elements of S^u and are boundary parallel. The components of $B^u \setminus\setminus B^s$ are exactly the components of $B^u \setminus\setminus \tau$; hence, (5b) for S^u follows from the axioms of a dynamic train track.

Take S^s to be the set of annuli added to (breached) $\boldsymbol{u}$-cusped torus pieces. By construction, every $\boldsymbol{suu}$-maw piece is attached to an element of S^s. By property (ii) above, every $\boldsymbol{suu}$-maw piece is boundary parallel as well. Property (5b) for S^s is clear from construction.

That $B^u \cap R_+$ does not carry Reeb annuli is part of the hypothesis. If $B^s \cap R_-$ carries a Reeb annulus, then the restriction of τ to the boundary of some $\boldsymbol{u}$-cusped product piece must carry a Reeb annulus. The boundary components of such a Reeb annulus will then lie on coherently dynamically oriented annulus $\boldsymbol{u}$-faces that meet along a $\boldsymbol{uu}$-cusp circle or bound cusped bigons, contradicting property (iii) above.

Now suppose B^s carries a closed surface C. By existence of the vector field V and atoroidality of Q, C is a torus which is either peripheral or bounds a solid torus.

If C bounds a solid torus, call it T. Otherwise let T be the component of $Q \setminus\setminus C$ containing a component of ∂Q parallel to C (necessarily a component of γ).

Since $C \cap B^u$ is an oriented train track on C with only converging switches, it is in fact a union of disjoint loops that cut C up into a collection of annuli. These annuli must be elements of S^s, which we defined above to be the set of annuli added to (breached) $\boldsymbol{u}$-cusped torus pieces. The complementary regions of $B^u \cup S^s$ are (breached) $\boldsymbol{suu}$-maw pieces, dynamic tori and $\boldsymbol{u}$-cusped product pieces, and T is a union of such regions. The $\boldsymbol{u}$-cusped product pieces cannot appear inside T since T has no $\boldsymbol{m}$-faces, and the breached $\boldsymbol{suu}$-maw pieces cannot appear inside T since T has no $\boldsymbol{p}$-faces. Thus T is a union of $\boldsymbol{suu}$-maw pieces and dynamic tori. But, by an index argument on a meridional disk (if T is a solid torus) or annulus (if T is a thickened torus), we see that this is impossible.

We conclude by applying Proposition A.8 to obtain a dynamic pair in Q.

For the "furthermore" statement, if the $\boldsymbol{u}$-cusped product complementary regions of B^u have no cusp circles and if β^u has no cusped bigon complementary regions, then we do not need to add sectors to B^u before constructing B^s. If β^u has no annulus complementary region, then (7) in Definition A.5 is automatically satisfied by the constructed (B'^u, B^s). If B^u does not have annulus or Möbius band sectors which meet $\boldsymbol{u}$-cusped torus pieces on both sides, then (5c) for S^s in Definition A.5 is satisfied for, by construction, the only places where the boundary components of these sources can meet are along such sectors. We apply the second bullet point of Proposition A.8 to finish the proof. □

A.3 From veering branched surfaces to dynamic pairs

Recall the definition of veering branched surfaces in Definition 6.11 and the definition of flow graphs in Definition 6.18 and Figure 26.

Proposition A.13 *Let B be a veering branched surface in a sutured manifold Q. The flow graph Φ of B is a dynamic train track on B.*

Proof From construction, it is clear that Φ is disjoint from ∂Q and the set of converging switches of Φ is equal to $\Phi \cap \operatorname{brloc}(B)$. Recall that Φ is obtained from the semiflow graph Φ_+ by deleting the branches whose forward trajectories all end on R_+ (Definition 6.18). We will show the remaining properties by first analyzing the situation for the semiflow graph Φ_+.

Recall from Definition 6.23 that, for each sector s, the components of $s \setminus\setminus \Phi_+$ are triangles, rectangles and tongues.

We define a vector field V_+ on B by requiring:

- V_+ is tangent to Φ_+.
- On a triangle, V_+ flows from the side cooriented inwards to the side cooriented outwards.
- On a rectangle, V_+ flows from the side cooriented inwards to the side cooriented outwards.
- On a tongue, V_+ flows from the cusp to the side on $\operatorname{brloc}(B)$ or R_+.
- V_+ is smooth on B except at the diverging switches of Φ_+, where backward trajectories are unique, and on $\operatorname{brloc}(B)$, where forward trajectories are unique.

We can recover the components of $B \setminus\setminus \Phi_+$ by gluing together components of $s \setminus\setminus \Phi_+$. To describe this gluing, construct a directed graph G by setting the vertices to be the set of components of $s \setminus\setminus \Phi_+$ for all sectors s, and an edge from a component c_1 to another c_2 if c_1 is followed by c_2. The definitions of Φ_+ and V_+ imply that G has the following properties:

- Each vertex has at most one outgoing edge; it has no outgoing edges if and only if it has a side on R_+.
- A vertex has no incoming edges if and only if it is a tongue
- Only tongues and rectangles can have edges entering a rectangle

Moreover, the components of G are in one-to-one correspondence with the components of $B \setminus\setminus \Phi_+$.

The first property above implies that each component H of G either has a vertex or a cycle as a sink. In the former case, every forward trajectory in the corresponding component of $B \setminus\setminus \Phi_+$ is finite and ends on R_+. In the latter case, the corresponding component of $B \setminus\setminus \Phi_+$ carries an annulus or Möbius band, formed by the union of triangles that make up the sink in H, which every forward trajectory in the component ends on. Moreover, in this latter case, the boundary of the component of $B \setminus\setminus \Phi_+$ lies on Φ_+ (and does not meet R_+). Indeed, none of the vertices in the corresponding component of G can have a side along R_+, or else it would be a sink.

We use this information to analyze the components of $B \setminus\setminus \Phi$. The components of $B \setminus\setminus \Phi_+$ that contain an annulus or Möbius band sink remain as components of $B \setminus\setminus \Phi$, since points of Φ_+ on their boundary have paths that go around the annulus/Möbius band and hence do not end on R_+. See Figure 65, right.

The other components of $B \setminus\setminus \Phi_+$ are glued together to form components of $B \setminus\setminus \Phi$, and every forward V_+-trajectory in the interior of the latter is finite and ends on R_+. See Figure 65, left. We remark that

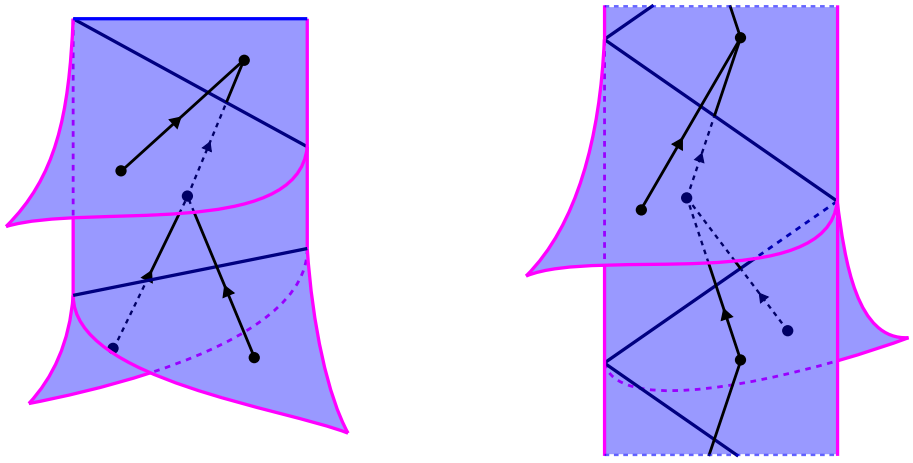

Figure 65: Analyzing the components of $B \setminus\setminus \Phi_+$ by gluing up the components of $s \setminus\setminus \Phi_+$.

this property is not necessarily true at the boundary: along Φ_+, forward V_+-trajectories are not unique in general and certain V_+-trajectories may glue up to form a loop.

In any case, it only remains to smooth V_+ near the switches of Φ_+ that are no longer switches of Φ. □

Theorem A.14 *If an atoroidal sutured manifold Q admits an unstable veering branched surface B, then it admits a dynamic pair (B^u, B^s, V).*

Proof By Proposition A.13, the branched surface contains a dynamic train track. By Proposition A.11, Q contains a dynamic pair. □

Corollary A.15 *Let Q be the compactified mapping torus of an endperiodic map $f : L \to L$. If Q is atoroidal, then there is a dynamic pair (B^u, B^s) on Q such that B^u is an unstable veering branched surface compatibly carrying the unstable Handel–Miller lamination of f.*

Proof Theorem 7.10 provides an unstable veering branched surface compatibly carrying the Handel–Miller lamination. We claim that when we apply Propositions A.11 and A.13 to B^u to get a dynamic pair, we do not need to modify B^u. To establish this, it suffices to check the hypotheses in the additional statement of Proposition A.11, and to show that splitting for goodness does not change B^u.

The boundary train track $B^u \cap R_+$ is efficient by the definition of veering branched surfaces, and hence has no annulus or cusped bigon complementary regions. The fact that the $\boldsymbol{u}$-cusped product complementary regions of B^u do not have cusp circles is shown in the proof of Theorem 7.10, specifically in Proposition 7.5.

As for the last additional condition of Proposition A.11, suppose there is an annulus or Möbius band sector s of B^u which meets $\boldsymbol{u}$-cusped torus pieces on both sides. Notice that s cannot have corners,

otherwise there would be some source on ∂s, but the cusp circles of a $\boldsymbol{u}$-cusped torus piece cannot have sources. With this in mind, the condition follows from Lemmas 7.8 and 7.9.

Finally, when one splits for goodness, one changes the boundary train track by a splitting move. But this cannot occur since the boundary train track of a veering branched surface is already spiraling. □

We remark that the above does not claim that B^s carries the stable Handel–Miller lamination, although presumably this is true. We would be interested to see a proof of this.

Acknowledgements

We thank John Cantwell and Larry Conlon for telling us about their work on foliation cones and Handel–Miller theory, David Gabai for explaining some of the history of his work on pseudo-Anosov flows transverse to finite-depth foliations, and Ian Agol and Eriko Hironaka for helpful conversations. We are additionally grateful to the referee for their numerous helpful comments and corrections.

This collaboration traces back to a topic group run by James Farre at the first *Nearly carbon neutral geometric topology conference* in June 2020, organized by Martin Bobb and Allison N Miller. We are grateful to James, Martin and Allison for putting on a great event in a creative way at a stressful time.

Landry was supported by the NSF under DMS 2013073 and thanks the Mathematisches Forschungsinstitut Oberwolfach for providing an ideal working environment during the final stages of this project. Tsang was supported by the Simons Foundation #376200.

References

[Agol 2011] **I Agol**, *Ideal triangulations of pseudo-Anosov mapping tori*, from "Topology and geometry in dimension three", Contemp. Math. 560, Amer. Math. Soc., Providence, RI (2011) 1–17 MR

[Altman 2014] **I Altman**, *The sutured Floer polytope and taut depth-one foliations*, Algebr. Geom. Topol. 14 (2014) 1881–1923 MR

[Calegari 2006] **D Calegari**, *Universal circles for quasigeodesic flows*, Geom. Topol. 10 (2006) 2271–2298 MR

[Calegari and Dunfield 2003] **D Calegari**, **N M Dunfield**, *Laminations and groups of homeomorphisms of the circle*, Invent. Math. 152 (2003) 149–204 MR

[Candel and Conlon 2000] **A Candel**, **L Conlon**, *Foliations, I*, Graduate Stud. in Math. 23, Amer. Math. Soc., Providence, RI (2000) MR

[Cantwell and Conlon 1993] **J Cantwell**, **L Conlon**, *Surgery and foliations of knot complements*, J. Knot Theory Ramifications 2 (1993) 369–397 MR

[Cantwell and Conlon 1994] **J Cantwell**, **L Conlon**, *Isotopy of depth one foliations*, from "Geometric study of foliations", World Sci., River Edge, NJ (1994) 153–173 MR

[Cantwell and Conlon 1999] **J Cantwell**, **L Conlon**, *Foliation cones*, from "Proceedings of the Kirbyfest", Geom. Topol. Monogr. 2, Geom. Topol. Publ., Coventry (1999) 35–86 MR

[Cantwell and Conlon 2017] **J Cantwell**, **L Conlon**, *Cones of foliations almost without holonomy*, from "Geometry, dynamics, and foliations 2013", Adv. Stud. Pure Math. 72, Math. Soc. Japan, Tokyo (2017) 301–348 MR

[Cantwell et al. 2021] **J Cantwell**, **L Conlon**, **S R Fenley**, *Endperiodic automorphisms of surfaces and foliations*, Ergodic Theory Dynam. Systems 41 (2021) 66–212 MR

[Fathi et al. 1979] **A Fathi**, **F Laudenbach**, **V Poenaru**, *Travaux de Thurston sur les surfaces: Séminaire Orsay*, Astérisque 66-67, Soc. Math. France, Paris (1979) MR

[Fenley 1997] **S R Fenley**, *End periodic surface homeomorphisms and* 3*-manifolds*, Math. Z. 224 (1997) 1–24 MR

[Fenley and Mosher 2001] **S Fenley**, **L Mosher**, *Quasigeodesic flows in hyperbolic* 3*-manifolds*, Topology 40 (2001) 503–537 MR

[Field et al. 2023] **E Field**, **H Kim**, **C Leininger**, **M Loving**, *End-periodic homeomorphisms and volumes of mapping tori*, J. Topol. 16 (2023) 57–105 MR

[Frankel et al. 2019] **S Frankel**, **S Schleimer**, **H Segerman**, *From veering triangulations to link spaces and back again*, preprint (2019) arXiv 1911.00006 To appear under Mem. Amer. Math. Soc.

[Fried 1979] **D Fried**, *Fibrations over S^1 with pseudo-Anosov monodromy*, from "Travaux de Thurston sur les surfaces: Séminaire Orsay", Astérisque 66-67, Soc. Math. France, Paris (1979) 251–266 MR

[Gabai 1983] **D Gabai**, *Foliations and the topology of* 3*-manifolds*, J. Differential Geom. 18 (1983) 445–503 MR

[Gabai 1987] **D Gabai**, *Foliations and the topology of* 3*-manifolds, II*, J. Differential Geom. 26 (1987) 461–478 MR

[Giannopolous et al. 2019] **A Giannopolous**, **S Schleimer**, **H Segerman**, *A census of veering structures*, electronic reference (2019) Available at `https://math.okstate.edu/people/segerman/veering.html`

[Hatcher 2008] **A Hatcher**, *The cyclic cycle complex of a surface*, preprint (2008) arXiv 0806.0326

[Hempel 1976] **J Hempel**, 3*-manifolds*, Ann. of Math. Stud. 86, Princeton Univ. Press (1976) MR

[Landry 2022] **M P Landry**, *Veering triangulations and the Thurston norm: homology to isotopy*, Adv. Math. 396 (2022) art. id. 108102 MR

[Landry 2023] **M Landry**, *Stable loops and almost transverse surfaces*, Groups Geom. Dyn. 17 (2023) 35–75 MR

[Landry and Tsang $\geq$ 2025] **M Landry**, **C C Tsang**, *Pseudo-Anosov flows and sutured hierarchies*, in preparation

[Landry et al. 2023a] **M P Landry**, **Y N Minsky**, **S J Taylor**, *Endperiodic maps via pseudo-Anosov flows*, preprint (2023) arXiv 2304.10620 To appear in Geom. Topol.

[Landry et al. 2023b] **M P Landry**, **Y N Minsky**, **S J Taylor**, *Flows, growth rates, and the veering polynomial*, Ergodic Theory Dynam. Systems 43 (2023) 3026–3107 MR

[Landry et al. 2024] **M P Landry**, **Y N Minsky**, **S J Taylor**, *A polynomial invariant for veering triangulations*, J. Eur. Math. Soc. 26 (2024) 731–788 MR

[Li 2002] **T Li**, *Laminar branched surfaces in* 3*-manifolds*, Geom. Topol. 6 (2002) 153–194 MR

[Li 2003] **T Li**, *Boundary train tracks of laminar branched surfaces*, from "Topology and geometry of manifolds", Proc. Sympos. Pure Math. 71, Amer. Math. Soc., Providence, RI (2003) 269–285 MR

[McMullen 2000] **C T McMullen**, *Polynomial invariants for fibered* 3*-manifolds and Teichmüller geodesics for foliations*, Ann. Sci. École Norm. Sup. 33 (2000) 519–560 MR

[McMullen 2015] **C T McMullen**, *Entropy and the clique polynomial*, J. Topol. 8 (2015) 184–212 MR

[Mosher 1992] **L Mosher**, *Dynamical systems and the homology norm of a* 3*-manifold, II*, Invent. Math. 107 (1992) 243–281 MR

[Mosher 1996] **L Mosher**, *Laminations and flows transverse to finite depth foliations*, preprint (1996)

[Penner and Harer 1992] **R C Penner**, **J L Harer**, *Combinatorics of train tracks*, Ann. of Math. Stud. 125, Princeton Univ. Press (1992) MR

[Schleimer and Segerman 2023] **S Schleimer**, **H Segerman**, *From veering triangulations to dynamic pairs*, preprint (2023) arXiv 2305.08799

[Thurston 1986] **W P Thurston**, *A norm for the homology of* 3*-manifolds*, Mem. Amer. Math. Soc. 339, Amer. Math. Soc., Providence, RI (1986) MR

[Tsang 2023] **C C Tsang**, *Veering branched surfaces, surgeries, and geodesic flows*, New York J. Math. 29 (2023) 1425–1495 MR

[Zhang 2023] **Y Zhang**, *Guts and the minimal volume orientable hyperbolic* 3*-manifold with* 3 *cusps*, preprint (2023) arXiv 2304.09950

MPL: *Department of Mathematics and Statistics, Saint Louis University*
St Louis, MO, United States

CCT: *Department of Mathematics, University of California, Berkeley*
Berkeley, CA, United States

Current address: *Département de mathématiques, Université du Québec à Montréal*
Montréal, QC, Canada

michael.landry@slu.edu, tsang.chi_cheuk@uqam.ca

Proposed: Mladen Bestvina
Seconded: Cameron Gordon, Dmitri Burago

Received: 18 May 2023
Revised: 2 August 2024

GEOMETRY & TOPOLOGY

msp.org/gt

See inside back cover or msp.org/gt for submission instructions.

The subscription price for 2025 is US $865/year for the electronic version, and $1210/year (+$75, if shipping outside the US) for print and electronic. Subscriptions, requests for back issues and changes of subscriber address should be sent to MSP. Geometry & Topology is indexed by Mathematical Reviews, Zentralblatt MATH, Current Mathematical Publications and the Science Citation Index.

Geometry & Topology (ISSN 1465-3060 printed, 1364-0380 electronic) is published 9 times per year and continuously online, by Mathematical Sciences Publishers, 2000 Allston Way # 59, Berkeley, CA 94701-4004. Periodical rate postage paid at Oakland, CA 94615-9651, and additional mailing offices. POSTMASTER: send address changes to Mathematical Sciences Publishers, 2000 Allston Way # 59, Berkeley, CA 94701-4004.

GT peer review and production are managed by EditFLOW® from MSP.

PUBLISHED BY

mathematical sciences publishers

nonprofit scientific publishing

http://msp.org/

GEOMETRY & TOPOLOGY

Volume 29 Issue 9 (pages 4477–4945) 2025